

POST-TRANSCRIPTIONAL REGULATION OF THE INNATE IMMUNE
RESPONSE BY RNA-BINDING PROTEINS

A Dissertation

by

KELSI OWENS WEST

Submitted to the Office of Graduate and Professional Studies of

Texas A&M University
in partial fulfillment of the requirements for the degree of

DOCTOR OF PHILOSOPHY

Chair of Committee,	Robert O. Watson
Committee Members,	Kristin L. Patrick
	A. Phillip West
	Michael F. Criscitiello
Head of Program,	David W. Threadgill

December 2020

Major Subject: Genetics

Copyright 2020 Kelsi Owens West

ABSTRACT

While transcriptional control of innate immune gene expression is well characterized, almost nothing is known about how pre-mRNA splicing decisions influence, or are influenced by, macrophage activation. I believe each step of RNA processing is just as important, if not more important than the initial transcription of an immune response gene, and RNA-processing can act as a major regulatory node of the innate immune response. Here, I demonstrate that splicing factors belonging to hnRNP and SRSF families are critical regulators of innate immune gene expression and their function is regulated by pathogen sensing cascades. My initial work focused on an RNA-binding protein, hnRNP M. Loss of hnRNP M led to hyperinduction of a unique regulon of inflammatory and antimicrobial genes following diverse innate immune stimuli. Mutating specific serines on hnRNP M had little effect on its ability to control pre-mRNA splicing or transcript levels of housekeeping genes in resting macrophages. However, these same serines greatly impacted hnRNP M's ability to dampen induction of specific innate immune transcripts following pathogen sensing. Conversely, additional studies focused around another hnRNP, hnRNP F, found a quite different phenotype, whereby loss of hnRNP F prevented activation of the complete family of interferon stimulatory genes following several innate immune stimuli and influenced intron inclusion of specific master regulators of ISGs, *Irf7* and *Ikbke*. I also found that mutating specific serines on hnRNP F influenced this gene expression of *Ifnb1*. My results reveal a previously unappreciated role for pattern recognition receptor signaling in controlling

splicing factor phosphorylation and establish pre-mRNA splicing as a critical regulatory node in defining innate immune outcomes. Lastly, with bioinformatic approaches, I discovered thousands of genes whose expression and splicing were regulated by hnRNP and SRSF RNA-binding proteins. My research demonstrates that these peripheral splicing factors carry out a wide range of functions to regulate distinct innate immune and housekeeping genes. Taken together, my results indicate that splicing is a major regulatory node of the innate immune response and these peripheral splicing factors are key players in regulation of gene expression.

DEDICATION

“The record shows I took the blows and did it my way.” - Frank Sinatra.

Tyler, this one is for you. You are the real MVP. The sacrifices you have made for me are the definition of love and I will spend forever trying to repay you. I love you forever times infinity. Dad, you taught me work ethic, drive, and patience and how to do everything I do to the best of my ability, no matter what it is. You deserve this degree as much as me. Like you said, “Science is a lot like fishing, you just got to keep casting until you get a bite.”

ACKNOWLEDGEMENTS

First, I would like to thank God for always watching out for me and having greater plans than I could have even dreamed of.

Tyler, all the things we have done and accomplished, who would have guessed that high school sweethearts from the Delmarva would go this far? I am eternally grateful for your love and thank God for you every day. You are my rock, my inspiration, my hero, my ride-or-die and the smartest, funniest person I know. You are the most selfless, hard-working, and genuine person I know. I am so excited for the adventure that we are just beginning.

To my parents, thank you for raising me with the most solid core values a person could have. Your faith, patience, and love have never given up on me. From the shy kid, to a difficult teenager, to a consumed, anxious academic, your love has never faded. Each of you are an example of Christ and this has guided me my whole life. To my sister, you are my person. Few will ever understand the bond we have. You are one of the few people I have always been my absolute true self with, and you have never judged or questioned me for it. I love you so much. I am so happy and blessed to be your sister. I am so proud of you and I am so excited for your future and all the amazing things God has waiting for you. To my brother, I thought about just poking fun at you, but alas. You are one of the greatest role models in my life. Your strength and pursuit of your dreams that started so young in your life has pushed me in my own pursuits to never give up on what I want.

I would like to thank my advisor, Dr. Robert Watson. You are an extremely fun and enthusiastic scientist, and person. Your excitement is literally infectious and got me through so many experiments that I was not that “excited” about. Thank you for taking the chance on me and the true investment you put into mentoring me. You have taught me the best experimental design, how to ask the right questions, and how to be the best scientist I can be. While the running joke seemed to be that I never liked you, I can tell you definitively that was untrue. I would not have traded joining your lab for anything. Try to get on the bench once and a while, okay? Please continue to give “no *cares*” as your resolutions always say. Stay passionate and keep the excitement going for new recruits. Dr. Kristin L. Patrick, thank you for allowing me to work on your brainchild with Dr. Watson and be the original member of the splicing cadets. You are one of the greatest educators and most ingenious writers and I will never forget our white board talks. I’m excited to see all the success both of you are destined to have in the future and check-in on where the research takes both of the labs.

Dr. Bell and Dr. Hoffpauir, the future is the brightest I have ever seen for you two. I hope you continue to care less and pursue what you want and not what others tell you. You have been the best coworkers and continue to be the greatest of friends. You both deserve all the of the joy and greatest things in life. Dr. Hoffpauir, your extreme kindness, love of science, and the light you shine has played a major impact in my life. I am so excited for the big things that life has in store for you. Dr. Bell, you are the smartest person I have ever met, and I am honored and proud to call you a mentor and

friend. You will be the best manager, scientist, and investigator the world has ever seen. I know this because you already are. I cannot wait to check-in on the Bell lab and make sure you are still pipetting. Stay true to you and do not listen to the noise. I will always be here for both of you, no matter where we all end up. Thank you both for your investment into my life and teaching me everything I know. I can only imagine the amazing adventures awaiting both of you and I cannot wait to be a part of them. Ms. Kaitlyn Carter, thank you for bringing new joy to the bench just when I needed it and realizing that mentoring the future like you, makes it all worth it. The world needs more enthusiastic, hardworking people like you. You have become one of my best friends and I know you have the brightest future ahead.

To my beloved Searcey, Wood, Owens, & Price family, your support and love do not go unnoticed and your constant inquisitions of “when I’m going to be done” kept reminding me to keep going, so I could finally tell you that I’m done! To my West, Whaley, Martin, & Outten family, you are the best in-laws I could have. The son you raised is the best gift in my entire life. Thank you for overflowing that love to me from day one and letting me steal him away for this wild adventure called life.

To my role models and life influencers Dr. Les Erikson, Dr. Stacey Wilson, Dr. Jennifer Doudna, Dr. Brandye Nobiling, Dr. Megan Quinn, & Dr. Chris Blazier, thank you for lighting a fire in me, being my scientific heroes, and creating true inspirations within me for the reasons behind the pursuits I am on today. Ms. Allison Wagner, I am so happy that you became my bench mate. Sharing laughs and struggles with you, truly helped me through the latter half of this degree. Do not forget to stand up for yourself

and what you want. To my genetics cohort, Kevin, Kristin, Casey, Matt, and Joe, I am so blessed to have been in the greatest, most genuine, and fun cohort of all time. I will miss you all so much and look forward to hearing about your wonderful lives and future endeavors. To the Watson and Patrick lab members, thank you for helping me and contributing to my success. I wish all of you continued accomplishments in your pursuits.

I would also like to thank my committee members, Dr. Robert Watson, Dr. Kristin Patrick, Dr. A. Phillip West, and Dr. Michael Criscitiello, for their guidance and support throughout the course of this research. You have challenged my understanding and have pushed me to know more. Thank you to my colleagues, faculty, and staff in the department of Microbial Pathogenesis and Immunology, especially the West and Samuels labs, for making my time at Texas A&M University a great experience. Lastly, while many problems were caused by COVID, without it, this probably would not have been written so fast, so thanks COVID.

CONTRIBUTORS AND FUNDING SOURCES

Contributors

This work was overseen by a dissertation committee comprising of Dr. Robert O. Watson, Dr. Kristin L. Patrick, and Dr. A. Phillip West of the Department of Microbial Pathogenesis and Immunology and Dr. Michael F. Criscitiello of the Department of Veterinary Pathobiology. The semi-quant PCR and IP/Western Blots were done in collaboration with Haley Scott and Allison Wagner, respectively. The samples analyzed for Chapter 3 was done in collaboration with Allison Wagner. The sequencing in Chapters 1 and 2 was conducted by Texas A&M AgriLife Genomics & Bioinformatics Services. The sequencing in Chapter 3 was conducted by Texas A&M Genome Sciences and Society (TIGSS). The IP/MS was done by Dr. Larry Dangott and the Protein Chemistry Lab at Texas A&M University. All other work conducted for the dissertation was completed by the student independently.

Funding Sources

This work was made possible in part by R01AI25512 (R.O.W.), R35GM133720 (K.L.P.), and R21AI4004 (R.O.W. and K.L.P.). Its contents are solely the responsibility of the authors and do not necessarily represent the official views of the National Institute of Allergy and Infectious Diseases.

NOMENCLATURE

RBP- RNA-Binding Protein

RNA- Ribonucleic Acid

DNA- Deoxyribonucleic Acid

ISG- Interferon-Stimulatory Gene

mRNA- Mature RNA/messenger RNA

UTR- Untranslated Region

DAMPs-Danger Associated Molecular Patterns

PRR- Patter Recognition Receptor

TLR- Toll-like Receptor

RRM- RNA Recognition Motif

KD- Knockdown

SCR- Scramble

shRNA- short hairpin RNA

gRNAs- guide RNAs

MOI- Multiplicity of Infection

NF- κ B- nuclear factor κ B

PAMPs- pathogen-associated molecular patterns

siRNA- small interfering RNAs

ISD- IFN stimulatory DNA

LS - local splice variation

MAJIQ- Modeling Alternative Junction Inclusion Quantification

VSV- vesicular stomatitis virus

NLS- nuclear localization signal

ChIP- chromatin immunoprecipitation

eCLIP- enhanced CLIP

LM- lipoglycan lipomannan

IFN- Interferon

Mtb- *Mycobacterium tuberculosis*

MDR- multi-drug resistance

cGAS- Cyclic GMP-AMP synthase

cGAMP- Cyclic guanosine monophosphate–adenosine monophosphate

STING- Stimulator of interferon genes

TBK1- Tank binding Kinase

IRF- Interferon-regulatory factor

ISRE- Ifn stimulated response element

CRISPR- Clustered Regularly Interspaced Short Palindromic Repeats

mtDNA- Mitochondrial DNA

IFNAR- Interferon- α/β receptor

JAK1- Janus kinase

TYK2- Tyrosine kinase 2

ISGF3- Interferon-stimulated gene factor 3

BMDM- Bone marrow derived macrophage

IL- Interleukin

TNF- Tumor necrosis factor

LC3- Light chain 3

ATG5- Autophagy related 5

MAVS- Mitochondrial antiviral signaling protein

RIG-I- Retinoic acid-inducible gene I

STAT- Signal Transducer and Activator of Transcription

NOS- Nitric oxide synthase

COMMD8- COMM Domain Containing 8

MX1- MX Dynamin Like GTPase 1

GBP- Guanylate Binding Protein

MARCKS- Myristoylated Alanine Rich Protein Kinase C Substrate

ADORA2A- Adenosine A2a Receptor

NMT2- N-myristoyltransferase

MyD88- Innate Immune Signal Transduction Adaptor

TRIF- Toll/interleukin-1 receptor-domain-containing adapter-inducing interferon- β

IPA- Ingenuity Pathway Analysis

HepG2- Human immortalized liver carcinoma cells

K562- Human immortalized myelogenous leukemia cell

RAW- Macrophage-like, Abelson leukemia virus transformed cell line

CXCL- C-X-C Motif Chemokine Ligand

CCL- C-C Motif Chemokine Ligand

RSAD2- Radical S-Adenosyl Methionine Domain Containing 2

MIP1A- Macrophage inflammatory protein 1- α

IRF- Interferon regulatory factor

μ g- micrograms

mL- milliliter

TDP- transactive response DNA binding protein

TABLE OF CONTENTS

	Page
ABSTRACT	ii
DEDICATION	iv
ACKNOWLEDGEMENTS	v
CONTRIBUTORS AND FUNDING SOURCES.....	ix
NOMENCLATURE.....	x
TABLE OF CONTENTS	xiv
CHAPTER I INTRODUCTION	1
Gene Expression and RNA-Processing.....	1
Pre-mRNA Splicing	2
Alternative Splicing.....	4
RNA-binding proteins (RBPs)	5
HnRNPs.....	6
HnRNP M.....	8
HnRNP F	10
HnRNP C, K, U.....	12
Post-translational Regulation of hnRNPs.....	14
SRSFs	15
Post-translational Regulation of SR proteins	18
The Innate Immune Response	19
Toll-Like Receptors.....	20
Nucleic Acid-Sensing Receptors.....	24
Bacterial Response	27
<i>Salmonella enterica</i> serovar Typhimurium.....	28
<i>Mycobacterium tuberculosis</i>	30
Innate Immune Response in Macrophages.....	32
Transcriptional Response	33
NF- κ B and AP1	34
IRFs and STATs.....	35
Post-transcriptional Response During Innate Immunity	36
Pre-mRNA Splicing in Innate Immunity	39
Post-translational Modifications During Innate Immunity	42

CHAPTER II THE SPLICING FACTOR HNRNP M IS A CRITICAL REGULATOR OF INNATE IMMUNE GENE EXPRESSION IN MACROPHAGES	45
Introduction	45
Results	48
RNA Sequencing (RNA-Seq) Analysis Reveals Immune Response Genes Are Regulated by hnRNP M during <i>Salmonella</i> Infection.....	48
hnRNP M Regulates a Specific Subset of Innate Immune Genes upon Treatment with Diverse Innate Immune Stimuli	50
hnRNP M Influences Gene Expression Outcomes at the Level of Pre-mRNA Splicing.....	53
hnRNP M Is Enriched at the Level of Chromatin and at the IL6 Genomic Locus ..	56
hnRNP M's Association with the <i>IL6</i> Locus Is RNA Dependent and Controlled by TLR4 Signaling	58
Phosphorylation of hnRNP M at S574 Downstream of TLR4 Activation Controls Its Ability to Repress Expression of Innate Immune Transcripts	60
Loss of hnRNP M Enhances Macrophages' Ability to Control Viral Infection	64
Discussion	66
CHAPTER III HNRNP M PROTEIN INTERACTIONS ARE REGULATED BY INNATE IMMUNE PHOSPHORYLATION EVENTS	69
Introduction	69
Results	71
hnRNP M Protein Interactions Reveal Paraspeckle Protein Associations	71
Phosphorylation of S574 Influences hnRNP M Protein Partners Associations	74
Paraspeckle Proteins Show Differential Regulation of Innate Immune Gene Expression	77
Discussion	78
CHAPTER IV HNRNP F REGULATE TYPE I INTERFERON RESPONSE DURING BACTERIAL INFECTION	81
Introduction	81
Results	84
Interferon Stimulatory Genes Are Regulated by hnRNP F during <i>S.</i> Typhimurium and <i>M. tuberculosis</i> Infection.....	84
hnRNP F Influences Innate Immune Gene Expression Through Splicing.....	87
hnRNP F Mass Spec Reveal Protein Interactions with Core Spliceosome Partners	95
Phosphorylation of hnRNP F influences ISG expression	97
Discussion	98

CHAPTER V GLOBAL ANALYSIS OF HNRNP AND SRSF FAMILY PROTEINS DURING THE INNATE IMMUNE RESPONSE	100
Introduction	100
Results	103
Depletion of hnRNPs Impacts Unique Sets of Innate Immune Genes	106
Depletion of SRSFs Impacts Unique Sets of Innate Immune Genes	107
IPA Analysis Reveals Targeted Pathways In hnRNP and SRSF Knockdowns	108
Reliance on Splicing Factors Does Not Correlate with Expression of <i>Salmonella</i> - Induced Innate Immune Genes	110
Discussion	114
CHAPTER VI MATERIALS AND METHODS.....	116
Cell lines.....	116
RAW 264.7 macrophages.....	116
BMDMs.....	116
Bacterial strains	117
RNA-SEQ.....	117
<i>S. Typhimurium</i> Infection.....	118
LPS Treatment.....	118
Immunofluorescence Microscopy	118
Western Blots	119
siRNA Transfection.....	119
Antibodies	119
Cellular fractionation.....	120
RNase Fractionation	121
Gene Ontology (GO) Canonical Pathway Analysis	121
RNA isolation and qPCR analysis	121
Immunoprecipitations.....	122
Mass Spec Immunoprecipitations	123
<i>M. tuberculosis</i> Infection.....	123
Chromatin Immunoprecipitation	124
FLAG Chromatin Immunoprecipitation.....	125
Alternative Splicing Analysis.....	125
VSV infection.....	126
Quantitation and Statistical Analysis	126
CHAPTER VII CONCLUSIONS	127
REFERENCES	133
APPENDIX A FIGURES.....	172
APPENDIX B TABLES	298

CHAPTER I

INTRODUCTION

Gene Expression and RNA-Processing

The central dogma of biology begins with transcription of DNA to RNA and ends with translation of the RNA into the final gene product of a protein (Figure 1). Thousands of genes are expressed in hundreds of cell types that influences a cell's function and inform its role in an organism. The processes and regulatory mechanisms that occur from DNA to RNA to protein play a crucial role in dictating not only which proteins are present in any cell, but also how much of those specific proteins.

Every minute, thousands of transcripts are produced in one cell. Therefore, the initiation of transcription and subsequent RNA transcript processing is an effective control point for a cell to regulate its proteome. In eukaryotes, this level of regulation is possible due to the presence of a nucleus in which both transcription and RNA processing occur. Additional RNA processing and translation mechanisms occur separately in the cytoplasm. While prokaryotes have express genes via simultaneous transcription and translation, meaning the translation of a transcript starts before the transcription event is complete¹. Eukaryotic transcripts are more complex, and the majority of the transcribed RNA does not encode for protein translation. To generate a protein coding RNA, these intervening sequences of nucleotides, called introns, need to be removed and protein-coding regions, known as exons, need to be joined together.

This process, known as pre-mRNA splicing, is required to produce mature messenger RNAs (mRNA).

Splicing is not the only RNA processing step that most eukaryotic transcripts endure in the nucleus. Before nascent transcripts can be translated into proteins, they need to undergo 5' capping, cleavage and polyadenylation, and the export into the cytoplasm (Figure 2). Each of these steps in RNA metabolism can impact the final outcome of gene expression, protein production. It is predicted that RNA processing steps such as alternative splicing and alternative polyadenylation account for more than half of the proteome diversity in a cell, with ~95% of all human transcripts produce several distinct mRNAs ².

Pre-mRNA Splicing

In the 1960s and 1970s, RNA regulation became a focus of gene expression studies. RNA processing through splicing was an extremely groundbreaking discovery in the 1970s. Initially, pre-mRNAs were identified to be long heterogenous nuclear RNAs. Examination of adenoviral mRNA at the nucleotide level led to the discovery that processing of pre-mRNA leads to splicing. This discovery began to highlight the extreme complexity RNA as compared to DNA. Splicing regulation of RNA allows many mRNA products and protein products to be produced from a single pre-mRNA. While many initial studies were conducted in yeast and several viral genes, these studies have been replicated in eukaryotic cells and tissues and splicing is now appreciated to be a critical point of regulation for gene expression in virtually all eukaryotes.

The process of splicing is carried out by five small nuclear ribonucleoproteins called snRNPs which, along with other core and peripheral factors, make up a protein complex termed the spliceosome. Virtually all mammalian transcripts contain introns, rendering pre-mRNA splicing a hugely important player in generating a functional transcriptome^{3,4}. Introns are removed by cleavage events facilitated by conserved nucleotide sequences. Generally, these intronic cis-splicing signals begin with a GU at the 5' end (the 5' splice site) and an AG at the 3' end (the 3' splice site), although occasionally these are AU and AC sites, respectively. These nucleotides have been found to be widely conserved and crucial for splicing reactions to occur. The initial step of intron removal is snRNP U1/U1-70K binding within an intron at the 5'SS (Figure 3). Subsequently, proteins known as U2 auxiliary proteins, U2AF1 and U2AF2, bind at the branch point (an adenosine roughly 20-30nt upstream of the 3'SS) and the polypyrimidine tract, respectively, along with the branchpoint binding protein SF1. Together, these proteins then recruit the U2 snRNP and a complex called the tri-snRNA, comprised of U4, U5, and U6 which is positioned at the 5' end of the intron. Components of the U2 snRNP displace SF1 and U2AF and the U6 snRNA displaces the U1 snRNA from the 5'SS, liberating the U4 snRNP from the tri-snRNP. Following release/destabilization of a subcomplex of U2 proteins known as SF3a and SF3b, the spliceosome becomes catalytically active and can carry out the process of intron removal. Following nucleophilic attack of the 5'SS guanine by the branchpoint adenosine, the 5' end of the intron is cleaved from the upstream exon forming a loop structure called the lariat intermediate. With the aid of U5, the downstream exon is

brought into proximity, cut, and ligated to the 3' end of the upstream exon via another transesterification reaction. This releases the lariat intron with U2, U5, and U6 bound. This leads to the final product of an mRNA with exons remaining and all introns removed (Figure 3).

Alternative Splicing

Thousands of transcripts are produced in every cell and many protein isoforms can be made from one single mRNA. The production of functionally diverse protein isoforms occurs via alternative splicing. This accounts for much of the diversity of the mammalian proteome (Figure 4). At the start of 1980, several research studies discovered the existence of alternative splicing in the *IgM* transcript. More recent research suggests that more than 90% of human genes are alternatively spliced and alternative splicing likely accounts for the complexity of organisms with smaller genomes. The consequences of alternatively spliced isoforms can be profound: some events generate proteins that play antagonistic functions to their canonical isoforms, while some isoforms are almost identical in structure and function to the canonical isoforms.

Alternative splicing can be accomplished through a variety of types of splicing events, including exon skipping, intron retention, mutually exclusive exons, alternative first and last exons, decoy exons, and the use of alternative 5' and 3' splice sites. The decisions that drive generation of these different isoforms are made in large part through binding of RNA binding proteins to sequences in the pre-mRNA, at sequences known as

exonic splicing enhancers (ESEs), exonic splicing silencers (ESSs), and intronic splicing enhancers (ISEs) and intronic splicing silencers (ISSs).

RNA-binding proteins (RBPs)

While splicing catalysis itself is carried out via the core components of the spliceosome, RBPs add an incredible amount of specificity and flexibility to the system by inhibiting or enhancing the association of the spliceosome with specific splice sites, introns, or exons (Figure 5). Even though these proteins are thought of as peripheral splicing factors, my research and others has demonstrated their importance in overall gene expression through impacting numerous RNA-processing events.

Many novel RBPs have been identified in recent studies using UV crosslinking of RBPs to RNA and quantitative mass spectrometry. From these experiments, over 800 RBPs were found in HeLa cells and 790 RBPs from HEK293s^{7,8}. RRM (RNA Recognition Motif), KH (K Homology), DEAD box helicase or zinc-finger domains are found in almost all of RBPs identified⁹. The majority of these factors identified fall into mRNA splicing factors or ribonucleoproteins¹⁰. Many RBPs are part of the families of heterogeneous nuclear ribonucleoprotein particles (hnRNPs) or serine-arginine-rich proteins (SRSF proteins), which represent the main groups of RBPs known as auxiliary factors³. hnRNPs and SRSFs interact with the spliceosome to conserve exons, remove introns, and impact overall splicing outcomes.

Although there are exceptions, the association of SRSF proteins with the spliceosome enhances splice site usage, whereas hnRNPs typically induce exon skipping¹¹. SRSF proteins and hnRNPs interact with components of the core spliceosome and,

depending on spatial organization/combinatorial diversity, they can promote exon skipping, exon inclusion, intron retention, etc. Mutations in these factors and subsequent mis-splicing can generate mutant proteins with deleterious activity or transcripts that lack protein-coding potential and become targets for nonsense mediated decay¹²⁻¹⁵.

HnRNPs

One large family of RBPs are the hnRNPs (heterogeneous nuclear RiboNucleoProteins). hnRNPs contribute to many processes of RNA metabolism including transcription where they can bind with transcription factors and RNA polymerase¹⁶. They have also been implicated in export, mRNA stabilization, and translational regulation¹⁷. hnRNPs have been identified in the nucleus and cytoplasm of several different cell types. hnRNPs can bind with transcription factors to enhance or promoter sequences to facilitate transcription. For example, hnRNP RALY can silence gene expression through interacting with transcriptionally active chromatin and when depleted in HeLa cells, causes a global reduction of RNAPII-dependent transcription¹⁸. HnRNP K has also been found to interact with RNAPII machinery¹⁹. These data suggest that while hnRNPs are characterized as RNA-binding proteins, and typically thought of as only binding to pre-mRNA, these factors have numerous functions in regulating gene production and expression.

hnRNP A/B and hnRNP C were the first hnRNPs to be identified in HeLa cells and lung fibroblasts²⁰. Many hnRNPs share general features but differ in domain composition and functional properties. hnRNPs differ in the number of RRM (RNA-recognition motifs) that occur in their protein structures. hnRNP L and hnRNP I have 4

RRMs while hnRNP C has one. Interestingly, hnRNP U does not have a typical RRM at all, rather several acidic (Aspartic and Glutamic Acid) and glycine rich regions ²¹. Most hnRNPs contain an NLS (nuclear localization signal), meaning they are found mostly in the nucleus. However, upon stimulation, post-translational modifications, or recruitment of other RBPs, hnRNPs have also been found to translocate to the cytoplasm ¹⁶. This points to their ability to move with a transcript throughout the cell, depending on the necessary functions an hnRNP is responsible for with a specific transcript. For example, many RNA processing events that occur in the cytoplasm, like NMD and translation, have been found to be regulated by hnRNPs ^{16,22}. hnRNPs also assist in nuclear export of mRNAs and have 3' and 5' UTR binding capabilities that control translation. Further UV crosslinking studies identified additional hnRNPs that bound to HeLa cell mRNA and uncovered that these binding capabilities can change from nuclear to cytoplasmic mRNA and binding depends on distinct nucleotide sequences ²³. Therefore, the export of mRNA requires dynamic interactions with RBPs and these binding capabilities are dependent on the step of RNA-processing, as hnRNPs that are needed for splicing may not be needed for translation, and vice-versa.

Although hnRNPs have been implicated in a wide variety of processes in RNA metabolism, they are mostly characterized as regulators of pre-mRNA splicing that influence splicing outcomes ²². Many hnRNPs are known to regulate alternative splicing leading to exon skipping or intron retention ¹⁷. hnRNP proteins can interfere with binding of spliceosome machinery or hinder communication between factors bound to different splice sites ¹⁷. More than half of the hnRNP proteins have been directly

implicated in splicing regulation. For example, hnRNP A1 can alter 5' splice site choice and promote exon skipping. Similarly, hnRNP H has been found to be a splicing inhibitor in several studies where it can bind to exonic splicing silencers and competes with U2AF35 for 3' splice sites. It can also act antagonistically with SRSF1 to influence exon skipping^{17,24,25}. hnRNP A1 and hnRNP F were identified to have similar binding motifs while having opposite functional effects. hnRNP F promotes exon 11 inclusion in the insulin receptor gene, while hnRNP A1 inhibits the inclusion of exon 11²⁶. hnRNP K was also found to influence splicing of *Runx1* through binding exon 6 and acting as a competitor for U2AF65 in 3' splice site usage²⁷. While several hnRNPs have been identified to be critical for splicing regulation in canonical mammalian cell models (generally HeLa), these factors have not been characterized in macrophages or during bacterial infection. Therefore, my project was based around a handful of hnRNPs (C,F,K,M,U) to elucidate their regulation of the innate immune response through splicing changes.

HnRNP M

hnRNP M primarily localizes in the nucleus and has three RRM domains located along the protein²⁸. hnRNP M has been identified as having several roles in the spliceosome and is a peripheral splicing factor with overlapping classification with hnRNP Q due to both having an affinity for poly GU binding motifs (Figure 6)²⁹⁻³². One of the first studies to declare hnRNP M as a regulator of splicing was done in 2007, where Hovhannisyan and Carstens found that it could enhance or silence splicing of alternative exons³³. In their research, overexpression of hnRNP M promoted exon skipping in

FGFR2³³. Numerous studies after this finding identified more predictive functions of hnRNP M as being a splicing repressor, where it influences the removal of exons in several different transcripts such as *Ceacam1*, *D2M*, *Smn1*, *Smn2*, and *Cd44*^{34–36} leading to alternatively spliced isoforms of these transcripts. Additionally, hnRNP M has been identified as a potential biomarker for diseases and cancers like colorectal cancer, prostate cancer, melanoma, aging, and ovarian cancer^{37–41}. Several studies have also implicated hnRNP M in promoting metastasis in breast cancer by competing with ESRP1 (epithelial splicing regulator) for cis-regulatory elements to influence *Cd44* alternatively-spliced isoforms^{42–47}.

hnRNP M has been found to interact with spliceosome proteins and other RBPs^{48,49}. These binding partners have widely been identified in co-regulating alternative splice sites of specific transcripts. One study identified that polypyrimidine tract-binding protein-associated splicing factor (PSF) and several paraspeckle proteins fractionate and immunoprecipitate with hnRNP M⁵⁰. hnRNP M and PSF seem to have opposing roles in this study as hnRNP M promoted exon skipping and PSF favors exon inclusion of a preprotachykinin minigene⁵⁰. hnRNP M also has been identified *ex vivo* to interact with cell division cycle 5-like (CDC5L) and pleiotropic regulator 1 (PLRG1) during the heat-shock response and this interaction is critical to impact alternative splicing of a minigene, adeno-E1A⁵¹. hnRNP M interacts with mTORC2 and influence alternative splicing decisions in the mTOR pathway and can influence muscle cell differentiation^{52,53}. Recent work has shown that hnRNP M interacts with a complex of proteins in neurons including Rbfox and MATR3 and researchers have found enrichment of hnRNP

M motifs nearby Rbfox binding sites⁵⁴. Several studies have found hnRNP M, hnRNP F, MATR3, NONO and SFPQ to interact. SFPQ and NONO have been found to be vital in paraspeckle complexes⁵⁴⁻⁵⁷. These protein interactions and how they are regulated remains unclear.

HnRNP F

The protein structure of hnRNP F is distinct from other hnRNP's because of the lack of conserved RRM. Only hnRNP F and hnRNP H have domains classified as quasi-RRMs (qRRMs) that interact with RNA by wrapping around the G-tract RNA sequence^{58,59}. This also plays into the function of the ability to recognize repetitive sequences in RNA like poly(G) and poly(U) motifs (Figure 6)^{21,29}. Along with the major function of most hnRNPs, hnRNP F has mostly been implicated in regulating alternative splicing. However, with the identification of an NES (nuclear export signal), hnRNP F has also been implicated in other RNA-processing steps including mRNA stabilization and nuclear export. HnRNP F was first characterized in 1992 by Matunis et. al. They found hnRNP F to bind to poly(rG) sequences and have overlapping characteristics with hnRNP H⁶⁰. Through NMR studies, researchers identified specific residues in hnRNP F that are important for interaction with the G-tract of the apoptosis gene, *Bcl-x*, as well as YAP, a transcription activator^{61,62}. Recent studies have identified hnRNP F in mediating mRNA decay through RNA-dependent interaction with TTP and BRF⁶³. hnRNP F can regulate *Snail1* mRNA stabilization during EMT in bladder cancer⁶⁴. hnRNP F has also been found to participate in nucleocytoplasmic shuttling and

import by interacting with import receptors and have transcription-dependent shuttling properties⁶⁵.

hnRNP F has been identified in affecting splicing of dozens of genes including *enox2*, *tpx2*, and fibroblast growth factor 2⁶⁶⁻⁶⁸. Similar hnRNP F-dependent splicing has also been shown in neurons and glia cells of the brain as well as regulation of myelin synthesis⁶⁹⁻⁷¹. Globally, exons that have flanking G-tracts were found to be targets of hnRNP F⁷⁰. Similarly to other hnRNPs, hnRNP F has also been implicated in several cancers such as breast cancer, colon cancer, and bladder cancer^{64,68,72-74}. In research conducted with breast cancer cells, knockdown of hnRNP F, showed an increase in the myeloid cell leukemia-1 (*Mcl-1*) short isoform⁷⁴. Triple knockdowns of hnRNP F, hnRNP K, and hnRNP H1, showed a 30-fold increase in the *Mcl-1* short isoform suggesting synergism between several hnRNPs in regulating splicing⁷⁴. This is not the only finding of cooperation between hnRNP F and other hnRNPs⁷⁵. hnRNP A1 and hnRNP F also work together to alternatively splice exons in the insulin receptor gene²⁶.

Interestingly, qRRMs of hnRNP F have also been found to be important for protein-protein interactions. Human telomerase RNA component (hTERC) was found to interact with hnRNP F via the first qRRM domain and play a role in telomerase activity and length⁷⁶. As mentioned previously, hnRNP F has been found to interact with FOXF3 and TTP and like hnRNP M, hnRNP F was identified in mass spec analysis of immunoprecipitation of paraspeckle proteins, SFPQ and NONO^{64,77,78}. Although widely understudied, researchers have also identified a few post-translational modifications that occur with hnRNP F. For example, in a gastric cancer model, ECD increased cancer

invasion by disabling ubiquitination and subsequent degradation of hnRNP F by ZFP91⁷⁹.

HnRNP C, K, U

Over the course of my studies, I also became interested in several other, generally understudied, hnRNPs. hnRNP C has been associated with splicing, translation, and transcript sorting. hnRNP C recognizes a poly U binding motif in transcripts it regulates (Figure 6)²⁹⁻³². Interestingly, hnRNP C has also been found to form polymers with other hnRNP C proteins. This formation allows more specificity in RNA interactions and enables hnRNP C to sort transcripts for export or retention, depending on their nucleotide length⁸⁰. hnRNP C was also found by Han et al. to promote the translation of *c-myc*, a transcription factor¹⁶. hnRNP A1 and hnRNP C form complexes with exosomal miRNA, dependent upon simulation of hnRNP A2/B1⁸¹. In addition, hnRNP C interacts with spliceosomal proteins through poly-U motifs, but this decreases at later steps suggesting an activation role in early splicing¹⁷. Together, these studies implicate hnRNP C in early gene expression through impacting transcription and splicing processes.

hnRNP K is known to bind to poly C regions (Figure 6) and has been implicated in translational, transcriptional, stability, and splicing regulation. hnRNP K has a unique protein domain called the “KH interaction region”⁸². This region allows hnRNP K to interact with multiple proteins and therefore influence mechanistic function of hnRNP K. In neural cells, hnRNP K and hnRNP E2 were identified to bind to a promoter region and facilitate transcription of the μ -opioid receptor gene in mouse neural cells⁸³. It has

also been found to interact with other splicing factors like hnRNP U, hnRNP L and Srp20, elongation factors of EF-1 α , and transcription factors like HMGB1, Zik1, and Kid1⁸². Similar to hnRNP C, hnRNP K has been found to regulate transcription but this has only been seen in neural cells; thus overall, hnRNP K seems to play more of a role in splicing and transcript stability.

hnRNP U is the biggest hnRNP at 120 kD. hnRNP U binds to regions containing a mixed nucleotide sequence resembling “GGACUGCRRUCGC” (Figure 6)²⁹⁻³². hnRNP U has been characterized in translational and transcriptional regulation as well as splicing and the protein has been shown to bind to ssDNA²¹. Research has shown hnRNP U is required for lncRNA accumulation to facilitate X inactivation⁸⁴. Bi et al. also identified hnRNP U to bind to H19 and this inhibits phosphorylation of RNA Pol II, preventing transcription⁸⁵.

hnRNPs have been characterized in a vast array of disease including cancer, ALS, Alzheimer’s, Fragile X syndrome, and SMA. Despite their importance in chronic disease, hnRNPs have not been described in the context of infection nor have they been previously identified as direct modulators of innate immune outcomes. While these hnRNPs have been studied extensively in the context of binding capability or protein interactions, few studies have identified global gene expression changes that are modulated by hnRNPs via splicing regulation or additional RNA-processing mechanisms.

Post-translational Regulation of hnRNPs

Signaling cascades that activate post-translational modification of hnRNPs are starting to be uncovered. As the most widely studied hnRNP, several studies have identified hnRNP K with several post-translational modifiers. hnRNP K has been shown to bind with several kinases including, ERK1/2, Src, Fyn, PCK, and the methyltransferase, PRMT1⁸². Phosphorylation of hnRNP K by JNK triggers posttranscriptional regulation in axons that assists with cell growth⁸⁶. Furthermore, MKK/p38 stress-signaling can lead to hyperphosphorylation of hnRNP A1. This leads to accumulation of hnRNP A1 in the cytoplasm⁸⁷. Similar results occur with phosphorylation of hnRNP I, where phosphorylation mutants at serine-16 lead to altered cellular localization⁸⁸. Phosphorylation of hnRNP L by CaMKIV kinase also regulates alternative splicing^{89,90}. Finally, phosphorylation of hnRNP U was found as an indicator of DNA damage⁹¹. While the importance of phosphorylation in hnRNP function is clear, the contribution of specific phosphorylation sites to altering hnRNP function are widely understudied.

Arginine methylation has also been identified to occur with hnRNP A1, A2, K and U and SUMO has also been found to modify hnRNP A1, C, K, H, and M¹⁷. While some of these modifications seem to influence hnRNP binding to nucleic acids, the majority of these modifications are less understood and their implications for regulating hnRNPs remain to be identified. Phosphorylation is generally thought to control subcellular localization and protein-protein interactions between these RBPs like hnRNPs⁹²⁻⁹⁷, but the kinases/phosphatases responsible for modifying them and the

conditions under which these modifications are controlled remain poorly understood. Furthermore, little to no research has been done on how cellular activation and bacterial infection can modulate their function through PTMs.

SRSFs

The SR protein family are another set of RBPs that have been implicated in many RNA-processing steps that impact gene expression. These RBPs are characterized by their C-terminal domains that are widely enriched with Serine (S) and Arginine (R) residues. They also have an RRM domain that is typically located near their N-terminal region⁹⁸. As their own expression and regulation varies between cell types, it has been hypothesized that SR proteins play distinct, curated roles in RNA-processing events⁹⁹. This is further supported by research showing that knocking out SRSF1, 2, or 3 in mice is embryonic lethal¹⁰⁰. While they are found primarily in the nucleus and nuclear speckles, SRSF1, SRSF4, SRSF6, SRSF10, SRSF3, and SRSF7 have been found to shuttle and translocate from the nucleus to the cytoplasm^{98,100}. As with many other RBPs, SRSF proteins have been implicated in cancers as by enhancing alternative splicing of protooncogenes^{101–105}. SRSF6 has also been implicated in wound healing where SRSF6-overexpressing mice had stem-cell depletion, mis-regulated splicing, and skin hyperplasia¹⁰⁶. While universally expressed in most cells, these results suggest that there are critical expression levels of expression for SRSFs. Collectively, these data indicate the importance of SRSF proteins to RNA processing events and to overall cell health and viability.

SR proteins play several roles in regulating gene expression (Figure 2). Several SR proteins have been found to associate with RNA polymerase II at the C-terminal domain where transcription factors and RBPs assemble¹⁰⁷. Furthermore, SRSF1 and SRSF3 have been found to bind to Histone 3 and associate with chromatin. Mass spec analysis of H3K9me found SRSF1 and SRSF3 as binding partners, implicating SR proteins in possible roles of epigenetic regulation of gene expression^{108,109}. SRSF2 is a nuclear SR protein that can also be associated with DNA and assists the release of Pol II to mediate transcript elongation^{110,111}. SRSF3 has been found to regulate 3' end processing by polyadenylation with U1 snRNP¹¹². SR proteins have also been shown to influence RNA modifications. Furthermore, SRSF3 and SRSF10 were recently discovered to impact N6-methyladenosine (m6A) RNA modification, where researchers found that the reader protein (YTHDC1) recruited SRSF3 and SRSF10 to modification sites¹¹³. SRSF9 represses ADAR2-mediated editing of *Cflar* and *cyFIP2* in the brain and SRSF9 was found to directly interact with ADAR^{114,115}.

Similar to hnRNPs, most SRSF proteins are located in the nucleus, aligning with their most widely known purpose of influencing splicing decisions in canonical and alternative splicing pathways (Figure 5). Generally, SR proteins recognize ESEs. SRSF proteins have been found to affect 5' splice site selection and enhance splicing activity via ESE binding¹¹⁶. Several studies have discovered SRSF-binding consensus motifs within RNA sequences using SELEX and eCLIP experimental techniques⁹⁸. SRSF1 was identified to bind to purine-rich motifs, whereas SRSF3 was shown to bind to a motif of CAUCA^{30,31,111,117,118,118-120}. SRSF4 has also been observed to bind to purine-rich

regions with poly(A) sequences ^{117,121}. SRSF1 and SRSF2 have been found to have similar binding motifs ¹²² (Figure 6). Interestingly, SRSF proteins seem to be beneficial in promoting co-transcriptional splicing more often than altering splicing outcomes post-transcriptionally ^{107,109}. Overexpression of SRSF1, SRSF2, SRSF7, SRSF5, and SRSF6 were discovered to influence 5' splice site selection and when researchers deleted the RS domain, SRSF1 did not alter 5'SS, suggesting a role for this domain in splice site selection ¹²³.

SRSF1 was the original SRSF protein to be defined and as such, there has been extensive research on the SRSF1-mediated splicing changes which includes *Bcl2l1*, *Bin1*, *Casp2*, *Cd44*, and *Tead1* which play roles in apoptosis, cell adhesion, and transcription ¹⁰⁰. Oncogenic mutations found in SRSF2 have been shown to alter RNA-binding capabilities and splicing, leading to premature termination of transcripts ¹²⁴⁻¹²⁶. Hara et. al. uncovered that SRSF6 alternatively splices *Bim*, leading to *BimS*, which promoted increased apoptosis ¹²⁷. SRSF6 is also upregulated in colorectal cancer samples and regulates *Zo-1* by binding to a SRSF6 motif in exon 23 of the transcript ¹²⁸. Research into age-dependent alternative splicing, has revealed SRSF7 as a major factor in adult isoform production of *Eif4a2* and *Rbm7* ¹²⁹. These RBPs have also been found to regulate splicing of other RBP transcripts. For example, SRSF9 interacts with an intronic element that promotes exon skipping and splicing repression of the hnRNP A1 pre-mRNA ¹³⁰. From my research and others, hnRNPs and SRSFs are found to frequently target and regulate other RBP transcripts. This regulation of many other RBPs has the

capacity to produce an onslaught of direct and indirect splicing changes when a single RBP is eliminated from a cell.

mRNA stability and NMD (Nonsense Mediated Decay) are also mediated by SR proteins. Zhang and Krainer showed SRSF1, SRSF2, SRSF7, SRSF5, and SRSF6 to all influence NMD of the *β -globulin* or *Gpx1*¹²³. Another known function of SR proteins is export of mRNA. SRSF3 and SRSF7 were found to shuttle the *H2a* gene and were found to associate with poly(A) RNA in the cytoplasm¹³¹. SRSF3, SRSF7, and SRS1 were identified to interact with export receptors, NXF1 and TAP, which can be influenced by the phosphorylation status of SR proteins^{95,132,133}. Furthermore, researchers identified SRSF1 regulates stabilization of *Pckl-1* in the cytoplasm by binding to the 3' UTR¹³⁴. Along with NMD or stabilization, SR proteins also have functions in mRNA translation. When researchers overexpress SRSF1, they found increased activity of ribosomes and translational activity or reporter constructs¹³⁵. While SR proteins have been studied in these contexts of resting cells, their contribution to cellular activation gene expression and regulation remains largely undefined.

Post-translational Regulation of SR proteins

Many SR proteins undergo specific PTMs, such as methylation, acetylation, and phosphorylation, that have been widely shown to modulate their function. Proteomic analysis of lysine residues identified acetylation events in SR proteins and SRP kinases and acetylation of SRSF2 resulted in protein turnover^{136,137}. Methylation of SRSF1 has also been described and implicated in cytosolic accumulation¹⁰⁰. Gui et. al. was amongst the first to implicate SR protein phosphorylation in modulating SRSF function

¹³⁸. The SR protein kinases SRPK1, SRPK2, and SRPK3 are highly conserved in eukaryotes and are capable of phosphorylating serines in the RS domains present in all SR proteins ^{138,138,139}. Other SR protein kinases include members of the Clk/Sty family and TOP1 ^{138,140–142}. SRSF1 has also been found to be dephosphorylated by PP1 and PP2A phosphatases ^{143,144}. Hypo-phosphorylation of SRSF1 in the cytoplasm directs SRSF1 into the nucleus where it aggregates in nuclear speckles. Alternatively, hyper-phosphorylated SRSF1 moves to co-transcriptional splicing activation where it is then transitioned back to hypo-phosphorylation, assisting in export of mRNA ¹⁰⁰. Interestingly, although phosphorylation is typically associated with protein activation, SRSF10 can only act as a splicing activator in its dephosphorylated state ^{145,146} suggesting that these proteins may toggle between phosphorylated states to regulate whether or not they can participate in splicing reactions. While these studies begin to elucidate the function of PTMs in RBPs, the dynamics, specificity, and splicing affects these events have on SR proteins remain a major gap in our knowledge of splicing regulation.

The Innate Immune Response

Although humans encounter pathogens like bacteria or viruses every day, we are mostly able to function properly without constantly being sick. Humans, as well as virtually all metazoan organisms, have a multilayered immune system. In vertebrate animals, the immune system can be classified into two types of responses: innate and adaptive. Adaptive immunity is focused on built up defenses based on genetic rearrangements that help the body mount specialized defenses over an individual's

lifetime. Conversely, innate immunity focuses on the initial, non-specific interaction that occurs when a host cell interacts with a pathogen. Innate immunity is a more conserved response across plants, invertebrates, and mammals¹⁴⁷. Innate immune responses are rapid and can be initiated without previous “knowledge” of a pathogen. The bulk of the innate immune response is carried out by the skin, mucous membranes, white blood cells, and various other blood substances. The innate immune system uses germline-encoded receptors to sense pathogen-associated molecular patterns (PAMPs) or nonpathogenic microbe-associated molecular patterns (MAMPs). There are several types of pattern recognition receptors (PRR) including membrane bound receptors like Toll-like (TLR), C-type lectin (CLR), and cytoplasmic receptors of NOD-like (NLR), RIG-I-like (RLR), and DNA sensors^{147,148}. Additionally, innate immunity can also be facilitated through mechanisms that are cell-dependent such as secreted antimicrobial proteins (AMPs), complement, alarmins, cytokines, chemokines, and proteases. Surprisingly, nucleic acids, pathogen components, and diverse pathogens that have entirely different life cycles are recognized by overlapping host PRRs¹⁴⁸.

Toll-Like Receptors

TLRs (Toll-like Receptors) have two subfamilies based on the PAMPs they recognize. TLR1, TLR2, TLR4, and TLR6 can recognize lipid-containing factors and TLR3, TLR7, TLR8 and TLR9 can sense nucleic acids¹⁴⁸ (Figure 7). Alternatively, these TLRs can be grouped based off their cellular location. TLR1, TLR2, TLR4, TLR5, TLR6, and TLR10 are expressed on the cellular membrane while TLR3, TLR7, TLR8, and TLR9 are almost always found intracellularly inside endosomes and lysosomes¹⁴⁸.

These TLRs are capable of directly binding to PAMPs but some also need additional proteins to recognize PAMPs (e.g. MD2 assists TLR4 in sensing lipopolysaccharide (LPS))¹⁴⁸. Additionally, some TLRs are able to sense multiple distinct ligands; TLR4 can recognize LPS, heat shock proteins (HSP), and respiratory syncytial virus (RSV)¹⁴⁸. TLRs can also form heterodimers with each other, such as TLR2 that can bind with TLR1 or TLR6. Historically, gram-negative bacteria are recognized by TLR4 through LPS signaling¹⁴⁹. Alternatively, gram positive bacteria have lipoproteins that are detected by TLR2^{150,151}. Gram-negative and gram-positive bacteria can also activate other TLRs with additional PAMPs, including intracellular TLRs¹⁵². TLR7 and TLR8 are responsible for detection of single-stranded RNA (ssRNA), while TLR3 recognizes dsRNA, both can be identified during viral infection¹⁵³⁻¹⁵⁵. Additionally, TLR9 can recognize CpG DNA that is found in both viruses and bacteria¹⁵⁶. Multiple TLRs can be activated via one pathogen and diverse pathogens can activate the same TLR. For example, *Salmonella enterica* serovar *Typhimurium* can cause signal-transduction through TLR4 (LPS), TLR9 (endosome), and TLR5 (flagellin) and activation of these TLRs is associated with pathogen virulence¹⁵⁷⁻¹⁵⁹.

TLR adaptor molecules lead to differential and specialized responses by the innate immune system. The adaptor protein MyD88 associates with many TLRs, with the exception of TLR3, which primarily uses TRIF (TIR Domain-Containing Adapter Protein Inducing IFN-Beta)¹⁶⁰. Several studies have been conducted to elucidate the mechanisms and kinetics of TLR4 signaling through these adaptor molecules. Knockout studies of MyD88 revealed compensatory mechanisms through other adaptor proteins of

Mal (MyD88 adaptor-like protein), TRIF, TRAM (TRIF-related adaptor molecule), and SARM (sterile alpha- and armadillo motif-containing protein)¹⁶¹⁻¹⁶⁴. Interestingly, TLR2 was found to require Mal to connect to MyD88 whereas TLR4 uses all four of these adaptors (Mal, MyD88, TRIF, & TRAM) to regulate different signal transduction pathways¹⁴⁸. Largely, these signaling cascades are categorized as MyD88-dependent or MyD88-independent. Each of these pathways are capable of activating MAPKs (mitogen-activated protein kinase), NF- κ B, and IRFs (interferon regulatory transcription factor)^{148,165}. However, the specialization of each receptor and its adaptors play a role in which transcriptional immune response is produced. During TLR7 and TLR9 signaling, IRF3 via MyD88 is responsible for producing IFN (Interferon) and ISGs (Interferon-Stimulatory Genes) expression^{148,166}. While in TLR2, TLR4, and TLR5 signaling, MyD88 has been shown to primarily produce proinflammatory gene expression like cytokines^{160,167-169}. Sensing of PAMPs by TLR and MyD88 leads to interactions with IRAK (IL-1R-associated kinase)^{167,168}. IRAK4, IRAK2, and IRAK1 are phosphorylated and associated with TRAF6 (TNF receptor (TNFR) associated factor). TRAF6 functions as an E3 ubiquitin ligase, forms polyubiquitin chains on itself and TAK1 (transforming growth factor-activated protein kinase 1), IKK (I κ B kinase), and NEMO (NF- κ B essential modifier)^{170,171}. Further along the pathway, TAB2 and TAB3 recruit TAK1^{172,173}. This activates two different pathways; IKK and MAPK¹⁷². Activation of the IKK complex starts with phosphorylation of I κ B. I κ B is normally an inhibitor of the IKK pathway, but undergoes degradation and when it is phosphorylated¹⁷⁴. This degradation event leads to NF- κ B translocation to the nucleus and initiates transcription

of proinflammatory genes¹⁷⁴. Alternatively, the MAPK family involves several members such as MKK3, MKK4, MKK6, and MKK7 (MAPK kinase)¹⁷⁵. These phosphorylate p38 and activate JNK (c-Jun N-terminal kinase), ultimately leading to transcription by AP1 (transcription factor activator protein 1)^{176,177}.

Contrarily, TRIF associates with TLR4 and TLR3. TRAM/TRIF signaling cascades can also activate TRAF6 and lead to similar paths of TAK1 and similar transcriptional responses. However, TRIF can also interact with TRAF3 leading to TBK1 phosphorylation of IRF3 and sequential activation of IFN and IFN-inducible genes^{148,163}. This was found when MyD88 knockout mice still had IFN production after exposure to endotoxin and lead to the finding of TRIF^{169,178}. Additional research led to the finding of critical players in the TRIF/IFN response pathway, TBK1 (TANK-binding kinase 1) and IKK ϵ ¹⁷⁹⁻¹⁸¹. These kinases are initiated through TRAF3 and TANK and directly phosphorylate IRF3 and IRF7^{179,181-183}. These phosphorylation events lead to formation of heterodimers or homodimers of IRF3 and IRF7, leading to translocation into the nucleus and activation of IFN production. Interestingly, TRAF3 and TRAF6 play a role in mediating the differential responses of TRIF signaling where TRIF can also signal to NF- κ B activation through TRAF6. TRAF6 binds to TRIF and this leads to recruitment of TAK1. Another adaptor molecule associated with this process is RIP1 (receptor-interacting protein 1). RIP1 is polyubiquitinated and leads to activation of TAK1^{184,185}. TAK1 activation then leads to IKK response and sequential triggering of MAPK and NF- κ B^{179,181}. Additional research has found an enhanceosome that involved NF- κ B, AP1, and IRFs forming a complex which induces IFN gene production¹⁸⁶.

Nucleic Acid-Sensing Receptors

Alongside TLRs, additional PRRs include NOD-like receptors, RIG-I like receptors, and intracellular nucleic acid-sensing receptors. Research has shown additional receptors were required to induce type I IFN (IFN- α and IFN- β) in response to DNA, RNA, or viral infections¹⁸⁷⁻¹⁹⁰. This led to the discovery of several cytosolic PRRs known as RIG-I (RLR) and NOD (NLR) receptors. NOD1 and NOD2 are the most widely characterized NLRs¹⁹¹. These receptors recognize peptidoglycan from bacteria. Where NOD1 primarily recognizes components from gram-negative bacteria, NOD2 can sense molecules produced by both gram-negative and gram-positive bacteria¹⁴⁸. Additionally, a protein complex containing NLR family members, ASC (apoptosis-associated speck-like protein containing CARD (caspase recruitment domain)), and NALP (Nacht LRR protein) was found to activate caspase-1 upon oligomerization through CARD-CARD interactions¹⁹¹. This complex was termed the inflammasome and leads to secretion of IL-1. Each NLR that is included in the different types of inflammasomes that have been identified, plays a role in the ability to recognize different pathogen signals¹⁴⁸. Additionally, AIM2, which is a cytosolic DNA receptor, was also found to interact with inflammasome components¹⁹². Furthermore, the DNA sensors IFI16, IFI204, as well as NLR1, NLR3 and NLR4 can trigger inflammasome activation^{193,194}.

RLRs have a crucial role in sensing RNA in the cytoplasm. RIG-I and MDA5 (melanoma differentiation-associated gene 5) are helicases that are IFN-inducible and part of the RLR family¹⁹⁵. These helicases have CARD domains that are critical in

recognizing RNA and activating the signal-transduction pathway to innate immune transcriptional outputs and antiviral type I IFN production^{148,195,196}. These RLRs have been implicated in regulating signaling of influenza, picornavirus, and norovirus. Furthermore, dsRNA from viruses can also be recognized by PKR (protein kinase R). PKR is a crucial contributor to the antiviral activities through induced IFN and mediating NF- κ B activation that leads to proinflammatory gene expression^{197–199}. Recent data suggests that PKR coordinates with RLR signaling but is not the main contributor to the antiviral defense^{200,201}.

Additional nucleic acid sensors are located in the cytoplasm and can work autonomously of TLR, NLR, and RLR sensing. DAI (DNA-dependent activator of IFN-regulatory factors), otherwise known as ZBP1 (Z-DNA binding protein), was one of the first cytosolic DNA receptors to be identified¹⁴⁸. Since DAI's discovery, several other cytosolic DNA receptors have been identified such as IFI16, DDX41, AIM2-like, and cGAS²⁰² (Figure 7). However, genetic data has convoluted the contribution of other DNA receptors, research has shown that *Cyclic GMP-AMP synthase* (cGAS) is the major contributor to cellular activation and IFN induction²⁰². cGAS was discovered in three separate studies to be the essential enzyme that binds DNA and activates the DNA sensing pathway during viral infection^{203–205}. Additional studies have also identified cGAS to be important in sensing Mtb DNA during infection, as well as being critical for the type I IFN response (Figure 8). Watson & Bell et. al showed cGAS KO BMDMs failed to induce IFN β or ISGs in response to Mtb infection²⁰⁶. In addition to bacterial or viral DNA initiating the type I IFN response, several studies suggest that host mtDNA

(mitochondrial DNA) also contributes to the induction of this response during later time points of macrophage infection and TFAM deficiency (transcription factor A, mitochondrial) ²⁰⁷.

In RLR/NLR sensing of viral dsRNA and ssRNA, RIG-I/MDA5 interacts with the adaptor proteins, MAVS or STING (stimulator of interferon genes) ²⁰⁸. MAVS and STING have been shown to interact with the mitochondrial membrane while STING also has been shown to interact with the endoplasmic reticulum (ER) ^{209–213}. STING is a critical component of nucleic acid signaling cascades that stimulate MAPK activation through several different pathways leading to cytokine, IFN, and ISG expression. Interaction of MAVS and STING leads to recruitment of the E3 ubiquitin ligase TRAF3 and the adaptor protein TANK ²¹⁴. This can lead to NEMO association to TBK1 activation and phosphorylation of IRF3 and IRF7 which both induce ISG expression ²¹⁵ (Figure 7). NEMO has also been shown to activate NF- κ B ^{209,215}. Additionally, RNA recognition can lead to activation of PKR, which can trigger TRAF2, p38, IKK α , and IKK β kinase activity leading to NF- κ B initiation and immune gene expression ^{197–199}. Furthermore, TRADD (TNF receptor-associated death domain) can interact with MAVS and lead to downstream activation of NF- κ B and IRF through Caspase 8/Caspase 10 and NEMO/TANK/TRAF3, respectively ^{182,195,196,215–218}. Taken together, each of these signal-transduction pathways can overlap with each other and join at critical components of innate immune signaling cascades, ultimately leading to activation of kinases, ubiquitinates, and gene expression of anti- and pro-inflammatory genes.

Bacterial Response

As mentioned previously, TLR2 plays a crucial role in detecting and initiating innate immune signaling cascades via recognition of cell wall components of gram-positive bacteria. Gram-positive bacteria like *Listeria monocytogenes* can contain peptidoglycan, glycolipid lipoteichoic acid and lipoproteins¹⁴⁸. This has been shown in genetic studies where TLR2 knockout mice show increased susceptibility to infection with *Streptococcus pneumoniae* and *Staphylococcus aureus*^{219–221}. TLR2 can also detect lipoarabinomannan found on *Mycobacteria*¹⁴⁸. Gram-positive bacteria can also activate TLR9 through CpG DNA and NOD2 and NALP1 by peptidoglycan^{222,223}.

Alternatively, the cell wall of gram-negative bacteria contains an outer membrane of LPS and other proteins. The endotoxin LPS is critical for most bacteria's survival. LPS is also known as the most stimulatory PAMPs and can cause endotoxic shock at high concentrations¹⁶⁶. Interestingly, many types of bacteria produce different structural variants of LPS, which can affect virulence and pathogenicity²²⁴. LPS is transferred from bacteria surfaces to MD2, which associates with TLR4, causing oligomerization and recruitment of MyD88 or TRIF activate NF- κ B or IRF signaling cascades, respectively¹⁴⁸ (Figure 9). TLR4 has been shown to be a critical factor for gram-negative bacteria and LPS detection, as well as control of bacterial infection. Mice lacking functional TLR4 were extremely susceptible to infection with *Neisseria meningitidis* and *Salmonella enterica* serotype Typhimurium¹⁴⁹. However, TLR4 is not the only PRR that can detect gram-negative bacteria: peptidoglycan can also stimulate

through TLR2 and NLR receptors and TLR5 is also able to detect flagellin in *Salmonella*, *Legionella pneumophila*, and *Escherichia coli*^{158,225,226}.

RLRs and NLRs can also detect bacterial infections. While TLRs sense through cell surfaces or intracellular vesicles, RIG-I and NODs play an important role in cytosolic detection of PAMPs. NOD1 and NOD2 recognize intracellular bacterial like *Mycobacterium tuberculosis*^{227,227}. This can lead to activation of the NALP3 inflammasome and upregulation of cytokines. In addition, dsDNA released by bacteria is detected by cGAS and signals through the DNA signaling cascades of cGAS/STING/TBK1 axis^{205,206,228} (Figure 8). Regardless of mechanism, each of these receptors induce signal-transduction pathways lead to a transcriptional upregulation of anti- and pro-inflammatory genes which can ultimately influenced innate immune outcomes.

***Salmonella enterica* serovar Typhimurium**

Salmonella, which causes over 1 million infections globally each year is one of the most common foodborne pathogens in the world and a major global cause of diarrheal diseases^{229 230}. The most common dissemination routes are animals and uncooked food. There is increasing importance of these infections due to continued outbreaks, high incidence rates worldwide, and the progression of antibiotic resistant *Salmonella* strains^{231 232}. This increase of antibiotic resistant *Salmonella* strains has led to an increase in mortality of infected patients in some countries²³³. This demonstrates there is a critical need to better understand the defense mechanisms employed by the host so that host-directed therapies can be developed to combat infections. Because of its

global public health relevance, much research has been conducted on the innate immune response to infection with *Salmonella* and other related gram-negative bacteria. There are several different types of subspecies, including the most widely studied, *Salmonella enterica* subspecies serovar Typhimurium (STm). Upon infection, STm initiates complex mechanisms to modulate host cell functions to establish an intracellular niche. Many virulence factors have been identified in STm, including plasmids, adhesion systems, flagella, and type III secretion systems²³⁴. During infection of epithelial cells of the gut, STm uses secreted proteins encoded by SPI-1 (*Salmonella* pathogenicity island-1)^{235,236}. However, this mechanism is slightly different in macrophages, which phagocytose the bacteria. After entry into a host cell, STm can replicate within a *Salmonella*-containing vacuole (SCV) which is composed of the host cell membrane²³⁷. Utilizing a type III secretion system, STm injects effector proteins from a second type III secretion system called SPI-2, that block lysosomal fusion and allows for replication of STm within the host cell^{237,238}. Each of the effectors encoded by SPI-1 and SPI-2 have been found to influence intracellular survival of STm or mediate cell invasion^{239,240}.

Several PRRs detect STm outside and inside host cells including TLR4, TLR2, TLR5, and TLR9 by endotoxins such as LPS and detection via lysosomes²⁴¹ (Figure 10).^{238,242} Upon detection of STm, LPS signals via TLR4 and triggers activation of the NF- κ B and MAPK pathways, leading to the overall production of proinflammatory cytokines, IFN, and ISGs²⁴². Importantly, mice lacking these TLRs are more susceptible to STm infection¹⁵⁷. Knockout of TLR2, TLR4, TLR7, and TLR9 reduced inflammatory responses in host cells and led to an increased susceptibility to STm infection^{243,244}. This

shows how TLRs can play a critical role for pathogen detection by inhibiting extracellular growth of STm through activation of TRIF/MYD88 signaling cascades leading to the production of proinflammatory gene expression. These studies also suggest TLRs are required for STm pathogenicity and increased susceptibility in host cells.

Mycobacterium tuberculosis

Mycobacterium tuberculosis (Mtb) is currently the number one infectious killer in the world. This human pathogen infects over a quarter of the world's population ²⁴⁵. Tuberculosis is spread when an infected individual with active disease coughs, sneezes, or spreads aerosolized droplets that contain the bacterium. These droplets are then inhaled by another individual and the bacterium is carried to the lungs where it is met by alveolar macrophages, one of the first lines of defense against Mtb.

Several different pattern recognition receptors such as TLR2, TLR4, TLR9, and NOD2 can recognize Mtb through PAMPs ^{227,246,247}. Macrophages phagocytize Mtb when it enters the lungs. *Mycobacterium tuberculosis* has five type VII secretion systems, ESX-1 – ESX-5. ESX-1 has been associated with virulence of *Mycobacterium tuberculosis* while ESX-3 has been shown to influence growth ^{248,249}. Once inside a macrophage, Mtb uses its ESX-1 secretion system to secrete ESAT-6. This substrate weakens the phagosome membrane and subsequently allows Mtb proteins and dsDNA access to the host cytosol. This release of dsDNA activates several immune defense pathways such as autophagy, DNA sensing, NOD sensing, and the inflammasome ^{192,203,206,250–253} While there are several DNA sensors that can detect DNA in the cytosol,

cGAS has been identified as the main DNA sensor in macrophages during Mtb infection^{206,253}.

cGAS recognizes Mtb dsDNA and this leads to synthesis of cGAMP (Cyclic guanosine monophosphate–adenosine monophosphate)²⁰⁶. cGAMP is a secondary messenger that binds to and activates STING which activates TBK1. This results in type I IFN and interferon stimulated gene (ISG) expression through the STING-TBK1-IRF3/7 axis (Figure 7& Figure 8). Researchers have found through Mtb infection of STING and NOD1/2 knockouts that STING is required for signaling transduction leading to IFN and ISG production, while NOD1/2 are not. During Mtb infection, type I IFN and selective autophagy are two different outcomes that follow the activation of TBK1^{206,254–256}. Selective autophagy and IFN responses have both been shown to play crucial roles in controlling Mtb infection. Interestingly, autophagy components localize with TBK1 at the Mtb containing autophagosome^{250,257–259}. Genetic studies have shown that ATG5 knockout mice are more susceptible to Mtb infection²⁵⁰. While type I IFN is thought to be antiviral, it has been correlated with negative outcomes for Mtb infection and enhanced Mtb pathogenesis²⁶⁰. When IRF3 is removed from mice and no IFN is produced, mice are more resistant to Mtb²⁵⁰. In addition, IL-1, IL-1R, or MyD88 show critical importance, as knockout mice for these factors are extremely susceptible to Mtb infection^{261–263}. During Mtb infection, DNA sensing leads to two opposing outcomes with one leading to increased susceptibility to Mtb and one leading to selective autophagy of the bacterium. There is a critical need to identify unique components and regulators of these responses to be targeted for host-directed therapies. As antibiotic

treatment and prevention methods are becoming ineffective, characterization of these components will allow for development of novel therapeutics that could activate selective autophagy to increase Mtb destruction while inhibiting the detrimental type I IFN response. The rise of multi-drug resistant tuberculosis is attributed to misuse of antibiotics in which only 56% of treatments are successful²⁴⁵. To be able to identify novel host-directed therapies that may enhance the efficacy of existing treatments, it is critical to understand the molecular interface between pathogens like *Salmonella* Typhimurium and *Mycobacterium tuberculosis* and the host cells they infect.

Innate Immune Response in Macrophages

Once a pathogen enters a host, phagocytes or scavenger cells are the first cells to detect a threat and mount a response. The most effective cells that phagocytize pathogens are macrophages and neutrophils. If a pathogen subverts each of these components and is not cleared, inflammatory cells, defense cells, and complement systems from the adaptive immunity are activated. If the adaptive immune response is prolonged, it can lead to swelling, fever, and potential autoimmune disease²⁶⁴. Prolonged macrophage activation and inflammatory responses can lead to swelling, fever, and autoimmune disease, therefore, it is critical for macrophages and other first lines of defense to eliminate pathogens. In the previous century, macrophages have been identified as critical to understanding innate immunity and abnormalities in their function have been found in cancer, arthritis, cystic fibrosis, and other diseases¹⁴⁷. Their canonical functions include phagocytosis of pathogens, engulfment of dead cells, and production of inflammatory cytokines that signal to other cells there is a threat. Upon

activation by infection or bacterial signal through PRRs, a macrophage mounts an innate immune response that promotes anti-inflammatory mechanisms. Overall, this activation facilitates the phagocytosis of bacteria and dead cells to reestablish the balance of tissue homeostasis. Interestingly, recent studies have contradicted the hypothesis that macrophages do not have “immune memory”, like the adaptive immune system¹⁴⁸. Researchers have found epigenetic reprogramming upon innate immune signaling that establishes innate immune memory and influences innate immune responses to further macrophage activation²⁶⁵.

Transcriptional Response

An essential characteristic of bacterial infection is the ability to promote the induction of a pro-inflammatory gene expression program by engagement of innate immune receptors. When innate immune cells like macrophages sense pathogens, they undergo a massive reprogramming of gene expression. Innate immune gene expression is mostly studied in the context of ligands, receptors, and signaling cascades that lead to the transcriptional output of the immune response mentioned previously. Signaling cascades of TLRs, NLRs, and RLRs ultimately lead to host gene expression that determines that outcome of infection (Figure 7). Some of these innate immune gene's expression are activated within minutes of bacterial or PAMP detection, while others are delayed in their expression. These kinetics may be affected by the signaling pathway, strength of signal, nucleosome remodeling, or RNA polymerase II availability²⁶⁶. Primary response genes include chemokines, cytokines, and other molecules to combat the bacterial infection. Additional transcription factors and signaling molecules are also

considered primary response genes, as they are needed to activate additional secondary response genes²⁶⁷⁻²⁶⁹.

NF-κB and AP1

AP1 is a transcription factor that plays a role in regulating proinflammatory cytokine expression. Interestingly, several members of the AP family of transcription factors have opposing roles. While some are activators of gene expression, some are repressors, similar to the NF-κB family of proteins²⁷⁰. NF-κB is often the dominant transcription factor complex of choice when the innate immune response is activated. It is composed of 5 transcription factors: p50, p52, RelA (aka p65), c-Rel and RelB²⁷¹. In resting cells, these components are inactive. However, when a bacterial signal is sensed by the cell, Iκβ is degraded allowing translocation of NF-κB into the nucleus. This process is almost always activated by IKK and NEMO leading to the phosphorylation and initiation of NF-κB, AP1 of pro-inflammatory cytokines, and IFN response. Depending on host factors, the NF-κB activation cycle can lead to various gene expression. NF-κB is important for transcription of cytokines like *Il-12b*, *Tnf*, *IL-1b*, *Il-10*, *Il-6* as well as apoptosis regulators *Bcl-XL* and *IAPs*, and cyclin growth factors such as *Mcsf*^{272,273}. Cytokines like *Il-6* play a significant roles in the pathogenesis of bacterial infections²⁷⁴. Interestingly, inhibitory Iκβ genes are also transcribed by NF-κB, representing a powerful negative feedback loop of NF-κB activation and regulation of immune gene expression²⁷².

IRFs and STATs

IRF and STAT (Signal Transducer and Activator of Transcription) are additional key transcription factors activated by innate immune signaling cascades. The IRF family of transcription factors contains IRF 1-9. Upon activation these IRFs form hetero- or homo-dimers, and bind to the IFN regulatory element or ISRE (IFN-stimulated response element) ²⁷⁵. IRF proteins contain several possible phosphorylation sites that are needed for activation. Phosphorylation at serine 386 for IRF3 or serine 477 and 479 on IRF7 are have been found to represent the main activation sites ²⁷⁶. Activation of type I IFN, IFN β , by IRF3/IRF7 has been studied thoroughly ²⁷⁵. Assembly of IRF3/IRF7 homo- and heterodimers and other transcription factors like AP1 and NF- κ B, forms the enhanceosome which allows for *Ifnb1* gene transcription ^{186,277}. Importantly, NF- κ B can assist with production of *Ifnb1* transcription, however, IRFs have not been found to take part in proinflammatory gene expression ²⁷⁸. After *Ifnb1* is transcribed, it is then released from the cell. Detection of IFN β in the extracellular space is accomplished by the IFN α/β receptor (IFNAR1) ²⁷⁹. Once IFNAR1 is activated, JAK1/TYK2 kinases recruit and phosphorylate STAT1/STAT2 dimer (signal transducer and activator of transcription), which assembles with IRF9 to form the IFN-stimulated gene factor 3 (ISGF3) complex ²⁷⁹⁻²⁸¹. Finally, this ISGF3 complex translocates into the nucleus and binds IFN stimulated response elements (ISRE) to induce expression of hundreds of IFN stimulated genes (ISG) such as *Isg15*, *Isg20*, *Irf9*, *Irf7*, and *Ifit1* (Figure 7, Figure 9, & Figure 10) ²⁷⁹⁻²⁸¹. Transcription of these ISGs is specific to the type I IFN response, as typically STAT proteins initiate transcription at Gamma activated sequence (GAS)

elements²⁸². Ultimately transcription of this response results in a positive feedback loop through the IFNAR receptor that further amplifies the Type I IFN response²⁸³.

Researchers are continually uncovering the importance of cytokines and ISGs in controlling bacterial infection and their regulation before transcription is widely appreciated. However, less is known about the post-transcriptional regulation of these factors during the innate immune response.

Post-transcriptional Response During Innate Immunity

Although much research has been conducted on the transcriptional innate immune response mounted by host cells following bacterial infection, very little is known about how the host regulates innate immune gene expression post-transcriptionally. Such a simplification neglects the dynamic processes that a transcript goes through before translation occurs^{12,284}. Regulation of post-transcriptional events has been majorly overlooked in the context of the innate immune response and includes mechanisms of regulation through several RNA-processing, translational events, as well as post-translational modifications of proteins. Understanding how each step in gene expression is regulated is critical for us to fully appreciate how the host immune response is shaped following infection. My project aims to challenge the paradigm of transcription as the primary regulatory checkpoint for macrophage innate immune activation.

Previous reports have shown several alternative pre-mRNA processing events that occur during bacterial infection in dendritic cells and macrophages¹². While some of those genes are housekeeping genes, others play a critical role in cellular defense.

Furthermore, LPS and IFN treatment of monocytes causes specific changes in terminal exons that have differential poly(A) sites leading to shortening of 3' UTRs¹². Alternative polyadenylation can occur within numerous sites on a transcript including exons and introns as well as UTRs. The polyadenylation of a last exon can shorten or extend a transcript's 3' UTR, whereas alternative polyadenylation within an intron can produce a transcript that leads to a truncated protein. TLR1-7 have also been shown to have two to four alternative polyadenylation sites²⁸⁵. Furthermore, the factor CSTF2, which utilizes weak polyadenylation sites, has increased protein expression upon LPS treatment in macrophages²⁸⁶. Poly(A) tails can also be differentially added to *TNF- α* and *Ccl5* (*Rantes*) transcripts following LPS treatment triggering their translation.^{287,288}.

The NXF1-NXT1 export complex is responsible for mRNA export of the majority of poly(A) mRNA²⁸⁹. CRM1 is also another exportin that mediates nuclear to cytoplasmic location of several mRNAs and snRNPs²⁸⁹. Although mRNA export has not been widely studied in the context of bacterial infection, many viruses disrupt export functions to assist in their own RNA processing. XPO1 (exportin 1) and NXF1 (nuclear export factors I) were identified by studying viral RNA and can inhibit or promote viral export and trafficking²⁸⁹. After export of a transcript, decisions are made by the cell to stabilize the mRNA for translation or send for destruction.

mRNA stability and decay are additional processes that can also be regulated during innate immunity. Metabolic labeling of RNA has shown that when cells are treated with immune agonists, the duration of inflammatory responses depends on the rate of RNA decay of dozens of immune transcripts^{290,291}. Several proteins have been

identified in regulating RNA turnover during innate immune responses, including TTP, HuR, BRF1, KSRP, HNRNPD, and HNRNPL^{12,292-294}. In a study looking at TTP, *Tnfa* mRNA stability was decreased when TTP was bound to the ARE (AU-rich element) of *Tnfa*. This study also found that when *TNFA* has increased expression, TTP expression also increases, demonstrating a feedback loop that will downregulate the inflammatory cytokine response and resolve prolonged inflammation^{292,295}. TTP has also been found to destabilize several other important infection modulators like *Il6*, *Inos*, *Ccl2*, *Ccl3*, and *Il10*²⁹⁵⁻²⁹⁷. Like TTP, ZC3H12A has also been shown to affect inflammation, whereby ZC3H12A knockout mice were shown to increase immunoglobins and hyperresponsive macrophages²⁹⁸. ZC3H12A destabilizes immune transcripts like *Il6* and *Il12-p40* by cleaning specific sites within the 3' UTR as an endonuclease²⁹⁸. Contrarily, ZCCHC11 has been found to bind to similar regions of *Il6* mRNA to stabilize the transcript²⁹⁹. These mechanisms of mRNA decay and stability are mechanisms that a host can modulate to promote survival during infection or could help a bacterium circumvent these host responses.

miRNA, ncRNAs, lncRNAs, also contribute to post-transcriptional regulation of gene expression during innate immune activation³⁰⁰. In combination with RISC (RNA-induced silencing complex), or acting on their own mechanisms with additional proteins, these ncRNAs can target transcripts by forming hairpin structures to bind to specific regions of a transcript. For example, MiR-146 has been shown to target *Irak1* and *Traf6*, both critical players in the innate immune response signaling cascade^{300,301}. LncRNAs have also been recently identified to regulate immune gene expression. Carpenter et. al

found lincRNA-Cox2 to be a major component in macrophages for regulation ISGs³⁰².

In cooperation with hnRNPA/B and hnRNPA2/B1, lincRNA-Cox2 was shown to be essential for expression of *Il6* and 700 additional secondary response genes³⁰².

LncRNAs have also been found to act as targets for miRNA to block their attachment to target genes and allow for upregulation of gene expression³⁰³.

The final step in RNA-processing is the initiation of translation of mRNA into the final product of a protein. Several components of the mTOR (Mammalian target of rapamycin), eIF (Eukaryotic Initiation Factor), eEF2 pathways play critical roles during innate immunity in finalizing the outcomes of inflammatory mediators. EIF2 is regulated by several kinases that are mediated by different environmental stimuli and dsRNA through PKR. Phosphorylation of eIF2 inhibits global translation³⁰⁴. During TLR activation, eIF2B has been found to be dephosphorylated through the TRIF pathway allowing for translation production of immune response genes. Phosphorylation of eIF4E plays a role in translating *TNF-a* and *Il6* through IRAK2 and IRAK3 signaling³⁰⁵. mTOR can also phosphorylate eIF4E, downstream of TRIF and MyD88 signaling³⁰⁶. Activation of macrophages with LPS has also shown mTOR-dependent phosphorylation of 4EBPs (eIF4E-binding proteins) which activates translation of *Cxcl1*, *Tnfa*, and *Il6*³⁰⁷. During bacterial infection, inactivation of mTOR by rapamycin has been found to promote pro-inflammatory gene expression³⁰⁸.

Pre-mRNA Splicing in Innate Immunity

The main focus of my thesis research is the role of pre-mRNA splicing in dictating innate immune outcomes. Much of this work was originally inspired by

experiments conducted by Bhatt et al. and Pandya-Jones et al., which demonstrated that when macrophages receive immune agonists, there is significant variation in the amount of time it takes for splicing of innate immune transcripts to occur. Some transcripts are processed several hours later or are never fully processed after upregulation of innate immune transcription^{4,309}. Previous studies have shown that innate immune response genes are alternatively spliced upon infection of various pathogens including dengue virus, *Mycobacterium tuberculosis*, *Listeria monocytogenes*, and *Salmonella Typhimurium*³¹⁰⁻³¹³. Critical components of innate immune signaling cascades like TLRs, MyD88, and IRAKs are alternatively spliced with alternative isoforms leading to opposing mechanisms of action^{12,291,314-316}. Several important innate immune molecules that function downstream of pattern recognition receptors, such as MyD88³¹⁷, the interleukin-1 receptor associated kinase 1, IRAK1³¹⁸, and even some of the TLRs themselves (TLR3, TLR4 co-receptor MD2)^{319,320}, are regulated through expression of truncated isoforms that auto-inhibit full-length protein function and dampen inflammatory responses. One of the *Tlr4* transcripts that is alternatively spliced to include an additional exon, contains a premature stop codon. This produces a TLR4 protein without transmembrane and intracellular domains and inhibits LPS signaling³¹⁵. In the case of MyD88, splicing factors like SF3a have been directly implicated in generating the MyD88 short isoform (MyD88-S), which inhibits expression of pro-inflammatory cytokines like *Il6* following LPS treatment. From this alternative splicing, MyD88-S is not able to bind to IRAK4 and mediate NF-κB activation^{15,321}. IRAK1 also has three isoforms that are produced by alternative splicing that lack kinase activity and

can suppress NF- κ B activation^{318,322,323}. Furthermore, TRAM and IRF3 are also alternatively spliced and can promote degradation of the canonical isoform and inhibit transactivation potential, respectively¹². One study also found the RNA sensing adapter MAVS has two spliced isoforms, with the canonical transcript inducing type I IFN production and the short isoform antagonizing the canonical isoform³²⁴. Indeed, many inflammatory mediators seem to encode isoforms with antagonistic activity, likely so that the cell can reduce deleterious inflammation by promoting one isoform over the other.

Little is known about how alternative splicing and pre-mRNA splicing decisions change in response to bacterial infection. Interestingly, in human dendritic cells and macrophages, gene expression of many splicing factors has been found to be upregulated during immune activation^{12,286}. Furthermore, large-scale proteomic datasets looking at phosphorylation changes upon bacterial infection reveal that over 20 splicing factors are differentially phosphorylated upon bacterial infection, strongly suggesting that splicing is regulated downstream of pathogen sensing^{325,326}. With regulation of RNA splicing and potential of pro-bacterial host factors, this widens the targets for host-directed therapy utilizing splicing inhibitors, enhancers, or targeting direct isoforms. My research focuses on how two of these splicing factors, hnRNP M and hnRNP F are regulated by phosphorylations during bacterial infection. Furthermore, I interrogated several members of hnRNP and SR RBPs that were identified from Budzik et. al. and Penn et. al. using bioinformatic analysis to identify their role in regulating the innate immune response

post-transcriptionally^{325,326}. My project is the first to identify PTMs of RBPs and how they influence gene expression regulation.

Post-translational Modifications During Innate Immunity

Post-translational modification of proteins constitutes a major mechanism by which cells regulate protein function, localization, and stability³²⁷. There are myriad PTMs, with the most well-studied being methylation, phosphorylation, ubiquitination, and acetylation. Each of these modifications have been found in PRR-dependent immune responses³²⁷. For examples, the RelA member of the NF- κ B family is modulated by multiple PTMs, including multiple acetylation, phosphorylation, and methylation events²⁶⁶. Methylation of arginine and lysine residues have been shown to impact NF- κ B responses³²⁸. TBK1, MyD88, and TRAF6, have been found to be differentially ubiquitinated, overall leading to inhibition of TLR-signaling³²⁷. STING has also been found to be ubiquitinated by RNF5, promoting its degradation and inhibiting IRF3-transcriptional responses during viral infection³²⁹. Several E3 ligases such as MARCH5, RNF5, AIP4, and SMURF2 can target MAVS for degradation through ubiquitination³²⁹⁻³³¹. Additionally, many deubiquitinating enzymes can inactivate RIG-I³³²⁻³³⁴. Ultimately, phosphorylation has been the most widely studied PTM during the innate immune response. Activation and deactivation of several components of TLR-signaling require phosphorylation including MAPKs, IKK α , IRF3, as well as MAVS, STING, TRIF, and TBK1³²⁷. TBK1, for example, autophosphorylates itself and can phosphorylate IRF3 leading to dimerization and translocation into the nucleus³³⁵. In some instances, phosphorylation of innate immune proteins downregulates

PRR signaling, as is the case for NLRX1, NLRC5, and MST4. For example, MST4 phosphorylates TRAF6, which leads to suppression of innate immune responses³³⁶⁻³³⁸. Two recent publications measured macrophage protein phosphorylation following infection with the intracellular pathogens *Mycobacterium tuberculosis* (Figure 11, Figure 12, & Figure 13)^{325,326} and *Cryptococcus neoformans*³³⁹. From each of these datasets, RNA-processing and splicing machinery were the top protein groups found to be differentially phosphorylated during infection. This data demonstrated that core spliceosome factors like SF3b1 and more peripheral splicing factors such as hnRNPs and SRs are differentially phosphorylated upon infection, suggesting an important role in the regulation of splicing during bacterial infection. Within this group of RBPs, very few have been studied in the framework of innate immunity. From these splicing proteins and RBPs that were differential phosphorylated (Figure 11, Figure 12, & Figure 13), my research honed in on the SR and hnRNP families of auxiliary splicing factors.

We hypothesize that pre-mRNA splicing regulation is a major component of the innate immune response; whereby cells can rapidly respond to pathogens by influencing the efficiency of pre-mRNA splicing of innate immune transcripts by posttranslational modification of RNA-binding proteins. Such changes lead to changes in total gene expression of crucial innate immune transcripts on top of those attributed to transcriptional activation. My experiments have shed light on how alternative splicing is impacted through direct modification of RNA-binding proteins and thus how splicing can influence the innate immune proteome as well. We chose to work with hnRNPs and SRs because: 1) they are known to affect splicing 2) they have significant changes in

their phosphorylation status upon bacterial infection 3) and they may be more easily manipulated than core splicing factors. These peripheral proteins can modulate splicing, but not necessarily impair it all together, so that cells can remain healthy. My initial research focused on hnRNP M with additional preliminary studies on hnRNP F. Finally, I took an unbiased bioinformatic approach to look more globally at how hnRNP and SRSF proteins differentially contribute to innate immune responses during bacterial infection.

CHAPTER II

THE SPLICING FACTOR HNRNP M IS A CRITICAL REGULATOR OF INNATE IMMUNE GENE EXPRESSION IN MACROPHAGES*

Introduction

When innate immune cells like macrophages sense pathogens, they undergo a massive reprogramming of gene expression. Although innate immune gene expression is mostly studied in the context of transcriptional activation, multiple lines of evidence support a crucial role for pre-mRNA splicing regulation in shaping the macrophage transcriptome. For example, when primary mouse macrophages are treated with a TLR4 agonist, individual transcripts show significant variation in the time it takes for them to be fully spliced, with some pre-mRNAs remaining unprocessed for hours after transcriptional activation^{4,309}. Likewise, computational analyses of human primary macrophages reveal a robust increase in mRNA isoform diversity and a global preference for exon inclusion following lipopolysaccharide (LPS) treatment or *Salmonella enterica serovar* Typhimurium infection³¹⁰. The production of functionally diverse protein isoforms via alternative splicing is also known to influence innate immune responses. Several important innate immune molecules that function downstream of pattern recognition receptors, such as the TLR adaptor protein MyD88³¹⁷, the interleukin-1 receptor associated kinase 1, IRAK1³¹⁸, and even some of the TLRs themselves (TLR3, TLR4 co-receptor MD2)^{319,320}, are regulated through expression of truncated isoforms that auto-inhibit full-length protein function and

dampen inflammatory responses. In the case of MyD88, splicing factors like SF3a have been directly implicated in generating the MyD88 short isoform (*Myd88-S*), which inhibits expression of pro-inflammatory cytokines like interleukin-6 (*Il-6*) following LPS treatment^{15,321}.

To date, only a handful of RNA-binding proteins (RBPs) have been studied in the context of the innate immune response. For example, TLR4 signaling via LPS treatment promotes the shuttling of hnRNP U (heterogeneous nuclear ribonucleoprotein particle U) from the nucleus to the cytosol, resulting in differential expression of several innate immune cytokines (TNF- α , IL-6, IL-1 β) via hnRNP U-dependent stabilization of cytosolic mRNAs³⁴⁰. Tristetraprolin (TTP), human antigen R (HuR), T cell intracellular antigen 1-related protein (TIAR), and hnRNP K have also been implicated in controlling gene expression in LPS-activated macrophages, with TTP and HuR regulating mRNA decay and TIAR and hnRNP K causing translational repression^{92,293,294,341}.

Phosphorylation is generally thought to control subcellular localization and protein-protein interactions between these RBPs⁹²⁻⁹⁷, but the kinases/phosphatases responsible for modifying them and the conditions under which these modifications are controlled remain poorly understood.

Two recent publications measured macrophage protein phosphorylation following infection with the intracellular pathogens *Mycobacterium tuberculosis*^{325,326} and *Cryptococcus neoformans*³³⁹. Intriguingly, a substantial number of these differentially phosphorylated peptides were derived from splicing factors. In fact, “spliceosome” was the top over-represented phosphorylated pathway in *C. neoformans*-

infected cells, suggesting that post-translational modification (PTM) of splicing factors is critical for controlling innate immune responses to pathogens. One of the proteins that was significantly differentially phosphorylated in each of these datasets was hnRNP M. hnRNP M is a splicing factor and RBP that has been repeatedly implicated in cancer metastasis and muscle differentiation^{37,42,45,52,53}. Its role in regulating innate immune gene expression in macrophages is unknown, although interestingly, it has also been found to influence dengue virus replication³⁴², suggesting a role in antiviral responses.

Here, we demonstrate that abrogating hnRNP M expression in a macrophage cell line leads to hyperinduction of over 100 transcripts following distinct innate immune stimuli, including infection with the gram-negative bacteria *Salmonella enterica serovar* Typhimurium, treatment with TLR2 and TLR4 agonists, and transfection of cytosolic dsDNA. While our data reveal that hnRNP M co-transcriptionally represses gene expression by influencing both constitutive and alternative splicing decisions, regulation of hnRNP M's function via phosphorylation at S574 specifically controls the protein's ability to inhibit intron removal of innate immune-activated transcripts. Consistent with its role in downregulating macrophage activation, macrophages lacking hnRNP M are better able to control viral replication, emphasizing the importance of pre-mRNA splicing regulation in modulating the innate immune response to infection.

Results

RNA Sequencing (RNA-Seq) Analysis Reveals Immune Response Genes Are Regulated by hnRNP M during *Salmonella* Infection

To investigate a role for hnRNP M in regulating the innate immune response, we first tested how loss of hnRNP M globally influenced macrophage gene expression. Stably selected, constitutive hnRNP M KD cell lines were generated by transducing RAW 264.7 mouse macrophages with lentiviral shRNA constructs designed to target hnRNP M or a control SCR shRNA. Western blot and qRT-PCR analysis confirmed ~80% and 60% knockdown of hnRNP M using two different shRNA constructs (KD1 and KD2, respectively) (Figure 1A). Because several attempts to knock out hnRNP M in RAW 264.7 macrophages by CRISPR/Cas9 gRNAs resulted exclusively in clones with in-frame insertions or deletions, we concluded that hnRNP M is essential in macrophages and continued our experiments using the viable knockdown cell lines. We next performed RNA-seq analysis on total poly(A)+ selected RNA collected from uninfected and *Salmonella* Typhimurium infected cells (MOI = 10) at the key innate immune time point of 4 h post-infection, at which time transcriptional activation downstream of both MyD88 and TRIF adapters would be expected³⁴³. Using CLC Genomics Workbench, we identified a number of genes that were differentially expressed in uninfected hnRNP M KD cells compared to SCR control cells, with 391 genes upregulated and 174 downregulated (Figure 1B). Looking specifically at transcripts with a fold change of $> \pm 1.5$ ($p < 0.05$), we observed similar numbers of impacted genes in uninfected hnRNP M KD and SCR macrophages (Figure 1C) and

those infected with *Salmonella* (Figure 1D). The ratio of upregulated (blue) and downregulated (red) transcripts was also quite similar between the two conditions and consistent with previous reports of hnRNP M repressing pre-mRNA splicing^{33,50}. Interestingly, we observed only 25% overlap between genes that were differentially expressed in uninfected and *Salmonella*-infected macrophages, suggesting that hnRNP M has distinct modes of operation depending on the activation state of a macrophage (Figure S1A). Unbiased canonical pathways analysis revealed strong enrichment for differentially expressed genes in innate immune signaling pathways in *Salmonella*-infected hnRNP M KD cells (Figure 1E), and manual analysis of these lists revealed a number of important chemokines (e.g., *Cxcl16*, *Ccl17*, *Ccl2*, *Ccl7*), antiviral molecules (e.g., *Isg15*, *Mx1*, *Rsad2*), and pro-inflammatory cytokines (e.g., *IL6*, *Mip1a* [*Ccl3*], *IL18*) whose expression were dramatically affected by loss of hnRNP M (Figure 1F). Additional pathways enriched for hnRNP M-dependent genes can be found in Figures S1B and S1C, and a list of all impacted genes (± 1.5 -fold change) can be found in Table S1.

To validate the RNA-seq gene expression changes, we used qRT-PCR to measure transcript levels of genes from both lists (uninfected SCR versus hnRNP M KD and *Salmonella*-infected SCR versus hnRNP M KD). We confirmed overexpression of several genes in uninfected hnRNP M KD cells (*Rnf26*, *Rnf128*, *Slc6a4*; Figure 1G), as well as hyperinduction of transcripts in hnRNP M KD cells at 2 and 4 h post-*Salmonella* infection (*IL6*, *Mx1*, *Gbp5*, *Adora2a*, and *Marcks*) (Figures 1H and S1D). Importantly, induction of other pro-inflammatory mediators such as *IL1 β* and *Tnfa* did not rely on

hnRNP M (Figure 1I), suggesting that hnRNP M's ability to regulate gene expression is conferred by specificity at the transcript level, rather than being common to a transcriptional regulon (e.g., NF- κ B, IRF3, STAT1). Together, these results reveal a previously unappreciated role for hnRNP M in repressing specific innate immune transcripts in macrophages.

hnRNP M Regulates a Specific Subset of Innate Immune Genes upon Treatment with Diverse Innate Immune Stimuli

Salmonella encodes several PAMPs that serve as potent activators of pattern recognition receptors. *Salmonella* can also activate pro-inflammatory gene expression via its virulence-associated type III secretion system³⁴⁴. To begin to determine the nature of the signal through which hnRNP M-dependent gene expression changes occur, we first tested whether LPS, a potent agonist of TLR4¹⁴⁹ and component of the *Salmonella* outer membrane, was sufficient to hyperinduce *IL6* expression in hnRNP M KD macrophages (Figure 2A). Similar to *Salmonella* infection, we observed a 3- to 4-fold hyperinduction of *IL6* in hnRNP M KD cells treated with 100 ng/mL LPS (from *E. coli*) for 2 and 4 h, confirming that hnRNP M acts downstream of TLR4 activation (Figure 2B). Importantly, hyperinduction of *IL6* mRNA in both LPS-treated and *Salmonella*-infected hnRNP M KD macrophages increased IL-6 protein levels 3- to 6-fold (Figure 2C), indicating that hnRNP M repression of *IL6* mRNA processing impacts protein outputs in a biologically meaningful way. We believe hnRNP M mainly functions to repress *IL6* expression early in macrophage activation, as we did not observe statistically significant differences in *IL6* mRNA levels between SCR and

hnRNP M KD at later time points (6 h) post-LPS treatment (Figure S2B), and this trend generally held for several other hnRNP M-dependent transcripts (Figure S2B). We did not observe any significant changes in hnRNP M protein expression over the same time course of LPS treatment (Figure S2C) nor did we observe significant differences in I κ B α degradation over a course of LPS treatment in hnRNP M KD versus SCR control cells (Figure S2D), demonstrating that signaling downstream of TLR4 activation is intact in the absence of hnRNP M. Consistent with our RNA-seq and qRT-PCR data from *Salmonella*-infected cells, *Mx1*, *Gbp5*, and *Marcks* were hyperinduced in hnRNP M KD cells after LPS treatment at 2 and 4 h (Figure 2E; Figure S2A), while *IL1 β* (Figure 2D) and *Tnfa* (Figure S2A) showed no changes in expression after LPS treatment in hnRNP M KD versus SCR control cells, despite both transcripts being tremendously upregulated. Rather than being activated by NF- κ B, transcription of *Mx1* and *Gbp5* occurs via STAT1 downstream of interferon (IFN)- β signaling, following IFN- β expression via the TRIF/IRF3 axis (Figure 2L). These results hinted at a mechanism for hnRNP M-dependent repression that is independent of transcription factor specificity and is instead dependent on individual transcripts.

In order to confirm that hnRNP M's ability to regulate innate immune gene expression was not unique to RAW 264.7 macrophages, we used siRNAs to knockdown hnRNP M in primary mouse bone marrow-derived macrophages (BMDMs) for 72 h, alongside negative control (designed to not target anything) and positive control (designed to target GAPDH) siRNAs (Figure 2F; Figure S2E) and treated these macrophages with LPS. Because BMDMs are incredibly responsive to innate immune

agonists, we used two different concentrations of LPS, 100 ng/mL (same as in the RAW 264.7 experiments) and 10 ng/mL. In both cases, hnRNP M siRNA KD in BMDMs recapitulated the phenotype that we observed in the RAW 264.7 KD macrophages, i.e., hyperinduction of *IL6* (Figures 2G, 100 ng/mL, and 2H, 10 ng/mL), albeit with slightly different kinetics and dose responses than we observed in the RAW 264.7 cell line. Importantly, we also measured hyperinduction of *Gpb5*, *Mx1*, and *Adora2a* and no change in *Tnfa* or *IL1β* (Figures 2I, 2J, and S2F) in hnRNP M siRNA KD cells, consistent with our results in the macrophage cell line. Together, these results argue for hnRNP M playing a crucial, conserved role in innate immune gene expression in both primary murine macrophages and murine macrophage cell lines.

To more directly test the idea that hnRNP M's target specificity is at the level of the transcript itself, we tested whether genes like *Mx1* and *IL6* were hyperinduced in hnRNP M KD RAW 264.7 macrophages treated with a panel of innate immune agonists. Treatment with 100 ng/mL of the TLR2/1 agonist Pam3CSK4 hyperinduced *IL6* expression in hnRNP M KD cells compared to SCR controls (Figure 2K; Figure S2G), while *Tnfa* and *IL1β* mRNA levels remained similar (Figure S2G). Likewise, transfection of hnRNP M KD cells with 1 μg/mL ISD a potent agonist of cytosolic DNA sensing and IRF3-mediated transcription downstream of the cGAS/STING/TBK1 axis¹⁹⁰ (Figure 2L), led to hyperinduction of *Mx1* in hnRNP M KD cells (Figure 2M). *Ifnb* and other IFN-stimulated genes (ISGs) regulated by IRF3 (*Ifit1* and *Irf7*) were expressed at similar levels (Figures 2M and 2N). Direct engagement of the IFN receptor (IFNAR) with recombinant IFN-β also resulted in *Mx1* hyperinduction in hnRNP M KD cells

(Figure 2O). Collectively, these results bolster a model whereby hnRNP M represses mRNA expression of a specific subset of innate immune genes, regardless of how those genes are induced.

hnRNP M Influences Gene Expression Outcomes at the Level of Pre-mRNA

Splicing

Because previous studies of hnRNP M have shown that it can enhance or silence splicing of alternatively spliced exons^{33–35,51}, we first asked whether loss of hnRNP M could specifically influence constitutive intron removal and/or alternative splicing in LPS-activated macrophages. We chose *IL6* as a model transcript because (1) it has a simple intron-exon architecture with four relatively short introns (165, 1,271, 3,059, and 1,226 nucleotides, respectively); (2) it was robustly hyperinduced by loss of hnRNP M (Figures 1F and 1H); and (3) it is a crucial component of the macrophage inflammatory response. Using qRT-PCR, we first measured the relative abundance of each *IL6* intron-exon junction (Figure 3A) in SCR control cells to assess how intron removal proceeded on *IL6* pre-mRNAs in cells containing hnRNP M. Primers were designed to only amplify introns that are still part of pre-mRNAs and not released intron lariats. At 2 h post-LPS treatment, most of the *IL6* transcripts we detected were partially processed, with intron 1 and to some extent intron 4 being preferentially removed and introns 2 and 3 being retained (Figure 3B). We then compared the relative abundance of *IL6* introns in SCR control cells to those in hnRNP M KD macrophages and observed a dramatic and specific decrease in intron 3-containing *IL6* pre-mRNAs in the absence of hnRNP M. This decrease in *IL6* intron 3 starkly contrasted other *IL6* intron-exon and exon-exon

junctions, which were overall more abundant in the absence of hnRNP M (Figure 3C). The fact that we observe vastly different amounts of intron 2 and 4-containing *IL6* pre-mRNAs compared to intron-3-containing *IL6* pre-mRNAs in hnRNP M KD macrophages speaks against hnRNP M impacting *IL6* expression transcriptionally and instead argues strongly for the protein playing a role in *IL6* pre-mRNA processing. These data demonstrate that *IL6* pre-mRNAs accumulate in the absence of hnRNP M and suggest that *IL6* intron 3 plays a privileged role in dictating the maturation of *IL6* mRNAs. Specifically, we propose that retention of intron 3 serves as a rate-limiting step in *IL6* pre-mRNA processing so that in the absence of hnRNP M, when *IL6* intron 3 is removed more efficiently, higher levels of mature *IL6* mRNA are made (Figures 1F, 1H, and 2B). Consistent with a role for hnRNP M in controlling splicing specifically, we did not observe any significant differences in the stability of *IL6* mRNAs in hnRNP M KD macrophages compared to SCR controls following a time course of Actinomycin D treatment (Figure S3A). We next wanted to explore whether loss of hnRNP M also influenced alternative splicing in uninfected and *Salmonella*-infected macrophages. To do so, we employed an algorithm for LSV analysis called MAJIQ³⁴⁵. MAJIQ allows identification, quantification, and visualization of diverse LSVs, including alternative 5' or 3' splice site usage and exon skipping, across different experimental conditions. MAJIQ identified a total of 94 LSVs in uninfected SCR versus hnRNP M KD macrophages and 67 LSVs in *Salmonella*-infected SCR versus hnRNP M KD macrophages (probability [$|\Delta \text{PSI}|, \geq 20\%$], $>95\%$) (Figure 3D). The vast majority of the LSVs identified in SCR versus hnRNP M KD cells were exon skipping events

(Figure 3D). Subsequent visualization of these LSVs by Voila analysis revealed that loss of hnRNP M generally correlated with increased exon inclusion in both uninfected and *Salmonella*-infected macrophages. In other words, the presence of hnRNP M led to more exon skipping, which is consistent with a role for hnRNP M in splicing repression. We also conducted IPA pathway analysis of alternatively spliced transcripts to identify pathways enriched for hnRNP M-dependent changes. In contrast to our global gene expression IPA analysis, we observed no enrichment for genes in innate immune-related pathways in either uninfected or *Salmonella*-infected macrophages (Figure 3E). In fact, only 3 transcripts had both significant expression changes (via RNA-seq) and significant delta PSI changes (via MAJIQ), suggesting that hnRNP M's role in influencing steady-state gene expression of innate immune transcripts is distinct from its role in controlling alternative splicing decisions (Figure S3B). Interestingly, the greatest number of splicing changes were induced by *Salmonella* infection itself (Figure S3C), consistent with previously published datasets^{310,311}.

Mx1, an anti-viral GTPase, was one of the three transcripts significantly impacted by loss of hnRNP M at the levels of gene expression (Figures 1F and 1H) and alternative splicing (Figure 3F). Specifically, MAJIQ identified an exon inclusion event of *Mx1* "exon 9" that was significantly more frequent in hnRNP M KD uninfected macrophages versus SCR control uninfected macrophages (delta PSI exon 8-exon 9 = 0.703 versus exon 8-exon 10 = 0.298) (Figure 3G). Inclusion of this exon 9 introduces a premature stop codon and exon-9-containing transcript isoforms of *Mx1* are annotated as nonsense-mediated decay targets. Together with our RNA-seq analysis, these results

suggest that the overall abundance of *Mxl* protein may be regulated by hnRNP M at multiple post-transcriptional processing steps, i.e., bulk transcript abundance and proportion of functional protein-encoding transcripts. MAJIQ also reported increased exon inclusion events for *Commd8*, a putative transcriptional regulator, and *Nmt2*, an N-myristoyltransferase. We confirmed each of these LSVs by semi-quantitative RT-PCR (Figures 3H, 3I, and S3D). Collectively, these data illustrate that hnRNP M can repress splicing of both constitutive and alternative introns, leading to distinct transcript and protein expression outcomes in macrophages.

hnRNP M Is Enriched at the Level of Chromatin and at the IL6 Genomic Locus

To get a better understanding of how hnRNP M controls pre-mRNA splicing, we next asked where hnRNP M localizes in RAW 264.7 macrophages and whether its localization changed upon TLR4 activation. Other hnRNP family members have been found to translocate to the cytoplasm in response to several different types of stimuli including VSV infection, osmotic shock, and inhibition of transcription^{93,346,347}, and hnRNP U has been shown to shuttle out of the nucleus following LPS treatment of macrophages³⁴⁰. Based on our data implicating hnRNP M in splicing, we predicted that it can function in the macrophage nucleus and indeed, several algorithms including NLS Mapper³⁴⁸ and PredictProtein³⁴⁹ predicted hnRNP M is a predominantly nuclear protein (NLS Mapper score 8.5/10; PredictProtein 98/100) (Figure 4A). To examine hnRNP M localization, we performed immunofluorescence microscopy in uninfected macrophages using an anti-hnRNP M antibody and observed significant nuclear enrichment (Figure 4B) with no major changes over a 2 h time course of LPS treatment (Figure 4C). This

was true for endogenous hnRNP M and a 3xFLAG-hnRNP M allele stably expressed in macrophages (Figure S4A). As a control, we monitored the translocation of hnRNP U upon LPS treatment and observed nuclear to cytoplasmic translocation, consistent with previous reports (Figure S4B). Based on these results, we concluded that hnRNP M is a nuclear protein in macrophages and that LPS treatment does not trigger translocation to another cellular compartment.

We next sought to understand more precisely where in the nucleus hnRNP M was enriched since intron recognition and removal can occur at the level of chromatin, while nascent transcripts are still tethered to RNA polymerase II^{309,350–352}. To this end, we performed a cellular fractionation experiment in RAW 264.7 macrophages over a time course of LPS treatment and visualized hnRNP M localization via western blot (Figure 4D). We observed hnRNP M in both the nucleoplasm and the chromatin over the course of LPS treatment, while no hnRNP M was detectable in the cytoplasmic fraction. Macrophages stably expressing 3xFLAG-hnRNP M showed a similar hnRNP M distribution between the nucleoplasm and chromatin (Figure S4C). We did not observe significant redistribution of either endogenous or 3xFLAG-hnRNP M between the nucleoplasm and chromatin fractions upon LPS treatment (Figures 4D and S4C). Residual hnRNP M protein expressed in KD cell lines was similarly distributed between the chromatin and nucleoplasm (Figure S4D). Together, fractionation and immunofluorescence experiments confirmed that a population of hnRNP M associates with chromatin, and the protein does not grossly redistribute in the cell upon LPS treatment.

hnRNP M's Association with the *IL6* Locus Is RNA Dependent and Controlled by TLR4 Signaling

We next wanted to determine whether hnRNP M's association with chromatin was specific for the genomic loci of genes whose regulation was impacted by hnRNP M (Figure 1F). We hypothesized that, if hnRNP M repression of *IL6* intron 3 removal occurs at the nascent transcript level, then hnRNP M may associate with the *IL6* genomic locus. To test this, we performed ChIP-qPCR. ChIP has been used extensively in yeast and to some extent in mammals as a spatiotemporal read out of splicing factor recruitment to nascent transcripts^{350,353–356}. Endogenous hnRNP M was immunoprecipitated from untreated macrophages, and association with the *IL6* locus (DNA) was determined using a series of tiling primers spaced approximately 500 bp apart (Figure 4E). We observed no enrichment of hnRNP M in the promoter region of *IL6*, consistent with it playing a mainly post-transcriptional role in *IL6* processing (Figure 4F, primer set 1). We did, however, observe significant enrichment of hnRNP M at several primer sets in the *IL6* gene, most notably over the intron 2-intron 3 region (Figure 4F, primer sets 3–5). Previously published cross-linking immunoprecipitation (CLIP)-seq experiments identified a GUGGUGG consensus site for hnRNP M²⁹; such a site exists in intron 2 of *IL6*, and several similar motifs are found in *IL6* intron 3 (Figure S4E). Indeed, of all the transcripts in Figure 1D, >75% of them contain at least one consensus hnRNP M motif in an intron (Table S2). ChIP-qPCR of histone H3, which showed clear depletion of nucleosomes around the *IL6* transcription start site (primer sets 1 and 2), was performed to control for genomic DNA accessibility and/or

primer set efficiency (Figure 4G). Together, these results reveal that hnRNP M can associate with the genomic locus of transcripts like *IL6* whose splicing it represses, suggesting that it functions co-transcriptionally. Importantly, treatment with RNase A shifted hnRNP M from the chromatin into the nucleoplasm (Figure 4H). Likewise, RNase A treatment³⁵⁶ abolished hnRNP M enrichment at the *IL6* genomic locus via ChIP-qPCR as well, confirming that its association with chromatin and the *IL6* gene depends on RNA (Figure 4I).

If hnRNP M acts as a repressor of *IL6* splicing by binding to nascent transcripts at the *IL6* locus, we hypothesized that this repression might be relieved upon TLR4 activation, thus allowing a cell to robustly induce IL-6 expression following pathogen sensing. To test this, we performed ChIP-qPCR of hnRNP M at the *IL6* locus in RAW 264.7 macrophages treated with LPS for 1 h. Remarkably, we observed a complete loss of hnRNP M enrichment at all primer sets along the *IL6* gene body, including those over intron 2 and 3, following LPS treatment (Figure 4J). This result strongly links hnRNP M's ability to repress *IL6* with its presence at the *IL6* genomic locus and suggests that TLR4 signaling controls hnRNP M's repressor activity.

Having demonstrated that hnRNP M's ability to associate with the *IL6* chromatin locus relies on RNA, we were curious to see whether hnRNP M directly binds to transcripts whose expression were hnRNP M dependent (Figures 1C and 1D). To begin to answer this question, we leveraged previously published datasets of hnRNP M-bound transcripts in two human cell lines HepG2 (human liver carcinoma cells) and K562 (human chronic myelogenous leukemia cells)³⁵⁷. Remarkably, we observed almost 60%

overlap between our MAJIQ genes and the eCLIP datasets (Figure 4K; Table S3), suggesting that hnRNP M's alternative splicing targets are highly conserved between mouse and human and that the transcripts identified in our MAJIQ analysis are direct hnRNP M targets. While the overlap between the eCLIP hits and differentially expressed transcripts from our RNA-seq analysis (RNA-seq hits, Figures 1C and 1D) was lower (22% for *Salmonella*-infected transcripts, 21% for uninfected transcripts), this result is not altogether surprising, as HepG2 cells and K562 cells would not be expected to express many of the same transcripts as a macrophage. However, together these data reinforce the idea that RBPs like hnRNP M can play specialized roles in different cellular contexts, while also regulating a core set of conserved target transcripts.

Phosphorylation of hnRNP M at S574 Downstream of TLR4 Activation Controls Its Ability to Repress Expression of Innate Immune Transcripts

A recently published phosphoproteomics dataset identified a number of splicing factors that were differentially phosphorylated during infection with the intracellular bacterium *Mycobacterium tuberculosis*^{325,326}. Because it is not a gram-negative bacterium, *M. tuberculosis* does not activate TLR4 via LPS, but it does express the LM and other lipoproteins, which are agonists of TLR2. Having confirmed hnRNP M-dependent regulation of IL6 following treatment with a TLR2 agonist (Pam3CSK4) (Figure 2K), we reasoned that TLR2 activation upon *M. tuberculosis* infection may lead to the same changes in hnRNP M phosphorylation as would TLR4 activation during *Salmonella* infection. We thus leveraged the *M. tuberculosis* global phosphoproteomics dataset from Penn et al.³²⁵, identified 5 differentially phosphorylated serine residues on

hnRNP M (S85, S431, S480, S574, and S636) (Figure 5A), and generated 3xFLAG-hnRNP M constructs with phosphomimic (S→D) or phosphodead (S→A) mutations at each of the serines and made stable RAW 264.7 macrophages expressing each of these alleles in wild-type RAW 264.7 macrophages that still contain a wild-type hnRNP M allele. Importantly, we did not observe any significant differences in the expression level of these mutant alleles compared to the wild-type 3xFLAG-hnRNP M either in resting macrophages or over a course of LPS treatment (Figure S5A). Although the phosphoproteomics dataset predicts infection-dependent gain of phosphorylation at some sites and loss of phosphorylation at others, we were curious as to whether we could detect bulk hnRNP M phosphorylation changes via western blot analysis. While we were unable to detect any higher- or lower-molecular-weight species using antibodies against the endogenous protein, we consistently measured accumulation of a higher-molecular-weight species of the wild-type 3xFLAG-hnRNP M allele over the course of LPS treatment, with an initial increase in the species seen as early as 15 min post-treatment (Figure S5B), consistent with a population of hnRNP M being post-translationally modified upon pathogen sensing.

To determine how these individual serine residues contribute to hnRNP M activity during macrophage activation, we infected each of the phosphomutant/mimic-expressing cell lines, as well as a control expressing a wild-type allele, with *Salmonella* and measured *IL6* and *Mx1* expression at 4 h. Remarkably, expression of hnRNP M harboring a single serine mutation (hnRNP M 574D) caused dramatic hyperinduction of both *IL6* and *Mx1* compared to cells expressing the wild-type 3xFLAG-hnRNP M allele

(Figures 5B and 5C). Several other phosphomutant alleles (S85D, red bar, S431A, light-blue bar, S480A/D, green bars) also affected *IL6* and *Mx1* induction but to a lesser extent (Figures 5B and 5C). Mutating S587, which is a repeat of the S574-containing sequence (MGANS(ph)LER), did not affect the regulation of *IL6* or *Mx1*, suggesting the location of these serines is critical and that phosphorylation-dependent regulation of hnRNP M is specific for select serine residues (Figure S5C). Curiously, expression of the S574D allele in the hnRNP M KD cell lines did not recapitulate this derepression phenotype, suggesting the 574D allele disrupts the activity of wild-type hnRNP M itself—perhaps via interfering with hnRNP M protein oligomerization and/or higher-order complexes that form at innate immune targets (Figure S5D).

Having implicated hnRNP M phosphorylation at S574 in controlling *IL6* and *Mx1* expression, we next wanted to see how phosphorylation affected transcripts whose expression in uninfected cells was higher in the absence of hnRNP M (Figure 1G). While we again observed elevated expression of these transcripts in the absence of hnRNP M (hnRNP M KD, gray bars), expression of the phosphomutant alleles (S431A/D and S574A/D) had no effect on *Rnf128*, *Rnf26*, or *Slc6a4* transcript levels (Figure 5D). Expression of these genes was similarly unaffected by the other hnRNP M phosphomutants (Figure S5E). Alternative splicing of *Commf8* was also unaffected by any of the phosphomutants in either uninfected or *Salmonella*-infected cells (Figure 5E). Together, these data provide strong evidence that hnRNP M's ability to regulate the expression of constitutively expressed genes and/or influence alternative splicing decisions does not rely on phosphorylation at serine 574, whereas its role in regulating

innate immune transcripts induced during infection is specifically controlled by PTMs downstream of pathogen sensing.

Like wild-type hnRNP M, each hnRNP M phosphomutant was enriched in the chromatin in untreated cells (Figure S5F). However, in ChIP experiments looking specifically at the *IL6* locus, the S574D phosphomimic allele displayed virtually no enrichment compared to the S574A phosphodead allele, whose enrichment profile was similar to that of wild-type hnRNP M (Figure 5F and Figure 4F). Indeed, hnRNP M S574D ChIPs more closely resembled those from RNase- or LPS-treated samples (Figures 4I and 4J). These data point to phosphorylation of residue S574 in controlling hnRNP M's ability to co-transcriptionally repress processing of chromatin-associated *IL6* pre-mRNAs.

We next sought to better understand how hnRNP M is phosphorylated at these key residues. TLR4 activation triggers a number of signaling cascades, including p38, MEK1/2 (ERK), and JNK MAP kinases. Previous reports have implicated each of these pathways in regulating *IL6* expression downstream of innate immune stimuli³⁵⁸, but it is not known whether these cascades control splicing factor phosphorylation. To test the role of each cascade in hnRNP M-dependent repression of *IL6*, we performed ChIP experiments in the presence of LPS and specific inhibitors of p38 (SB203580), JNK (SP600125), or MEK (U0126). We again observed LPS-dependent loss of hnRNP M enrichment at *IL6* (primer sets 4–6), and treatment with JNK and MEK inhibitors had no effect on hnRNP M release. However, in the presence of the p38 inhibitor, hnRNP M remained associated with the *IL6* genomic locus after LPS treatment (Figure 5G),

demonstrating that p38 signaling promotes release of hnRNP M from the *IL6* genomic locus.

Last, to interrogate the mechanism driving *IL6* hyperinduction in hnRNP M S574D-expressing cells, we asked whether *IL6* intron removal was affected by expression of the phosphomutant alleles. Using the same qRT-PCR approach used in Figure 3B, we detected an increase in *IL6* pre-mRNAs containing introns 2 and 3 in macrophages overexpressing a wild-type hnRNP M allele, consistent with hnRNP M slowing *IL6* intron removal. Conversely, these same introns were removed more efficiently in the presence of hnRNP M S574D, while no difference was observed in S574A-expressing cells (Figure 5H). These data strongly support a model whereby phosphorylation of hnRNP M at S574 relieves its ability to act as a splicing repressor, allowing for rapid removal of *IL6* introns and upregulation of *IL6* mRNA, and demonstrate a previously unappreciated role for constitutive intron removal in mediating *IL6* expression in macrophages.

Loss of hnRNP M Enhances Macrophages' Ability to Control Viral Infection

Because loss of hnRNP M resulted in hyperinduction of a variety of cell-intrinsic antimicrobial molecules and ISGs, we hypothesized that hnRNP M KD cells would be better at controlling viral replication. We infected SCR and hnRNP M KD RAW 264.7 macrophages with VSV, an enveloped RNA virus that can replicate and elicit robust gene expression changes in RAW 264.7 macrophages³⁵⁹. Viral replication (levels of VSV-G) was measured over an 8 h time course by qRT-PCR in cells infected with a viral MOI of 1 and 0.1. At both MOIs, loss of hnRNP M correlated with dramatic

restriction of VSV replication, particularly at the 8 h time point (Figure 6A). As expected, infection with VSV, a potent activator of cytosolic RNA sensing via RIG-I/MAVS³⁵⁹, led to robust induction of *Ifnb* levels in an hnRNP M-independent fashion at both MOIs, as we previously observed in hnRNP M KD cells transfected with cytosolic dsDNA (Figures 6B, S6A, and 2M, respectively). Consistent with hnRNP M-dependent regulation occurring downstream of diverse immune stimuli (Figure 2), VSV-infected hnRNP M KD cells at MOI = 1 and MOI = 0.1 hyperinduced both *Mx1* and *IL6* (Figures 6C, 6D, S6B, and S6C). While *Mx1* itself is a well-known anti-viral GTPase, cell lines derived from inbred mouse strains like RAW 264.7 have been shown to carry non-functional *Mx1* alleles (Shin et al., 2015). Therefore, to begin to predict what other hnRNP M-regulated genes may be responsible for enhanced VSV restriction, we manually examined hnRNP M-regulated transcripts in our RNA-seq data from uninfected and *Salmonella*-infected (i.e., TLR4-activated) macrophages and identified a number of genes known to be important for controlling RNA viral replication (Figure 6E). qRT-PCR confirmed hyperinduction of several antiviral ISGs in hnRNP M KD macrophages at 4 h post-VSV infection including *Rsad2* (*Viperin*), *Ifit1*, *Irf7*, and *Gbp5* (Figure 6F). Interestingly, neither *Ifit1* nor *Irf7* was identified as an hnRNP M-dependent transcript during *Salmonella* infection, even though both can be expressed downstream of TLR4 through IRF3/IFNAR/STAT1 signaling. This difference may simply reflect kinetic differences in transcript induction following RNA sensing versus TLR4 activation or may indicate that hnRNP M regulates an even broader set of transcripts in macrophages following RNA virus infection. We propose that inhibition of VSV

replication in hnRNP M KD macrophages ultimately results from a combination of pro-viral gene downregulation (red genes, Figure 6E) and anti-viral gene upregulation (blue genes, Figure 6E and Figure 6F). Collectively, these data are consistent with hnRNP M playing a critical role in slowing innate immune gene expression and suggest that the presence of hnRNP M can actually blunt macrophage antiviral defenses at early time points following infection with VSV.

Discussion

Despite the substantial impact pre-mRNA splicing has on gene expression outcomes, little is known about how components of the spliceosome are modified and regulated during cellular reprogramming events, such as macrophage pathogen sensing. Here, we demonstrate that the splicing factor hnRNP M is a critical repressor of a unique regulon of innate immune transcripts (see model in Figure 7). These transcripts were hyperinduced in hnRNP M KD macrophages downstream of a variety of innate immune stimuli (i.e., *Salmonella* infection, TLR4/TLR2 agonists, recombinant IFN- β , cytosolic dsDNA, RNA virus infection [VSV]) (Figure 2; Figure 6), and hyperinduction of this regulon correlated with enhanced capacity of hnRNP M KD macrophages to control VSV replication at early time points (Figure 6). We propose that in innate immune cells like macrophages repression of pre-mRNA splicing by hnRNP M serves as a safeguard, dampening the initial ramping up of innate immune gene expression and preventing spurious expression of potent pro-inflammatory molecules in situations where the cell has not fully engaged with a pathogen. The latter situation is supported by experiments in which low doses of LPS (10 and 50 ng/mL), were sufficient to hyperinduce *IL6* in the

absence of hnRNP M without inducing significant a change in the amount of *IL6* mRNA expressed in SCR control cells (Figure S7A). These data support a role for hnRNP M in slowing *IL6* processing in macrophages that are “sampling” PAMPs or that have just received an initial innate immune stimulus. The requirement for cells to tightly control expression of potent inflammatory mediators like *IL6* is evidenced by the fact that multiple transcriptional and post-transcriptional mechanisms exist to regulate *IL6*, including chromatin remodeling²⁶⁷, mRNA stability³⁶⁰, subcellular localization³⁶¹, and now, based on these data, pre-mRNA splicing. While hnRNP M’s role in regulating many alternative splicing decisions is conserved across diverse cell types in mice and humans (as evidenced by overlap in our MAJIQ hits and eCLIP datasets [Figure 4K]), its role in controlling innate immune transcripts is uniquely influenced by phosphorylation downstream of pathogen sensing. Based on these observations, we propose that hnRNP M and likely other splicing factors possess distinct capacities for interacting with RNAs and/or proteins depending on how they are post-translationally modified. In this way, innate immune sensing cascades may remodel splicing complexes, for example, by promoting release of hnRNP M from chromatin-associated RNA-proteins complexes via p38-MAPK cascades.

While we do not fully understand the mechanisms driving hnRNP M’s target specificity, our RNA-seq data as well as other datasets³⁰⁹ demonstrate the presence of cryptic exons in a number of hnRNP M-regulated transcripts (Figure S7). Previous work investigating the RNA-binding landscape of a panel of hnRNP proteins in a non-macrophage cell line (HEK293Ts, human embryonic kidney cells) revealed that hnRNP

M has a strong preference for binding distal intronic regions (>2 kb from an exon-intron junction)²⁹. Its binding profile was somewhat unique among the hnRNPs queried and was more reminiscent of another RBP, TDP-43. TDP-43 also binds UG-rich sites in distal introns and is crucial for repressing splicing of cryptic exons for a set of transcripts in the brain^{362,363}. We speculate that hnRNP M regulates splicing of macrophage transcripts through a similar mechanism where it binds to UG-rich regions downstream of cryptic exons and inhibits assembly of the spliceosome on these introns, thus slowing intron removal.

While hnRNP M's ability to associate with the *IL6* genomic locus via ChIP is RNA dependent, it is conceivable that hnRNP M controls innate immune gene expression through mechanisms that are independent of direct contacts between hnRNP M and regulated transcripts. Because a number of splicing factors have been shown to impact histone markers and chromatin remodeling, it is possible that hnRNP M promotes epigenetic changes at specific target transcripts³⁶⁴⁻³⁶⁷. hnRNP M may also interact with one or more long non-coding RNAs (lncRNAs), a number of which are regulated by TLR activation³⁰² and have been shown to control *IL6* expression^{302,368}. Experiments designed to identify hnRNP M-associated RNAs in uninfected and infected macrophages will provide important insights into how hnRNP M recognizes chromatin-associated target transcripts and help illuminate how pre-mRNA splicing decisions shape the innate immune transcriptome.

CHAPTER III

HNRNP M PROTEIN INTERACTIONS ARE REGULATED BY INNATE

IMMUNE PHOSPHORYLATION EVENTS

Introduction

Historically, the regulation of gene expression during the immune response has been hyper-focused on transcriptional and signaling regulation. However, we have challenged this paradigm with our work on the RBP hnRNP M. Defining the hnRNP M protein interactome is essential to further elucidating the mechanism behind *I/6* repression. In previous research, hnRNP M was found to interact with spliceosome proteins CDC5L and PLRG1 in HeLa cells⁵¹. hnRNP M has also been found to be associated with TAF15/FUS, which are transcription factors in HeLa cells^{369(p15)}. Additional research has identified hnRNP M as a regulator of muscle differentiation through interaction with mTOR/Rictor.^{53(p2)} There has not been a high-throughput approach of hnRNP M protein partners and specifically not in macrophages or in the context of the innate immune response.

Our lab's previous findings showed hnRNP M is a critical repressor of pre-mRNA splicing and gene expression during macrophage activation. We also identified specific serine residues that play a role in the repressor function of hnRNP M. We next wanted to identify mechanistic function of hnRNP M and how protein partners could contribute to hnRNP M repressor function. Additionally, we wanted to identify if specific serine residues could influence these interactions with other protein partners.

Our IP/MS findings conclude that hnRNP M interacts with core paraspeckle complex factors, SFPQ and MATRIN3.

Upon infection with *Salmonella* or activation of macrophages, this association is almost completely abolished. Interestingly, S574 phosphomutant and mimic alleles had differential binding capacity with these same core spliceosome factors and different splicing proteins, suggesting that interactions within these paraspeckle complexes and the repressor function of hnRNP M may be regulated by phosphorylation. Paraspeckle proteins such as SFPQ and NONO form protein-RNA structures with the lncRNA NEAT1. Paraspeckles are known for their role in nuclear retention of RNA and controlling gene expression in stress responses and viral infection³⁷⁰. Their role in gene regulation has been implicated in many RNA processes and transcription^{370,371}. Recently, SFPQ and NONO were found to associate with a TB effector protein, Apa, suggesting a possible role for paraspeckles in innate immunity to bacterial infection³²⁵. Surprisingly, knockdowns of SFPQ, NONO, and MATR3 protein partners showed phenotypes similar to hnRNP M knockdowns. These results identify novel interactors and the critical function of phosphorylation in regulating these complexes. While typically recognized in the context of paraspeckles, our results also implicate SFPQ, NONO, and MATR3 in having distinct roles in regulation of gene expression during innate immune activation.

Results

hnRNP M Protein Interactions Reveal Paraspeckle Protein Associations

Based on hnRNP M's localization in the nucleus in the presence and absence of immune agonists, we hypothesized that hnRNP M may interact with core spliceosome factors and RNA-processing proteins. To test this, we generated 3XFL-hnRNP M stably expressing RAW 264.7 macrophages and performed nuclear FLAG immunoprecipitation followed by mass spectrometry peptide identification analysis from resting cell lysates. We found peptides aligning with PTBP3 (Polypyrimidine Tract Binding Protein 3), RBM14, and SNRPD3 (Small nuclear ribonucleoprotein Sm D3) (Figure 28 & Figure 29). Each of these proteins are well annotated to function in core spliceosome assembly and splicing processes. Similarly, we found several hnRNPs (hnRNPF, hnRNPH1, RALY), and SRSF proteins (SRSF7, SRSF6) to interact with hnRNP M. PRPF31 (Pre-mRNA Processing Factor 31) is part of the U4/U6 complex and interacts with hPRP6 to form the U4/U6-U5 complex. While we have previously discovered splicing processes that hnRNP M regulates, our IP/MS analysis further confirms this mechanism by identifying that these splicing factors interact with hnRNP M.

Interestingly, we also found hnRNP M to be associated with Matr3 (Matrin 3), ILF3 (Interleukin enhancer-binding factor 3), RBM14, and SFPQ (Splicing Factor Proline and Glutamine Rich). These proteins have been found to play a role in paraspeckle formation leading to transcriptional and splicing regulation of target transcripts^{362,370,372}. Previously, these factors have been reported to associate in 293Ts⁵⁷, but have not been characterized in the context of macrophages. Likewise, hnRNP M

association with paraspeckle complexes in resting macrophages has not been explored. Paraspeckle formation requires NEAT-1 lncRNA. NEAT-1, NONO, and SFPQ are essential factors in paraspeckle formation and function. In work done in HeLa cells, SFPQ was found to regulate *Il8* expression through repression of transcription. Specifically, induction of NEAT1 expression served to sequester SFPQ from the promoter of *Il8*, allowing for induction of *Il8* gene expression³⁷³. These data strongly suggest that inflammatory gene expression can be regulated by moving proteins to and from the paraspeckle. Our previous studies found hnRNP M at the level of chromatin in the gene body of *Il6*, specifically around the vicinity of intron 2. While we initially hypothesized that this association corresponded to co-transcriptional splicing regulation of intron 2, we did not rule out a role for hnRNP M in regulating *Il6* transcription, much in the same way as SFPQ.

Our findings that hnRNP M's interaction with the *Il6* chromatin locus was relieved upon macrophage activation suggested to us that the protein was somehow altered in activated macrophage. Therefore, we wanted to know which protein partners were associated with hnRNP M during immune activation. To test this, we took the same 3XFL-hnRNP M stably expressing RAW 264.7 macrophages as above and again performed nuclear FLAG immunoprecipitation and subsequent mass spectrometry analysis, this time in cells treated with LPS for 2h. Strikingly, our results identified far less protein interactions upon LPS stimulation (Figure 30). This result suggests that upon immune activation, hnRNP M relieves its repression of gene expression by also relieving association with its protein partners. Following immune activation, we found hnRNP M-

interacting peptides derived from hnRNP U, SRSF7, and SNRPD3. While SRSF7 and SNRPD3 were also found to interact with hnRNP M in resting cells, hnRNP U was only identified in the +LPS samples. PRMT5 (a protein arginine methyltransferase) and SUPT5 (Suppressor of Ty 5, DSIF elongation factor) were also only identified in our +LPS samples. Interestingly, SFPQ, RBM14, MATR3, and ILF3 paraspeckle proteins were not found in our IP/MS following innate immune activation in our cells. We hypothesize that relief of hnRNP M repression may occur via disassociation with this paraspeckle complex.

To validate our IP/MS analysis and to investigate additional hnRNP M protein interactions, we set up a system for immunoprecipitation/western blot analysis, whereby we treated cells with LPS, immunopurified hnRNP M, and probed for SFPQ, NONO, and MATR3 by western blot. Notably, we observed less SFPQ interaction with hnRNP M upon following LPS treatment (Figure 32). Similarly, MATR3 immunoprecipitated with hnRNP M in resting cells, but not LPS-treated cells. Our immunoprecipitation validated our initial IP/MS, and we did not observe NONO association with hnRNP M in resting cells or immune activated cells. This result is curious because the literature strongly suggests that SFPQ and NONO are always found as a heterodimer; these factors may have novel distinct functions during the innate immune response. Collectively, these results demonstrate that hnRNP M is associated with paraspeckle complexes, which may play a role in splicing repression. During innate immune activation, hnRNP M appears to dissociate from these partners, allowing for splicing activation and gene expression.

We also investigated whether hnRNP M and paraspeckle proteins colocalize in macrophage by immunofluorescence. hnRNP M demonstrated nuclear localization as seen in our previous report (Figure 31). Consistent with previous reports, SFPQ and NONO displayed punctate staining within the nucleus^{55,371}. Interestingly, MATR3 showed a similar speckle pattern, but with additional localization inside the cytoplasm. Consistent with our IP/MS we saw co-localization of SFPQ and MATR3 with hnRNP M within the nucleus. Interestingly, we also saw co-localization of hnRNP M with NONO.

Phosphorylation of S574 Influences hnRNP M Protein Partners Associations

Our published work demonstrates that phosphorylation of hnRNP M at S574 alters the protein's ability to function as repressor of *Ilf6* expression. In order to dissect if protein-protein partners of hnRNP M depend on the phosphorylation status of hnRNP M, we generated 3XFLAG-hnRNP M constructs with phosphomimic (S→D) or phosphodead (S→A) mutations at each of the serines and made stable RAW 264.7 macrophages expressing each of these alleles in wild-type RAW 264.7 macrophages and performed nuclear FLAG immunoprecipitation and subsequent mass spectrometry analysis in resting cells. In S574A samples, peptides for NCL and H2AFY were found, similarly aligning with WT hnRNP M. Furthermore, ILF3, RBM14, and SFPQ, which have been previously been found in paraspeckle complexes, were also found to associate with hnRNP M-S574A. Interestingly, the 574A mutant also associated with the splicing factors SNRPN, SRSF1 and SRSF9 (Figure 33). hnRNP F and SRSF6 were surprisingly not found in our mass spec analysis of hnRNP M-S574A mutant. Alternatively, RBM14 and ILF3 were also found to interact with hnRNP M-S574D mutant. Remarkably,

S574D samples had peptides aligning to Matrin3, another paraspeckle factor and RBP. This interaction was not identified in WT-hnRNP M or S574A samples. S574D interacted with several splicing factors and RBPs such as hnRNP U, hnRNP K, hnRNP F, SRSF1, and SRSF7(Figure 35). Surprisingly, SFPQ and NONO peptides were not found in S574D samples. Tables showing overlapping factors between WT-hnRNP M, S574A, and S574D are shown in Table 4. These results argue that phosphorylation of hnRNP M plays an unappreciated role in regulating protein-protein interactions of hnRNP M.

Because we observed that hnRNP M lost interactions upon innate immune activation, we wanted to test whether this same phenomenon occurred with hnRNP M phosphomutants. To test this, we treated our 3XFL-hnRNP M phosphomutant stably expressing RAW 264.7 macrophages and performed nuclear IP/MS analysis in cells treated with LPS and treated for 2h. Similar to WT-hnRNP M, our 574D and 574A phosphomutants both had fewer interacting peptides identified when cells were treated with LPS (Figure 34 & Figure 36). MATR3, NONO, and ILF3 were found to interact with S574A+LPS. We also found splicing proteins of SRSF1, NCL, SNRPN, and SNRPD3 to appear to be decreased upon LPS treatment, suggesting a relief of splicing associated factors. Interestingly, SRSF9 was found in S574A uninfected and S574A+LPS, suggesting it plays a role with hnRNP M regardless of macrophage activation status. hnRNP U and SRSF7 interacted with hnRNP M S574D in both resting and LPS-treated macrophages. Surprisingly, although SFPQ and Matrin3 were consistent hits in our hnRNP M mass spectrometry analysis, we did not detect peptides from these

factors interacting with hnRNP M S574D in the presence of LPS, suggesting that either phosphorylation at this site and/or LPS treatment promotes dissociation between hnRNP M and these factors.

Interestingly, PRMT5 was identified in both phosphomutants during LPS treatment, similar to WT-hnRNP M+LPS. This suggests that PRMT5 may play a role in methylating hnRNP M upon innate immune activation to influence splicing outcomes³⁷⁴.

To test if the interaction between hnRNP M and Matrin3 or SFPQ is phosphorylation-dependent, we immunoprecipitated 3XFL-hnRNP M S574A and 3XFL-hnRNP M S574D from stably expressing RAW cells and probed for either endogenous Matrin 3 or SFPQ via western blot in resting cells and cells treated with LPS for 2h. In resting cells, we found that Matrin 3 immunoprecipitated with 3XFL-hnRNP M S574A S574D, S392A/D, and S85A/D (Figure 37). Interestingly, SFPQ was not found in resting cells or cells treated with LPS in 3XFL-hnRNP M S574D and S392D mutant immunoprecipitations. (Figure 37). This aligns with our IP/MS, as SFPQ was only found to interact with S574A mutants and WT-hnRNP M in resting cells. This suggests hnRNP M and SFPQ interaction is relieved upon immune activation and that S574A resembles the resting cell phosphorylation status of hnRNP M.

As mentioned above, MATR3 immunoprecipitated with hnRNP M in resting cells, but not LPS-treated cells (Table 4). Interestingly, upon activation Matrin3 seemed to stay with S574A upon activation. This is contrary to S574D where we see loss of Matrin3 upon LPS treatment, similar to WT-hnRNP M+LPS. While more research is needed on hnRNP M and paraspeckle interactions, together, this data suggests that SFPQ

and Matrin3 associate with hnRNP M in resting cells, with WT-hnRNP M having similar association as S574A. Alternatively, upon immune activation, S574A retains interaction with MATR3, while S574D loses interaction with SFPQ and MATR3, similar to WT-hnRNP M. Ultimately, our results suggest that MATR3 and SFPQ interaction with hnRNP M is influenced by phosphorylation of hnRNP M at S574. We have also identified differences in requirements of phosphorylation status of hnRNP M, where S574 seems to be critical with MATR3 and but SFPQ interaction does not depend on this serine alone for interaction with hnRNP M. Our research has identified novel phosphorylation-dependent interactions that could potentially influence innate immune expression, similar to hnRNP M.

Paraspeckle Proteins Show Differential Regulation of Innate Immune Gene Expression

Previous reports have shown that paraspeckle proteins play a role in regulating the innate immune response to viral infections, whereby SFPQ can regulate replication of hepatitis delta-virus, influenza A, and HIV³⁷⁵. Additionally, NONO has been found to be essential for immune activation following HIV infection³⁷⁶. Interestingly, Matrin3 has not been characterized widely in the innate immune response, but was found to be ubiquitinated by TRAF6, a critical player in innate immune signaling³⁷⁷. Having identified SFPQ, NONO, and Matrin3 as interactors of hnRNP M, we hypothesized that removing these factors could have an effect on gene expression of the same regulon of innate immune genes whose expression was altered in the absence of hnRNP M. To test this idea, we generated stably selected, constitutive SFPQ, NONO, and Matrin3

knockdown cell lines by transducing RAW 264.7 mouse macrophages with lentiviral shRNA constructs designed to target SFPQ, NONO, MATR3, or a control SCR shRNA. qRT-PCR analysis confirmed ~50%, ~80%, and ~90% knockdown of SFPQ, NONO, and MATR3, respectively using two different shRNA constructs (Figure 38). We treated these knockdown cells with LPS for 2HR and 4HR and collected RNA. To first test if these factors regulate the same regulon as hnRNP M, we performed qRT-PCRs to measure *Il6* mRNA levels. Remarkably, *Il6* was upregulated in SFPQ, NONO, and MATR3 KD samples compared to SCR control (Figure 38). In MATR3 KD cells, we saw an upregulation at 2HR and 4HR, suggesting a possible earlier role in regulation of *Il6* gene expression. Since we observed the strongest phenotype with MATR3, we performed qRT-PCR for additional hnRNP M regulated genes, *Mx1* and *Gbp5*. Interestingly, MATR3 KD did not show a significant difference in *Mx1* and *Gbp5* gene expression when compared to SCR control. These results suggest that while the hnRNP M and MATR3 regulons are seemingly distinct, loss of SFPQ and NONO do appear to phenocopy loss of hnRNP M. Ultimately, these data demonstrate novel regulation of *Il6* expression by NONO, SFPQ, and MATR3 that warrants further investigation.

Discussion

Our studies have identified novel protein partners that interact with hnRNP M that are dependent on the phosphorylation status of hnRNP M at S574. The most interesting partners of hnRNP M were several paraspeckle core factors, NONO, SFPQ, and MATR3. Our studies also suggest that hnRNP M protein complexes are dissociated in response to macrophage activation.

Consistent with our observation that hnRNP M associates with chromatin, we found hnRNP M interacts with a number of paraspeckle proteins that also fractionate with chromatin³⁷⁰. Additional chromatin immunoprecipitation experiments looking at the distribution of hnRNP M, MATR3, and SFPQ at target genes will help illuminate whether these proteins regulate innate immune gene expression through similar or disparate mechanisms. Notably, a recent study by Cao et. al showed that hnRNP M moves outside of the nucleus at an 8h time point following viral infection³⁷⁸. My studies did not show relocalization of hnRNP M into the cytosol although we never looked at an 8h time point. It will be interesting to see if we can recapitulate these results in our cells and determine whether relocation of hnRNP M explains some of its protein-protein interaction dynamics.

While knockdown of NONO, SFPQ, and MATR3 appear to phenocopy loss of hnRNP M, the timing of when each of these KDs showed maximal phenotypic differences in terms of *Il6* hyperinduction was not the same across the board. Therefore, while we can implicate each of these factors in regulating *Il6* expression, it is likely that they do so through different or independent mechanisms. Further studies using RNA-seq to look at the entire MATR3, SFPQ, and NONO-dependent innate immune regulons will allow us to unbiasedly identify the genes that are regulated by each factor and determine to what degree they phenocopy loss of hnRNP M.

While additional research is needed to identify kinases/phosphatases of the hnRNP M/SFPQ/NONO/Matrin3 complex, our research has identified specific serines on hnRNP M that are required for Matrin 3-hnRNP M interaction. Furthermore, our

research has identified a loss of hnRNP M protein interactions upon innate immune activation which aligns with the role of hnRNP M de-repression of innate immune gene expression upon activation. We hypothesize that hnRNP M repression of innate immune genes is relieved when hnRNP M loses interaction with specific factors like Matrin3. Our results also indicate that upon activation or differential phosphorylation, hnRNP M loses protein partners. Our S574D mutant appeared similar to immune activation with mostly loss of protein partners while S574A having more associations, similar to Uninfected WT-hnRNP M. The kinetics of these interactions are also important to study as our mass-spec studies only followed up using an IP at a single time point of 2h. While mutation of S574 did not cause complete protein dissociation with its interactors, this could suggest that other serines or PTMs of hnRNP M may be in play when regulating protein-protein interfaces. In addition, more research needs to be conducted on which kinases and phosphatases are responsible for the differences in the association and interactions of this complex with hnRNP M. Another factor in the paraspeckle complex is lncRNA NEAT-1. Initial RNA binding studies with hnRNP M have not shown interaction with Neat-1 and our studies also revealed these interactions are RNA-independent (data not shown). This suggests that Neat-1 plays other functions in the paraspeckle complex that may not involve hnRNP M and its regulon. More research will help illuminate hnRNP M-dependent and independent functions for the lncRNA Neat1 and paraspeckles in regulating innate immune gene expression.

CHAPTER IV
HNRNP F REGULATE TYPE I INTERFERON RESPONSE DURING BACTERIAL
INFECTION

Introduction

The innate immune response requires robust expression of thousands of immune response genes that are activated downstream of myriad signal transduction cascades. This response also requires powerful regulation that occurs through coordinated control of gene expression that can occur at each level of RNA processing. Such regulation can occur through changes to histones and nucleosome, transcription factor modifications, pre-mRNA splicing decisions, export, translation regulation, and post-translational modifications of proteins involved in any of these steps^{266,327,379}. While conventional research has focused on transcriptional outputs of the innate immune response, our studies have found that RNA processing, specifically at the level of splicing, is a critical regulatory node of the innate immune response in macrophages. Up to 95% of the human genome is alternatively spliced and these splicing events occur more frequently in the nervous and immune systems^{11,380,381} and recent studies have identified many alternatively spliced isoforms during the context of bacterial infection³¹⁰⁻³¹². Although alternative splicing has been repeatedly identified as a form of regulation during infection, little to no research has identified the splicing factors or RNA-binding proteins that regulate these events or how these proteins themselves are functionally altered upon innate immune stimuli. Although hnRNP U, TTP Tristetraprolin (TTP), human antigen

R (HuR), T cell intracellular antigen 1-related protein (TIAR), and hnRNP K have been shown to regulate mRNA decay and translation during LPS treatment^{92,293,294,340}, there is a critical void in the understanding of how pre-mRNA splicing is regulated and how splicing factors are modified during bacterial infection.

Previously, our lab discovered a role for the splicing factor hnRNP M in regulating expression of key innate immune transcripts during *Salmonella* infection. hnRNP M was originally found in studies focusing on phosphorylation changes that occur during infection with *Mycobacterium tuberculosis* and *Cryptococcus neoformans*^{325,326,339}. Intriguingly, several other splicing factors were identified in these data sets, with “mRNA processing” and the “spliceosome” being top hits amongst pathways with infection-specific phosphorylation changes. Among these proteins hnRNP F, which has a similar RNA binding consensus to hnRNP M (G-U rich sequences), rose to the top of our list. We initially hypothesized that hnRNP F could have similar functions or bind antagonistically to sites occupied by hnRNP M. Aligning with this hypothesis, research conducted on exon 8 of *Cd44* found hnRNP M to decrease exon inclusion. Contrastingly on this same exon 8 of *Cd44*, hnRNP F was found to increase exon inclusion⁴⁷.

hnRNP F is an RNA-binding protein and splicing factor. It has been identified to affect splicing of dozens of genes including *Enox2*, *Tpx2*, *Mcl-1*, *Sirtuin-1*, *Nrf2*, *Agt*, *insulin receptor gene*, and *fibroblast growth factor 2*^{26,66-68,74,382}. Researchers have also identified hnRNP F-dependent splicing changes in neurons and glia cells of the brain and it has been implicated in regulation of myelin synthesis⁶⁹⁻⁷¹. Deletion of hnRNP F in HeLa cells was found to decrease the efficiency of pre-mRNA splicing via its interaction

with cap binding proteins, CBP20 and CBP80³⁸³. hnRNP F has also been identified to interact paraspeckle proteins^{64,77,78}. As has been reported for other hnRNPs, hnRNP F has been associated with several cancers such as breast, colon, and bladder cancer^{64,68,72-74}. Interestingly, studies conducted in T cells and B cells showed overexpression of hnRNP F resulted in reduced T cell functions and reduced Ig heavy-chain mRNA, respectively^{384,77}. While the contribution of hnRNP F in regulating the innate immune response is largely uncharacterized unknown, one study treated macrophages with LPS and found hnRNP F to be involved in nonsense mediated decay, along with other RNA binding proteins, TTP a zinc finger protein, and BRF1, a component of RNA III polymerase⁶³.

In my current studies, I have implicated hnRNP F in a mechanistically different form of regulation for hundreds of interferon stimulatory gene (ISG) transcripts. We demonstrate that hnRNP F is required for the activation of *Ifnb1* expression. Consequently, loss of hnRNP F leads to a dramatic silencing of ISG induction following a number of innate immune stimuli, although we find IFNAR signaling itself to remain intact. In our attempt to understand how hnRNP F could simultaneously impact the expression of the entire type I IFN regulon, we identified that several master regulators of ISGs, *Irf7*, *Ikbke*, and *Irak1*, were differentially spliced in the absence of hnRNP F. HnRNP F-dependent exon exclusion and intron retention events would target transcripts like *Irf7*, *Ikbke*, and *Irak1* for nonsense mediated decay, perhaps leading to lower proteins levels and a subsequent loss of ISG induction during both *Salmonella* Typhimurium infection and *Mycobacterium tuberculosis* infection. Interestingly,

mutating several serine residues (predicted to be differentially phosphorylated during infection) on hnRNP F resulted in modulated expression of *Ifnb1* and ISGs, suggesting phosphorylation is a critical point of regulation for hnRNP F. We further demonstrated hnRNP F interacts with a core spliceosome factor Sf3b1. Taken together, this data suggests a novel function for hnRNP F in modulating *Ifnb1* expression. We propose that hnRNP F's ability to interact with core spliceosome partners may be facilitated by innate immune phosphorylation and may control hnRNP F's ability to influence splicing of immune-activated transcripts.

Results

Interferon Stimulatory Genes Are Regulated by hnRNP F during *S. Typhimurium* and *M. tuberculosis* Infection

To evaluate the global impact of hnRNP F on regulation of the macrophage innate immune response, we performed RNA-seq analysis on total poly(A)⁺ selected RNA. RNA was collected from stably selected, constitutive hnRNP F KD cell lines that were generated by transducing RAW 264.7 mouse macrophages with lentiviral shRNA constructs designed to target hnRNP F or a control SCR shRNA. Western blot and qRT-PCR analysis confirmed ~90% and 80% knockdown of hnRNP F using two different shRNA constructs (KD1 and KD2, respectively) (Figure 39). RNA was isolated from resting macrophages or from cells following *Salmonella* Typhimurium (STm) infection (MOI = 5), or *Mycobacterium tuberculosis* (Mtb) infection (MOI=10) at the key innate immune time point of 4 h post-infection, at which time transcriptional activation downstream of TLRs and cGAS is expected^{206,343}. RNA-Seq gene expression profiling

was done using CLC Genomics Workbench. With this analysis, we identified hundreds of genes whose expression was affected in hnRNP F KD cells compared to SCR control cells, with 1,094 genes upregulated and 904 downregulated (Figure 39) in uninfected cells. Strikingly, this ratio of genes that are downregulated to upregulated upon depletion of hnRNP F shifted upon infection with STm or Mtb. Whereas roughly equal numbers of genes were impacted in resting macrophages, we observed an overwhelming number of downregulated transcripts in the absence of hnRNP F at 4h post STm or Mtb infection (Figure 40). The vast majority of these hnRNP F-dependent transcripts were ISGs (Figure 39 & Figure 40), suggesting a major defect in the type I IFN response. While *Salmonella* infection had more differential gene expression than *Tuberculosis* infection, the ratio of upregulated (orange) and downregulated (purple) transcripts was quite similar between the two conditions, with more downregulated genes than upregulated in the absence of hnRNP F. The differences in gene expression can possibly be explained by the differential dynamics of STm and Mtb infection; STm elicits gene expression mainly through TLR4/MyD88/TRIF pathways with peak induction of most innate immune genes seen between 2-4h post-infection. Mtb sensing takes a bit longer, with gene expression downstream of TLR2 peaking between 2-4h post-infection and cytosolic DNA sensing responses typically peaking between 4-6h post-infection (Figure 9 & Figure 10). Despite this, similar ISGs are downregulated in hnRNP F KD cells in both infections (e.g. *Mx2*, *Irf7*, *Isg15*, *Ifit1*, *Ifitm3*, *Oasl1*) (Figure 39 & 40, dot plots). This global downregulation of ISG expression in STm or Mtb-infected hnRNP F macrophages is consistent with previous reports of hnRNP F playing a role in activating

pre-mRNA splicing^{26,75,77,384–386}. Interestingly, we observed less than a 25% overlap between genes that were differentially expressed in uninfected, STm-infected, and Mtb-infected macrophages, suggesting that hnRNP F has distinct modes of operation depending on the activation state of a macrophage (Figure 40). We next used Qiagen IPA Analysis to identify cellular pathways that were enriched for hnRNP F-dependent genes (pval<0.05, SCR vs. hnRNP F KD), we found “mTOR Signaling” and “EIF2 Signaling” pathways among the top hnRNP F-dependent pathways in uninfected samples. STm-infected samples revealed strong enrichment for “Activation of IRF” and “Interferon Signaling” as well as “Communication between adaptive and innate immune cells” (Figure 39 & Figure 40). These pathways were consistent with the remarkable amount of ISGs we found that were downregulated in the absence of hnRNP F. A complete list of IPA analysis results can be found in Figure 40. Further manual analysis of these lists revealed dozens of key ISGs (e.g., *Mx1*, *Idi47*, *Ifit3*, *Ifit1*, *Isg15*, *Isg20*). These ISGs have been implicated as antiviral molecules and play a crucial role in pathogenesis of Mtb and other bacterial infections³⁸⁷. Several additional chemokines and cytokines were also found to be downregulated upon depletion of hnRNP F (e.g., *Ccl2*, *Ccl17*, *Il6*, *Il1β*) (Figure 39 and Figure 40). Consistent with the general overlap between the hnRNP F-dependent gene expression changes in STm and Mtb infection, the Mtb-infected samples had similar pathways enriched like “Interferon signaling” and “Activation of IRF.” Additional pathways enriched for hnRNP F-dependent genes can be found in Figure 40.

To validate the RNA-seq gene expression changes, we used qRT-PCR to measure transcript levels of genes from each list (uninfected, STm-infected, and Mtb-infected SCR vs. hnRNP F KD). We verified expression of several genes in uninfected hnRNP F KD cells (*Fcgr1* & *Ubt2* Figure 45), as well as downregulation of transcripts in hnRNP F KD cells at 4 h post-*Salmonella* and *Tuberculosis* infection (*Irf7*, *Mx2*, *Ifnβ*, *Ifit1*, and *Il6*) (Figure 41). Consistent with our RNA-seq data, induction of other pro-inflammatory mediators such as *Tnfa* and *Irf9* did not rely on hnRNP F (Figure 41).

To provide additional insight into how hnRNP F may be regulating ISG expression, we next tested the kinetics of this response by infecting hnRNP F KD and SCR control cells with STm and collecting RNA at 2h and 6h post-infection. Interestingly, at 2h, we did not see an hnRNP F-dependent difference in ISG expression, but we did observe downregulation of *Ifnb* transcript levels. At 6h, we saw a similar ISG phenotype to 4h post-*Salmonella*.

hnRNP F Influences Innate Immune Gene Expression Through Splicing

hnRNP F has been widely shown to regulate RNA-processing through regulation of mRNA decay, transport, and enhanced splicing by facilitating exon inclusion or the usage of alternative 5'SS in multiple types of cells including fibroblasts, neurons, and oligodendrocytes^{26,64,66,71,75,77,384–386,388,389}. To understand how hnRNP F may be affecting RNA-processing in macrophages upon activation and immune response gene expression, we first wanted to explore how loss of hnRNP F impacted alternative splicing in uninfected and STm- and Mtb-infected macrophages. To do this, we employed an algorithm for LSV (local splice variant) analysis called MAJIQ³⁴⁵. MAJIQ

allows identification, quantification, and visualization of diverse LSVs, including alternative 5' or 3' splice site usage, exon skipping, and intron retention across different experimental conditions. MAJIQ identified a total of 3,463 LSVs (2,067 genes) in uninfected, 967 LSVs (725 genes) in STm-infected, and 770 LSVs (594 genes) in Mtb-infected, and SCR versus hnRNP F KD macrophages (probability [Δ PSI], $\geq 10\%$), $>95\%$) (Figure 47, Figure 48, Figure 49, & Figure 50). The majority of the LSVs identified in SCR versus hnRNP F KD cells were exon skipping events (Figure 47). Visualizations of these LSVs by Voila displayed an increase of intron inclusion and exon skipping in uninfected, STm-infected and Mtb-infected macrophages. These results suggest that in the presence of hnRNP F, there is more exon inclusion, which aligns with hnRNP F's previously characterized role in splicing activation.

Genes that were predicted to undergo hnRNP F-dependent alternative splicing by our MAJIQ analysis, were then subjected to IPA pathway analysis to identify pathways and upstream regulators enriched for hnRNP F-dependent changes. Consistent with our global gene expression analysis, we found changes in "Activation of IRF" and "Role of PKR in Interferon Induction" in our STm-infected samples. Uninfected MAJIQ results showed enrichment for "Molecular Mechanisms of Cancer" and "Estrogen Receptor Signaling". Additionally, Mtb-infected samples had hits of "TNFR1 Signaling" and "Death Receptor Signaling" (Figure 47 & Figure 50). A more comprehensive list of IPA analysis hits is found in Figure 50. When comparing our RNA-seq and MAJIQ analysis data sets (p val <0.05 , [Δ PSI], $\geq 10\%$), 387 transcripts had an overlap of significant gene expression changes and LSV changes in uninfected samples. In contrast, there was

virtually no overlap between genes undergoing alternative splicing with those whose expression changed in the absence of hnRNP F in STm-infected or Mtb-infected cells, with only 65 and 4 transcripts overlap in LSV and gene expression changes, respectively. Interestingly, there were almost 5 times the number of genes with differences in alternative splicing compared to overall gene expression in Mtb-infected samples. Displaying this data using Venn diagram illustrates that uninfected and STm-infected macrophages share 331 hnRNP F-dependent alternatively spliced genes, whereas uninfected and Mtb-infected macrophages share 249 hnRNP F-dependent genes. These data suggest that hnRNP F's influence on gene expression can be attached to its function in controlling alternative splicing decisions, but also leaves room for distinction of gene regulation by hnRNP F through diverse mechanisms ³⁹⁰.

We next manually cataloged genes with hnRNP F LSV changes to try to identify master regulators of ISG expression whose alternative splicing could be regulated by hnRNP F. We found several interesting candidates, including *Irf7*, *Ikbke*, *Irf9*, *Irf5*, and *Irf1*, that were significantly impacted by loss of hnRNP F at the levels of gene alternative splicing (Figure 47, Figure 48, & Figure 49). Specifically, the MAJIQ-identified LSV events of *Irf7*, *Ikbke*, *Irf9*, *Irf5*, and *Irf1* were found significantly more in hnRNP F KD macrophages vs. SCR control macrophages.

Two hnRNP F-dependent LSVs were identified by the MAJIQ algorithm in *Irf7* (delta PSI exon 9-exon 10 = -0.168 versus exon 8-exon 9 = -0.145) (Figure 47, Figure 48, & Figure 49). Specifically, exclusion of exon 9 or retention of intron 9, happens more frequently in hnRNP F depleted macrophages in our MAJIQ analysis. MAJIQ uses

pseudo-transcript diagrams to identify every possible exon and intron annotated in a specific gene. Exon 9 and intron 9 relate to genomic coordinates of exon 7 and intron 7 in the canonical *Irf7* transcript. Ultimately, our results align with hnRNP F's role in activating splicing. To quantify these events in hnRNP F KD macrophages, we performed qPCR using primers designed around exon 9 and exon 10 to detect intron retention in *Irf7*. This intron retention event occurred more in hnRNP K KD macrophages upon different immune agonists (LPS, ISD, and IFN β) (Figure 47). Previous research done by Frankiw et. al also showed that *Irf7* expression could be regulated at the level of intron retention, although they examined a different *Irf7* intron.

To identify possible RNA-binding motifs in *Irf7*, we performed manual analysis of annotated hnRNP F consensus motifs along the *Irf7* transcript. In Voila visualization, a “quasi-gene” is formed utilizing all of the known LSVs and exons. Figure 48 shows a canonical depiction of *Irf7* transcript. Interestingly, the region of exon 3-exon 5 (aligning with MAJIQ highlighted region in yellow), show several possible hnRNP F binding sites, suggesting hnRNP F may regulate intron removal and exon inclusion by binding to target transcripts.

Although these data do not quite implicate *Irf7* as the ISG phenotype “smoking gun” these analyses certainly demonstrate that hnRNP F is an activator of splicing and can act on alternative exon inclusion events or intron removal changes that may impact the outcomes of innate immune activation in macrophages.

Similar to our previous report on hnRNP M, we wanted to test whether hnRNP F target specificity is at the level of the transcript itself, we treated hnRNP F KD

macrophages with a panel of innate immune agonists including LPS, ISD, polyI:C, and IFN β . LPS is a potent agonist of TLR4^{149,391} and component of the *Salmonella* outer membrane as well as tuberculosis having cell wall component of lipoarabinomannan (LBP), resembles LPS with its ability to induce inflammatory gene expression³⁹²⁻³⁹⁴. Treatment with LPS was sufficient to reproduce downregulation of *Ifnb* and ISG expression in hnRNP F KD macrophages (Figure 42). Similar to *Salmonella* and *Tuberculosis* infection, we observed a 5- to 6-fold reduction of *Isg15*, *Ifit1*, and *Ifnb* in hnRNP F KD cells treated with 100 ng/mL LPS (from *E. coli*) at 4h. Interestingly, at 2h we do not see statistical difference in SCR vs hnRNP F KD ISG expression. However, we do continue to see a decrease in *Ifnb* gene expression at 2h post-LPS and STm infection (Figure 42). Transfection of hnRNP F KD cells with 1 μ g/mL ISD led to reduction of *Ifnb* and ISGs in hnRNP F KD cells (Figure 43). In hnRNP F KD cells, we see downregulation of *Isg15*, *Ifit1*, and *Ifnb* (Figure 43). Similarly, upon treatment with Poly I:C, which activates IRF through MAVS/RIG-I, we see a similar downregulation of *Ifnb1* and ISGs in hnRNP F KD cells. However, we observe less differences in earlier activation but stronger differences later in activation and this suggests that hnRNP F regulation of ISG expression occurs continuously during activation.

In our data we consistently see lower *Ifnb1* gene expression across time points, agonists and infections. As several ISGs are upregulated during the IRF3/IRF7 axis, but these same ISGs are also upregulated upon IFN- β /IFNAR signaling that requires IFN β protein expression. Therefore, we wanted to test whether the *Ifnb1* gene expression differences in hnRNP F KD macrophages lead to differences in IFN β protein expression.

We infected cells with STm for 4h and collected supernatants. Supernatants were then placed on ISRE:IFNB cells for 6h, lysed, and analyzed using the plate reading capacity of the Cytation 5 Cell Imaging Multi-mode Reader. At 4h we saw a consistent downregulation of IFNB protein levels in our hnRNP F KD macrophages when compared to our SCR control cells (Figure 46). This suggests that lower IFNB levels could lead to a downregulation of signaling through IFNAR/STAT and lower ISG expression in our hnRNP F KD macrophages.

To further explore our hypothesis that lower IFN β expression in hnRNP F KD macrophages is leading to an overall decrease in ISG expression, we wanted to treat IFNAR directly with recombinant IFN β for 4h. With equal amounts of IFN β , our hypothesis is that hnRNP F KD cells would recover the ISG phenotype. RNA was collected at 4h post-treatment and analyzed via qRT-PCR. Upon IFN β treatment, hnRNP F KD cells showed similar upregulation of *Irf7*, *Ifit1*, *Isg15*, and *Mx2* (Figure 44), rescuing the phenotype of lower ISG expression in hnRNP F KD cells. This finding suggests the effects hnRNP F has on ISG expression happen in the first part of the TRIF-TBK1 sensing cascade, before IFNAR signaling occurs. Overall, our results argue for hnRNP F playing a crucial, conserved role in regulating IFN β expression leading to and overall immune response gene expression through IFN β regulation dependent on the TBK1-IKK ϵ axis.

Numerous transcription factors play a role in *Ifnb* expression termed the “enhanceosome”²⁷⁸. Several of these same transcription factors are downregulated in hnRNP F KD cells during STm and Mtb infection (e.g. *Irf7*, *Irf3*, *Irf1*, & *Irf5*). Our IFN β

results suggests that the component that hnRNP F may be regulating could be part of the initial TBK1-IKK ϵ -IRF3/IRF7 axis, rather than downstream of IFNAR and IFN- β signaling. IRF7 and IRF3 are known as critical components of the IFN- α /IFN- β in response to bacterial and viral infections^{395(p3),396,397(p7)}. Since STAT1 and STAT2 are downstream of IFNAR and IFN treatment did not lead to a downregulation of ISGs in the hnRNP F KD cells, we first tested IRF7 and IRF3 activation and expression levels. As alternative splicing can produce *Irf7* transcripts that can be sent for decay or affect protein domains, we wanted to identify if *Irf7* alternative splicing in hnRNP F KD cells could affect protein levels. Cells were treated with LPS and ISD and then RNA samples were collected at 4h in order to look at gene expression of each of these factors (Figure 42 & Figure 43). Consistent with our RNA-Seq results, we saw a downregulation of *Irf7*, but not *Irf3* during agonist treatment. To further confirm our gene expression results, we treated SCR control and hnRNP F KD cells with LPS and ISD for 4h and 8h and collected protein samples to look at IRF7 protein levels. In uninfected, 4h, and 8h we saw a decrease in IRF7 protein levels in hnRNP F KD macrophages compared to SCR control (Figure 51). These results suggest that hnRNP F plays a role in promoting *Irf7* expression, possibly via alternative splicing, such that loss of hnRNP F decreases IRF7 protein abundance. This consequence of hnRNP F KD could be explain the lack of ISG induction during STm or Mtb infection.

Data presented thus far strongly suggests that loss of hnRNP F impacts initial *Ifnb* activation without impacting ISG expression downstream of IFNAR. One obvious way to modulate *Ifnb1* expression is through altering the activity of its major

transcription factor IRF3. Indeed, while IRF7 can play a role in regulating *Ifnb1*, IRF3 has been identified as the primary activator of *Ifnb1* gene expression³⁹⁸. IRF3 is located in the cytoplasm of resting cells. Upon immune activation, phosphorylation of IRF3 promotes homo-dimerization and translocation into the nucleus. To investigate if hnRNP F is needed for IRF3 translocation into the nucleus, we performed cellular fractionation and measured cytoplasmic and nuclear IRF3 during LPS and ISD treatment in hnRNP F KD and SCR control macrophages via western blot. During each agonist treatment, we found similar levels of IRF3 at each time point in our hnRNP F KD vs. SCR control cells. Nuclear translocation upon agonist treatment occurred similarly in our hnRNP F KD cells and SCR control cells (Figure 52). This suggests IRF3 signaling in hnRNP F KD macrophages is intact and is not the cause of lower *Ifnb1* expression. Additionally, we did not observe any significant changes in hnRNP F protein expression over the same time course of LPS, ISD, or poly I:C treatment. This suggests that the mechanism for which hnRNP F regulates *Ifnb1* and overall ISG expression is independent of IRF3 translocation.

Taking into account the more dramatic phenotype we observe for *Ifnb1* expression in the absence of hnRNP F and the fact that hnRNP F is dispensable for ISG expression if IFNAR is stimulated directly with IFN- β , we developed two possible explanations: (1) hnRNP F alters the splicing/expression of a transcription factor of signaling component required for *Ifnb1* expression downstream of TRIF activation and/or dsDNA sensing, or (2) hnRNP F acts directly to promote transcription of *Ifnb1*

(because *Ifnb1* does not contain an annotated intron it is extremely unlikely for hnRNP F to be acting on *Ifnb1* transcripts at the level of splicing).

hnRNP F Mass Spec Reveal Protein Interactions with Core Spliceosome Partners

To further elucidate how hnRNP F regulates *Ifnb1* gene expression, we sought to identify the protein binding partners of hnRNP F. We began by hypothesizing that hnRNP F localization in macrophages may inform its function. We performed bioinformatics analysis to look for a nuclear export signal within hnRNP F's amino acid sequence. Surprisingly, we identified a nuclear export signal near the N-terminal end of hnRNP F (Figure 53). Interestingly, we did not find a strong nuclear localization signal, suggesting hnRNP F may translocate frequently. We then performed immunofluorescence microscopy experiments using 3XFL-hnRNP FLAG stably expressing macrophages to look at the localization of hnRNP F in resting and activated cells. We treated cells with LPS for 1h, 2h, and 4h and detected hnRNP F with an anti-FLAG antibody. In resting macrophages, hnRNP F seemed to be dispersed within the cell and was detectable in nuclear and cytoplasmic compartments. When cells were treated with LPS, we observed a similar diffuse localization pattern. Using Cytation 5 imaging software, we analyzed cytoplasm compartments, nuclear compartments, and hnRNP F signal to quantitatively measure translocation. As expected, hnRNP F showed a similar translocation score during each time point compared to resting cells (Figure 55). Together, these results suggest hnRNP F can potentially regulate RNA processing and gene expression at steps occurring in either the cytoplasm or the nucleus.

To identify hnRNP F protein partners, we performed immunoprecipitation and mass spectrometry (IP-MS) from macrophages as we previously described for hnRNP M, only this time we analyzed both the cytoplasm and the nucleus, as immunofluorescence experiments revealed the protein can be found in both cellular compartments. (Figure 56). Briefly, we generated 3XFL-hnRNP F stably expressing RAW264.7 macrophages, fractionated the cytoplasm and nuclear fractions, immunoprecipitated 3XFL-hnRNP F from each fraction using FLAG beads, and sent these samples for analysis via LCMS/MS. Utilizing STRING databases, we overlaid our data with previously known hnRNP F interactions. Mass spec analysis of the cytoplasm identified hnRNP F-associated peptides derived from hnRNP H1, hnRNP U, and SRSF6, which align with published mRNA decay/translation functions of these proteins^{16,135}. Interestingly, a few immune-related proteins were found in hnRNP F IP/MS, including JAK1 (Janus Kinase 1), which interacts with the IFNAR receptor (Figure 57 and Figure 58). We also identified peptides derived from EIF2s1, a translation initiation factor, suggesting a possible role for hnRNP F in protein translation.

The proteins hnRNP F interacts with in the nucleus are primarily involved in RNA-processing. Remarkably, we identified peptides derived from several critical core spliceosomal proteins including SF3b1, SNRPN and SNRPA. Sf3b1 encodes the U2 snRNP and plays a role in 3' branch site recognition^{399(p1)} while SNRPN and SNRPA are components of the U1snRNP. We also found that nuclear hnRNP F interacted with NONO, a component of paraspeckles that regulates transcription and promotes spliceosome assembly^{371,400}. To confirm our mass spec analysis interactions, we

immunoprecipitation followed by western blot. This approach confirmed that hnRNP F can interact with Sf3b1. Curiously, this interaction was seemingly enhanced in cells treated with LPS for 2h (Figure 59). These results suggest that hnRNP F is involved in splicing decisions with the core spliceosome complex of Sf3b1, although it also may interact with alternative complexes and paraspeckle factors that regulate non-splicing steps of RNA processing. hnRNP F was also found to interact with SAFB and SSB, which have previously been shown to negatively regulate *Ifnb1* expression^{401,402}, NPM1, which can regulate DNA-binding of NF- κ B to *Ifnb1*, and TRIM28, which is a positive regulator of *Ifnb1*^{403,404}. It is possible that hnRNP F's contribution to *Ifnb1* expression is through one or more of these interactions.

Phosphorylation of hnRNP F influences ISG expression

We next leveraged the *Mycobacterium tuberculosis* global phosphoproteomics dataset and identified 4 differentially phosphorylated serine residues on hnRNP F (S23, S104, S237, and S310) (Figure 53)³²⁶. We then generated 3xFLAG-hnRNP F constructs with phosphomimic (S→D) or phosphodead (S→A) mutations at each of the serines and made stable RAW 264.7 macrophages expressing each of these alleles in wild-type RAW 264.7 macrophages that still contain a wild-type hnRNP F. To begin to elucidate the impact of phosphorylation on regulating hnRNP F and thereby ISG expression, we infected these cells with STm and collected RNA at 4h. Remarkably, there were clear differences in *Ifnb1* and ISG expression when these hnRNP F phospho-mutant alleles were expressed (Figure 54). Specifically, S21D, 104D, and 237A showed decreased *Ifnb1* and essentially phenocopied knockdown of hnRNP F. While not statistically

significant, several mutants showed an increased in *Ifnb1* expression. Further studies will be needed to investigate how these mutants impact alternative splicing of transcripts like *Irf7* and whether they alter interactions with hnRNP F protein binding partners.

Regardless of the exact mechanism, these enticing results suggest that phosphorylation of hnRNP F can have functional consequences on innate immune gene expression.

Discussion

We conclude that hnRNP F regulates the expression of dozens of ISGs, likely through controlling *Ifnb1* expression. HnRNP F-dependent changes to *Ifnb1* expression occur downstream of diverse innate immune agonists and different bacterial infections (Figure 60). Interestingly, hnRNP F was found to differentially splice several master regulators of ISGs, including *Irf7* and *Ikbke*. These intron retention and exon exclusion events that increase in the absence of hnRNP F are predicted to target these transcripts for degradation, which leads to lower protein levels in the case of IRF7. Future experiments will continue to elucidate the contributions of these alternatively spliced isoforms to the ISG phenotype we observe in hnRNP F KD macrophages.

Overall, our data support a whereby knocking down hnRNP F in macrophages causes a failure to induce *Ifnb1* expression, perhaps via generation of alternatively spliced isoform of the transcription factor IRF7 that target the transcript for nonsense mediated decay. Because *Ifnb1* transcript and protein levels remain low, hnRNP F KD macrophages are defective at engaging IFNAR and activating STAT-dependent transcription of ISGs (Figure 60). While the molecular mechanisms driving hnRNP F-dependent phenotypes in infected macrophages remain unconfirmed, our studies have

uncovered a novel role for hnRNP F in regulating IFN β and innate immune gene expression. We have also implicated phosphorylation of hnRNP F in regulating *Ifnb1* expression during the innate immune response. We hypothesize that some of these modifications influence localization of hnRNP F and/or its ability to interact with some of the protein binding partners we identified in our mass spectrometry analysis like Sf3b1. Indeed, my work shows that interaction between Sf3b1 and hnRNP F may be stronger following LPS treatment. It is possible that this increase in affinity between the two proteins occurs via post-translational modification of one or both of these factors. It is also possible that strengthening the interaction between hnRNP F and Sf3b1 serves to help the spliceosome promote innate immune gene expression by encouraging exon inclusion and limiting exon skipping/intron retention (which are increased in cells lacking hnRNP F). It will be interesting to determine the specific serine residues whose phosphorylation modulates hnRNP F's interaction with Sf3b1 and investigate whether mutation of these residues alters splicing efficiency/fidelity during macrophage activation. It will also be interesting to following up on the interaction between hnRNP F and NONO, as our work on hnRNP M suggests that modulation of the paraspeckle formation and/or dissociation constitutes a major way that macrophages control innate immune gene expression.

CHAPTER V

GLOBAL ANALYSIS OF HNRNP AND SRSF FAMILY PROTEINS DURING THE INNATE IMMUNE RESPONSE

Introduction

When innate immune cells like macrophages sense pathogens they undergo dramatic gene expression reprogramming, with some genes being transcriptionally induced >1000-fold²⁶⁶. Despite these mind-boggling levels of gene expression activation, the innate immune response needs to be tightly regulated—too weak of a response may not be sufficient to ensure pathogen elimination and a too strong of a response risks chronic inflammation and/or autoimmunity^{264,405}. Upon PAMP recognition, signal transduction factors activate several transcription factors that have been widely studied. Overall, this activation leads to transcription of pro-inflammatory cytokines, interferons, and ISGs. From our previous research with hnRNP M, we have shown the post-transcriptional regulation of the innate immune response is a major, albeit underappreciated, regulatory node in balancing chronic inflammation and resolution of infection.

Very limited research has been conducted on viral or bacterial infections and their effects on phosphorylation, regulation, or splicing changes mediated by SR proteins. Of the immune-related research conducted, much has focused on T-cell and B-cell function. SRSF1, SRSF9, SRSF3, and SRSF7 regulates *Cd45* by promoting exon inclusion during T-cell activation⁴⁰⁶. SRSF1 has been implicated in T-cell activation

through binding to the 3' UTR of CD3 ζ , promoting intron retention⁴⁰⁷. SRSF2 was also found to play a role in splicing *Cd45*, suggesting regulating expression of this gene by SRs is held in critical regard by T-cells⁴⁰⁸.

During Human Papilloma virus infection, SRSF1, SRSF2, and SRSF3 are up-regulated⁴⁰⁹. SRSFs were also found to be upregulated as autoantigens in autoimmune disorders, such as lupus⁴¹⁰. Some work has been done looking at SRSF functions in innate immunity in plants. Yeast two-hybrid study showed SRSF proteins required interaction with MOS14, which is an important regulatory factor in pathogen defense in plants⁴¹¹. This interaction impacted splicing patterns of MOS14 regulated genes, *snc1* and *rsp4* and compromised resistance⁴¹¹. While unclassified as an SRSF because of its lack of RRM domain, an SRSF-like protein, termed SR15, was also found to be a splicing inhibitor of HSV1 (Herpes simplex virus I)⁴¹². Beyond this work, there is a clear lack of studies on SRSF proteins during the innate immune response. Here, we aim to shine a spotlight on the diverse contribution SRSF proteins make to modulating the macrophage transcriptome during infection with the important human pathogen STm.

Having previously identified completely distinct contributions of two RNA binding proteins, hnRNP M and hnRNP F, to macrophage gene expression during infection, we set out to unbiasedly survey a panel of hnRNP and SRSF family proteins to understand how they individually, and as proteins families, regulate innate immune gene expression. To these ends, we selected 5 hnRNPs, (C, F, K, M, U) and 5 SRSFs (1, 2, 6, 7, 9) that were identified as being either differentially phosphorylated and/or ubiquitinated upon *Mycobacterium tuberculosis* infection of primary bone marrow

derived macrophages, suggesting they, over other RNA binding proteins, play a privileged role in the innate immune response³²⁶. While these proteins, particularly the SRSFs, are well-known to be phosphorylated, little is known about the regulatory potential of specific phosphorylated serines on SRSF proteins or hnRNPs, nor do we fully appreciate how PTM of splicing factors could be coupled to pathogen sensing. We hypothesize that PTM of splicing factors downstream of PRRs specialize the spliceosome in a way that helps promote the macrophage innate immune gene expression program. By altering (1) the capacity of SRSF and hnRNPs to engage in protein complexes, (2) protein-RNA interactions, and (3) subcellular localization of these factors, PTMs can control splicing decisions to fine-tune innate immune gene expression and control infection. In this way, a splicing factor can make splicing decisions in activated macrophages distinct from those it controls in resting cells.

In uninfected and *S. Typhimurium* infected cells, we found that loss of hnRNPs and SRSFs impacts expression of completely different sets of genes. Interestingly, we also found hnRNP and SRSF protein families do not equally contribute to innate immune gene expression. We also found that not all innate immune transcripts rely on these hnRNPs and SRSFs for proper regulated. These results suggest that splicing regulation is not a blanket mechanism whereby all intron containing genes are equally dependent on splicing factors for proper induction. Rather, our results suggest that certain innate immune transcripts are uniquely sensitive to loss of splicing regulation. In addition to looking at steady-state gene expression changes, we also measured alternative splicing changes induced by loss of SRSFs and hnRNPs. Using the MAJIQ

algorithm, we identified several critical innate immune transcripts that rely on these factors to generate canonical isoforms, including genes in the *NF-Irf*, *Mapk*, *Ifit*, and *Gbp* families. Together, our work uses unbiased high-throughput sequencing and bioinformatic approaches to highlight a neglected role for hnRNPs and SRSFs in global regulation of innate immune gene expression.

Results

Determining the Contribution of Splicing Regulatory Proteins to Macrophage Gene Expression During *Salmonella* Infection

To begin to understand how individual splicing factors impact innate immune gene expression in macrophages, we first generated stable knockdown RAW 264.7 macrophage-like cell lines for individual hnRNPs and SRSFs via lentiviral transduction of shRNA constructs. SRSF and hnRNP family members were prioritized for inclusion in this analysis on basis of whether or not they were identified as differentially phosphorylated in a recently published phosphoproteomics dataset of Mtb-infected macrophages.

Although the shRNA constructs were all drug selected, alongside scramble (SCR) controls at the same time, for the same length of time, under the same conditions, it was immediately apparent that certain splicing factors tolerated knockdown better than others. For example, we were never able to achieve more than ~50% knockdown for factors like SRSF1 and 2, while factors like SRSF6 and 9 could be knocked down to about 10% their initial transcript levels. These differences likely reflect the cell's reliance on each of these factors for splicing pre-mRNAs of essential genes. While

differences in knockdown efficiency constitute a clear caveat in these studies, we are careful not to make conclusions based on the “strength” of a particular phenotype, as the number of genes affected by loss of an SRSF or hnRNP is likely highly dependent on how much of that factor is actually lost by the cell. We instead simply report on what happens when each of these factors is ablated by X amount, whether it be 50% or 90%, which will still provide important insights into how each of these factors control gene expression in resting and activated macrophages.

Each of these KD RAW 264.7 cell lines was infected with the gram-negative bacterial pathogen, *S. Typhimurium*. We confirmed that our *Salmonella* infection was successful by measuring *Il1b* and *Tnfa* expression at the key innate immune transcripts at 4hr post infection, at which point, robust induction is well-characterized (data not shown). Total RNA was collected for RNA-seq from resting macrophages and STm-infected macrophages at this 4h time point and sent for bulk RNA sequencing. An average of ~60.2 million raw sequencing reads were generated from three biological replicates of each knockdown (for Uninfected and *Salmonella*-infected samples). Reads were aligned, quantified, and analyzed using CLC Genomics Workbench (Qiagen).

To begin to compare how loss of individual regulatory splicing factors influences innate immune gene expression, we compiled all genes that were differentially expressed either in resting macrophages (top) or at 4h post—STm (bottom) infection in at least one knockdown cell line (compared to SCR control) ($p < 0.05$) to create the profiles shown in Figure 61. We found 2,659 genes that were affected by at least one knockdown in resting cells and 1,600 genes were affected by at least one knockdown specifically during STm

infection. In looking at the “profiles” generated for each of these knockdowns, it is immediately apparent that each hnRNP/SRSF, for the most part, impacts expression of a distinct set of genes. With the exception of hnRNP M, which we have previously characterized as a repressor of innate immune gene expression, knockdown of hnRNPs and SRSFs led to downregulation of target genes, consistent with these factors generally promoting or activating splicing/gene expression. This trend was similar in resting macrophages and during STm infection. Although many of these affected gene profiles were distinct, we did observe obvious overlap between genes regulated by hnRNP C, K, U and to a lesser extent, hnRNP F, suggesting hnRNPs may work cooperatively, as was previously shown by Huelga et al ²⁹.

Surprisingly, SRSF1 and SRSF2 did not appear to regulate many innate immune transcripts upon STm infection. In our macrophage cells, we did not see drastic gene expression changes with SRSF1 or SRSF2 knockdown cells. While this may be attributed in part to knockdown efficiency, SRSF2 has similar knockdown to hnRNP U, SRSF9, and SRSF6. These hnRNPs and SRSFs showed drastic differences in dozens of different genes. Therefore, we believe that SRSF2 and SRSF1 may not be contributing to the innate immune response at 4h but may contribute at a later time or by different mechanisms unappreciated by RNA-Seq differential expression. Interestingly, SRSF2 was not found to be differentially phosphorylated during Mtb infection which also contributes to the notion of later or minimal contributions during the innate immune response by SRSF2³²⁵.

Depletion of hnRNPs Impacts Unique Sets of Innate Immune Genes

We measured a total of 2,952 differentially expressed genes in hnRNP knockdown macrophages upon STm infection (vs. SCR control), compared to 3,693 differentially expressed cells in hnRNP knockdown samples. The top 30 genes with >1.5-fold change in gene expression and a p-value of 0.05 that were differentially expressed between *Salmonella*-infected hnRNP knockdowns and their respective SCR controls are displayed in Figure 62. Heatmaps are representative of down-regulated vs. up-regulated genes.

Dozens of innate immune response genes were found dysregulated in hnRNP depleted cells. Expression of several key innate immune response genes are found decreased in the majority of hnRNPs. For example, *Gbp5*, *Gbp2*, *Mx1*, and *Ifit2* have decreased expression in hnRNP C, F, K, and U. Interestingly, hnRNP M was the only hnRNP to show upregulation of these same genes, as we have previously shown. Furthermore, hnRNP F had a striking phenotype, whereby its depletion almost exclusively caused downregulation of gene expression in STm-infected macrophages, with only 3 genes significantly up-regulated.

Surprisingly, hnRNP C, K, and U had a similar gene expression profile with down-regulated genes and up-regulated genes. *Wnt1*, *Dmpk*, and *Dusp2* were some of the genes up-regulated in hnRNP C, K, and U, while *Nos2*, *Ifi47* and *Cmpk2* were all down-regulated in these samples when compared to SCR control. This suggests a possible collaborative function of these hnRNPs in coordinate a specific regulon of gene expression during *Salmonella* infection.

To further investigate the overlap of hnRNP regulons, we utilized Venn diagrams to plot all differentially expressed genes with $pval > 0.05$ (Figure 66). Upon analysis of hnRNP overlap of differentially expressed genes in uninfected macrophages, we identified 67 genes whose expression was altered by all five hnRNPs. Upon STm infection, this common node increased to 104 genes. By far, hnRNP F depletion impacted the most genes, with 1,943 genes changing expression in uninfected samples, compared to ~400 genes whose expression was altered in resting hnRNP C, K, and U knockdown cells. When comparing uninfected vs. STm-infected differentially expressed genes, only ~20% of hnRNP F regulated genes were found in both uninfected and STm infected samples, compared to other hnRNPs where ~40-50% of genes were found in each condition. This suggest that: 1. hnRNP F plays a role as a master regulator of gene expression compared to other hnRNP family members and 2. hnRNP F's canonical function is modulated under innate immune activation.

Depletion of SRSFs Impacts Unique Sets of Innate Immune Genes

Differential expression analysis revealed a total of 1,777 differentially expressed genes upon in SRSF knockdown resting cells compared to SCR controls and 1,525 differentially expressed genes in STm-infected knockdowns vs. SCRs. The top 30 genes with >1.5-fold change in gene expression and a p-value of 0.05 that were differentially expressed between STm-infected SRSF knockdowns and their respective SCR controls are displayed in Figure 63. Unlike the hnRNPs, SRSFs were less uniform in the overall number of genes they up vs. downregulated. For example, SRSF1 and SRSF7 displayed an overall trend of down-regulated genes when they were depleted in macrophages

suggesting an activation role in innate immune gene expression. Alternatively, SRSF9, SRSF2, and SRSF6 demonstrated a trend of 50/50 split of down-regulated and up-regulated genes. While several similar immune genes like *Mx1* and *Ifi204* were also found in the majority of hnRNP knockdowns, SRSF regulated genes did not show a striking overlap amongst SRSF 1, 2, 6, 7, or 9. This suggests that even more so than hnRNPs, SRSF proteins have independent and diverse impacts on macrophage gene expression regulation upon bacterial infection.

Likewise, SRSF-regulated genes showed less overlap compared to those regulated by hnRNPs (Figure 62). In uninfected samples, only 17 genes were found to be regulated by each SRSF and only 11 genes during STM infection. Venn diagram analysis showed SRSF6 and SRSF7 overlap with 55 genes in uninfected samples and an increase to 82 genes in STM infected samples (Figure 67). Similar to hnRNP F, SRSF6 and SRSF7 regulate dozens more genes, comparatively. Interestingly, SRSF1 regulates over 300 genes in uninfected samples with a small overlap with STM infected genes. However, SRSF1 only regulates a little over 100 genes upon infection. This suggests that SRSF1 function is also regulated during infection, with the cell promoting less regulation of genes by SRSF1.

IPA Analysis Reveals Targeted Pathways In hnRNP and SRSF Knockdowns

To gain insight into what is common about the genes whose expression was impacted by loss of specific hnRNP or SRSF proteins, we performed functional classification and Ingenuity Pathway Analysis (IPA) of differentially expressed genes ($p_{val} > 0.05$). IPA delivers a tool to assemble and extract relevant information from our

RNA-Seq. While the caveat is that it relies on published research and databases, it is able to combine individual genes to identify biological themes and mechanistic regulatory networks. The top functions identified by IPA in our RNA-Seq for uninfected and STm-infected are shown in Figure 64 and Figure 65. IPA Canonical Pathways identified *EIF2 Signaling*, *Unfolded Protein Response*, and *NRF2-mediated Oxidative Stress Response* as some of the top affected pathways by hnRNPs and SRSFs in resting macrophages. In STm-infected RNA-Seq IPA Canonical Pathway Analysis, there were more drastic changes in z-scores compared to hnRNPs. Role of PRRs, Interferon Signaling, and Role of PKR were pathways enriched for differentially expressed genes in several of the hnRNP- and SRSF-depleted cell lines (Figure 64 & Figure 65). Strikingly, hnRNP F and hnRNP M showed opposing z-scores aligning with hnRNP F's activation function and hnRNP M's repression function during the innate immune response that we previously identified ³⁹⁰.

Upstream Regulator Analysis (URA) of IPA was used to identify molecules upstream of the differentially expressed genes that had a high probability to cause the observed gene expression changes. URA has two outputs - an overlap P-value measuring enrichment of network-regulated genes in the dataset and an activation Z-score. Using predicted patterns based on published data, the Z-score measures a statistically significant corresponding match between the detected gene expression changes. In uninfected samples, MYC (proto-oncogene, bHLH transcription factor), IRF3 (Interferon Regulator Factor), and MLKIPL (MAX Dimerization Protein Interacting Protein Like), were some of the upstream regulators implicated in the gene expression

changes that occur in the hnRNP and SRSF knockdown samples (Figure 69 & Figure 70). Interestingly, URA analysis identified a unique set of possible upstream regulators for SRSF1 and SRFS6, where these factors have opposing z-scores. Additionally, this analysis further separated hnRNP C, K, and U where hnRNP K and hnRNP U have similar upstream regulators and z-scores, where hnRNP C has similar upstream regulators, but the activation z-score differs. This may suggest that hnRNP C, K, and U may regulate similar genes, but this occurs during different regulation mechanisms or with different kinetics.

The CNA (Causal Network Analysis) generalizes URA by incorporating pathways from regulators to regulated molecules. Similar to the URA analysis, MLXIPL, MYC, and RICTOR were some of the top z-scores among hnRNPs and SRSFs in uninfected samples (Figure 71 & Figure 72). Interestingly for each of the URA and CNA, while hnRNP M and hnRNP F have the most drastic gene changes, hnRNP C, K, and U have the most drastic z-scores. This further supports our hypothesis that hnRNP C, K, and U are regulating a similar regulon of genes.

Reliance on Splicing Factors Does Not Correlate with Expression of *Salmonella*-Induced Innate Immune Genes

We next asked whether genes whose expression is most induced by STm infection were more reliant on hnRNPs or SRSFs for proper expression. To identify the most transcriptionally activated in STm-infected macrophages, we pooled together each SCR used in our original analysis and identified differentially expressed genes using CLC Genomics Workbench. Consistent with previous literature, genes like *Illb*, *Rsad2*,

Ifnb1, *Ifit1*, *Tnf*, and *Il6*, were massively upregulated upon *Salmonella* infection at our 4h time point (Figure 68). Interestingly, as we continue to look down this list, to genes whose expression is induced via a much smaller fold-change, we still see hnRNP and/or SRSF expression changes. This observation suggests that RNA-processing regulation is uncoupled from the level of transcription induction and supports a model whereby certain innate immune transcripts are more reliant on RBP for proper expression than are other innate immune transcripts. This also points to the idea that highly expressed genes are not necessarily subject to more splicing regulation. This also aligns with Pandya-Jones et. al where they report that only certain innate immune transcripts displayed obvious co-transcriptional splicing regulation⁴.

From this same analysis, we identified several genes that are highly regulated by hnRNPs and SRSFs and others that do not seem to be affected by depletion of these factors. Several critical cytokines like *Il1a* and *Il6* were found to be affected by knockdown of several hnRNPs and SRSFs. Similarly, many interferon stimulatory genes such as *Ifnb1*, *Ifit3b*, *Mx1*, *Rgs16* were affected by knockdown of several hnRNPs and SRSFs. With each of the genes that were affected by hnRNP or SRSF knockdown, the extent to their dysregulation varied between factors. As our analysis is conducted at 4h, this suggests that these factors regulate the same genes although with different kinetics. On the other hand, there were some genes that are highly induced upon *Salmonella* infection that had no change in expression when hnRNPs and SRSFs were depleted; *Ccl17*, *Il33*, *Cish*, *Mtmr7*, and *Cx3cl1*. This may be due to the kinetics of these gene's regulation, specific structure, or alternative RBPs that regulate these transcripts. Overall,

this data supports our hypothesis that RNA-processing and splicing-dependent changes are independent of expression level.

Alternative Splicing Changes Do Not Account for the Vast Majority of Expression Changes

The discovery that hnRNPs and SRSFs do not correlate with transcriptional upregulation during STm infection advocates that RNA-processing mechanisms like splicing and mRNA export may be critical procedures in regulating the innate immune response, outside of transcriptional upregulation. To understand how hnRNPs and SRSFs influence RNA-processing via alternative splicing changes, we utilized MAJIQ. MAJIQ quantifies LSV's (local splice variants). This enables detection of intron retention, exon skipping, alternative 5', and alternative 3' events.

To compare alternative splicing differences, we performed deltapsi calculations using MAJIQ with SCR control samples and respective hnRNP and SRSF knockdowns. Upon examination of the types of alternative splicing events MAJIQ quantifies, exon skipping was the major event affected seen in all knockdowns (Figure 73, Figure 74, & Figure 75). Interestingly, the total number of LSV events went down during STm infection for each event. hnRNP F had the most LSVs in both uninfected and STm-infected cells, correlating with the number of genes that we saw differentially expressed in our RNA-Seq data.

To understand if these alternative splicing changes contribute to the gene expression we see with hnRNP and SRSF knockdown, we used Venn diagrams to overlap the differences in our RNA-Seq data to the genes identified in our MAJIQ

analysis. As seen in our previous studies with hnRNP M, we did not see a significant overlap with genes differentially expressed and genes identified to have alternative splicing events in our MAJIQ analysis (Figure 76 & Figure 77). hnRNP F, SRSF6, and SRSF7 had the most overlap with ~10% of genes overlapping in each data set. Interestingly, in uninfected and *Salmonella*-infected SRSF samples we see many more genes affected in our MAJIQ analysis vs. our differential gene expression analysis. This suggests while SRSFs may not be altering expression of these genes, these proteins are critical in controlling splicing changes.

Interestingly, hnRNP K and SRSF9 had the least amount of overlap between RNA-Seq and MAJIQ data. hnRNP K had zero overlap in both uninfected and STm-infected, while SRSF9 had only 5 genes overlap in uninfected and in STm-infected samples. With our MAJIQ splicing analysis revealing distinct genes regulated by hnRNP and SRSF factors, we performed IPA analysis of alternatively spliced genes to identify pathways enriched for hnRNP and SRSF-dependent changes. Notably, we observed enrichment for several cancer pathways including *BRCA1 DNA Damage*, *Molecular Mechanisms of Cancer*, and *Myeloid Leukemia Signaling* in our uninfected samples (Figure 78 & Figure 79). This aligns with dozens of reports supporting splicing regulation in cancer processes⁴¹³. Interestingly, we also observed enrichment for *TNFR2 signaling*, *SAPK/JNK Signaling*, in uninfected samples. These pathways play important roles in the innate immune response. While displaying increased significance, IPA analysis of STm-infected samples also showed enrichment for similar pathways as uninfected samples.

We further explored our hnRNP and SRSF-dependent alternatively spliced genes through Causal Pathway Analysis (Figure 80 & Figure 81). Remarkably, our uninfected and *Salmonella*-infected pathways showed similar results like our IPA analysis mentioned previously, with increased significance in STm-infected samples. The top enriched pathways were *camptothecin* and *monobutyl phthalate*. *Camptothecin* is a compound that inhibits DNA and RNA synthesis while *monobutyl phthalate* has been found to inhibit steroidogenesis. Intriguingly, *IFN alpha/beta* and *IFNAR* pathways showed enrichment for alternatively spliced genes across the majority of factors in uninfected and STm-infected macrophages, further demonstrating the importance of RNA-processing in the innate immune response. *IRF7* was also found to be enriched in *Salmonella*-infected samples, suggesting genes regulated by *Irf7* are more affected by knockdown of splicing factors. As our previous work on hnRNP M did not show enrichment of many innate immune pathways in IPA analysis of hnRNP M-dependent alternatively spliced genes, our current global analysis highlights the dynamics of each of these families of splicing factors. Taken these data together, we can generally conclude that the ability of hnRNPs and SRSFs to influence gene expression is distinct from their ability to controlling specific alternative splicing decisions.

Discussion

In this study, we implicate hnRNPs and SRSFs as critical components of the innate immune response. Regulation of these factors come primarily in the form of activation, as when the majority of these factors are removed, we see a downregulation of genes. Furthermore, we found hnRNP and SRSF-dependent gene regulation was

independent of Salmonella-induction of innate immune response genes. Identification of alternative splicing affects show thousands of genes that were affected by hnRNP and SRSF knockdown. Furthermore, these genes showed enrichment for several innate immune related pathways, such as cancer and kinase regulation.

Our research provides insight into the role of hnRNPs and SRSFs as part of macrophage activation upon pathogen sensing. We believe each of these RNA-binding proteins is specialized upon this response through PTMs and is designated to differential gene regulation. We suspect that this functionalization is at least in part driven by differential phosphorylation of these splicing factors. Our results suggest specialization of the spliceosome during the innate immune response. Future research will be dedicated to how these hnRNP and SRSF dependent alternatively spliced isoforms impact innate immune outcomes as well as how kinetics, gene length, intron/exon count, and binding motifs play a role in the differential regulation we see of the same gene by different hnRNPs and SRSFs.

CHAPTER VI

MATERIALS AND METHODS

Cell lines

RAW 264.7 macrophages

RAW 264.7 macrophages (ATCC) (originally isolated from male BALB/c mice) were cultured at 37°C with a humidified atmosphere of 5% CO₂ in DMEM (Thermo Fisher) with 10% FBS (Sigma Aldrich) 0.5% HEPES (Thermo Fisher). For RAW 264.7 macrophages stably expressing scramble knockdown and hnRNP M knockdown, cells were transfected with scramble non-targeting shRNA constructs and hnRNP M shRNA constructs targeted toward the 3' UTR of hnRNP M. After 48 hours, media was supplemented with hygromycin (Invitrogen) to select for cells containing the shRNA plasmid. RAW 264.7 macrophages stably expressing GFP-FL and 3XFL-hnRNP M were transfected for 48 hours and then selected through addition of puromycin (Invivogen).

BMDMs

C57BL/6J mice were used to generate bone marrow derived macrophages (BMDMs). All animals were housed, bred at Texas A&M Health Science Center under approved IACUC guidelines. BMDMs were differentiated from BM cells isolated by washing mouse femurs with 10 mL DMEM. Cells were then centrifuged for 5 min at 1000 rpm and resuspended in BMDM media (DMEM, 20% FBS (Millipore), 1mM sodium pyruvate (Lonza), 10% MCSF conditioned media (Waston lab)). BM cells were

counted and plated at 3×10^6 in 15 cm non-TC treated dishes in 30 mL complete BMDM media. Cells were fed with an additional 15 mL of BMDM media on day 3 of culture.

Cells were harvested on day 7 with 1 X PBS EDTA (Lonza).

Bacterial strains

Salmonella enterica serovar Typhimurium (SL1344) was obtained from Helene Andrews-Polymenis, TAMHSC. Infections with *S. Typhimurium* were conducted by plating RAW 264.7 macrophages on tissue-cultured treated 12-well dishes at 7.5×10^5 and incubated overnight. Overnight cultures of *S. Typhimurium* were diluted 1:20 in LB broth containing 0.3M NaCl and grown until they reached an OD600 of 0.9.

RNA-SEQ

The RNA-Seq experiment was made up of 12 samples: biological triplicate of SCR uninfected, SCR *Salmonella*-infected, knockdown uninfected, and *Salmonella*-infected knockdown cells. RNA-Seq and library prep was performed by Texas A&M AgriLife Genomics and Bioinformatics Service. Samples were sequenced on Illumina 4000 using 2×75 -bp paired-end reads. Raw reads were filtered and trimmed and Fastq data was mapped to the *Mus musculus* Reference genome (RefSeq) using CLC Genomics Workbench 8.0.1. Differential expression analyses were performed using CLC Genomics Workbench. Relative transcript expression was calculated by counting Reads Per Kilobase of exon model per Million mapped reads (RPKM). The differentially expressed genes were selected as those with p value threshold < 0.05 and a fold change value > 1.5 to include in the heatmaps represented. Follow up RT-qPCR analysis was done with both knockdowns, while the best knockdown was selected for sequencing, as

the phenotype often tracked with the knockdown efficiency (M1 = ~80%, M2 = ~60%). Genes with p values < 0.05 were displayed in volcano plots and heatmaps using GraphPad Prism software (GraphPad, San Diego, CA).

S. Typhimurium Infection

Unless specified, cell lines at a confluency of 80% were infected with the S. Typhimurium strains at an MOI of 10 (hnRNP M and hnRNP F experiemtns) and and MOI of 5 (hnRNP and SRRF RNA-Seq) for 30 minutes in Hank's buffered salt solution (HBSS), and subsequently cells were spun for 10 minutes at 1,000rpm, washed twice in HBSS containing 100µg/ml of gentamycin, and refilled with media plus gentamicin (10 µg/ml). Supernatants were collected at 2 hours and 4 hours and analyzed using IL6 ELISA (Biolegend). After removal of supernatant, cells were lysed in Trizol (Thermo Fisher) for RNA collection and analyzed using RT-qPCR.

LPS Treatment

RAW 264.7 macrophages were plated on 12-well tissue-culture treated plates at a density of 7.5×10^5 and allowed to acclimate overnight. Cells were then treated with E. Coli Lipopolysaccharide (Sigma-Aldrich) at 100ng/mL for the respective time points where supernatants and RNA were collected for analysis.

Immunofluorescence Microscopy

RAW 264.7 macrophages were plated on glass coverslips in 48-well plates. Cells were treated with LPS as described above. At the designated time points, cells were washed with PBS (Thermo Fisher) and then fixed in 4% paraformaldehyde for 10 minutes. Cells were washed with PBS 3x and then permeabilized with 0.2% Triton-X

(Thermo Fisher). Coverslips were placed in primary antibody for 1 hour then washed 3x in PBS and placed in secondary antibody. These were washed twice in PBS and twice in deionized water, followed by mounting onto a glass slide using ProLong Diamond antifade mountant (Invitrogen). Images were acquired on a Nikon A1-Confocal Microscope.

Western Blots

Protein samples were run on Any kD Mini-PROTEAN TGX precast protein gels (BioRad) and transferred to 0.45 um nitrocellulose membranes (GE Healthcare). The membranes were incubated in the primary antibody of interest overnight and washed with TBS-Tween 20. Membranes were then incubated in secondary antibody for 1-2 hours and imaged using LI-COR Odyssey FC Imaging System.

siRNA Transfection

BMDMs were plated at 3×10^5 in 12-well TC-treated plates and incubated overnight. Viromer Blue (Lipocalyx) was used to transfect siRNAs according to the manufacturer's instructions. The siRNAs directed against Gapdh, hnRNP M, or hnRNP F were purchased from Thermo Fisher with a negative control present. After 48 hr of siRNA transfection, LPS was added and RNA was collected at the respective time points.

Antibodies

The following primary antibodies were used: rabbit polyclonal hnRNP M (Abcam, #177957), hnRNP F (Abcam, # 50982) rabbit polyclonal Histone 3 (Abcam, #1791), mouse monoclonal Beta-Actin (Abcam, #6276), mouse monoclonal hnRNP L

(Abcam, #6106-100), rabbit polyclonal Beta-Tubulin (Abcam, #179513), mouse monoclonal hnRNP U (Santa-Cruz, sc-32315), DAPI nuclear staining (Thermo Fisher), and mouse monoclonal ANTI-FLAG M2 antibody (Sigma-Aldrich, F3165). Secondary antibodies used were as follows: IR Dye CW 680 goat anti-rabbit, IR Dye CW800 goat anti-mouse (LI-COR), Alexfluor-488 anti-rabbit and Alexfluor-647 anti-mouse secondary antibodies for immunofluorescence (LI-COR).

Cellular fractionation

Macrophage cellular fractionation was done as described in Pandya-Jones et al., 2013. RAW 264.7 macrophages were plated on in 10 cm tissue-culture treated plates at $1-3 \times 10^7$ per plate. Cells and buffers were kept on ice unless noted otherwise. Cells were rinsed twice in cold PBS-EDTA (Lonza) and scraped into 15 mL conical tubes. Cells were spun at 1,000 g for 5 minutes at 4C and resuspended in NP-40 lysis buffer (10 mM Tris-HCl [pH 7.5], 0.05% NP40 [Sigma], 150 mM NaCl, protease inhibitor tablet (Thermo Fisher)) and incubated for 5 min on ice. Lysate was added to 2.5 volumes of a sucrose cushion (Lysis buffer with 24% sucrose) and centrifuged for at 14,000 rpm for 10min at 4C. The supernatant was collected and saved for cytoplasmic protein sample. The nuclear pellet was resuspended in glycerol buffer (20 mM Tris-HCl [pH 7.9], 75 mM NaCl, 0.5 mM EDTA, 0.85 mM DTT, 50% glycerol, protease inhibitor tablet) and lysed with nuclear lysate buffer in equal volume and vortexed 2X for 2 s (10 mM HEPES [pH 7.6], 1 mM DTT, 7.5 mM MgCl₂, 0.2 mM EDTA, 0.3 M NaCl, 1 M UREA, 1% NP-40, protease inhibitor tablet). Lysates were chilled on ice for 2 minutes and then spun at 10,000 rpm for 2 minutes at 4C. Supernatant was collected and used for

nucleoplasmic protein samples. The remaining chromatin pellet was gently rinsed in PBS-EDTA and treated with DNase in DNase buffer for 1 hr at 37C. After incubation, the supernatant was collected for chromatin protein samples. Sample buffer (BIO-RAD) and 2-Mercaptoethanol (BIO-RAD) was added to every protein sample with 5 minutes boiling prior to running on gels for western blots. Approximately 10% of sample was loaded for western blots.

RNase Fractionation

For nuclear lysates treated with RNase, nuclear pellets were resuspended in glycerol buffer. Nuclear lysis buffer was added, and lysates were incubated on ice for 5 minutes. Samples were then divided into two samples with one receiving 1 ul of RNase A (Thermo Fisher) per 50 ul sample and another with no RNase A. Both were incubated at 37C for 30 mins. Lysates were then spun at 10,000rpm for 2 mins and the rest of the fractionation proceeded as described.

Gene Ontology (GO) Canonical Pathway Analysis

To determine the most affected pathways in control versus knockdown RAW 264.7 macrophages, canonical pathway analysis was conducted using Ingenuity Pathway Analysis software from QIAGEN Bioinformatics. Genes that were differentially expressed with a p value < 0.05 from our RNA-SEQ analysis were used as input from uninfected and *Salmonella* Typhimurium infected cells.

RNA isolation and qPCR analysis

For transcript analysis, cells were harvested in Trizol and RNA was isolated using Direct-zol RNA Miniprep kits (Zymo Research) with 1 hr DNase treatment. cDNA

was synthesized with iScript cDNA Synthesis Kit (Bio-Rad). CDNA was diluted to 1:20 for each sample. A pool of cDNA from each treated or infected sample was used to make a 1:10 standard curve with each standard sample diluted 1:5 to produce a linear curve. RT-qPCR was performed using Power-Up SYBR Green Master Mix (Thermo Fisher) using a Quant Studio Flex 6 (Applied Biosystems). Samples were run in triplicate wells in a 96-well plate. Averages of the raw values were normalized to average values for the same sample with the control gene, beta-actin. To analyze fold induction, the average of the treated sample was divided by the untreated control sample, which was set at 1.

Immunoprecipitations

1×10^7 RAW 264.7 macrophages stably expressing FL-hnRNP M, FL-hnRNP F, or FL-GFP in a 10cm plate were harvested in PBS+0.5M EDTA 24 hours post-transfection and pellets were lysed on ice with lysis buffer (50 mM Tris HCl pH 7.4, 150 mM NaCl, 1 mM EDTA, 0.075% NP-40) containing protease inhibitor (Pierce A32955). Strep-tactin superflow plus beads (Qiagen) were washed using buffer containing 5% 1M Tris at pH 7.4, 3% NaCl, and 0.2% 0.5M EDTA. 1000 μ l of the cleared lysate was added to the beads and inverted for 2 hr at 4°C. Beads were then washed 4 times with wash buffer (50 mM Tris HCl pH 7.4 150 mM NaCl 0.5M EDTA, 0.05% NP-40) and eluted using 5x FLAG peptide. Whole cell lysate inputs and elutions were boiled in 4x SDS loading buffer with 10% 2-mercapethanol. Samples were analyzed via western blot.

Mass Spec Immunoprecipitations

Similarly, 5×10^7 RAW 264.7 macrophages stably expressing FL-hnRNP M, FL-hnRNP F, or FL-GFP in 2x15cm plates were harvested in PBS+0.5M EDTA 24 hours post-transfection and pellets were lysed on ice with lysis buffer (50 mM Tris HCl pH 7.4, 150 mM NaCl, 1 mM EDTA, 0.075% NP-40) containing protease inhibitor (Pierce A32955). EZview Red ANTI-FLAG® M2 Affinity Gel Beads (Sigma) were washed using buffer containing 5% 1M Tris at pH 7.4, 3% NaCl, and 0.2% 0.5M EDTA. 1000 μ l of the cleared lysate was added to the beads and inverted for 2 hr at 4°C. Beads were then washed 4 times with wash buffer (50 mM Tris HCl pH 7.4 150 mM NaCl 0.5M EDTA, 0.05% NP-40) and eluted using 5x FLAG peptide. Whole cell lysate inputs and elutions were boiled in 4x SDS loading buffer with 10% 2-mercapethanol. Samples were loaded onto SDS-Page gel and each band was extracted and purified and analyzed via Mass-Spec.

***M. tuberculosis* Infection**

Low passaged lab stocks of each Mtb strain (Erdman strain WT, Erdman *luxBCADE*, or Erdman m-Cherry) were thawed for each experiment to ensure virulence was preserved. *M. tuberculosis* was cultured in roller bottles at 37°C in Middlebrook 7H9 broth (BD Biosciences) supplemented with 10% OADC, 0.5% glycerol, and 0.1% Tween-80. All work with Mtb was performed under Biosafety Level 3 (BSL3) containment using procedures approved by the Texas A&M University Institutional Biosafety Committee. To prepare the inoculum, bacteria grown to log phase (OD 0.6-0.8) were spun at low speed (500g) to remove clumps and then pelleted and washed with PBS twice. Resuspended bacteria were briefly sonicated and spun at low speed once again to further remove clumps.

The bacteria were diluted in DMEM + 10% horse serum and added to cells at an MOI of 10 for RNA and cytokine analysis and MOI of 1 for microscopy studies. Cells were spun with bacteria for 10 min at 1000 x g to synchronize infection, washed twice with PBS, and then incubated in fresh media. RAW 264.7 or CRISPR/Cas9 RAW 264.7 macrophages were plated on 12-well tissue-culture treated plates at a density of 3×10^5 cells/well and allowed to grow overnight. Where applicable, RNA was harvested from infected cells using 0.5 ml Trizol reagent at each time point.

Chromatin Immunoprecipitation

Chromatin Immunoprecipitation (ChIP) was adapted from Abcam's protocol. Briefly, two confluent 15 cm dishes of RAW 264.7 macrophages were crosslinked in formaldehyde to a final concentration of 0.75% and rotated for 10 minutes. Glycine was added to stop the cross linking by shaking for 5 minutes at a concentration of 125 mM. Cells were rinsed with PBS twice and then scraped into 5 mL PBS and centrifuged at 1,000 g for 5 min at 4°C. Cellular pellets were resuspended in ChIP lysis buffer (750 μ L per 1×10^7 cells) and incubated for 10 min on ice. Cellular lysates were sonicated for 40 minutes (30sec ON, 30sec OFF) on high in a Bioruptor UCD-200 (Diagenode). After sonication, cellular debris was pelleted by centrifugation for 10 min, 4°C, 8,000 x g. Input samples were taken at this step and stored at -80°C until decrosslinking. For RNase treated samples, RNase A was added to cell lysates and incubated for 30 mins at 37°C. Approximately 25 μ g of DNA diluted to 1:10 with RIPA buffer was used for overnight immunoprecipitation. Each ChIP had one sample for the specific antibody and one sample for Protein G beads only which were pre-blocked for 1 hr with single stranded

herring sperm DNA (75 ng/ μ L) and BSA (0.1 μ g/ μ L). The respective primary antibody was added to all samples except the beads-only sample at a concentration of 5 μ g and rotated at 4°C overnight. Beads were washed 3x in with a final wash in high salt (500mM NaCl). DNA was eluted with elution buffer and rotated for 15 min at 30C. Centrifuge for 1 min at 2,000 x g and transfer the supernatant into a fresh tube. Supernatant was incubated in NaCl, RNase A (10 mg/mL) and proteinase K (20 mg/mL) and incubated at 65°C for 1 h. The DNA was purified using phenol:chloroform extraction. DNA levels were measure by RT-qPCR. Primers were designed by tiling each respective gene every 500 base pairs that were inputted into NCBI primer design.

FLAG Chromatin Immunoprecipitation

In RAW 264.7 macrophages stably expressing FL-hnRNP M, FL-hnRNP F, or FL-GFP, ChIP was conducted as described above with minor adjustments. Lysates were incubated overnight at 4C with ANTI-FLAG M2 antibody. After washing, DNA was eluted with FLAG peptide (Sigma-Aldrich F4799) by adding 20 μ l of 5X FLAG peptide, vortexed at room temperature for 15 mins and supernatants were collected. This process was repeated a total of 3x followed by decrosslinking as described.

Alternative Splicing Analysis

Alternative splicing events were analyzed using MAJIQ and VOILA with the default parameters (Vaquero-Garcia et al., 2016). Briefly, uniquely mapped, junction-spanning reads were used by MAJIQ to construct splice graphs for transcripts by using the RefSeq annotation supplemented with de-novo detected junctions. Here, de-novo refers to junctions that were not in the RefSeq transcriptome database but had sufficient

evidence in the RNA-Seq data. The resulting gene splice graphs were analyzed for all identified local splice variations (LSVs). For every junction in each LSV, MAJIQ then quantified expected percent spliced in (PSI) value in control and knockdown samples and expected change in PSI (dPSI) between control and knockdown samples. Results from VOILA were then filtered for high confidence changing LSVs (whereby one or more junctions had at least a 95% probability of expected dPSI of at least an absolute value of 20 PSI units (noted as “20% dPSI”) between control and KD) and candidate changing LSVs (95% probability, 10% dPSI). For the high confidence results (dPSI \geq 20%), the events were further categorized as single exon cassette, multi-exon cassette, alternative 5' and/or 3' splice site, or intron-retention.

VSV infection

7x10⁵ RAW cells were seeded in 12-well plates 16h before infection. Cells were infected with VSV-GFP virus (Dalton and Rose, 2001) at multiplicity of infection (MOI) of 1 and 0.1 in serum-free DMEM (HyClone SH30022.01). After 1h of incubation with media containing virus, supernatant was removed, and fresh DMEM plus 10% FBS was added to each well. At indicated times post infection, cells were harvested with Trizol and prepared for RNA isolation.

Quantitation and Statistical Analysis

Statistical analysis of data was performed using GraphPad Prism software. Two-tailed unpaired Student's t tests were used for statistical analyses, and unless otherwise noted, all results are representative of at least three biological experiments (mean \pm SEM (n = 3 per group)).

CHAPTER VII

CONCLUSIONS

My work has shown that the regulation of gene expression through RBPs and RNA processing is essential to provide the proper gene expression profiles needed during bacterial infection. My research indicates that RNA processing plays a critical role in regulating the expression of innate immune response genes and I have identified novel roles for hnRNPs and SRSFs in regulating the innate immune response.

Through my work I discovered hnRNP M to be a repressor of specific innate immune genes upon innate immune agonists and *Salmonella* infection. In this model, hnRNP M associates with chromatin at the target gene locus and represses innate immune gene expression through influencing intron removal. This is facilitated through TLR signaling and differential phosphorylation of hnRNP M at S574. While my data supports this model, specific mechanisms of hnRNP M signaling and mechanisms remain to be resolved; specifically, which kinases or phosphatases are responsible for differential phosphorylation of hnRNP M upon bacterial infection. Interestingly, several factors have been found to regulate SRSFs phosphorylation^{92,136,142,414}. Similarly, DUSP proteins are found to have differential gene expression in several of our RBP RNA-Seq datasets. DUSP2, an important phosphatase that specifically inactivates MAPK, was also found to have similar gene expression profiles of *IL6* as hnRNP M⁴¹⁵. Therefore, knockdown of DUSP phosphatases, or other kinases involved in SRSF phosphorylation, may identify specific factors that regulate hnRNP M phosphorylation and overall gene expression and protein interactions mechanisms of hnRNP M.

Another unknown mechanism the level of hnRNP M chromatin regulation found at other innate immune transcripts. To investigate which transcripts hnRNP M regulates at the level of chromatin, ChIP-Seq would unbiasedly illuminate which innate immune transcripts or other canonical transcripts are regulated by hnRNP M. This could identify hnRNP M-dependent splicing events that occur at the level of chromatin. To identify which transcripts are bound by hnRNP M in a resting cell, ICLIP or CLIP-Seq would identify the innate immune transcripts RNA bound by hnRNP M. Furthermore, I predict that specific phosphorylation events will enable particular RNA and/or protein interactions and that some of these interactions will remain “trapped” since the phosphate will not be able to be added or removed from the mutated serine. For this experiment, CLIP-seq can also be performed using macrophages expressing 3xFL tagged hnRNP M phosphomutant alleles.

My studies have also identified opposing mechanisms in RBPs in gene regulation by identifying hnRNP M to be a repressor of gene expression and hnRNP F to be an activator of gene expression following diverse innate immune stimuli. Interestingly, hnRNP F was found to down regulate gene expression of dozens of ISGs and differentially splice several master regulators of ISGs, including *Irf7* and *Ikbke*. Mis-splicing events in the absence of hnRNP F could target these transcripts for degradation leading to loss of *Ifnb* transcript and overall ISG expression. While more questions remain for hnRNP F, my studies have shown that *Ifnb1* expression is highly dependent on the presence of hnRNP F. Along with their opposing regulation, surprisingly I found

hnRNP F and hnRNP M to interact with similar proteins in paraspeckle complexes like SFPQ, MATR3, and NONO. Interestingly, hnRNP F was also found to interact with several core splicing factors like Sf3b1. While hnRNP M did not have many core splicing factors identified in my IP/MS, this further suggests their opposing function. I propose a model whereby hnRNP M and hnRNP F are regulators of similar innate immune transcripts. In resting cells, hnRNP M represses splicing factors from being associated with transcripts, while hnRNP F as an activator, brings core splicing factors to a transcript to facilitate gene expression and hnRNP M is removed from the transcript following innate immune activation. This is also supported by my findings of release of hnRNP M protein-protein interactions and hnRNP F interaction with Sf3b1 increasing upon macrophage activation. Kinetics of these interactions will be important to follow-up on as my studies were only conducted at 2H post-macrophage activation and splicing processes occur dynamically throughout the innate immune response.

As these proteins were found to be differentially phosphorylated upon infection, my work also identified specific serines that play a role in regulating gene expression upon bacterial infection. Mutating specific serines on hnRNP M greatly impacted the protein's ability to dampen induction of specific innate immune transcripts following pathogen sensing. Alternatively, mutating specific serines on hnRNP F showed a wide range in regulation abilities of innate immune transcripts. This suggests that while hnRNP M may have a singular critical phosphorylation event, hnRNP F function may be regulated by several events and contribute to hnRNP F localization, RNA-binding, and protein-protein interactions. This could suggest additional modes of regulation by

hnRNP F and also various roles in different complexes such as splicing, RNA-processing, and mRNA export complexes. As aforementioned with hnRNP M, additional research is also needed to identify kinases/phosphatases of this hnRNP F and how these events regulate hnRNP F's function.

In my work, I have performed a genome-wide analysis of gene expression and splicing regulation of several ubiquitously expressed hnRNPs and SRSFs in resting macrophages and *Salmonella*-infected macrophages. I identified __ AS events that are regulated by hnRNP C, F, K, M, U and SRSF 1, 2, 6, 7, and 9. With this data, I have established that hnRNPs and SRSFs have independent functions in regulating gene expression. While hnRNPs seem to collaborate more on the same transcripts, SRSFs seem to regulate in distinct mechanisms as many genes in our RNA-Seq did not show much overlap amongst SRSFs. Additionally, while hnRNP M was found as the major repressor of gene expression, the majority of other RBPs were found to be activators of gene expression upon innate immune activation. While this set of proteins does not cover all hnRNPs and SRSFs, this may indicate a macrophages priority of activating gene expression rather than gene repression. Differential gene expression in hnRNP and SRSF knockdowns also identified transcription-dependent gene regulation, as the most upregulated transcripts upon *Salmonella* infection alone, were not the most affected by hnRNP and SRSF knockdown.

Interestingly, hnRNP C, K, and U had over 40% of RNA-Seq differentially expressed genes overlap in resting and infected macrophages. Surprisingly, only hnRNP C and U showed significant overlap in my MAJIQ analysis, while hnRNP K showed no

overlap with hnRNP C and U. This suggest hnRNP K is influencing similar transcripts, but through different RNA processing functions like export or translation. More research will need to be conducted on how these hnRNPs and SRSFs distinct and collaborative mechanisms play a part in RNA processing steps like splicing and mRNA translation.

My research demonstrates a wide range of regulation by these peripheral splicing factors in regulating distinct innate immune genes and housekeeping genes. MAJIQ analysis of my hnRNP and SRSF RNA-Seq data has identified several transcripts whose alternative splicing requires these RBPs that may play a role in cell-intrinsic innate immunity. For example, several RBPs I looked at control generation of distinct protein-coding isoforms of several genes involved in signaling and transcription (e.g. *Irf7*, *Atf4*, *Ikbkg*, *Tlr7*), which are major mechanisms through which macrophages control ST replication. In order to implicate these hnRNP and SRSF-dependent transcript isoforms in controlling bacterial infection, I will knockdown these transcripts with shRNA targeted towards the 3'UTR, as this will target the majority of transcript isoforms, allowing me to complement with cloned cDNAs from alternatively spliced isoforms of the gene of interest. I can then infect these cell lines with ST and look at survival outcomes (ST intracellular trafficking, CFUs) to implicate these alternatively spliced isoforms in host survival outcomes. Further research is needed to characterize these previously unstudied alternatively spliced isoforms and identify new roles for RNA-binding proteins in controlling cell-intrinsic innate immunity. Together, my data has identified novel mechanisms of RBP functions. I believe that RNA processing is a critical level of regulation during the innate immune response and understanding the

specific functions of each RBP will identify unique and collaborative mechanisms by which RBPs play a critical role in regulating the innate immune response.

REFERENCES

1. Gene Expression | Learn Science at Scitable. Accessed June 3, 2020. <https://www.nature.com/scitable/topicpage/gene-expression-14121669/>
2. Nilsen TW, Graveley BR. Expansion of the eukaryotic proteome by alternative splicing. *Nature*. 2010;463(7280):457-463. doi:10.1038/nature08909
3. Gallego-Paez LM, Bordone MC, Leote AC, Saraiva-Agostinho N, Ascensão-Ferreira M, Barbosa-Morais NL. Alternative splicing: the pledge, the turn, and the prestige. *Hum Genet*. 2017;136(9):1015-1042. doi:10.1007/s00439-017-1790-y
4. Pandya-Jones A, Bhatt DM, Lin C-H, Tong A-J, Smale ST, Black DL. Splicing kinetics and transcript release from the chromatin compartment limit the rate of Lipid A-induced gene expression. *RNA*. 2013;19(6):811-827. doi:10.1261/rna.039081.113
5. Black DL. Protein Diversity from Alternative Splicing: A Challenge for Bioinformatics and Post-Genome Biology. *Cell*. 2000;103(3):367-370. doi:10.1016/S0092-8674(00)00128-8
6. Early P, Huang H, Davis M, Calame K, Hood L. An immunoglobulin heavy chain variable region gene is generated from three segments of DNA: VH, D and JH. *Cell*. 1980;19(4):981-992. doi:10.1016/0092-8674(80)90089-6
7. Baltz AG, Munschauer M, Schwanhäusser B, et al. The mRNA-Bound Proteome and Its Global Occupancy Profile on Protein-Coding Transcripts. *Mol Cell*. 2012;46(5):674-690. doi:10.1016/j.molcel.2012.05.021
8. Castello A, Fischer B, Eichelbaum K, et al. Insights into RNA Biology from an Atlas of Mammalian mRNA-Binding Proteins. *Cell*. 2012;149(6):1393-1406. doi:10.1016/j.cell.2012.04.031
9. Hentze MW, Castello A, Schwarzl T, Preiss T. A brave new world of RNA-binding proteins. *Nat Rev Mol Cell Biol*. 2018;19(5):327-341. doi:10.1038/nrm.2017.130
10. Liepelt A, Naarmann-de Vries IS, Simons N, et al. Identification of RNA-binding Proteins in Macrophages by Interactome Capture. *Mol Cell Proteomics*. 2016;15(8):2699-2714. doi:10.1074/mcp.M115.056564

11. Martinez NM, Lynch KW. Control of Alternative Splicing in Immune Responses: Many Regulators, Many Predictions, Much Still to Learn. *Immunol Rev.* 2013;253(1):216-236. doi:10.1111/imr.12047
12. Carpenter S, Ricci EP, Mercier BC, Moore MJ, Fitzgerald KA. Post-transcriptional regulation of gene expression in innate immunity. *Nat Rev Immunol.* 2014;14(6):361-376. doi:10.1038/nri3682
13. Hardy MP, O'Neill LAJ. The murine IRAK2 gene encodes four alternatively spliced isoforms, two of which are inhibitory. *J Biol Chem.* 2004;279(26):27699-27708. doi:10.1074/jbc.M403068200
14. Lee FF-Y, Chuang H-C, Chen N-Y, Nagarajan G, Chiou PP. Toll-Like Receptor 9 Alternatively Spliced Isoform Negatively Regulates TLR9 Signaling in Teleost Fish. *PLOS ONE.* 2015;10(5):e0126388. doi:10.1371/journal.pone.0126388
15. De Arras L, Alper S. Limiting of the Innate Immune Response by SF3A-Dependent Control of MyD88 Alternative mRNA Splicing. *PLoS Genet.* 2013;9(10). doi:10.1371/journal.pgen.1003855
16. Han SP, Tang YH, Smith R. Functional diversity of the hnRNPs: past, present and perspectives. *Biochem J.* 2010;430(3):379-392. doi:10.1042/BJ20100396
17. Contreras R, Cloutier P, Shkreta L, Fisette J-F, Revil T, Chabot B. hnRNP Proteins and Splicing Control. *Adv Exp Med Biol.* 2007;623:123-147. doi:10.1007/978-0-387-77374-2_8
18. Cornella N, Tebaldi T, Gasperini L, et al. The hnRNP RALY regulates transcription and cell proliferation by modulating the expression of specific factors including the proliferation marker E2F1. *J Biol Chem.* 2017;292(48):19674-19692. doi:10.1074/jbc.M117.795591
19. Michelotti EF, Michelotti GA, Aronsohn AI, Levens D. Heterogeneous nuclear ribonucleoprotein K is a transcription factor. *Mol Cell Biol.* 1996;16(5):2350-2360.
20. Beyer AL, Christensen ME, Walker BW, LeSturgeon WM. Identification and characterization of the packaging proteins of core 40S hnRNP particles. *Cell.* 1977;11(1):127-138. doi:10.1016/0092-8674(77)90323-3
21. Geuens T, Bouhy D, Timmerman V. The hnRNP family: insights into their role in health and disease. *Hum Genet.* 2016;135(8):851-867. doi:10.1007/s00439-016-1683-5

22. Dreyfuss G, Matunis MJ, Pinol-Roma S, Burd CG. hnRNP PROTEINS AND THE BIOGENESIS OF mRNA. *Annu Rev Biochem.* 1993;62(1):289-321. doi:10.1146/annurev.bi.62.070193.001445
23. Eekelen CA van, Riemen T, Venrooij WJ van. Specificity in the interaction of hnRNA and mRNA with proteins as revealed by in vivo cross linking. *FEBS Lett.* 1981;130(2):223-226. doi:10.1016/0014-5793(81)81125-8
24. Jacquenet S, Méreau A, Bilodeau PS, Damier L, Stoltzfus CM, Branlant C. A Second Exon Splicing Silencer within Human Immunodeficiency Virus Type 1 tat Exon 2 Represses Splicing of Tat mRNA and Binds Protein hnRNP H. *J Biol Chem.* 2001;276(44):40464-40475. doi:10.1074/jbc.M104070200
25. Rahman MA, Azuma Y, Nasrin F, et al. SRSF1 and hnRNP H antagonistically regulate splicing of COLQ exon 16 in a congenital myasthenic syndrome. *Sci Rep.* 2015;5(1):13208. doi:10.1038/srep13208
26. Talukdar I, Sen S, Urbano R, Thompson J, Yates JR, Webster NJG. hnRNP A1 and hnRNP F Modulate the Alternative Splicing of Exon 11 of the Insulin Receptor Gene. *PLoS ONE.* 2011;6(11). doi:10.1371/journal.pone.0027869
27. Cao W, Razanau A, Feng D, Lobo VG, Xie J. Control of alternative splicing by forskolin through hnRNP K during neuronal differentiation. *Nucleic Acids Res.* 2012;40(16):8059-8071. doi:10.1093/nar/gks504
28. Chen Q, Jin M, Zhu J, Xiao Q, Zhang L. Functions of Heterogeneous Nuclear Ribonucleoproteins in Stem Cell Potency and Differentiation. *BioMed Res Int.* 2013;2013:623978. doi:10.1155/2013/623978
29. Huelga SC, Vu AQ, Arnold JD, et al. Integrative Genome-wide Analysis Reveals Cooperative Regulation of Alternative Splicing by hnRNP Proteins. *Cell Rep.* 2012;1(2):167-178. doi:10.1016/j.celrep.2012.02.001
30. Ray D, Kazan H, Chan ET, et al. Rapid and systematic analysis of the RNA recognition specificities of RNA-binding proteins. *Nat Biotechnol.* 2009;27(7):667-670. doi:10.1038/nbt.1550
31. Castle JC, Zhang C, Shah JK, Kulkarni AV, Cooper TA, Johnson JM. Differential expression of 24,426 human alternative splicing events and predicted cis-regulation in 48 tissues and cell lines. *Nat Genet.* 2008;40(12):1416-1425. doi:10.1038/ng.264
32. Paradis C, Cloutier P, Shkreta L, Toutant J, Klarskov K, Chabot B. hnRNP I/PTB can antagonize the splicing repressor activity of SRp30c. *RNA.* 2007;13(8):1287-1300. doi:10.1261/rna.403607

33. Hovhannisyan RH, Carstens RP. Heterogeneous Ribonucleoprotein M Is a Splicing Regulatory Protein That Can Enhance or Silence Splicing of Alternatively Spliced Exons. *J Biol Chem.* 2007;282(50):36265-36274. doi:10.1074/jbc.M704188200
34. Park E, Iaccarino C, Lee J, et al. Regulatory Roles of Heterogeneous Nuclear Ribonucleoprotein M and Nova-1 Protein in Alternative Splicing of Dopamine D2 Receptor Pre-mRNA. *J Biol Chem.* 2011;286(28):25301-25308. doi:10.1074/jbc.M110.206540
35. Cho S, Moon H, Loh TJ, et al. hnRNP M facilitates exon 7 inclusion of SMN2 pre-mRNA in spinal muscular atrophy by targeting an enhancer on exon 7. *Biochim Biophys Acta BBA - Gene Regul Mech.* 2014;1839(4):306-315. doi:10.1016/j.bbagr.2014.02.006
36. Dery KJ, Gaur S, Gencheva M, Yen Y, Shively JE, Gaur RK. Mechanistic Control of Carcinoembryonic Antigen-related Cell Adhesion Molecule-1 (CEACAM1) Splice Isoforms by the Heterogeneous Nuclear Ribonuclear Proteins hnRNP L, hnRNP A1, and hnRNP M. *J Biol Chem.* 2011;286(18):16039-16051. doi:10.1074/jbc.M110.204057
37. Chen S, Zhang J, Duan L, et al. Identification of HnRNP M as a novel biomarker for colorectal carcinoma by quantitative proteomics. *Am J Physiol-Gastrointest Liver Physiol.* 2013;306(5):G394-G403. doi:10.1152/ajpgi.00328.2013
38. Harvey SE, Xu Y, Lin X, et al. Coregulation of alternative splicing by hnRNPM and ESRP1 during EMT. *RNA.* 2018;24(10):1326-1338. doi:10.1261/rna.066712.118
39. Košec A, Novak R, Konjevoda P, Trkulja V, Bedeković V, Grgurević L. Tumor tissue hnRNP M and HSP 90α as potential predictors of disease-specific mortality in patients with early-stage cutaneous head and neck melanoma: A proteomics-based study. *Oncotarget.* 2019;10(62):6713-6722. doi:10.18632/oncotarget.27333
40. Yang T, An Z, Zhang C, et al. HnRNPM is a potential mediator of YY1 which promotes EMT in prostate cancer cells. *The Prostate.* 2019;79(11):1199-1210. doi:10.1002/pros.23790
41. Bjersand K, Seidal T, Sundström-Poromaa I, Åkerud H, Skirnisdóttir I. The clinical and prognostic correlation of HRNPM and SLC1A5 in pathogenesis and prognosis in epithelial ovarian cancer. *PLoS ONE.* 2017;12(6). doi:10.1371/journal.pone.0179363

42. Xu Y, Gao XD, Lee J-H, et al. Cell type-restricted activity of hnRNPM promotes breast cancer metastasis via regulating alternative splicing. *Genes Dev.* 2014;28(11):1191-1203. doi:10.1101/gad.241968.114
43. Zhang F-L, Cao J-L, Xie H-Y, et al. Cancer-Associated MORC2-Mutant M276I Regulates an hnRNPM-Mediated CD44 Splicing Switch to Promote Invasion and Metastasis in Triple-Negative Breast Cancer. *Cancer Res.* 2018;78(20):5780-5792. doi:10.1158/0008-5472.CAN-17-1394
44. Yang W-H, Ding M-J, Cui G-Z, Yang M, Dai D-L. Heterogeneous nuclear ribonucleoprotein M promotes the progression of breast cancer by regulating the axin/ β -catenin signaling pathway. *Biomed Pharmacother.* 2018;105:848-855. doi:10.1016/j.biopha.2018.05.014
45. Thomas P, Forse RA, Bajenova O. Carcinoembryonic antigen (CEA) and its receptor hnRNP M are mediators of metastasis and the inflammatory response in the liver. *Clin Exp Metastasis.* 2011;28(8):923-932. doi:10.1007/s10585-011-9419-3
46. Sun H, Liu T, Zhu D, et al. HnRNPM and CD44s expression affects tumor aggressiveness and predicts poor prognosis in breast cancer with axillary lymph node metastases. *Genes Chromosomes Cancer.* 2017;56(8):598-607. doi:10.1002/gcc.22463
47. Hu X, Harvey SE, Zheng R, et al. The RNA-binding protein AKAP8 suppresses tumor metastasis by antagonizing EMT-associated alternative splicing. *Nat Commun.* 2020;11. doi:10.1038/s41467-020-14304-1
48. Wahl MC, Will CL, Lührmann R. The Spliceosome: Design Principles of a Dynamic RNP Machine. *Cell.* 2009;136(4):701-718. doi:10.1016/j.cell.2009.02.009
49. Rappsilber J, Ryder U, Lamond AI, Mann M. Large-Scale Proteomic Analysis of the Human Spliceosome. *Genome Res.* 2002;12(8):1231-1245. doi:10.1101/gr.473902
50. Marko M, Leichter M, Patrino-Georgoula M, Guialis A. hnRNP M interacts with PSF and p54nrb and co-localizes within defined nuclear structures. *Exp Cell Res.* 2010;316(3):390-400. doi:10.1016/j.yexcr.2009.10.021
51. Llères D, Denegri M, Biggiogera M, Ajuh P, Lamond AI. Direct interaction between hnRNP-M and CDC5L/PLRG1 proteins affects alternative splice site choice. *EMBO Rep.* 2010;11(6):445-451. doi:10.1038/embor.2010.64

52. Passacantilli I, Frisone P, De Paola E, Fidaleo M, Paronetto MP. hnRNPM guides an alternative splicing program in response to inhibition of the PI3K/AKT/mTOR pathway in Ewing sarcoma cells. *Nucleic Acids Res.* 2017;45(21):12270-12284. doi:10.1093/nar/gkx831
53. Chen W-Y, Lin C-L, Chuang J-H, et al. Heterogeneous nuclear ribonucleoprotein M associates with mTORC2 and regulates muscle differentiation. *Sci Rep.* 2017;7(1):1-13. doi:10.1038/srep41159
54. Damianov A, Ying Y, Lin C-H, et al. Rbfox proteins regulate splicing as part of a large multiprotein complex LASR. *Cell.* 2016;165(3):606-619. doi:10.1016/j.cell.2016.03.040
55. Yadav SP, Hao H, Yang H-J, et al. The transcription-splicing protein NonO/p54nrb and three NonO-interacting proteins bind to distal enhancer region and augment rhodopsin expression. *Hum Mol Genet.* 2014;23(8):2132-2144. doi:10.1093/hmg/ddt609
56. Luisier R, Tyzack GE, Hall CE, et al. Intron retention and nuclear loss of SFPQ are molecular hallmarks of ALS. *Nat Commun.* 2018;9(1):2010. doi:10.1038/s41467-018-04373-8
57. Iradi MCG, Triplett JC, Thomas JD, et al. Characterization of gene regulation and protein interaction networks for Matrin 3 encoding mutations linked to amyotrophic lateral sclerosis and myopathy. *Sci Rep.* 2018;8(1):4049. doi:10.1038/s41598-018-21371-4
58. Samatanga B, Dominguez C, Jelesarov I, Allain FH-T. The high kinetic stability of a G-quadruplex limits hnRNP F qRRM3 binding to G-tract RNA. *Nucleic Acids Res.* 2013;41(4):2505-2516. doi:10.1093/nar/gks1289
59. Dominguez C, Fiset J-F, Chabot B, Allain FH-T. Structural basis of G-tract recognition and encaging by hnRNP F quasi-RRMs. *Nat Struct Mol Biol.* 2010;17(7):853-861. doi:10.1038/nsmb.1814
60. Matunis MJ, Xing J, Dreyfuss G. The hnRNP F protein: unique primary structure, nucleic acid-binding properties, and subcellular localization. *Nucleic Acids Res.* 1994;22(6):1059-1067.
61. Dominguez C, Allain FH-T. NMR structure of the three quasi RNA recognition motifs (qRRMs) of human hnRNP F and interaction studies with Bcl-x G-tract RNA: a novel mode of RNA recognition. *Nucleic Acids Res.* 2006;34(13):3634-3645. doi:10.1093/nar/gkl488

62. Chu W-K, Hung L-M, Hou C-W, Chen J-K. Heterogeneous ribonucleoprotein F regulates YAP expression via a G-tract in 3'UTR. *Biochim Biophys Acta BBA - Gene Regul Mech.* 2019;1862(1):12-24. doi:10.1016/j.bbagr.2018.10.003
63. Reznik B, Clement SL, Lykke-Andersen J. hnRNP F complexes with tristetraprolin and stimulates ARE-mRNA decay. *PloS One.* 2014;9(6):e100992. doi:10.1371/journal.pone.0100992
64. Li F, Zhao H, Su M, et al. HnRNP-F regulates EMT in bladder cancer by mediating the stabilization of Snail1 mRNA by binding to its 3' UTR. *EBioMedicine.* 2019;45:208-219. doi:10.1016/j.ebiom.2019.06.017
65. Van Dusen CM, Yee L, McNally LM, McNally MT. A Glycine-Rich Domain of hnRNP H/F Promotes Nucleocytoplasmic Shuttling and Nuclear Import through an Interaction with Transportin 1. *Mol Cell Biol.* 2010;30(10):2552-2562. doi:10.1128/MCB.00230-09
66. Tang X, Kane VD, Morr e DM, Morr e DJ. hnRNP F directs formation of an exon 4 minus variant of tumor-associated NADH oxidase (ENOX2). *Mol Cell Biochem.* 2011;357(1):55-63. doi:10.1007/s11010-011-0875-5
67. Mauger DM, Lin C, Garcia-Blanco MA. hnRNP H and hnRNP F Complex with Fox2 To Silence Fibroblast Growth Factor Receptor 2 Exon IIIc. *Mol Cell Biol.* 2008;28(17):5403-5419. doi:10.1128/MCB.00739-08
68. Li F, Su M, Zhao H, et al. HnRNP-F promotes cell proliferation by regulating TPX2 in bladder cancer. *Am J Transl Res.* 2019;11(11):7035-7048.
69. Min H, Chan RC, Black DL. The generally expressed hnRNP F is involved in a neural-specific pre-mRNA splicing event. *Genes Dev.* 1995;9(21):2659-2671. doi:10.1101/gad.9.21.2659
70. Mandler MD, Ku L, Feng Y. A cytoplasmic quaking I isoform regulates the hnRNP F/H-dependent alternative splicing pathway in myelinating glia. *Nucleic Acids Res.* 2014;42(11):7319-7329. doi:10.1093/nar/gku353
71. White R, Gonsior C, Bauer NM, Kr amer-Albers E-M, Luhmann HJ, Trotter J. Heterogeneous Nuclear Ribonucleoprotein (hnRNP) F Is a Novel Component of Oligodendroglial RNA Transport Granules Contributing to Regulation of Myelin Basic Protein (MBP) Synthesis. *J Biol Chem.* 2012;287(3):1742-1754. doi:10.1074/jbc.M111.235010
72. Balasubramani M, Day BW, Schoen RE, Getzenberg RH. Altered Expression and Localization of Creatine Kinase B, Heterogeneous Nuclear Ribonucleoprotein F, and High Mobility Group Box 1 Protein in the Nuclear Matrix Associated with

- Colon Cancer. *Cancer Res.* 2006;66(2):763-769. doi:10.1158/0008-5472.CAN-05-3771
73. Honoré B, Baandrup U, Vorum H. Heterogeneous nuclear ribonucleoproteins F and H/H' show differential expression in normal and selected cancer tissues. *Exp Cell Res.* 2004;294(1):199-209. doi:10.1016/j.yexcr.2003.11.011
74. Tyson-Capper A, Gautrey H. Regulation of Mcl-1 alternative splicing by hnRNP F, H1 and K in breast cancer cells. *RNA Biol.* 2018;15(12):1448-1457. doi:10.1080/15476286.2018.1551692
75. Martinez-Contreras R, Fisette J-F, Nasim FH, Madden R, Cordeau M, Chabot B. Intronic binding sites for hnRNP A/B and hnRNP F/H proteins stimulate pre-mRNA splicing. *PLoS Biol.* 2006;4(2):e21. doi:10.1371/journal.pbio.0040021
76. Xu C, Xie N, Su Y, et al. HnRNP F/H associate with hTERC and telomerase holoenzyme to modulate telomerase function and promote cell proliferation. *Cell Death Differ.* Published online December 20, 2019:1-16. doi:10.1038/s41418-019-0483-6
77. Du J, Wang Q, Ziegler SF, Zhou B. FOXP3 interacts with hnRNPF to modulate pre-mRNA alternative splicing. *J Biol Chem.* 2018;293(26):10235-10244. doi:10.1074/jbc.RA117.001349
78. Benegiamo G, Mure LS, Erikson G, et al. The RNA-Binding Protein NONO Coordinates Hepatic Adaptation to Feeding. *Cell Metab.* 2018;27(2):404-418.e7. doi:10.1016/j.cmet.2017.12.010
79. Xu S-H, Zhu S, Wang Y, et al. ECD promotes gastric cancer metastasis by blocking E3 ligase ZFP91-mediated hnRNP F ubiquitination and degradation. *Cell Death Dis.* 2018;9(5):1-11. doi:10.1038/s41419-018-0525-x
80. McCloskey A, Taniguchi I, Shinmyozu K, Ohno M. hnRNP C Tetramer Measures RNA Length to Classify RNA Polymerase II Transcripts for Export. *Science.* 2012;335(6076):1643-1646. doi:10.1126/science.1218469
81. Villarroya-Beltri C, Gutiérrez-Vázquez C, Sánchez-Cabo F, et al. Sumoylated hnRNPA2B1 controls the sorting of miRNAs into exosomes through binding to specific motifs. *Nat Commun.* 2013;4. doi:10.1038/ncomms3980
82. Bomsztyk K, Denisenko O, Ostrowski J. hnRNP K: One protein multiple processes. *BioEssays.* 2004;26(6):629-638. doi:10.1002/bies.20048
83. Malik AK, Flock KE, Godavarthi CL, Loh HH, Ko JL. Molecular basis underlying the poly C binding protein 1 as a regulator of the proximal promoter of

- mouse μ -opioid receptor gene. *Brain Res.* 2006;1112(1):33-45.
doi:10.1016/j.brainres.2006.07.019
84. Hasegawa Y, Brockdorff N, Kawano S, Tsutui K, Tsutui K, Nakagawa S. The Matrix Protein hnRNP U Is Required for Chromosomal Localization of Xist RNA. *Dev Cell.* 2010;19(3):469-476. doi:10.1016/j.devcel.2010.08.006
85. Bi H, Yang X, Yuan J, et al. H19 inhibits RNA polymerase II-mediated transcription by disrupting the hnRNP U-actin complex. *Biochim Biophys Acta BBA - Gen Subj.* 2013;1830(10):4899-4906. doi:10.1016/j.bbagen.2013.06.026
86. Hutchins EJ, Szaro BG. c-Jun N-Terminal Kinase Phosphorylation of Heterogeneous Nuclear Ribonucleoprotein K Regulates Vertebrate Axon Outgrowth via a Posttranscriptional Mechanism. *J Neurosci.* 2013;33(37):14666-14680. doi:10.1523/JNEUROSCI.4821-12.2013
87. van der Houven van Oordt W, Diaz-Meco MT, Lozano J, Krainer AR, Moscat J, Cáceres JF. The Mkk3/6-p38-Signaling Cascade Alters the Subcellular Distribution of Hnrnp A1 and Modulates Alternative Splicing Regulation. *J Cell Biol.* 2000;149(2):307-316.
88. Xie J, Lee J-A, Kress TL, Mowry KL, Black DL. Protein kinase A phosphorylation modulates transport of the polypyrimidine tract-binding protein. *Proc Natl Acad Sci U S A.* 2003;100(15):8776-8781.
doi:10.1073/pnas.1432696100
89. Yu J, Hai Y, Liu G, Fang T, Kung SKP, Xie J. The Heterogeneous Nuclear Ribonucleoprotein L Is an Essential Component in the Ca²⁺/Calmodulin-dependent Protein Kinase IV-regulated Alternative Splicing through Cytidine-Adenosine Repeats. *J Biol Chem.* 2009;284(3):1505-1513.
doi:10.1074/jbc.M805113200
90. Liu G, Razanau A, Hai Y, et al. A Conserved Serine of Heterogeneous Nuclear Ribonucleoprotein L (hnRNP L) Mediates Depolarization-regulated Alternative Splicing of Potassium Channels. *J Biol Chem.* 2012;287(27):22709-22716.
doi:10.1074/jbc.M112.357343
91. Berglund FM, Clarke PR. hnRNP-U is a specific DNA-dependent protein kinase substrate phosphorylated in response to DNA double-strand breaks. *Biochem Biophys Res Commun.* 2009;381(1):59-64. doi:10.1016/j.bbrc.2009.02.019
92. Ostareck-Lederer A, Ostareck DH, Cans C, et al. c-Src-Mediated Phosphorylation of hnRNP K Drives Translational Activation of Specifically Silenced mRNAs. *Mol Cell Biol.* 2002;22(13):4535-4543. doi:10.1128/MCB.22.13.4535-4543.2002

93. Allemand E, Guil S, Myers M, Moscat J, Caceres JF, Krainer AR. Regulation of heterogeneous nuclear ribonucleoprotein A1 transport by phosphorylation in cells stressed by osmotic shock. *Proc Natl Acad Sci*. 2005;102(10):3605-3610. doi:10.1073/pnas.0409889102
94. Cobianchi F, Calvio C, Stoppini M, Buvoli M, Riva S. Phosphorylation of human hnRNP protein A1 abrogates in vitro strand annealing activity. *Nucleic Acids Res*. 1993;21(4):949-955.
95. Huang Y, Yario TA, Steitz JA. A molecular link between SR protein dephosphorylation and mRNA export. *Proc Natl Acad Sci*. 2004;101(26):9666-9670. doi:10.1073/pnas.0403533101
96. Shin D-L, Hatesuer B, Bergmann S, Nedelko T, Schughart K. Protection from Severe Influenza Virus Infections in Mice Carrying the *Mx1* Influenza Virus Resistance Gene Strongly Depends on Genetic Background. Perlman S, ed. *J Virol*. 2015;89(19):9998-10009. doi:10.1128/JVI.01305-15
97. Stamm S. Regulation of Alternative Splicing by Reversible Protein Phosphorylation. *J Biol Chem*. 2008;283(3):1223-1227. doi:10.1074/jbc.R700034200
98. Jeong S. SR Proteins: Binders, Regulators, and Connectors of RNA. *Mol Cells*. 2017;40(1):1-9. doi:10.14348/molcells.2017.2319
99. Zahler AM, Lane WS, Stolk JA, Roth MB. SR proteins: a conserved family of pre-mRNA splicing factors. *Genes Dev*. 1992;6(5):837-847. doi:10.1101/gad.6.5.837
100. Das S, Krainer AR. Emerging functions of SRSF1, splicing factor and oncoprotein, in RNA metabolism and cancer. *Mol Cancer Res MCR*. 2014;12(9):1195-1204. doi:10.1158/1541-7786.MCR-14-0131
101. Karni R, de Stanchina E, Lowe SW, Sinha R, Mu D, Krainer AR. The gene encoding the splicing factor SF2/ASF is a proto-oncogene. *Nat Struct Mol Biol*. 2007;14(3):185-193. doi:10.1038/nsmb1209
102. Anczuków O, Rosenberg AZ, Akerman M, et al. The splicing factor SRSF1 regulates apoptosis and proliferation to promote mammary epithelial cell transformation. *Nat Struct Mol Biol*. 2012;19(2):220-228. doi:10.1038/nsmb.2207
103. Jia R, Li C, McCoy JP, Deng C-X, Zheng Z-M. SRp20 is a proto-oncogene critical for cell proliferation and tumor induction and maintenance. *Int J Biol Sci*. Published online 2010:806-826. doi:10.7150/ijbs.6.806

104. Ghigna C, Giordano S, Shen H, et al. Cell Motility Is Controlled by SF2/ASF through Alternative Splicing of the Ron Protooncogene. *Mol Cell*. 2005;20(6):881-890. doi:10.1016/j.molcel.2005.10.026
105. Cohen-Eliav M, Golan-Gerstl R, Siegfried Z, et al. The splicing factor SRSF6 is amplified and is an oncoprotein in lung and colon cancers. *J Pathol*. 2013;229(4):630-639. doi:10.1002/path.4129
106. Jensen MA, Wilkinson JE, Krainer AR. Splicing factor SRSF6 promotes hyperplasia of sensitized skin. *Nat Struct Mol Biol*. 2014;21(2):189-197. doi:10.1038/nsmb.2756
107. Das R, Dufu K, Romney B, Feldt M, Elenko M, Reed R. Functional coupling of RNAP II transcription to spliceosome assembly. *Genes Dev*. 2006;20(9):1100-1109. doi:10.1101/gad.1397406
108. Loomis RJ, Naoe Y, Parker JB, et al. Chromatin Binding of SRp20 and ASF/SF2 and Dissociation from Mitotic Chromosomes Is Modulated by Histone H3 Serine 10 Phosphorylation. *Mol Cell*. 2009;33(4):450-461. doi:10.1016/j.molcel.2009.02.003
109. Luco RF, Allo M, Schor IE, Kornblihtt AR, Misteli T. Epigenetics in Alternative Pre-mRNA Splicing. *Cell*. 2011;144(1):16-26. doi:10.1016/j.cell.2010.11.056
110. Sapra AK, Änkö M-L, Grishina I, et al. SR Protein Family Members Display Diverse Activities in the Formation of Nascent and Mature mRNPs In Vivo. *Mol Cell*. 2009;34(2):179-190. doi:10.1016/j.molcel.2009.02.031
111. Ji X, Zhou Y, Pandit S, et al. SR Proteins Collaborate with 7SK and Promoter-Associated Nascent RNA to Release Paused Polymerase. *Cell*. 2013;153(4):855-868. doi:10.1016/j.cell.2013.04.028
112. Lou H, Neugebauer KM, Gagel RF, Berget SM. Regulation of Alternative Polyadenylation by U1 snRNPs and SRp20. *Mol Cell Biol*. 1998;18(9):4977-4985. doi:10.1128/MCB.18.9.4977
113. Xiao W, Adhikari S, Dahal U, et al. Nuclear m6A Reader YTHDC1 Regulates mRNA Splicing. *Mol Cell*. 2016;61(4):507-519. doi:10.1016/j.molcel.2016.01.012
114. Tariq A, Garnarcz W, Handl C, Balik A, Pusch O, Jantsch MF. RNA-interacting proteins act as site-specific repressors of ADAR2-mediated RNA editing and fluctuate upon neuronal stimulation. *Nucleic Acids Res*. 2013;41(4):2581-2593. doi:10.1093/nar/gks1353

115. Shanmugam R, Zhang F, Srinivasan H, et al. SRSF9 selectively represses ADAR2-mediated editing of brain-specific sites in primates. *Nucleic Acids Res.* 2018;46(14):7379-7395. doi:10.1093/nar/gky615
116. Huang Y, Steitz JA. SRprises along a Messenger's Journey. *Mol Cell.* 2005;17(5):613-615. doi:10.1016/j.molcel.2005.02.020
117. Änkö M-L, Müller-McNicoll M, Brandl H, et al. The RNA-binding landscapes of two SR proteins reveal unique functions and binding to diverse RNA classes. *Genome Biol.* 2012;13(3):R17. doi:10.1186/gb-2012-13-3-r17
118. Wang X, Juan L, Lv J, Wang K, Sanford JR, Liu Y. Predicting sequence and structural specificities of RNA binding regions recognized by splicing factor SRSF1. *BMC Genomics.* 2011;12(Suppl 5):S8. doi:10.1186/1471-2164-12-S5-S8
119. Cavaloc Y, Bourgeois CF, Kister L, Stévenin J. The splicing factors 9G8 and SRp20 transactivate splicing through different and specific enhancers. *RNA.* 1999;5(3):468-483.
120. Akerman M, David-Eden H, Pinter RY, Mandel-Gutfreund Y. A computational approach for genome-wide mapping of splicing factor binding sites. *Genome Biol.* 2009;10(3):R30. doi:10.1186/gb-2009-10-3-r30
121. Änkö M-L, Morales L, Henry I, Beyer A, Neugebauer KM. Global analysis reveals SRp20- and SRp75-specific mRNPs in cycling and neural cells. *Nat Struct Mol Biol.* 2010;17(8):962-970. doi:10.1038/nsmb.1862
122. Pandit S, Zhou Y, Shiue L, et al. Genome-wide analysis reveals SR protein cooperation and competition in regulated splicing. *Mol Cell.* 2013;50(2):223-235. doi:10.1016/j.molcel.2013.03.001
123. Zhang Z, Krainer AR. Involvement of SR Proteins in mRNA Surveillance. *Mol Cell.* 2004;16(4):597-607. doi:10.1016/j.molcel.2004.10.031
124. Rahman MA, Lin K-T, Bradley RK, Abdel-Wahab O, Krainer AR. Recurrent SRSF2 mutations in MDS affect both splicing and NMD. *Genes Dev.* Published online January 30, 2020. doi:10.1101/gad.332270.119
125. Masaki S, Ikeda S, Hata A, et al. Myelodysplastic Syndrome-Associated SRSF2 Mutations Cause Splicing Changes by Altering Binding Motif Sequences. *Front Genet.* 2019;10. doi:10.3389/fgene.2019.00338
126. Zhang J, Lieu YK, Ali AM, et al. Disease-associated mutation in SRSF2 misregulates splicing by altering RNA-binding affinities. *Proc Natl Acad Sci.* 2015;112(34):E4726-E4734. doi:10.1073/pnas.1514105112

127. Hara H, Takeda T, Yamamoto N, et al. Zinc-induced modulation of SRSF6 activity alters Bim splicing to promote generation of the most potent apoptotic isoform BimS. *FEBS J.* 2013;280(14):3313-3327. doi:10.1111/febs.12318
128. Wan L, Yu W, Shen E, et al. SRSF6-regulated alternative splicing that promotes tumour progression offers a therapy target for colorectal cancer. *Gut.* 2019;68(1):118-129. doi:10.1136/gutjnl-2017-314983
129. Kadota Y, Jam FA, Yukiue H, et al. Srsf7 Establishes the Juvenile Transcriptome through Age-Dependent Alternative Splicing in Mice. *iScience.* 2020;23(3):100929. doi:10.1016/j.isci.2020.100929
130. Simard MJ, Chabot B. SRp30c Is a Repressor of 3' Splice Site Utilization. *Mol Cell Biol.* 2002;22(12):4001-4010. doi:10.1128/MCB.22.12.4001-4010.2002
131. Huang Y, Steitz JA. Splicing Factors SRp20 and 9G8 Promote the Nucleocytoplasmic Export of mRNA. *Mol Cell.* 2001;7(4):899-905. doi:10.1016/S1097-2765(01)00233-7
132. Huang Y, Gattoni R, Stévenin J, Steitz JA. SR Splicing Factors Serve as Adapter Proteins for TAP-Dependent mRNA Export. *Mol Cell.* 2003;11(3):837-843. doi:10.1016/S1097-2765(03)00089-3
133. Lai M-C, Tarn W-Y. Hypophosphorylated ASF/SF2 Binds TAP and Is Present in Messenger Ribonucleoproteins. *J Biol Chem.* 2004;279(30):31745-31749. doi:10.1074/jbc.C400173200
134. Lemaire R, Prasad J, Kashima T, Gustafson J, Manley JL, Lafyatis R. Stability of a PKCI-1-related mRNA is controlled by the splicing factor ASF/SF2: a novel function for SR proteins. *Genes Dev.* 2002;16(5):594-607. doi:10.1101/gad.939502
135. Sanford JR, Gray NK, Beckmann K, Cáceres JF. A novel role for shuttling SR proteins in mRNA translation. *Genes Dev.* 2004;18(7):755-768. doi:10.1101/gad.286404
136. Edmond V, Moysan E, Khochbin S, et al. Acetylation and phosphorylation of SRSF2 control cell fate decision in response to cisplatin. *EMBO J.* 2011;30(3):510-523. doi:10.1038/emboj.2010.333
137. Choudhary C, Kumar C, Gnad F, et al. Lysine Acetylation Targets Protein Complexes and Co-Regulates Major Cellular Functions. *Science.* 2009;325(5942):834-840. doi:10.1126/science.1175371

138. Gui J-F, Lane WS, Fu X-D. A serine kinase regulates intracellular localization of splicing factors in the cell cycle. *Nature*. 1994;369(6482):678-682. doi:10.1038/369678a0
139. Zhou Z, Fu X-D. Regulation of Splicing by SR proteins and SR Protein-Specific Kinases. *Chromosoma*. 2013;122(3):191-207. doi:10.1007/s00412-013-0407-z
140. Colwill K, Pawson T, Andrews B, et al. The Clk/Sty protein kinase phosphorylates SR splicing factors and regulates their intranuclear distribution. *EMBO J*. 1996;15(2):265-275.
141. Koizumi J, Okamoto Y, Onogi H, Mayeda A, Krainer AR, Hagiwara M. The Subcellular Localization of SF2/ASF Is Regulated by Direct Interaction with SR Protein Kinases (SRPKs). *J Biol Chem*. 1999;274(16):11125-11131. doi:10.1074/jbc.274.16.11125
142. Rossi F, Labourier E, Forné T, et al. Specific phosphorylation of SR proteins by mammalian DNA topoisomerase I. *Nature*. 1996;381(6577):80-82. doi:10.1038/381080a0
143. Novoyatleva T, Heinrich B, Tang Y, et al. Protein phosphatase 1 binds to the RNA recognition motif of several splicing factors and regulates alternative pre-mRNA processing. *Hum Mol Genet*. 2008;17(1):52-70. doi:10.1093/hmg/ddm284
144. Misteli T, Spector DL. Serine/threonine phosphatase 1 modulates the subnuclear distribution of pre-mRNA splicing factors. *Mol Biol Cell*. 1996;7(10):1559-1572.
145. Shin C, Feng Y, Manley JL. Dephosphorylated SRp38 acts as a splicing repressor in response to heat shock. *Nature*. 2004;427(6974):553-558. doi:10.1038/nature02288
146. Shin C, Manley JL. The SR Protein SRp38 Represses Splicing in M Phase Cells. *Cell*. 2002;111(3):407-417. doi:10.1016/S0092-8674(02)01038-3
147. Gasteiger G, D’Osualdo A, Schubert DA, Weber A, Bruscia EM, Hartl D. Cellular Innate Immunity: An Old Game with New Players. *J Innate Immun*. 2017;9(2):111-125. doi:10.1159/000453397
148. Mogensen TH. Pathogen Recognition and Inflammatory Signaling in Innate Immune Defenses. *Clin Microbiol Rev*. 2009;22(2):240-273. doi:10.1128/CMR.00046-08
149. Poltorak A, He X, Smirnova I, et al. Defective LPS Signaling in C3H/HeJ and C57BL/10ScCr Mice: Mutations in Tlr4 Gene. *Science*. 1998;282(5396):2085-2088.

150. Schwandner R, Dziarski R, Wesche H, Rothe M, Kirschning CJ. Peptidoglycan- and lipoteichoic acid-induced cell activation is mediated by toll-like receptor 2. *J Biol Chem*. 1999;274(25):17406-17409. doi:10.1074/jbc.274.25.17406
151. Yoshimura A, Lien E, Ingalls RR, Tuomanen E, Dziarski R, Golenbock D. Cutting edge: recognition of Gram-positive bacterial cell wall components by the innate immune system occurs via Toll-like receptor 2. *J Immunol Baltim Md 1950*. 1999;163(1):1-5.
152. Mogensen TH, Paludan SR, Kilian M, Ostergaard L. Live *Streptococcus pneumoniae*, *Haemophilus influenzae*, and *Neisseria meningitidis* activate the inflammatory response through Toll-like receptors 2, 4, and 9 in species-specific patterns. *J Leukoc Biol*. 2006;80(2):267-277. doi:10.1189/jlb.1105626
153. Diebold SS, Kaisho T, Hemmi H, Akira S, Reis e Sousa C. Innate antiviral responses by means of TLR7-mediated recognition of single-stranded RNA. *Science*. 2004;303(5663):1529-1531. doi:10.1126/science.1093616
154. Heil F, Hemmi H, Hochrein H, et al. Species-specific recognition of single-stranded RNA via toll-like receptor 7 and 8. *Science*. 2004;303(5663):1526-1529. doi:10.1126/science.1093620
155. Alexopoulou L, Holt AC, Medzhitov R, Flavell RA. Recognition of double-stranded RNA and activation of NF-kappaB by Toll-like receptor 3. *Nature*. 2001;413(6857):732-738. doi:10.1038/35099560
156. Hemmi H, Takeuchi O, Kawai T, et al. A Toll-like receptor recognizes bacterial DNA. *Nature*. 2000;408(6813):740-745. doi:10.1038/35047123
157. Arpaia N, Godec J, Lau L, et al. TLR signaling is required for *Salmonella typhimurium* virulence. *Cell*. 2011;144(5):675-688. doi:10.1016/j.cell.2011.01.031
158. Hawn TR, Verbon A, Lettinga KD, et al. A common dominant TLR5 stop codon polymorphism abolishes flagellin signaling and is associated with susceptibility to legionnaires' disease. *J Exp Med*. 2003;198(10):1563-1572. doi:10.1084/jem.20031220
159. Hayashi F, Smith KD, Ozinsky A, et al. The innate immune response to bacterial flagellin is mediated by Toll-like receptor 5. *Nature*. 2001;410(6832):1099-1103. doi:10.1038/35074106
160. O'Neill LAJ, Bowie AG. The family of five: TIR-domain-containing adaptors in Toll-like receptor signalling. *Nat Rev Immunol*. 2007;7(5):353-364. doi:10.1038/nri2079

161. Fitzgerald KA, Palsson-McDermott EM, Bowie AG, et al. Mal (MyD88-adaptor-like) is required for Toll-like receptor-4 signal transduction. *Nature*. 2001;413(6851):78-83. doi:10.1038/35092578
162. Oshiumi H, Matsumoto M, Funami K, Akazawa T, Seya T. TICAM-1, an adaptor molecule that participates in Toll-like receptor 3-mediated interferon-beta induction. *Nat Immunol*. 2003;4(2):161-167. doi:10.1038/ni886
163. Fitzgerald KA, Rowe DC, Barnes BJ, et al. LPS-TLR4 signaling to IRF-3/7 and NF-kappaB involves the toll adaptors TRAM and TRIF. *J Exp Med*. 2003;198(7):1043-1055. doi:10.1084/jem.20031023
164. Carty M, Goodbody R, Schröder M, Stack J, Moynagh PN, Bowie AG. The human adaptor SARM negatively regulates adaptor protein TRIF-dependent Toll-like receptor signaling. *Nat Immunol*. 2006;7(10):1074-1081. doi:10.1038/ni1382
165. Mitchell G, Isberg RR. Innate Immunity to Intracellular pathogens: balancing microbial elimination and inflammation. *Cell Host Microbe*. 2017;22(2):166-175. doi:10.1016/j.chom.2017.07.005
166. Akira S, Uematsu S, Takeuchi O. Pathogen recognition and innate immunity. *Cell*. 2006;124(4):783-801. doi:10.1016/j.cell.2006.02.015
167. Burns K, Martinon F, Esslinger C, et al. MyD88, an adapter protein involved in interleukin-1 signaling. *J Biol Chem*. 1998;273(20):12203-12209. doi:10.1074/jbc.273.20.12203
168. Wesche H, Henzel WJ, Shillinglaw W, Li S, Cao Z. MyD88: an adapter that recruits IRAK to the IL-1 receptor complex. *Immunity*. 1997;7(6):837-847. doi:10.1016/s1074-7613(00)80402-1
169. Kawai T, Takeuchi O, Fujita T, et al. Lipopolysaccharide stimulates the MyD88-independent pathway and results in activation of IFN-regulatory factor 3 and the expression of a subset of lipopolysaccharide-inducible genes. *J Immunol Baltim Md 1950*. 2001;167(10):5887-5894. doi:10.4049/jimmunol.167.10.5887
170. Suzuki N, Suzuki S, Duncan GS, et al. Severe impairment of interleukin-1 and Toll-like receptor signalling in mice lacking IRAK-4. *Nature*. 2002;416(6882):750-756. doi:10.1038/nature736
171. Li S, Strelow A, Fontana EJ, Wesche H. IRAK-4: a novel member of the IRAK family with the properties of an IRAK-kinase. *Proc Natl Acad Sci U S A*. 2002;99(8):5567-5572. doi:10.1073/pnas.082100399

172. Wang C, Deng L, Hong M, Akkaraju GR, Inoue J, Chen ZJ. TAK1 is a ubiquitin-dependent kinase of MKK and IKK. *Nature*. 2001;412(6844):346-351. doi:10.1038/35085597
173. Kanayama A, Seth RB, Sun L, et al. TAB2 and TAB3 activate the NF-kappaB pathway through binding to polyubiquitin chains. *Mol Cell*. 2004;15(4):535-548. doi:10.1016/j.molcel.2004.08.008
174. Häcker H, Karin M. Regulation and function of IKK and IKK-related kinases. *Sci STKE Signal Transduct Knowl Environ*. 2006;2006(357):re13. doi:10.1126/stke.3572006re13
175. Chang L, Karin M. Mammalian MAP kinase signalling cascades. *Nature*. 2001;410(6824):37-40. doi:10.1038/35065000
176. Shim J-H, Xiao C, Paschal AE, et al. TAK1, but not TAB1 or TAB2, plays an essential role in multiple signaling pathways in vivo. *Genes Dev*. 2005;19(22):2668-2681. doi:10.1101/gad.1360605
177. Sato S, Sanjo H, Takeda K, et al. Essential function for the kinase TAK1 in innate and adaptive immune responses. *Nat Immunol*. 2005;6(11):1087-1095. doi:10.1038/ni1255
178. Kawai T, Adachi O, Ogawa T, Takeda K, Akira S. Unresponsiveness of MyD88-deficient mice to endotoxin. *Immunity*. 1999;11(1):115-122. doi:10.1016/s1074-7613(00)80086-2
179. Fitzgerald KA, McWhirter SM, Faia KL, et al. IKKepsilon and TBK1 are essential components of the IRF3 signaling pathway. *Nat Immunol*. 2003;4(5):491-496. doi:10.1038/ni921
180. Hemmi H, Takeuchi O, Sato S, et al. The roles of two IkappaB kinase-related kinases in lipopolysaccharide and double stranded RNA signaling and viral infection. *J Exp Med*. 2004;199(12):1641-1650. doi:10.1084/jem.20040520
181. Sharma S, tenOever BR, Grandvaux N, Zhou G-P, Lin R, Hiscott J. Triggering the interferon antiviral response through an IKK-related pathway. *Science*. 2003;300(5622):1148-1151. doi:10.1126/science.1081315
182. Guo B, Cheng G. Modulation of the interferon antiviral response by the TBK1/IKKi adaptor protein TANK. *J Biol Chem*. 2007;282(16):11817-11826. doi:10.1074/jbc.M700017200
183. Sato S, Sugiyama M, Yamamoto M, et al. Toll/IL-1 receptor domain-containing adaptor inducing IFN-beta (TRIF) associates with TNF receptor-associated factor

- 6 and TANK-binding kinase 1, and activates two distinct transcription factors, NF-kappa B and IFN-regulatory factor-3, in the Toll-like receptor signaling. *J Immunol Baltim Md 1950*. 2003;171(8):4304-4310. doi:10.4049/jimmunol.171.8.4304
184. Meylan E, Burns K, Hofmann K, et al. RIP1 is an essential mediator of Toll-like receptor 3-induced NF-kappa B activation. *Nat Immunol*. 2004;5(5):503-507. doi:10.1038/ni1061
185. Cusson-Hermance N, Khurana S, Lee TH, Fitzgerald KA, Kelliher MA. Rip1 mediates the Trif-dependent toll-like receptor 3- and 4-induced NF- κ B activation but does not contribute to interferon regulatory factor 3 activation. *J Biol Chem*. 2005;280(44):36560-36566. doi:10.1074/jbc.M506831200
186. Thanos D, Maniatis T. Virus induction of human IFN beta gene expression requires the assembly of an enhanceosome. *Cell*. 1995;83(7):1091-1100. doi:10.1016/0092-8674(95)90136-1
187. Edelmann KH, Richardson-Burns S, Alexopoulou L, Tyler KL, Flavell RA, Oldstone MBA. Does Toll-like receptor 3 play a biological role in virus infections? *Virology*. 2004;322(2):231-238. doi:10.1016/j.virol.2004.01.033
188. Hochrein H, Schlatter B, O'Keeffe M, et al. Herpes simplex virus type-1 induces IFN-alpha production via Toll-like receptor 9-dependent and -independent pathways. *Proc Natl Acad Sci U S A*. 2004;101(31):11416-11421. doi:10.1073/pnas.0403555101
189. Ishii KJ, Coban C, Kato H, et al. A Toll-like receptor-independent antiviral response induced by double-stranded B-form DNA. *Nat Immunol*. 2006;7(1):40-48. doi:10.1038/ni1282
190. Stetson DB, Medzhitov R. Recognition of Cytosolic DNA Activates an IRF3-Dependent Innate Immune Response. *Immunity*. 2006;24(1):93-103. doi:10.1016/j.immuni.2005.12.003
191. Kanneganti T-D, Lamkanfi M, Núñez G. Intracellular NOD-like receptors in host defense and disease. *Immunity*. 2007;27(4):549-559. doi:10.1016/j.immuni.2007.10.002
192. Houben D, Demangel C, van Ingen J, et al. ESX-1-mediated translocation to the cytosol controls virulence of mycobacteria. *Cell Microbiol*. 2012;14(8):1287-1298. doi:10.1111/j.1462-5822.2012.01799.x
193. Unterholzner L, Keating SE, Baran M, et al. IFI16 is an innate immune sensor for intracellular DNA. *Nat Immunol*. 2010;11(11):997-1004. doi:10.1038/ni.1932

194. Fernandes-Alnemri T, Yu J-W, Datta P, Wu J, Alnemri ES. AIM2 activates the inflammasome and cell death in response to cytoplasmic DNA. *Nature*. 2009;458(7237):509-513. doi:10.1038/nature07710
195. Yoneyama M, Kikuchi M, Natsukawa T, et al. The RNA helicase RIG-I has an essential function in double-stranded RNA-induced innate antiviral responses. *Nat Immunol*. 2004;5(7):730-737. doi:10.1038/ni1087
196. Kato H, Sato S, Yoneyama M, et al. Cell type-specific involvement of RIG-I in antiviral response. *Immunity*. 2005;23(1):19-28. doi:10.1016/j.immuni.2005.04.010
197. Nallagatla SR, Hwang J, Toroney R, Zheng X, Cameron CE, Bevilacqua PC. 5'-triphosphate-dependent activation of PKR by RNAs with short stem-loops. *Science*. 2007;318(5855):1455-1458. doi:10.1126/science.1147347
198. Yang YL, Reis LF, Pavlovic J, et al. Deficient signaling in mice devoid of double-stranded RNA-dependent protein kinase. *EMBO J*. 1995;14(24):6095-6106.
199. Zamanian-Daryoush M, Mogensen TH, DiDonato JA, Williams BR. NF-kappaB activation by double-stranded-RNA-activated protein kinase (PKR) is mediated through NF-kappaB-inducing kinase and IkappaB kinase. *Mol Cell Biol*. 2000;20(4):1278-1290. doi:10.1128/mcb.20.4.1278-1290.2000
200. McAllister CS, Samuel CE. The RNA-activated protein kinase enhances the induction of interferon-beta and apoptosis mediated by cytoplasmic RNA sensors. *J Biol Chem*. 2009;284(3):1644-1651. doi:10.1074/jbc.M807888200
201. Zhang P, Samuel CE. Induction of protein kinase PKR-dependent activation of interferon regulatory factor 3 by vaccinia virus occurs through adapter IPS-1 signaling. *J Biol Chem*. 2008;283(50):34580-34587. doi:10.1074/jbc.M807029200
202. Vance RE. Cytosolic DNA Sensing: The Field Narrows. *Immunity*. 2016;45(2):227-228. doi:10.1016/j.immuni.2016.08.006
203. Collins AC, Cai H, Li T, et al. Cyclic GMP-AMP Synthase Is an Innate Immune DNA Sensor for Mycobacterium tuberculosis. *Cell Host Microbe*. 2015;17(6):820-828. doi:10.1016/j.chom.2015.05.005
204. Sun L, Wu J, Du F, Chen X, Chen ZJ. Cyclic GMP-AMP synthase is a cytosolic DNA sensor that activates the type I interferon pathway. *Science*. 2013;339(6121):786-791. doi:10.1126/science.1232458

205. Schoggins JW, MacDuff DA, Imanaka N, et al. Pan-viral specificity of IFN-induced genes reveals new roles for cGAS in innate immunity. *Nature*. 2014;505(7485):691-695. doi:10.1038/nature12862
206. Watson RO, Bell SL, MacDuff DA, et al. The cytosolic sensor cGAS detects Mycobacterium tuberculosis DNA to induce type I interferons and activate autophagy. *Cell Host Microbe*. 2015;17(6):811-819. doi:10.1016/j.chom.2015.05.004
207. West AP, Khoury-Hanold W, Staron M, et al. Mitochondrial DNA stress primes the antiviral innate immune response. *Nature*. 2015;520(7548):553-557. doi:10.1038/nature14156
208. Kawai T, Takahashi K, Sato S, et al. IPS-1, an adaptor triggering RIG-I- and Mda5-mediated type I interferon induction. *Nat Immunol*. 2005;6(10):981-988. doi:10.1038/ni1243
209. Seth RB, Sun L, Ea C-K, Chen ZJ. Identification and characterization of MAVS, a mitochondrial antiviral signaling protein that activates NF-kappaB and IRF 3. *Cell*. 2005;122(5):669-682. doi:10.1016/j.cell.2005.08.012
210. Ishikawa H, Barber GN. STING is an endoplasmic reticulum adaptor that facilitates innate immune signalling. *Nature*. 2008;455(7213):674-678. doi:10.1038/nature07317
211. Tanaka Y, Chen ZJ. STING specifies IRF3 phosphorylation by TBK1 in the cytosolic DNA signaling pathway. *Sci Signal*. 2012;5(214):ra20. doi:10.1126/scisignal.2002521
212. Zhong B, Yang Y, Li S, et al. The adaptor protein MITA links virus-sensing receptors to IRF3 transcription factor activation. *Immunity*. 2008;29(4):538-550. doi:10.1016/j.immuni.2008.09.003
213. Marinho FV, Benmerzoug S, Oliveira SC, Ryffel B, Quesniaux VFJ. The Emerging Roles of STING in Bacterial Infections. *Trends Microbiol*. 2017;25(11):906-918. doi:10.1016/j.tim.2017.05.008
214. Saha SK, Pietras EM, He JQ, et al. Regulation of antiviral responses by a direct and specific interaction between TRAF3 and Cardif. *EMBO J*. 2006;25(14):3257-3263. doi:10.1038/sj.emboj.7601220
215. Zhao T, Yang L, Sun Q, et al. The NEMO adaptor bridges the nuclear factor-kappaB and interferon regulatory factor signaling pathways. *Nat Immunol*. 2007;8(6):592-600. doi:10.1038/ni1465

216. Michallet M-C, Meylan E, Ermolaeva MA, et al. TRADD protein is an essential component of the RIG-like helicase antiviral pathway. *Immunity*. 2008;28(5):651-661. doi:10.1016/j.immuni.2008.03.013
217. Takahashi K, Kawai T, Kumar H, Sato S, Yonehara S, Akira S. Roles of caspase-8 and caspase-10 in innate immune responses to double-stranded RNA. *J Immunol Baltim Md 1950*. 2006;176(8):4520-4524. doi:10.4049/jimmunol.176.8.4520
218. Balachandran S, Thomas E, Barber GN. A FADD-dependent innate immune mechanism in mammalian cells. *Nature*. 2004;432(7015):401-405. doi:10.1038/nature03124
219. Echchannaoui H, Frei K, Schnell C, Leib SL, Zimmerli W, Landmann R. Toll-like receptor 2-deficient mice are highly susceptible to *Streptococcus pneumoniae* meningitis because of reduced bacterial clearing and enhanced inflammation. *J Infect Dis*. 2002;186(6):798-806. doi:10.1086/342845
220. Mancuso G, Midiri A, Beninati C, et al. Dual role of TLR2 and myeloid differentiation factor 88 in a mouse model of invasive group B streptococcal disease. *J Immunol Baltim Md 1950*. 2004;172(10):6324-6329. doi:10.4049/jimmunol.172.10.6324
221. Takeuchi O, Hoshino K, Akira S. Cutting edge: TLR2-deficient and MyD88-deficient mice are highly susceptible to *Staphylococcus aureus* infection. *J Immunol Baltim Md 1950*. 2000;165(10):5392-5396. doi:10.4049/jimmunol.165.10.5392
222. Girardin SE, Boneca IG, Viala J, et al. Nod2 is a general sensor of peptidoglycan through muramyl dipeptide (MDP) detection. *J Biol Chem*. 2003;278(11):8869-8872. doi:10.1074/jbc.C200651200
223. Faustin B, Lartigue L, Bruey J-M, et al. Reconstituted NALP1 inflammasome reveals two-step mechanism of caspase-1 activation. *Mol Cell*. 2007;25(5):713-724. doi:10.1016/j.molcel.2007.01.032
224. Maldonado RF, Sá-Correia I, Valvano MA. Lipopolysaccharide modification in Gram-negative bacteria during chronic infection. *FEMS Microbiol Rev*. 2016;40(4):480-493. doi:10.1093/femsre/fuw007
225. Andersen-Nissen E, Hawn TR, Smith KD, et al. Cutting edge: Tlr5^{-/-} mice are more susceptible to *Escherichia coli* urinary tract infection. *J Immunol Baltim Md 1950*. 2007;178(8):4717-4720. doi:10.4049/jimmunol.178.8.4717

226. Simon R, Samuel CE. Activation of NF-kappaB-dependent gene expression by Salmonella flagellins FliC and FljB. *Biochem Biophys Res Commun.* 2007;355(1):280-285. doi:10.1016/j.bbrc.2007.01.148
227. Ferwerda G, Girardin SE, Kullberg B-J, et al. NOD2 and toll-like receptors are nonredundant recognition systems of Mycobacterium tuberculosis. *PLoS Pathog.* 2005;1(3):279-285. doi:10.1371/journal.ppat.0010034
228. Ishii KJ, Akira S. Innate immune recognition of, and regulation by, DNA. *Trends Immunol.* 2006;27(11):525-532. doi:10.1016/j.it.2006.09.002
229. World Health Organization, ed. *WHO Estimates of the Global Burden of Foodborne Diseases.* World Health Organization; 2015.
230. Salmonella Homepage | CDC. Published June 24, 2020. Accessed July 15, 2020. <https://www.cdc.gov/salmonella/index.html>
231. Angulo FJ, Mølbak K. Human Health Consequences of Antimicrobial Drug—Resistant Salmonella and Other Foodborne Pathogens. *Clin Infect Dis.* 2005;41(11):1613-1620. doi:10.1086/497599
232. Cianflone NFC. Salmonellosis and the GI Tract: More than Just Peanut Butter. *Curr Gastroenterol Rep.* 2008;10(4):424-431.
233. Chiu C-H, Wu T-L, Su L-H, et al. The emergence in Taiwan of fluoroquinolone resistance in Salmonella enterica serotype choleraesuis. *N Engl J Med.* 2002;346(6):413-419. doi:10.1056/NEJMoa012261
234. Jajere SM. A review of Salmonella enterica with particular focus on the pathogenicity and virulence factors, host specificity and antimicrobial resistance including multidrug resistance. *Vet World.* 2019;12(4):504-521. doi:10.14202/vetworld.2019.504-521
235. Sansonetti P. Phagocytosis of bacterial pathogens: implications in the host response. *Semin Immunol.* 2001;13(6):381-390. doi:10.1006/smim.2001.0335
236. Drecktrah D, Knodler LA, Ireland R, Steele-Mortimer O. The mechanism of Salmonella entry determines the vacuolar environment and intracellular gene expression. *Traffic Cph Den.* 2006;7(1):39-51. doi:10.1111/j.1600-0854.2005.00360.x
237. Eng S-K, Pusparajah P, Mutalib N-SA, Ser H-L, Chan K-G, Lee L-H. Salmonella: A review on pathogenesis, epidemiology and antibiotic resistance. *Front Life Sci.* 2015;8(3):284-293. doi:10.1080/21553769.2015.1051243

238. Kurtz JR, Goggins JA, McLachlan JB. Salmonella infection: interplay between the bacteria and host immune system. *Immunol Lett.* 2017;190:42-50. doi:10.1016/j.imlet.2017.07.006
239. Galán JE. Salmonella interactions with host cells: type III secretion at work. *Annu Rev Cell Dev Biol.* 2001;17:53-86. doi:10.1146/annurev.cellbio.17.1.53
240. Figueira R, Holden DW. Functions of the Salmonella pathogenicity island 2 (SPI-2) type III secretion system effectors. *Microbiol Read Engl.* 2012;158(Pt 5):1147-1161. doi:10.1099/mic.0.058115-0
241. Royle MCJ, Töttemeyer S, Alldridge LC, Maskell DJ, Bryant CE. Stimulation of Toll-like receptor 4 by lipopolysaccharide during cellular invasion by live Salmonella typhimurium is a critical but not exclusive event leading to macrophage responses. *J Immunol Baltim Md 1950.* 2003;170(11):5445-5454. doi:10.4049/jimmunol.170.11.5445
242. Azimi T, Zamirnasta M, Sani MA, Soltan Dallal MM, Nasser A. Molecular Mechanisms of Salmonella Effector Proteins: A Comprehensive Review. *Infect Drug Resist.* 2020;13:11-26. doi:10.2147/IDR.S230604
243. Sivick KE, Arpaia N, Reiner GL, Lee BL, Russell BR, Barton GM. Toll-like receptor-deficient mice reveal how innate immune signaling influences Salmonella virulence strategies. *Cell Host Microbe.* 2014;15(2):203-213. doi:10.1016/j.chom.2014.01.013
244. Gogoi M, Shreenivas MM, Chakravorty D. Hoodwinking the Big-Eater to Prosper: The Salmonella-Macrophage Paradigm. *J Innate Immun.* 2019;11(3):289-299. doi:10.1159/000490953
245. WHO | Global tuberculosis report 2019. WHO. Accessed May 7, 2020. http://www.who.int/tb/publications/global_report/en/
246. Means TK, Wang S, Lien E, Yoshimura A, Golenbock DT, Fenton MJ. Human Toll-Like Receptors Mediate Cellular Activation by Mycobacterium tuberculosis. *J Immunol.* 1999;163(7):3920-3927.
247. Jo E-K. Mycobacterial interaction with innate receptors: TLRs, C-type lectins, and NLRs. *Curr Opin Infect Dis.* 2008;21(3):279-286. doi:10.1097/QCO.0b013e3282f88b5d
248. Feltcher ME, Sullivan JT, Braunstein M. Protein export systems of Mycobacterium tuberculosis: novel targets for drug development? *Future Microbiol.* 2010;5(10):1581-1597. doi:10.2217/fmb.10.112

249. Brodin P, Majlessi L, Marsollier L, et al. Dissection of ESAT-6 system 1 of *Mycobacterium tuberculosis* and impact on immunogenicity and virulence. *Infect Immun*. 2006;74(1):88-98. doi:10.1128/IAI.74.1.88-98.2006
250. Watson RO, Manzanillo PS, Cox JS. Extracellular *M. tuberculosis* DNA Targets Bacteria for Autophagy by Activating the Host DNA-Sensing Pathway. *Cell*. 2012;150(4):803-815. doi:10.1016/j.cell.2012.06.040
251. Raghavan S, Manzanillo P, Chan K, Dovey C, Cox JS. Secreted transcription factor controls *Mycobacterium tuberculosis* virulence. *Nature*. 2008;454(7205):717-721. doi:10.1038/nature07219
252. Simeone R, Bottai D, Brosch R. ESX/type VII secretion systems and their role in host-pathogen interaction. *Curr Opin Microbiol*. 2009;12(1):4-10. doi:10.1016/j.mib.2008.11.003
253. Wassermann R, Gulen MF, Sala C, et al. *Mycobacterium tuberculosis* Differentially Activates cGAS- and Inflammasome-Dependent Intracellular Immune Responses through ESX-1. *Cell Host Microbe*. 2015;17(6):799-810. doi:10.1016/j.chom.2015.05.003
254. Yu T, Yi Y-S, Yang Y, Oh J, Jeong D, Cho JY. The pivotal role of TBK1 in inflammatory responses mediated by macrophages. *Mediators Inflamm*. 2012;2012:979105. doi:10.1155/2012/979105
255. Takeshita F, Ishii KJ. Intracellular DNA sensors in immunity. *Curr Opin Immunol*. 2008;20(4):383-388. doi:10.1016/j.coi.2008.05.009
256. Weidberg H, Elazar Z. TBK1 mediates crosstalk between the innate immune response and autophagy. *Sci Signal*. 2011;4(187):pe39. doi:10.1126/scisignal.2002355
257. Thurston TLM, Ryzhakov G, Bloor S, von Muhlinen N, Randow F. The TBK1 adaptor and autophagy receptor NDP52 restricts the proliferation of ubiquitin-coated bacteria. *Nat Immunol*. 2009;10(11):1215-1221. doi:10.1038/ni.1800
258. Castillo EF, Dekonenko A, Arko-Mensah J, et al. Autophagy protects against active tuberculosis by suppressing bacterial burden and inflammation. *Proc Natl Acad Sci U S A*. 2012;109(46):E3168-3176. doi:10.1073/pnas.1210500109
259. Bradfute SB, Castillo EF, Arko-Mensah J, et al. Autophagy as an immune effector against tuberculosis. *Curr Opin Microbiol*. 2013;16(3):355-365. doi:10.1016/j.mib.2013.05.003

260. Manca C, Tsenova L, Bergtold A, et al. Virulence of a Mycobacterium tuberculosis clinical isolate in mice is determined by failure to induce Th1 type immunity and is associated with induction of IFN-alpha /beta. *Proc Natl Acad Sci U S A*. 2001;98(10):5752-5757. doi:10.1073/pnas.091096998
261. Mayer-Barber KD, Andrade BB, Oland SD, et al. Host-directed therapy of tuberculosis based on interleukin-1 and type I interferon crosstalk. *Nature*. 2014;511(7507):99-103. doi:10.1038/nature13489
262. Mayer-Barber KD, Barber DL, Shenderov K, et al. Caspase-1 independent IL-1beta production is critical for host resistance to mycobacterium tuberculosis and does not require TLR signaling in vivo. *J Immunol Baltim Md 1950*. 2010;184(7):3326-3330. doi:10.4049/jimmunol.0904189
263. Fremont CM, Togbe D, Doz E, et al. IL-1 receptor-mediated signal is an essential component of MyD88-dependent innate response to Mycobacterium tuberculosis infection. *J Immunol Baltim Md 1950*. 2007;179(2):1178-1189. doi:10.4049/jimmunol.179.2.1178
264. Information NC for B, Pike USNL of M 8600 R, MD B, Usa 20894. *The Innate and Adaptive Immune Systems*. Institute for Quality and Efficiency in Health Care (IQWiG); 2016. Accessed May 12, 2020. <https://www.ncbi.nlm.nih.gov/books/NBK279396/>
265. Trained immunity: A program of innate immune memory in health and disease | Science. Accessed May 12, 2020. <https://science.sciencemag.org/content/352/6284/aaf1098>
266. Smale ST. Transcriptional regulation in the innate immune system. *Curr Opin Immunol*. 2012;24(1):51-57. doi:10.1016/j.coi.2011.12.008
267. Ramirez-Carrozzi VR, Braas D, Bhatt DM, et al. A Unifying Model for the Selective Regulation of Inducible Transcription by CpG Islands and Nucleosome Remodeling. *Cell*. 2009;138(1):114-128. doi:10.1016/j.cell.2009.04.020
268. Fowler T, Sen R, Roy AL. Regulation of primary response genes. *Mol Cell*. 2011;44(3):348-360. doi:10.1016/j.molcel.2011.09.014
269. Ramirez-Carrozzi VR, Nazarian AA, Li CC, et al. Selective and antagonistic functions of SWI/SNF and Mi-2beta nucleosome remodeling complexes during an inflammatory response. *Genes Dev*. 2006;20(3):282-296. doi:10.1101/gad.1383206
270. Singh SK, Ruzek D. *Viral Hemorrhagic Fevers*. CRC Press; 2016.

271. Hayden MS, West AP, Ghosh S. NF- κ B and the immune response. *Oncogene*. 2006;25(51):6758-6780. doi:10.1038/sj.onc.1209943
272. Dorrington MG, Fraser IDC. NF- κ B Signaling in Macrophages: Dynamics, Crosstalk, and Signal Integration. *Front Immunol*. 2019;10. doi:10.3389/fimmu.2019.00705
273. Oeckinghaus A, Ghosh S. The NF- κ B Family of Transcription Factors and Its Regulation. *Cold Spring Harb Perspect Biol*. 2009;1(4). doi:10.1101/cshperspect.a000034
274. Van der Poll T, Van Deventer SJH. Interleukin-6 in Bacterial Infection and Sepsis: Innocent Bystander or Essential Mediator? In: Vincent J-L, ed. *Yearbook of Intensive Care and Emergency Medicine 1999*. Yearbook of Intensive Care and Emergency Medicine. Springer; 1999:43-53. doi:10.1007/978-3-662-13453-5_5
275. Mogensen TH. IRF and STAT Transcription Factors - From Basic Biology to Roles in Infection, Protective Immunity, and Primary Immunodeficiencies. *Front Immunol*. 2019;9. doi:10.3389/fimmu.2018.03047
276. IRF7: activation, regulation, modification and function | Genes & Immunity. Accessed May 14, 2020. <https://www.nature.com/articles/gene201121>
277. Lee C-K, Bluysen HAR. Editorial: STATs and IRFs in Innate Immunity: From Transcriptional Regulators to Therapeutic Targets. *Front Immunol*. 2019;10:1829. doi:10.3389/fimmu.2019.01829
278. Kim TK, Maniatis T. The mechanism of transcriptional synergy of an in vitro assembled interferon-beta enhanceosome. *Mol Cell*. 1997;1(1):119-129. doi:10.1016/s1097-2765(00)80013-1
279. Malmgaard L. Induction and regulation of IFNs during viral infections. *J Interferon Cytokine Res Off J Int Soc Interferon Cytokine Res*. 2004;24(8):439-454. doi:10.1089/1079990041689665
280. Plataniias LC. Mechanisms of type-I- and type-II-interferon-mediated signalling. *Nat Rev Immunol*. 2005;5(5):375-386. doi:10.1038/nri1604
281. Marchetti M, Monier M-N, Fradagrada A, et al. Stat-mediated Signaling Induced by Type I and Type II Interferons (IFNs) Is Differentially Controlled through Lipid Microdomain Association and Clathrin-dependent Endocytosis of IFN Receptors. *Mol Biol Cell*. 2006;17(7):2896-2909. doi:10.1091/mbc.E06-01-0076

282. Decker T, Kovarik P, Meinke A. GAS elements: a few nucleotides with a major impact on cytokine-induced gene expression. *J Interferon Cytokine Res Off J Int Soc Interferon Cytokine Res*. 1997;17(3):121-134. doi:10.1089/jir.1997.17.121
283. Lee AJ, Ashkar AA. The Dual Nature of Type I and Type II Interferons. *Front Immunol*. 2018;9:2061. doi:10.3389/fimmu.2018.02061
284. Schaub A, Glasmacher E. Splicing in immune cells-mechanistic insights and emerging topics. *Int Immunol*. 2017;29(4):173-181. doi:10.1093/intimm/dxx026
285. Stevenson BJ, Iseli C, Beutler B, Jongeneel CV. Use of Transcriptome Data to Unravel the Fine Structure of Genes Involved in Sepsis. *J Infect Dis*. 2003;187(Supplement_2):S308-S314. doi:10.1086/374755
286. Shell SA, Hesse C, Morris SM, Milcarek C. Elevated levels of the 64-kDa cleavage stimulatory factor (CstF-64) in lipopolysaccharide-stimulated macrophages influence gene expression and induce alternative poly(A) site selection. *J Biol Chem*. 2005;280(48):39950-39961. doi:10.1074/jbc.M508848200
287. Crawford EK, Ensor JE, Kalvakolanu I, Hasday JD. The role of 3' poly(A) tail metabolism in tumor necrosis factor-alpha regulation. *J Biol Chem*. 1997;272(34):21120-21127. doi:10.1074/jbc.272.34.21120
288. Swanson BJ, Murakami M, Mitchell TC, Kappler J, Marrack P. RANTES production by memory phenotype T cells is controlled by a posttranscriptional, TCR-dependent process. *Immunity*. 2002;17(5):605-615. doi:10.1016/s1074-7613(02)00456-9
289. Kuss SK, Mata MA, Zhang L, Fontoura BMA. Nuclear Imprisonment: Viral Strategies to Arrest Host mRNA Nuclear Export. *Viruses*. 2013;5(7):1824-1849. doi:10.3390/v5071824
290. Rabani M, Levin JZ, Fan L, et al. Metabolic labeling of RNA uncovers principles of RNA production and degradation dynamics in mammalian cells. *Nat Biotechnol*. 2011;29(5):436-442. doi:10.1038/nbt.1861
291. Chang J-S, Huggett JF, Dheda K, Kim LU, Zumla A, Rook GAW. Myobacterium tuberculosis induces selective up-regulation of TLRs in the mononuclear leukocytes of patients with active pulmonary tuberculosis. *J Immunol Baltim Md 1950*. 2006;176(5):3010-3018. doi:10.4049/jimmunol.176.5.3010
292. Anderson P. Post-transcriptional regulons coordinate the initiation and resolution of inflammation. *Nat Rev Immunol*. 2010;10(1):24-35. doi:10.1038/nri2685

293. Chen Y-L, Jiang Y-W, Su Y-L, Lee S-C, Chang M-S, Chang C-J. Transcriptional regulation of tristetraprolin by NF- κ B signaling in LPS-stimulated macrophages. *Mol Biol Rep*. 2013;40(4):2867-2877. doi:10.1007/s11033-012-2302-8
294. Liepelt A, Mossanen JC, Denecke B, et al. Translation control of TAK1 mRNA by hnRNP K modulates LPS-induced macrophage activation. *RNA*. 2014;20(6):899-911. doi:10.1261/rna.042788.113
295. Carballo E, Lai WS, Blackshear PJ. Feedback Inhibition of Macrophage Tumor Necrosis Factor- α Production by Tristetraprolin. *Science*. 1998;281(5379):1001-1005. doi:10.1126/science.281.5379.1001
296. Sauer I, Schaljo B, Vogl C, et al. Interferons limit inflammatory responses by induction of tristetraprolin. *Blood*. 2006;107(12):4790-4797. doi:10.1182/blood-2005-07-3058
297. Linker K, Pautz A, Fechir M, Hubrich T, Greeve J, Kleinert H. Involvement of KSRP in the post-transcriptional regulation of human iNOS expression-complex interplay of KSRP with TTP and HuR. *Nucleic Acids Res*. 2005;33(15):4813-4827. doi:10.1093/nar/gki797
298. Matsushita K, Takeuchi O, Standley DM, et al. Zc3h12a is an RNase essential for controlling immune responses by regulating mRNA decay. *Nature*. 2009;458(7242):1185-1190. doi:10.1038/nature07924
299. Jones MR, Quinton LJ, Blahna MT, et al. Zcchc11-dependent uridylation of microRNA directs cytokine expression. *Nat Cell Biol*. 2009;11(9):1157-1163. doi:10.1038/ncb1931
300. Baltimore D, Boldin MP, O'Connell RM, Rao DS, Taganov KD. MicroRNAs: new regulators of immune cell development and function. *Nat Immunol*. 2008;9(8):839-845. doi:10.1038/ni.f.209
301. Taganov KD, Boldin MP, Chang K-J, Baltimore D. NF- κ B-dependent induction of microRNA miR-146, an inhibitor targeted to signaling proteins of innate immune responses. *Proc Natl Acad Sci*. 2006;103(33):12481-12486. doi:10.1073/pnas.0605298103
302. Carpenter S, Atianand M, Aiello D, et al. A long noncoding RNA induced by TLRs mediates both activation and repression of immune response genes. *Science*. 2013;341(6147):789-792. doi:10.1126/science.1240925
303. Salmena L, Poliseno L, Tay Y, Kats L, Pandolfi PP. A ceRNA hypothesis: the Rosetta Stone of a hidden RNA language? *Cell*. 2011;146(3):353-358. doi:10.1016/j.cell.2011.07.014

304. Gordiyenko Y, Llácer JL, Ramakrishnan V. Structural basis for the inhibition of translation through eIF2 α phosphorylation. *Nat Commun.* 2019;10(1):2640. doi:10.1038/s41467-019-10606-1
305. Wan Y, Xiao H, Affolter J, et al. Interleukin-1 receptor-associated kinase 2 is critical for lipopolysaccharide-mediated post-transcriptional control. *J Biol Chem.* 2009;284(16):10367-10375. doi:10.1074/jbc.M807822200
306. Schmitz F, Heit A, Dreher S, et al. Mammalian target of rapamycin (mTOR) orchestrates the defense program of innate immune cells. *Eur J Immunol.* 2008;38(11):2981-2992. doi:10.1002/eji.200838761
307. López-Pelaéz M, Fumagalli S, Sanz C, et al. Cot/tpl2-MKK1/2-Erk1/2 controls mTORC1-mediated mRNA translation in Toll-like receptor-activated macrophages. *Mol Biol Cell.* 2012;23(15):2982-2992. doi:10.1091/mbc.E12-02-0135
308. Weichhart T, Costantino G, Poglitsch M, et al. The TSC-mTOR signaling pathway regulates the innate inflammatory response. *Immunity.* 2008;29(4):565-577. doi:10.1016/j.immuni.2008.08.012
309. Bhatt DM, Pandya-Jones A, Tong A-J, et al. Transcript Dynamics of Proinflammatory Genes Revealed by Sequence Analysis of Subcellular RNA Fractions. *Cell.* 2012;150(2):279-290. doi:10.1016/j.cell.2012.05.043
310. Pai AA, Baharian G, Pagé Sabourin A, et al. Widespread Shortening of 3' Untranslated Regions and Increased Exon Inclusion Are Evolutionarily Conserved Features of Innate Immune Responses to Infection. *PLoS Genet.* 2016;12(9). doi:10.1371/journal.pgen.1006338
311. Kalam H, Fontana MF, Kumar D. Alternate splicing of transcripts shape macrophage response to Mycobacterium tuberculosis infection. *PLOS Pathog.* 2017;13(3):e1006236. doi:10.1371/journal.ppat.1006236
312. Zhang W, Niu C, Fu R-Y, Peng Z-Y. Mycobacterium tuberculosis H37Rv infection regulates alternative splicing in Macrophages. *Bioengineered.* 2018;9(1):203-208. doi:10.1080/21655979.2017.1387692
313. De Maio FA, Risso G, Iglesias NG, et al. The Dengue Virus NS5 Protein Intrudes in the Cellular Spliceosome and Modulates Splicing. *PLoS Pathog.* 2016;12(8). doi:10.1371/journal.ppat.1005841
314. Jaresová I, Rozková D, Spísek R, Janda A, Brázová J, Sedivá A. Kinetics of Toll-like receptor-4 splice variants expression in lipopolysaccharide-stimulated antigen

- presenting cells of healthy donors and patients with cystic fibrosis. *Microbes Infect.* 2007;9(11):1359-1367. doi:10.1016/j.micinf.2007.06.009
315. Iwami KI, Matsuguchi T, Masuda A, Kikuchi T, Musikacharoen T, Yoshikai Y. Cutting edge: naturally occurring soluble form of mouse Toll-like receptor 4 inhibits lipopolysaccharide signaling. *J Immunol Baltim Md 1950.* 2000;165(12):6682-6686. doi:10.4049/jimmunol.165.12.6682
 316. Haehnel V, Schwarzfischer L, Fenton MJ, Rehli M. Transcriptional regulation of the human toll-like receptor 2 gene in monocytes and macrophages. *J Immunol Baltim Md 1950.* 2002;168(11):5629-5637. doi:10.4049/jimmunol.168.11.5629
 317. Janssens S, Burns K, Vercammen E, Tschopp J, Beyaert R. MyD88S, a splice variant of MyD88, differentially modulates NF- κ B- and AP-1-dependent gene expression. *FEBS Lett.* 2003;548(1):103-107. doi:10.1016/S0014-5793(03)00747-6
 318. Rao N, Nguyen S, Ngo K, Fung-Leung W-P. A Novel Splice Variant of Interleukin-1 Receptor (IL-1R)-Associated Kinase 1 Plays a Negative Regulatory Role in Toll/IL-1R-Induced Inflammatory Signaling. *Mol Cell Biol.* 2005;25(15):6521-6532. doi:10.1128/MCB.25.15.6521-6532.2005
 319. Gray P, Michelsen KS, Sirois CM, et al. Identification of a Novel Human MD-2 Splice Variant That Negatively Regulates Lipopolysaccharide-Induced TLR4 Signaling. *J Immunol.* 2010;184(11):6359-6366. doi:10.4049/jimmunol.0903543
 320. Seo J-W, Yang E-J, Kim SH, Choi I-H. An inhibitory alternative splice isoform of Toll-like receptor 3 is induced by type I interferons in human astrocyte cell lines. *BMB Rep.* 2015;48(12):696-701. doi:10.5483/BMBRep.2015.48.12.106
 321. De Arras L, Seng A, Lackford B, et al. An Evolutionarily Conserved Innate Immunity Protein Interaction Network. *J Biol Chem.* 2013;288(3):1967-1978. doi:10.1074/jbc.M112.407205
 322. Jensen LE, Whitehead AS. IRAK1b, a novel alternative splice variant of interleukin-1 receptor-associated kinase (IRAK), mediates interleukin-1 signaling and has prolonged stability. *J Biol Chem.* 2001;276(31):29037-29044. doi:10.1074/jbc.M103815200
 323. Yanagisawa K, Tago K, Hayakawa M, Ohki M, Iwahana H, Tominaga S-I. A novel splice variant of mouse interleukin-1-receptor-associated kinase-1 (IRAK-1) activates nuclear factor-kappaB (NF-kappaB) and c-Jun N-terminal kinase (JNK). *Biochem J.* 2003;370(Pt 1):159-166. doi:10.1042/BJ20021218

324. Brubaker SW, Gauthier AE, Mills EW, Ingolia NT, Kagan JC. A bicistronic MAVS transcript highlights a class of truncated variants in antiviral immunity. *Cell*. 2014;156(4):800-811. doi:10.1016/j.cell.2014.01.021
325. Penn BH, Netter Z, Johnson JR, et al. An Mtb-Human Protein-Protein Interaction Map Identifies a Switch between Host Antiviral and Antibacterial Responses. *Mol Cell*. 2018;71(4):637-648.e5. doi:10.1016/j.molcel.2018.07.010
326. Budzik JM, Swaney DL, Jimenez-Morales D, et al. Dynamic post-translational modification profiling of Mycobacterium tuberculosis-infected primary macrophages. Garrett WS, Kana BD, Dhar N, eds. *eLife*. 2020;9:e51461. doi:10.7554/eLife.51461
327. Liu J, Qian C, Cao X. Post-Translational Modification Control of Innate Immunity. *Immunity*. 2016;45(1):15-30. doi:10.1016/j.immuni.2016.06.020
328. Levy D, Kuo AJ, Chang Y, et al. Lysine methylation of the NF- κ B subunit RelA by SETD6 couples activity of the histone methyltransferase GLP at chromatin to tonic repression of NF- κ B signaling. *Nat Immunol*. 2011;12(1):29-36. doi:10.1038/ni.1968
329. Zhong B, Zhang L, Lei C, et al. The ubiquitin ligase RNF5 regulates antiviral responses by mediating degradation of the adaptor protein MITA. *Immunity*. 2009;30(3):397-407. doi:10.1016/j.immuni.2009.01.008
330. Pan Y, Li R, Meng J-L, Mao H-T, Zhang Y, Zhang J. Smurf2 Negatively Modulates RIG-I-Dependent Antiviral Response by Targeting VISA/MAVS for Ubiquitination and Degradation. *J Immunol*. 2014;192(10):4758-4764. doi:10.4049/jimmunol.1302632
331. Yoo Y-S, Park Y-Y, Kim J-H, et al. The mitochondrial ubiquitin ligase MARCH5 resolves MAVS aggregates during antiviral signalling. *Nat Commun*. 2015;6. doi:10.1038/ncomms8910
332. Cui J, Song Y, Li Y, et al. USP3 inhibits type I interferon signaling by deubiquitinating RIG-I-like receptors. *Cell Res*. 2014;24(4):400-416. doi:10.1038/cr.2013.170
333. Pauli E-K, Chan YK, Davis ME, et al. The Ubiquitin-Specific Protease USP15 Promotes RIG-I-Mediated Antiviral Signaling by Deubiquitylating TRIM25. *Sci Signal*. 2014;7(307):ra3. doi:10.1126/scisignal.2004577
334. Fan Y, Mao R, Yu Y, et al. USP21 negatively regulates antiviral response by acting as a RIG-I deubiquitinase. *J Exp Med*. 2014;211(2):313-328. doi:10.1084/jem.20122844

335. Lei C-Q, Zhong B, Zhang Y, Zhang J, Wang S, Shu H-B. Glycogen Synthase Kinase 3 β Regulates IRF3 Transcription Factor-Mediated Antiviral Response via Activation of the Kinase TBK1. *Immunity*. 2010;33(6):878-889. doi:10.1016/j.immuni.2010.11.021
336. Jiao S, Zhang Z, Li C, et al. The kinase MST4 limits inflammatory responses through direct phosphorylation of the adaptor TRAF6. *Nat Immunol*. 2015;16(3):246-257. doi:10.1038/ni.3097
337. Cui J, Zhu L, Xia X, et al. NLRC5 Negatively Regulates the NF- κ B and Type I Interferon Signaling Pathways. *Cell*. 2010;141(3):483-496. doi:10.1016/j.cell.2010.03.040
338. Xia X, Cui J, Wang HY, et al. NLRX1 Negatively Regulates TLR-Induced NF- κ B Signaling by Targeting TRAF6 and IKK. *Immunity*. 2011;34(6):843-853. doi:10.1016/j.immuni.2011.02.022
339. Pandey A, Ding SL, Qin Q-M, et al. Global Reprogramming of Host Kinase Signaling in Response to Fungal Infection. *Cell Host Microbe*. 2017;21(5):637-649.e6. doi:10.1016/j.chom.2017.04.008
340. Zhao W, Wang L, Zhang M, et al. Nuclear to Cytoplasmic Translocation of Heterogeneous Nuclear Ribonucleoprotein U Enhances TLR-Induced Proinflammatory Cytokine Production by Stabilizing mRNAs in Macrophages. *J Immunol*. 2012;188(7):3179-3187. doi:10.4049/jimmunol.1101175
341. Ostareck DH, Ostareck-Lederer A. RNA-Binding Proteins in the Control of LPS-Induced Macrophage Response. *Front Genet*. 2019;10. doi:10.3389/fgene.2019.00031
342. Viktorovskaya OV, Greco TM, Cristea IM, Thompson SR. Identification of RNA Binding Proteins Associated with Dengue Virus RNA in Infected Cells Reveals Temporally Distinct Host Factor Requirements. *PLoS Negl Trop Dis*. 2016;10(8). doi:10.1371/journal.pntd.0004921
343. Yamamoto M, Sato S, Hemmi H, et al. Role of Adaptor TRIF in the MyD88-Independent Toll-Like Receptor Signaling Pathway. *Science*. 2003;301(5633):640-643. doi:10.1126/science.1087262
344. Sun H, Kamanova J, Lara-Tejero M, Galán JE. Salmonella stimulates pro-inflammatory signalling through p21-activated kinases bypassing innate immune receptors. *Nat Microbiol*. 2018;3(10):1122-1130. doi:10.1038/s41564-018-0246-z

345. A new view of transcriptome complexity and regulation through the lens of local splicing variations | eLife. Accessed April 21, 2020. <https://elifesciences.org/articles/11752>
346. Lichtenstein M, Guo W, Tartakoff AM. Control of Nuclear Export of hnRNP A1. *Traffic*. 2001;2(4):261-267. doi:10.1034/j.1600-0854.2001.1o002.x
347. Pettit Kneller EL, Connor JH, Lyles DS. hnRNPs Relocalize to the Cytoplasm following Infection with Vesicular Stomatitis Virus. *J Virol*. 2009;83(2):770-780. doi:10.1128/JVI.01279-08
348. Kosugi S, Hasebe M, Tomita M, Yanagawa H. Systematic identification of cell cycle-dependent yeast nucleocytoplasmic shuttling proteins by prediction of composite motifs. *Proc Natl Acad Sci*. 2009;106(25):10171-10176. doi:10.1073/pnas.0900604106
349. Yachdav G, Kloppmann E, Kajan L, et al. PredictProtein--an open resource for online prediction of protein structural and functional features. *Nucleic Acids Res*. 2014;42(Web Server issue):W337-343. doi:10.1093/nar/gku366
350. Moehle EA, Ryan CJ, Krogan NJ, Kress TL, Guthrie C. The Yeast SR-Like Protein Npl3 Links Chromatin Modification to mRNA Processing. *PLoS Genet*. 2012;8(11). doi:10.1371/journal.pgen.1003101
351. Nojima T, Gomes T, Carmo-Fonseca M, Proudfoot NJ. Mammalian NET-seq analysis defines nascent RNA profiles and associated RNA processing genome-wide. *Nat Protoc*. 2016;11(3):413-428. doi:10.1038/nprot.2016.012
352. Pandya-Jones A, Black DL. Co-transcriptional splicing of constitutive and alternative exons. *RNA*. 2009;15(10):1896-1908. doi:10.1261/rna.1714509
353. Neves LT, Douglass S, Spreafico R, Venkataramanan S, Kress TL, Johnson TL. The histone variant H2A.Z promotes efficient cotranscriptional splicing in *S. cerevisiae*. *Genes Dev*. 2017;31(7):702-717. doi:10.1101/gad.295188.116
354. Nissen KE, Homer CM, Ryan CJ, et al. The histone variant H2A.Z promotes splicing of weak introns. *Genes Dev*. 2017;31(7):688-701. doi:10.1101/gad.295287.116
355. Patrick KL, Ryan CJ, Xu J, et al. Genetic Interaction Mapping Reveals a Role for the SWI/SNF Nucleosome Remodeler in Spliceosome Activation in Fission Yeast. *PLoS Genet*. 2015;11(3). doi:10.1371/journal.pgen.1005074

356. Bieberstein NI, Carrillo Oesterreich F, Straube K, Neugebauer KM. First exon length controls active chromatin signatures and transcription. *Cell Rep.* 2012;2(1):62-68. doi:10.1016/j.celrep.2012.05.019
357. Van Nostrand EL, Pratt GA, Shishkin AA, et al. Robust transcriptome-wide discovery of RNA-binding protein binding sites with enhanced CLIP (eCLIP). *Nat Methods.* 2016;13(6):508-514. doi:10.1038/nmeth.3810
358. Costa-Pereira AP. Regulation of IL-6-type cytokine responses by MAPKs. *Biochem Soc Trans.* 2014;42(1):59-62. doi:10.1042/BST20130267
359. Kandasamy RK, Vladimer GI, Snijder B, et al. A time-resolved molecular map of the macrophage response to VSV infection. *Npj Syst Biol Appl.* 2016;2(1):1-12. doi:10.1038/npjjsba.2016.27
360. Masuda K, Ripley B, Nishimura R, et al. Arid5a controls IL-6 mRNA stability, which contributes to elevation of IL-6 level in vivo. *Proc Natl Acad Sci.* 2013;110(23):9409-9414. doi:10.1073/pnas.1307419110
361. Higa M, Oka M, Fujihara Y, Masuda K, Yoneda Y, Kishimoto T. Regulation of inflammatory responses by dynamic subcellular localization of RNA-binding protein Arid5a. *Proc Natl Acad Sci.* 2018;115(6):E1214-E1220. doi:10.1073/pnas.1719921115
362. Ling JP, Pletnikova O, Troncoso JC, Wong PC. TDP-43 repression of nonconserved cryptic exons is compromised in ALS-FTD. *Science.* 2015;349(6248):650-655. doi:10.1126/science.aab0983
363. Ling JP, Chhabra R, Merran JD, et al. PTBP1 and PTBP2 Repress Nonconserved Cryptic Exons. *Cell Rep.* 2016;17(1):104-113. doi:10.1016/j.celrep.2016.08.071
364. de Almeida SF, Grosso AR, Koch F, et al. Splicing enhances recruitment of methyltransferase HYPB/Setd2 and methylation of histone H3 Lys36. *Nat Struct Mol Biol.* 2011;18(9):977-983. doi:10.1038/nsmb.2123
365. Kim S, Kim H, Fong N, Erickson B, Bentley DL. Pre-mRNA splicing is a determinant of histone H3K36 methylation. *Proc Natl Acad Sci.* 2011;108(33):13564-13569. doi:10.1073/pnas.1109475108
366. Martins SB, Rino J, Carvalho T, et al. Spliceosome assembly is coupled to RNA polymerase II dynamics at the 3' end of human genes. *Nat Struct Mol Biol.* 2011;18(10):1115-1123. doi:10.1038/nsmb.2124

367. Saldi T, Cortazar MA, Sheridan RM, Bentley DL. Coupling of RNA Polymerase II Transcription Elongation with Pre-mRNA Splicing. *J Mol Biol.* 2016;428(12):2623-2635. doi:10.1016/j.jmb.2016.04.017
368. Atianand MK, Hu W, Satpathy AT, et al. A Long Noncoding RNA lincRNA-EPS Acts as a Transcriptional Brake to Restrain Inflammation. *Cell.* 2016;165(7):1672-1685. doi:10.1016/j.cell.2016.05.075
369. Marko M, Leichter M, Patrino-Georgoula M, Guialis A. Selective interactions of hnRNP M isoforms with the TET proteins TAF15 and TLS/FUS. *Mol Biol Rep.* 2014;41(4):2687-2695. doi:10.1007/s11033-014-3128-3
370. Fox AH, Lamond AI. Paraspeckles. *Cold Spring Harb Perspect Biol.* 2010;2(7):a000687. doi:10.1101/cshperspect.a000687
371. Fox AH, Nakagawa S, Hirose T, Bond CS. Paraspeckles: Where Long Noncoding RNA Meets Phase Separation. *Trends Biochem Sci.* 2018;43(2):124-135. doi:10.1016/j.tibs.2017.12.001
372. Boehringer A, Garcia-Mansfield K, Singh G, Bakkar N, Pirrotte P, Bowser R. ALS Associated Mutations in Matrin 3 Alter Protein-Protein Interactions and Impede mRNA Nuclear Export. *Sci Rep.* 2017;7. doi:10.1038/s41598-017-14924-6
373. Imamura K, Imamachi N, Akizuki G, et al. Long Noncoding RNA NEAT1-Dependent SFPQ Relocation from Promoter Region to Paraspeckle Mediates IL8 Expression upon Immune Stimuli. *Mol Cell.* 2014;53(3):393-406. doi:10.1016/j.molcel.2014.01.009
374. Tan DQ, Li Y, Yang C, et al. PRMT5 Modulates Splicing for Genome Integrity and Preserves Proteostasis of Hematopoietic Stem Cells. *Cell Rep.* 2019;26(9):2316-2328.e6. doi:10.1016/j.celrep.2019.02.001
375. Knott GJ, Bond CS, Fox AH. The DBHS proteins SFPQ, NONO and PSPC1: a multipurpose molecular scaffold. *Nucleic Acids Res.* 2016;44(9):3989-4004. doi:10.1093/nar/gkw271
376. Lahaye X, Gentili M, Silvin A, et al. NONO Detects the Nuclear HIV Capsid to Promote cGAS-Mediated Innate Immune Activation. *Cell.* 2018;175(2):488-501.e22. doi:10.1016/j.cell.2018.08.062
377. Fang J, Bolanos LC, Choi K, et al. Ubiquitination of hnRNPA1 by TRAF6 links chronic innate immune signaling with myelodysplasia. *Nat Immunol.* 2017;18(2):236-245. doi:10.1038/ni.3654

378. Cao P, Luo W-W, Li C, et al. The heterogeneous nuclear ribonucleoprotein hnRNPM inhibits RNA virus-triggered innate immunity by antagonizing RNA sensing of RIG-I-like receptors. *PLoS Pathog.* 2019;15(8):e1007983. doi:10.1371/journal.ppat.1007983
379. Parseghian MH, Luhrs KA. Beyond the walls of the nucleus: the role of histones in cellular signaling and innate immunity This paper is one of a selection of papers published in this Special Issue, entitled 27th International West Coast Chromatin and Chromosome Conference, and has undergone the Journal's usual peer review process. *Biochem Cell Biol.* 2006;84(4):589-595. doi:10.1139/o06-082
380. Ergun A, Doran G, Costello JC, et al. Differential splicing across immune system lineages. *Proc Natl Acad Sci.* 2013;110(35):14324-14329. doi:10.1073/pnas.1311839110
381. Pan Q, Shai O, Lee LJ, Frey BJ, Blencowe BJ. Deep surveying of alternative splicing complexity in the human transcriptome by high-throughput sequencing. *Nat Genet.* 2008;40(12):1413-1415. doi:10.1038/ng.259
382. Lo C-S, Shi Y, Chenier I, et al. Heterogeneous Nuclear Ribonucleoprotein F Stimulates Sirtuin-1 Gene Expression and Attenuates Nephropathy Progression in Diabetic Mice. *Diabetes.* 2017;66(7):1964-1978. doi:10.2337/db16-1588
383. Gamberi C, Izaurralde E, Beisel C, Mattaj IW. Interaction between the human nuclear cap-binding protein complex and hnRNP F. *Mol Cell Biol.* 1997;17(5):2587-2597.
384. Veraldi KL, Arhin GK, Martincic K, Chung-Ganster L-H, Wilusz J, Milcarek C. hnRNP F Influences Binding of a 64-Kilodalton Subunit of Cleavage Stimulation Factor to mRNA Precursors in Mouse B Cells. *Mol Cell Biol.* 2001;21(4):1228-1238. doi:10.1128/MCB.21.4.1228-1238.2001
385. Huang H, Zhang J, Harvey SE, Hu X, Cheng C. RNA G-quadruplex secondary structure promotes alternative splicing via the RNA-binding protein hnRNPF. *Genes Dev.* 2017;31(22):2296-2309. doi:10.1101/gad.305862.117
386. Min H. The generally expressed hnRNP F is involved in a neural-specific pre-mR splicing event. :14.
387. Schneider WM, Chevillotte MD, Rice CM. Interferon-stimulated genes: a complex web of host defenses. *Annu Rev Immunol.* 2014;32:513-545. doi:10.1146/annurev-immunol-032713-120231

388. Wang E, Dimova N, Cambi F. PLP/DM20 ratio is regulated by hnRNPH and F and a novel G-rich enhancer in oligodendrocytes. *Nucleic Acids Res.* 2007;35(12):4164-4178. doi:10.1093/nar/gkm387
389. White R, Gonsior C, Bauer NM, Kraemer-Albers EM, Luhmann HJ, Trotter J. HnRNP F is a novel component of oligodendroglial RNA transport granules contributing to the regulation of MBP protein synthesis. *J Biol Chem.* Published online November 29, 2011:jbc.M111.235010. doi:10.1074/jbc.M111.235010
390. West KO, Scott HM, Torres-Odio S, West AP, Patrick KL, Watson RO. The Splicing Factor hnRNP M Is a Critical Regulator of Innate Immune Gene Expression in Macrophages. *Cell Rep.* 2019;29(6):1594-1609.e5. doi:10.1016/j.celrep.2019.09.078
391. Hoffpauir CT, Bell SL, West KO, et al. TRIM14 Is a Key Regulator of the Type I IFN Response during Mycobacterium tuberculosis Infection. *J Immunol.* Published online May 13, 2020. doi:10.4049/jimmunol.1901511
392. Juffermans NP, Verbon A, van Deventer SJ, et al. Serum concentrations of lipopolysaccharide activity-modulating proteins during tuberculosis. *J Infect Dis.* 1998;178(6):1839-1842. doi:10.1086/314492
393. Savedra R, Delude RL, Ingalls RR, Fenton MJ, Golenbock DT. Mycobacterial lipoarabinomannan recognition requires a receptor that shares components of the endotoxin signaling system. *J Immunol Baltim Md 1950.* 1996;157(6):2549-2554.
394. Zhang Y, Doerfler M, Lee TC, Guillemin B, Rom WN. Mechanisms of stimulation of interleukin-1 beta and tumor necrosis factor-alpha by Mycobacterium tuberculosis components. *J Clin Invest.* 1993;91(5):2076-2083. doi:10.1172/JCI116430
395. Taniguchi T, Takaoka A. The interferon- α/β system in antiviral responses: a multimodal machinery of gene regulation by the IRF family of transcription factors. *Curr Opin Immunol.* 2002;14(1):111-116. doi:10.1016/S0952-7915(01)00305-3
396. Sakaguchi S, Negishi H, Asagiri M, et al. Essential role of IRF-3 in lipopolysaccharide-induced interferon- β gene expression and endotoxin shock. *Biochem Biophys Res Commun.* 2003;306(4):860-866. doi:10.1016/S0006-291X(03)01049-0
397. Sato M, Suemori H, Hata N, et al. Distinct and Essential Roles of Transcription Factors IRF-3 and IRF-7 in Response to Viruses for IFN- α/β Gene Induction. *Immunity.* 2000;13(4):539-548. doi:10.1016/S1074-7613(00)00053-4

398. Juang Y-T, Lowther W, Kellum M, et al. Primary activation of interferon A and interferon B gene transcription by interferon regulatory factor 3. *Proc Natl Acad Sci*. 1998;95(17):9837-9842. doi:10.1073/pnas.95.17.9837
399. SF3B1 - an overview | ScienceDirect Topics. Accessed July 17, 2020. <https://www.sciencedirect.com/topics/biochemistry-genetics-and-molecular-biology/sf3b1>
400. Rosonina E, Ip JYY, Calarco JA, et al. Role for PSF in Mediating Transcriptional Activator-Dependent Stimulation of Pre-mRNA Processing In Vivo. *Mol Cell Biol*. 2005;25(15):6734-6746. doi:10.1128/MCB.25.15.6734-6746.2005
401. Hammerich-Hille S, Kaiparettu BA, Tsimelzon A, et al. SAFB1 mediates repression of immune regulators and apoptotic genes in breast cancer cells. *J Biol Chem*. 2010;285(6):3608-3616. doi:10.1074/jbc.M109.066431
402. Bitko V, Musiyenko A, Bayfield MA, Maraia RJ, Barik S. Cellular La Protein Shields Nonsegmented Negative-Strand RNA Viral Leader RNA from RIG-I and Enhances Virus Growth by Diverse Mechanisms. *J Virol*. 2008;82(16):7977-7987. doi:10.1128/JVI.02762-07
403. Lin J, Kato M, Nagata K, Okuwaki M. Efficient DNA binding of NF- κ B requires the chaperone-like function of NPM1. *Nucleic Acids Res*. 2017;45(7):3707-3723. doi:10.1093/nar/gkw1285
404. Krischuns T, Günl F, Henschel L, et al. Phosphorylation of TRIM28 Enhances the Expression of IFN- β and Proinflammatory Cytokines During HPAIV Infection of Human Lung Epithelial Cells. *Front Immunol*. 2018;9. doi:10.3389/fimmu.2018.02229
405. Cui J, Chen Y, Wang HY, Wang R-F. Mechanisms and pathways of innate immune activation and regulation in health and cancer. *Hum Vaccines Immunother*. 2015;10(11):3270-3285. doi:10.4161/21645515.2014.979640
406. ten Dam GB, Zilch CF, Wallace D, et al. Regulation of alternative splicing of CD45 by antagonistic effects of SR protein splicing factors. *J Immunol Baltim Md 1950*. 2000;164(10):5287-5295. doi:10.4049/jimmunol.164.10.5287
407. Moulton VR, Tsokos GC. Alternative Splicing Factor/Splicing Factor 2 Regulates the Expression of the ζ Subunit of the Human T Cell Receptor-associated CD3 Complex. *J Biol Chem*. 2010;285(17):12490-12496. doi:10.1074/jbc.M109.091660

408. Wang H-Y, Xu X, Ding J-H, Bermingham JR, Fu X-D. SC35 Plays a Role in T Cell Development and Alternative Splicing of CD45. *Mol Cell*. 2001;7(2):331-342. doi:10.1016/S1097-2765(01)00181-2
409. Mole S, McFarlane M, Chuen-Im T, Milligan SG, Millan D, Graham SV. RNA splicing factors regulated by HPV16 during cervical tumour progression. *J Pathol*. 2009;219(3):383-391. doi:10.1002/path.2608
410. Neugebauer KM, Merrill JT, Wener MH, Lahita RG, Roth MB. SR proteins are autoantigens in patients with systemic lupus erythematosus: Importance of phosphoepitopes. *Arthritis Rheum*. 2000;43(8):1768-1778. doi:10.1002/1529-0131(200008)43:8<1768::AID-ANR13>3.0.CO;2-9
411. Xu S, Zhang Z, Jing B, et al. Transportin-SR Is Required for Proper Splicing of Resistance Genes and Plant Immunity. *PLoS Genet*. 2011;7(6):e1002159. doi:10.1371/journal.pgen.1002159
412. Li Q, Zhao H, Jiang L, et al. An SR-protein Induced by HSV1 Binding to Cells Functioning as a Splicing Inhibitor of Viral pre-mRNA. *J Mol Biol*. 2002;316(4):887-894. doi:10.1006/jmbi.2001.5318
413. Scotti MM, Swanson MS. RNA mis-splicing in disease. *Nat Rev Genet*. 2016;17(1):19-32. doi:10.1038/nrg.2015.3
414. Lin S, Xiao R, Sun P, Xu X, Fu X-D. Dephosphorylation-Dependent Sorting of SR Splicing Factors during mRNP Maturation. *Mol Cell*. 2005;20(3):413-425. doi:10.1016/j.molcel.2005.09.015
415. Hsiao K-Y, Chang N, Tsai J-L, Lin S-C, Tsai S-J, Wu M-H. Hypoxia-inhibited DUSP2 expression promotes IL-6/STAT3 signaling in endometriosis. *Am J Reprod Immunol N Y N 1989*. 2017;78(4). doi:10.1111/aji.12690

APPENDIX A
FIGURES

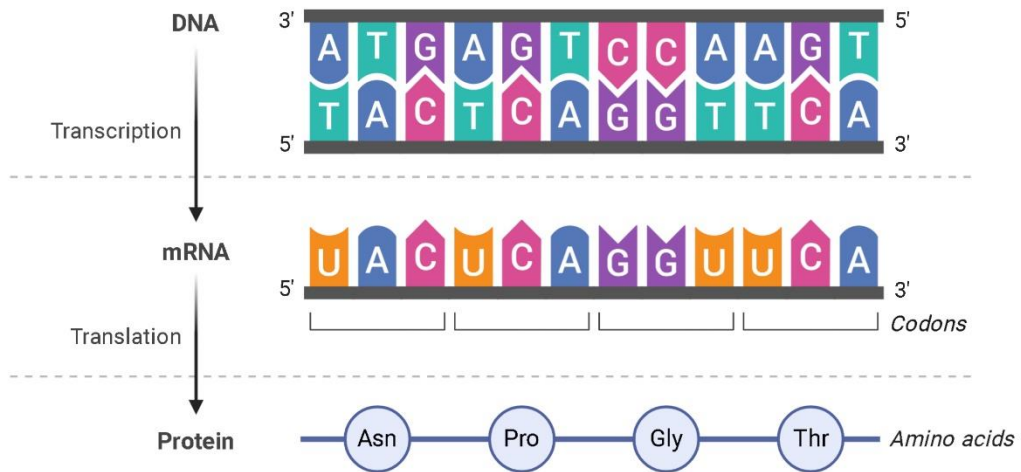


Figure 1. The Central Dogma of Biology

Genetic information from DNA is transcribed into messenger RNA (mRNA). These mRNAs code for amino acids that are produced during the process of translation, leading to the final product of a protein.

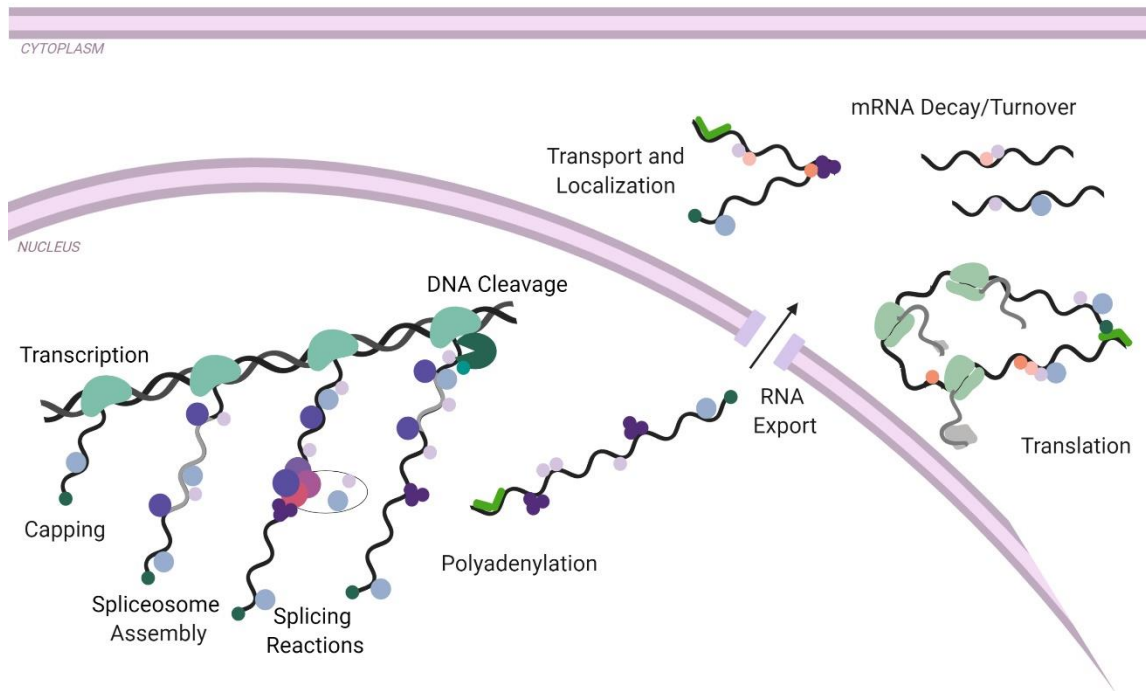


Figure 2. RNA Processing Steps in Eukaryotic Cells

Following transcription, pre-mRNA goes through several RNA processing steps; 5' capping, removing introns through splicing, polyadenylation at the 3' end, and export out of the nucleus. mRNAs are determined to be sent for decay or translated into a protein. Each of these processes are facilitated by various RNA-binding proteins (gray and purple circles).

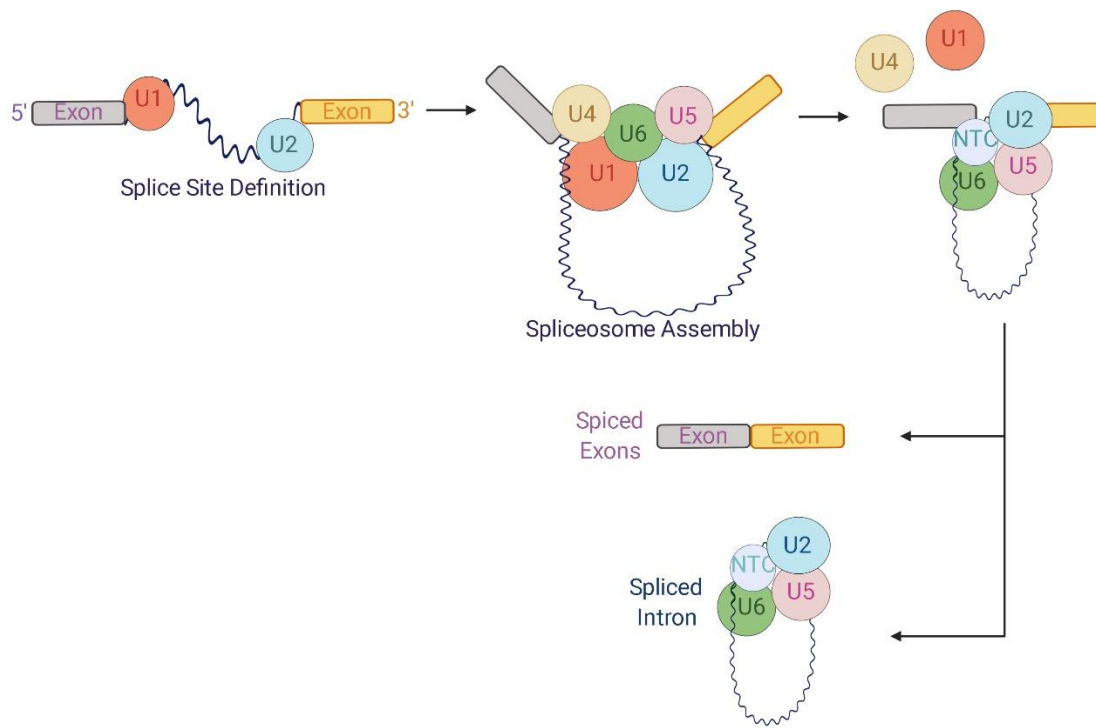


Figure 3. Spliceosome Assembly and Removal of an Intron from a Pre-mRNA

U1 and U2 snRNPs bind to conserved sequences that define a splice site on either end of an intron. U4/U5/U6 snRNPs form the full spliceosome leading to formation of a lariat loop structure of the intron to be removed. U1 and U4 are removed, leading to the final reaction with two exons spliced together and the spliced intron removed.

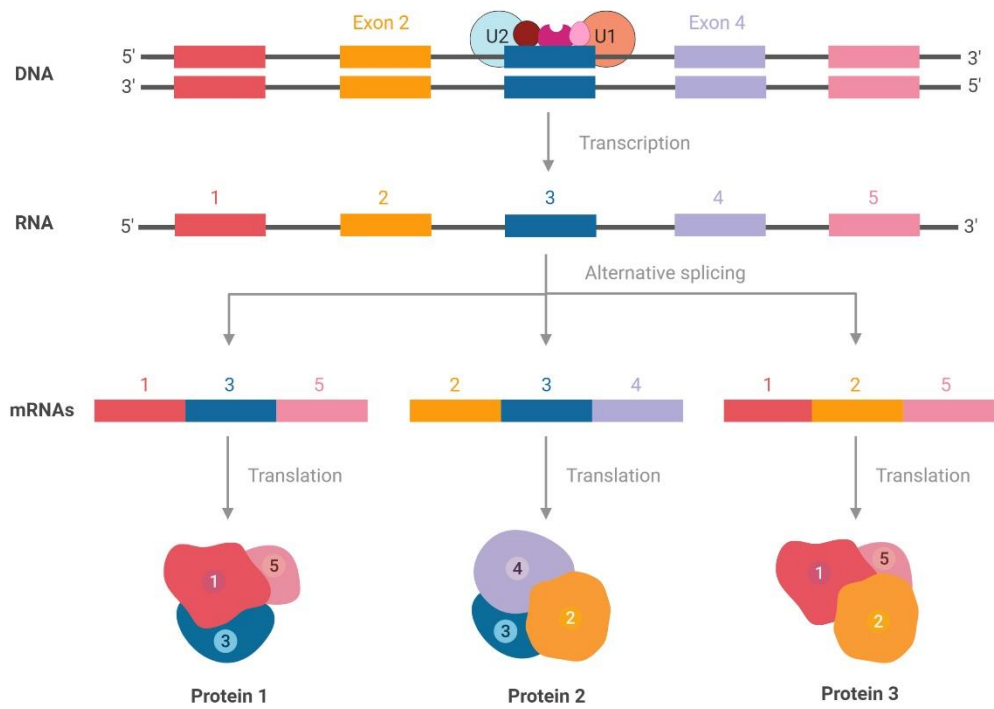


Figure 4. Alternative Splicing Produces Different Protein Isoforms from One RNA

During alternative splicing, exons from pre-mRNA are spliced together in alternating sequences. These mRNA sequences lead to different protein isoforms that can have diverse functions.

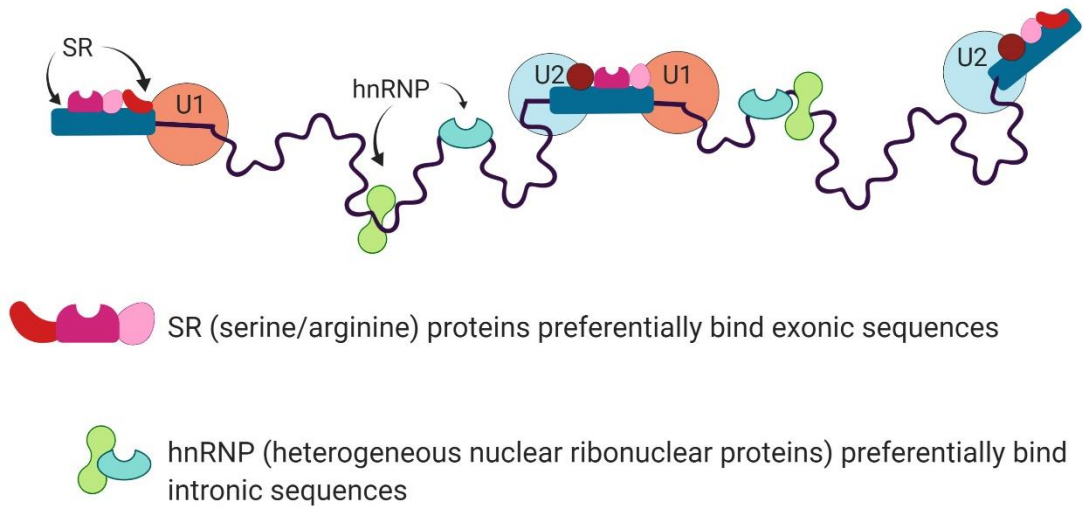


Figure 5. RBPs Influence Splicing Reactions Through Defining Exons and Introns

hnRNP and SRSF RNA-binding proteins can bind to consensus motifs in exons and introns to enhance or repress spliceosome function. These leads to influencing spliceosome assembly and reactions that impacts canonical and alternative splicing.

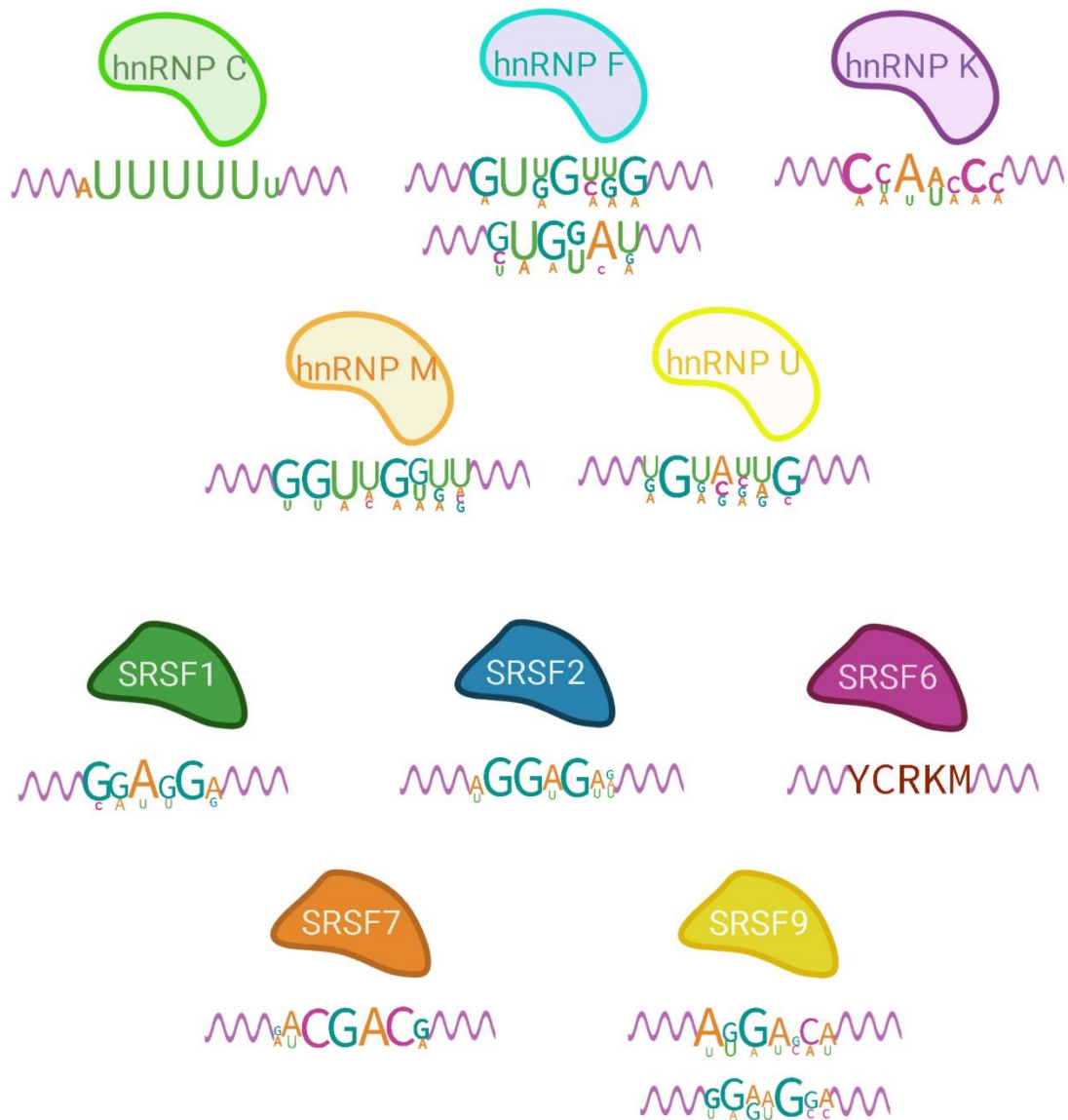


Figure 6. hnRNP and SRSF Proteins Identified Binding Motifs

Visualizations of hnRNP and SRSF binding motifs identified via CLIP-seq experiments from Huelga et. al., Ray et. al., Castle et al., and Paradis et. al. ²⁹⁻³²

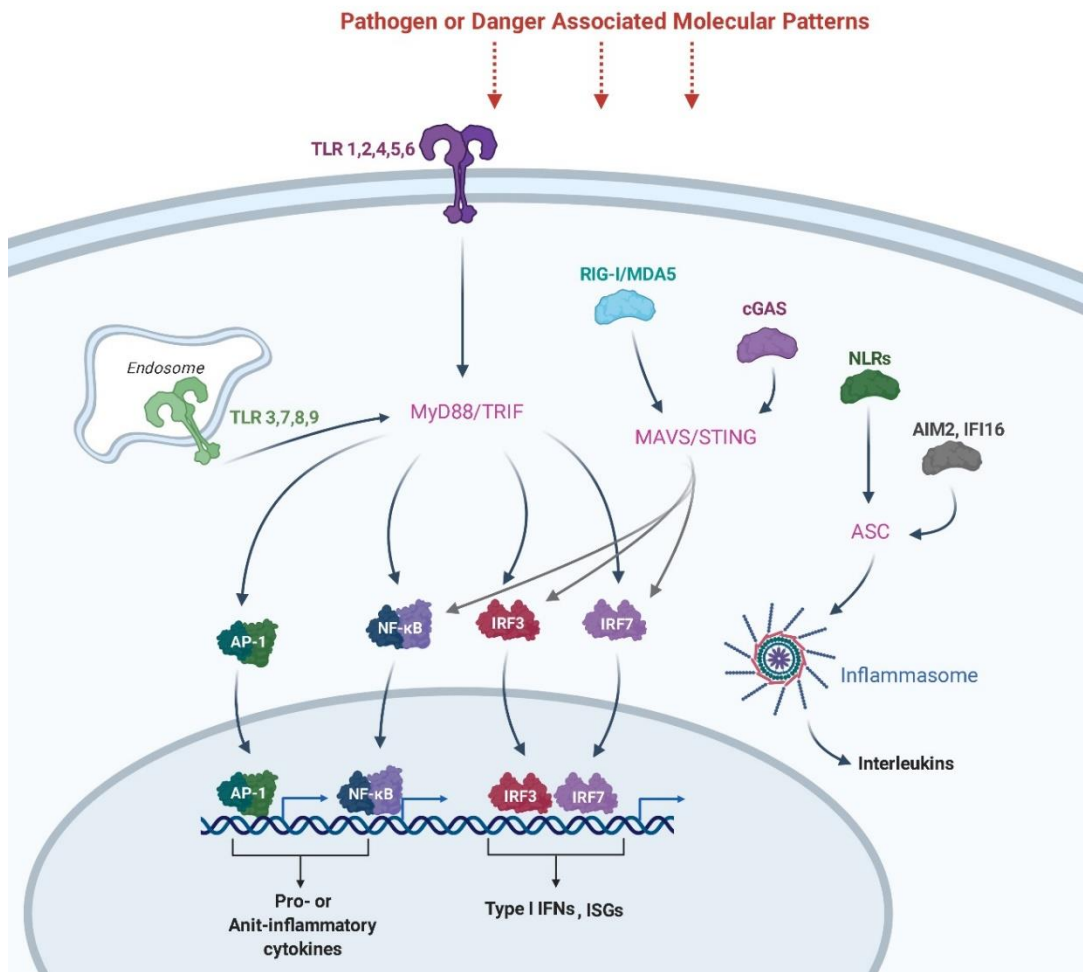


Figure 7. Innate Immune Receptors and Signaling Cascades Lead to Cytokine, Interferon, and Interferon-Stimulatory Genes Production

PAMPs or DAMPs from microbes are sensed via Toll-like receptors and Nucleic acid receptors. These receptors signal to adaptor molecules that activate transcription factors like AP-1, NF- κ B, and IRFs. These transcription factors stimulate cytokine, interferon, and interferon-stimulatory genes production to help combat the invading pathogen.

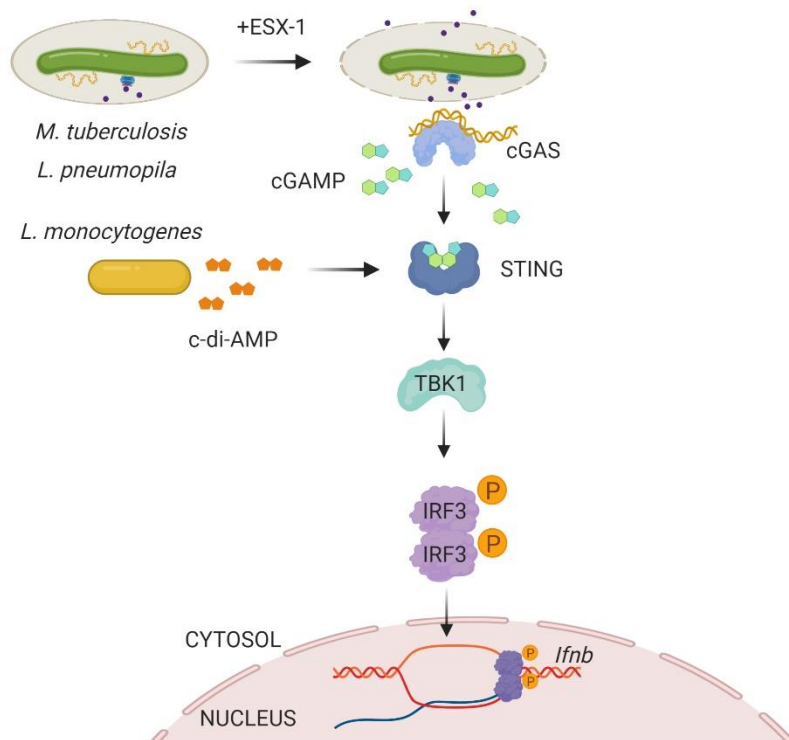


Figure 8. Innate Immune Sensing of Cytosolic DNA From Bacterial Pathogens by cGAS

Upon entry into a macrophage, *Mycobacterium tuberculosis* uses its ESX-1 secretion system to secrete proteins that permeabilize the bacterium-containing phagosome. Host cytosolic DNA sensor cGAS detects Mtb. Alternatively, *Listeria monocytogenes* can release c-di-AMP, which directly activates STING. Each outcome leads to TBK1 activation and IFN production.

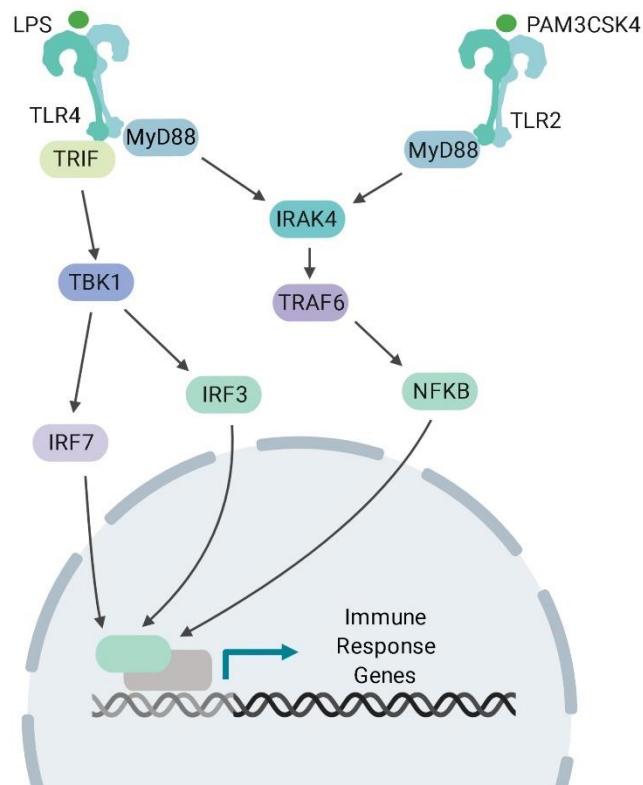


Figure 9. Model of TLR4 and TLR2 Signaling

TLR4 can recognize LPS from gram-negative pathogens. TLR2 senses PAM3CSK4 from gram-positive pathogens. TLR4 and TLR2 stimulate through MYD88 dependent signaling cascades. TLR4 can also stimulate through TRIF. MYD88 independent pathways initiate IRAK4/TRAF6 and trigger NF- κ B transcription of innate immune response genes. TRIF signaling activates TBK1 and IRF transcription of interferon.

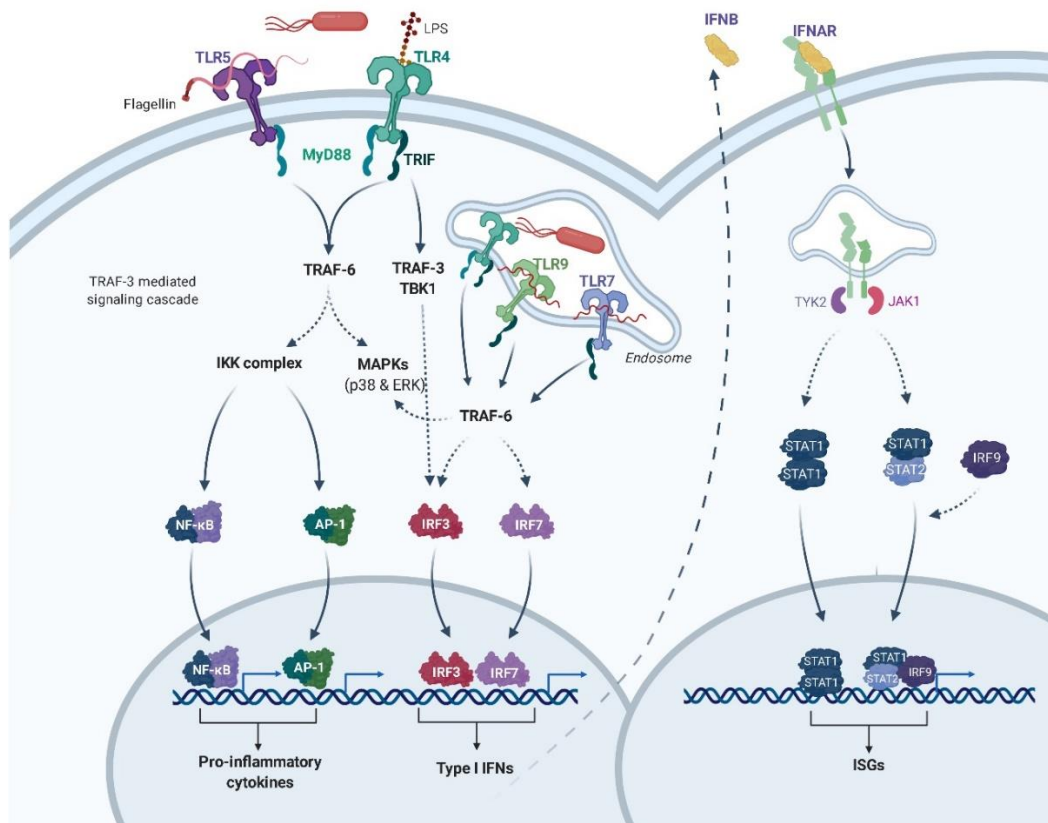


Figure 10. *Salmonella* Detection and Innate Immune Response Via Toll-like Receptors

Toll-like receptors detect the presence of *Salmonella*, which detect LPS, flagellin, and endocytosed *Salmonella*. Upon TLR binding, engage adaptors MYD88 and TRIF. This triggers kinase and phosphatase activation of MAPK and IKKs. These MAPKs and IKKs modulate NF- κ B and IRF function, sending them to the nucleus. Upon nuclear entry, these transcription factors stimulate cytokine and Type I Interferon production. IFN β that is produced then signals through IFNAR. This leads to STAT activation and production of Interferon-stimulatory genes.

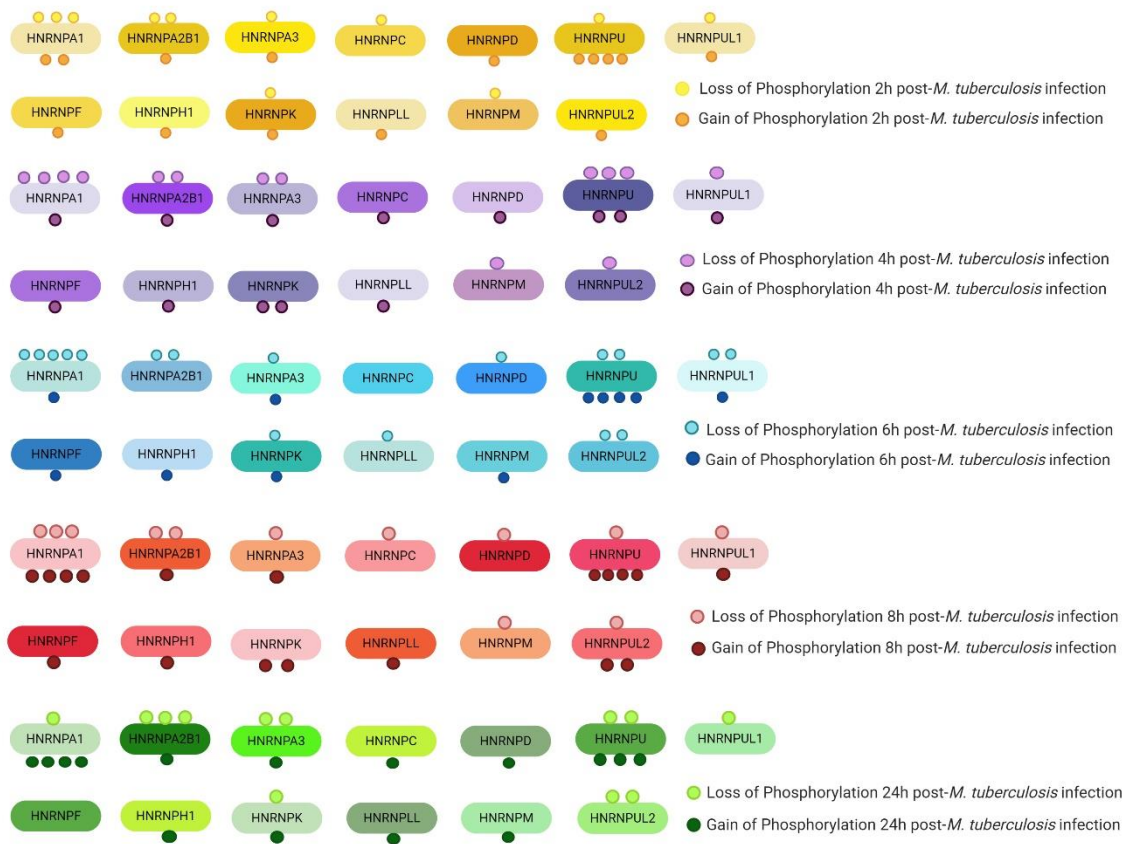


Figure 11. hnRNPs are Differentially Phosphorylated Upon *M. tuberculosis* Infection

Diagram of Phosphorylation events of hnRNPs identified by Budzik et. al and Penn et. al. ^{325,326}

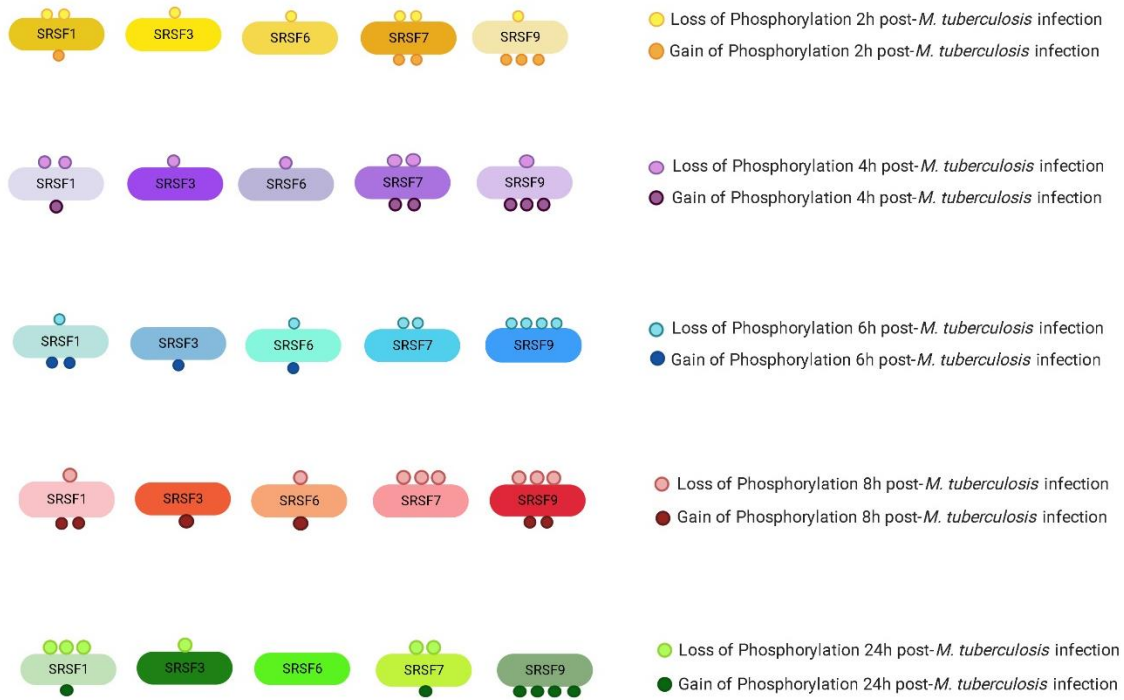


Figure 12. SRSFs are Differentially Phosphorylated Upon *M. tuberculosis* Infection

Diagram of Phosphorylation events of SRSFs identified by Budzik et. al and

Penn et. al. ^{325,326}

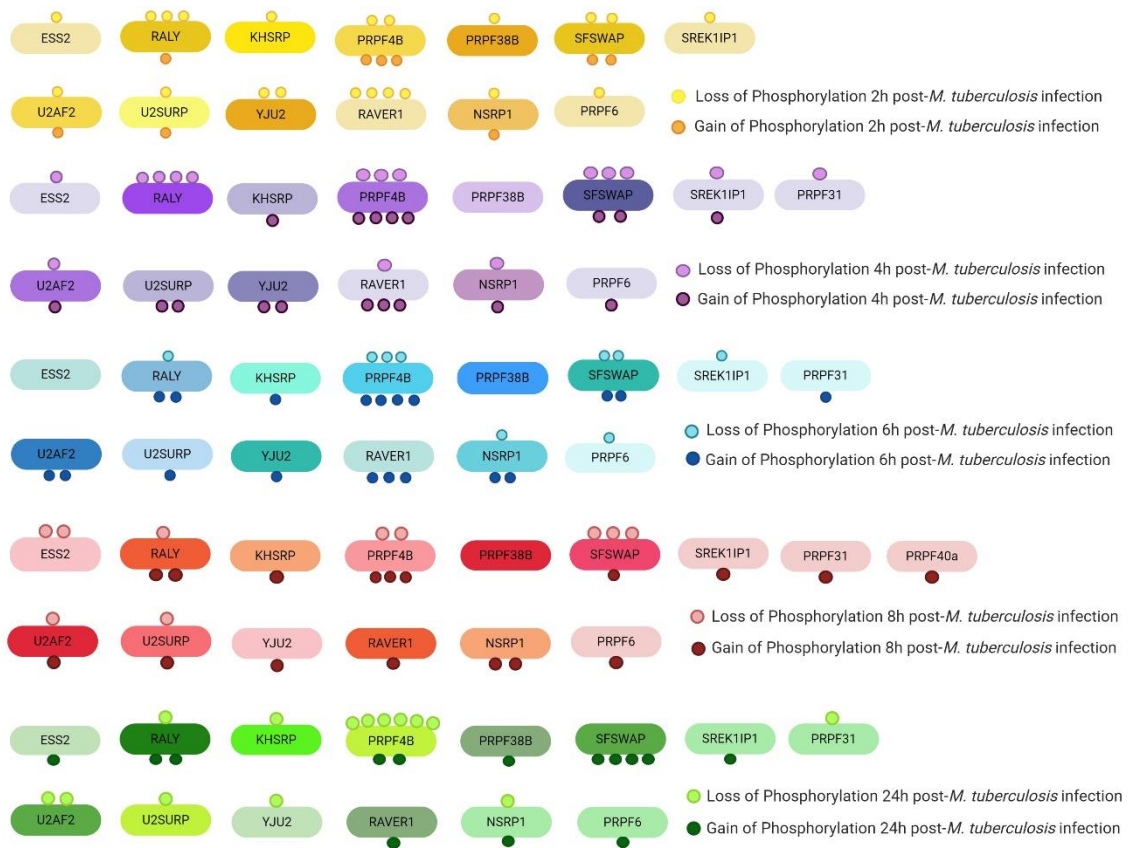


Figure 13. Core Spliceosome Factors are Differentially Phosphorylated Upon *M. tuberculosis* Infection

Diagram of Phosphorylation events of core spliceosome factors identified by Budzik et. al and Penn et. al. ^{325,326}

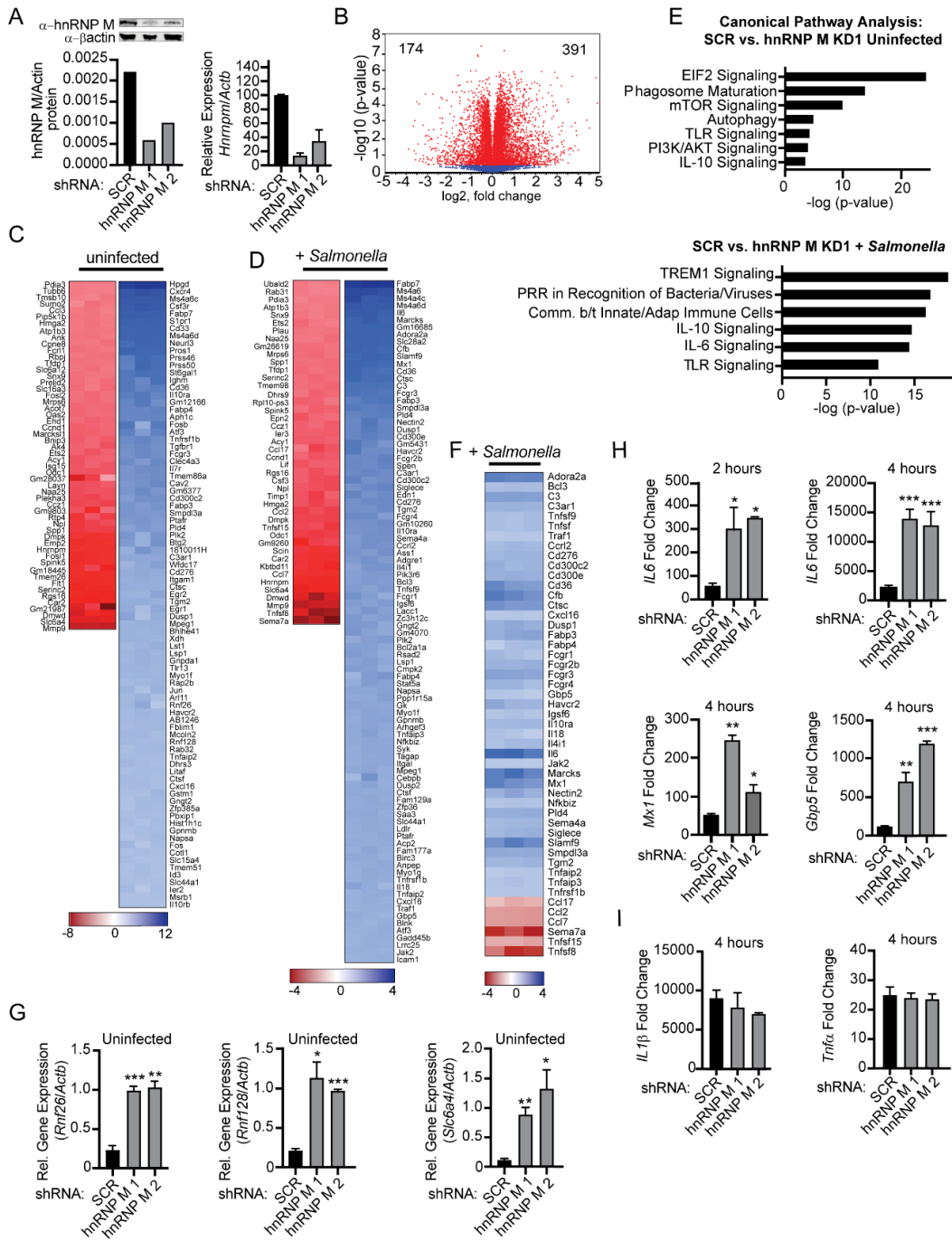


Figure 14. (Figure 1) hnRNP M Regulates Expression of Innate Immune Genes during *Salmonella Typhimurium* Infection

(A) Western blot analysis and qRT-PCR of hnRNP M in RAW 264.7 macrophages with b-actin as a loading control. Values are mean (SD) representative of 3 biological replicates. (B) Volcano plot (t test) showing gene expression analysis of hnRNP M KD RNA-seq data from uninfected cells. x axis shows fold change of gene expression, and y axis shows statistical significance. Downregulated genes are plotted on the left, and upregulated genes are on the right. (C) Gene expression analysis of hnRNP M KD cells compared to SCR control for uninfected cells. Each column represents a biological replicate. Red, genes downregulated in hnRNP M KD; blue, genes upregulated in hnRNP M KD. (D) Gene expression analysis of hnRNP M KD cells compared to SCR control for Salmonella-infected cells. Each column represents a biological replicate. (E) Ingenuity pathway analysis of gene expression changes in uninfected and Salmonella-infected cells. (F) Manually annotated hnRNP M-dependent innate immune genes. Each column represents a biological replicate. (G) qRT-PCR of *Rnf26*, *Rnf128*, and *Slc6a4* in uninfected hnRNP M KD cells. (H) qRT-PCR of mature *IL6*, *Mx1*, and *Gbp5* transcripts in Salmonella-infected hnRNP M KD cells at 2 and 4 h post-infection. (I) qRT-PCR of *IL1 β* and *Tnfa* transcripts in Salmonella-infected hnRNP M KD cells at 4 h post-infection. (G)–(I) represent 3 biological replicates \pm SEM, n = 3. For all experiments in this study, statistical significance was determined using two-tailed Students' t test. *p < 0.05, **p < 0.01, ***p < 0.001, n.s., not significant.

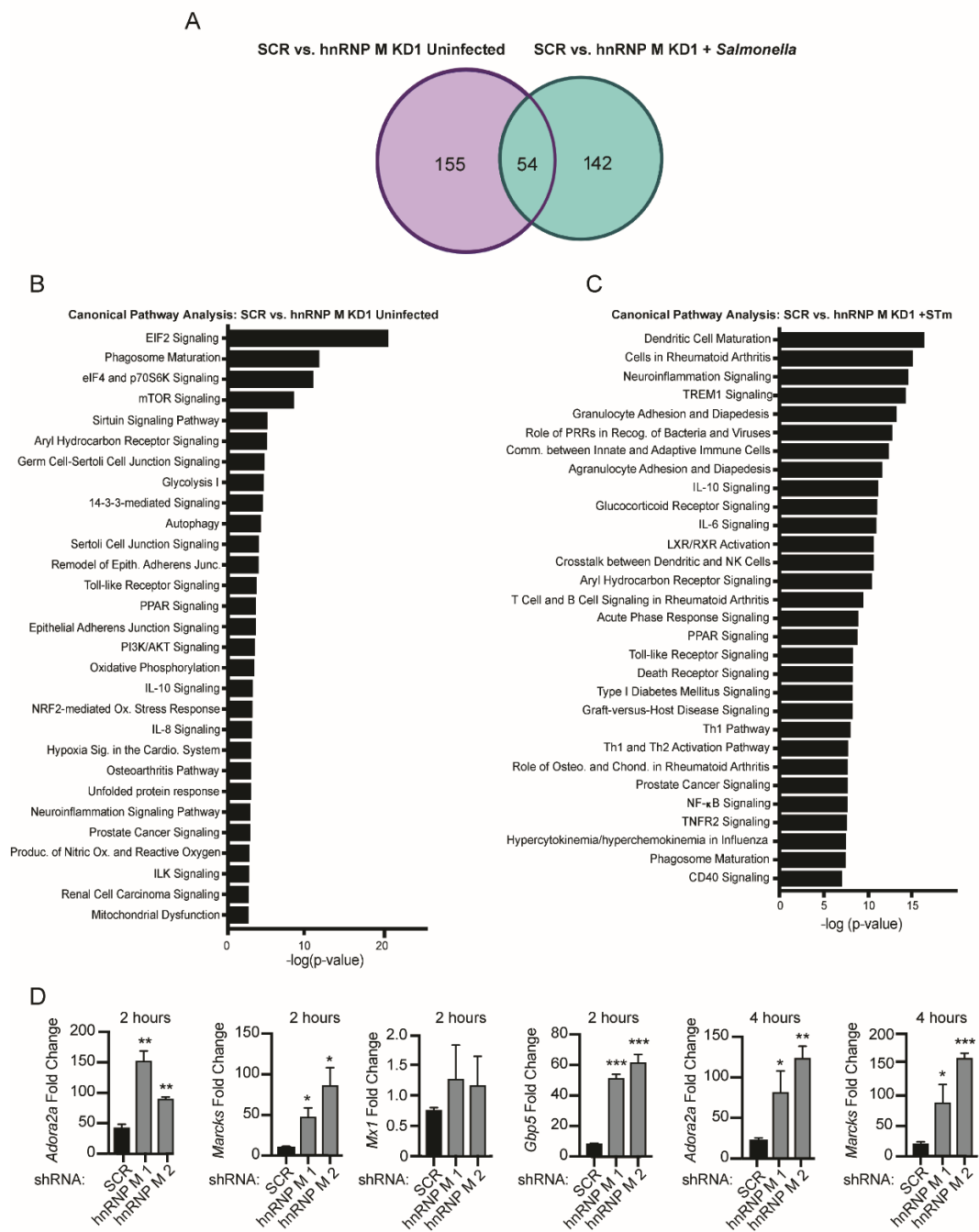


Figure 15 (Figure S1). HnRNP M regulates expression of specific immune genes during *Salmonella Typhimurium* Infection.

(a) Venn diagram to represent overlap between hnRNP M-regulated transcripts in uninfected and Salmonella-infected macrophages. (b) Complete ingenuity pathway analysis for SCR vs. hnRNP M KD uninfected macrophages. (c) Complete ingenuity pathway analysis for SCR vs. hnRNP M KD Salmonella-infected macrophages. (d) Gene expression by RT-qPCR in SCR, hnRNP M KD 1, and hnRNP M KD 2 2hr post-Salmonella infection for *Adora2a*, *Marcks*, *Mxl*, *Gbp5*, and 4hr for *Adora2a* and *Marcks*.

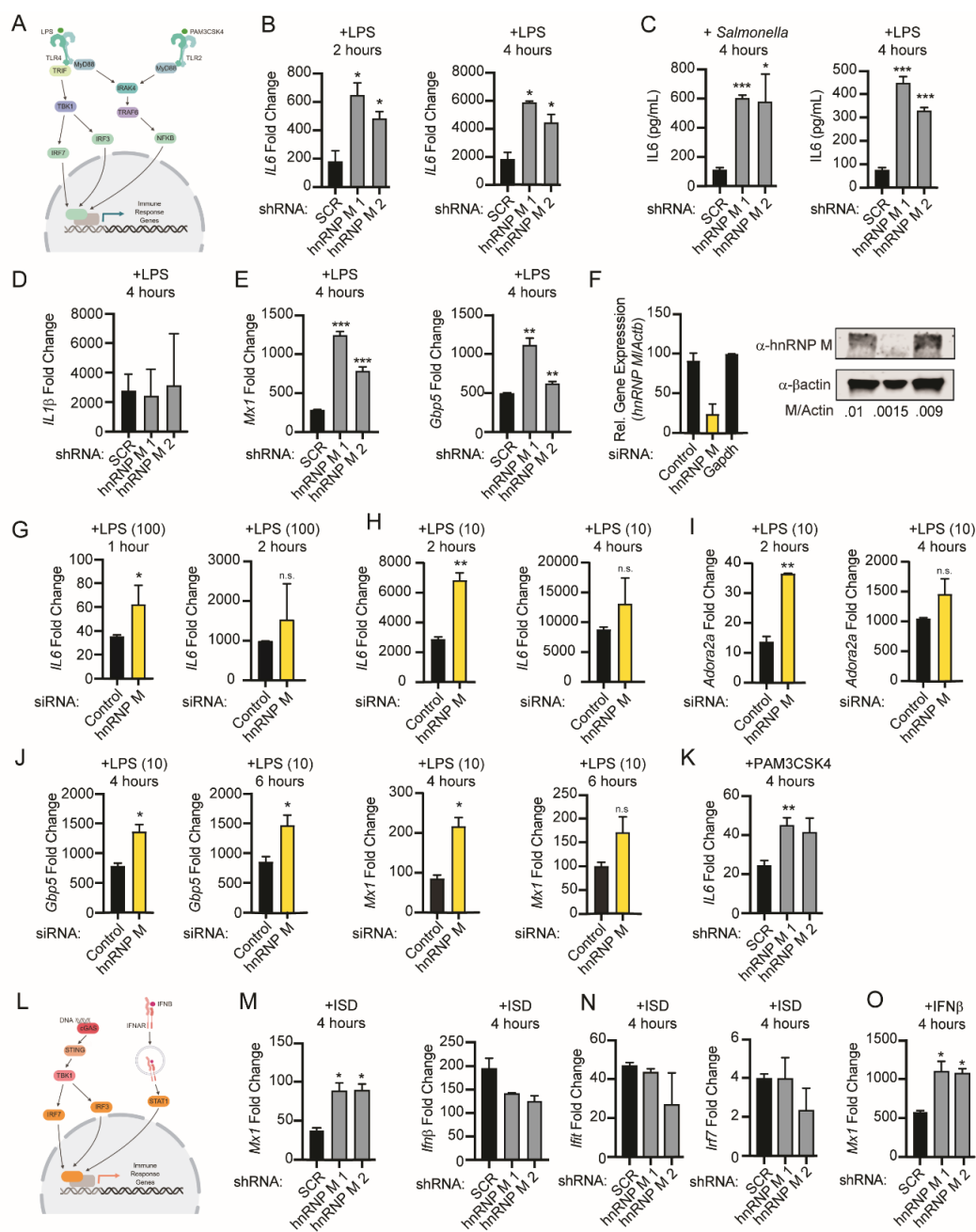


Figure 16 (Figure 2). hnRNP M-Dependent Regulation of Innate Immune Gene Expression Occurs Downstream of Sensing Multiple Innate Immune Stimuli

(A) Model of TLR4 and TLR2 signaling. (B) qRT-PCR of *IL6* mRNA levels in SCR control and hnRNP M KD cells treated with LPS for 2 and 4 h. (C) IL6 ELISA with supernatants collected 4 h post-Salmonella infection or LPS treatment. (D) qRT-PCR of *IL1 β* transcripts in LPS-treated hnRNP M KD cells (4 h). (E) qRT-PCR of *Mx1* and *Gbp5* mRNA levels in SCR control and hnRNP M KD cells treated with LPS (4 h). (F) qRT-PCR and western analysis demonstrating effective depletion of hnRNP M in siRNA-transfected BMDMs. b-actin was used as a loading control. (G) qRT-PCR of mature *IL6* in negative control and hnRNP M siRNA BMDMs treated with 100 ng/mL of LPS for 1 and 2 h. (H) qRT-PCR of mature *IL6* in negative control and hnRNP M siRNA BMDMs treated with 10 ng/mL of LPS for 2 and 4 h. (I) As in (H) but *Adora2a*. (J) qRT-PCR of *Gbp5* and *Mx1* in negative control and hnRNP M siRNA BMDMs treated with 10 ng/mL of LPS for 4 and 6 h. (K) qRT-PCR of mature *IL6* in SCR control and hnRNP M KD cells treated with Pam3CSK4 for 4 h. (L) Model of cGAS-mediated cytosolic DNA sensing and IFNAR signaling. (M) qRT-PCR of *Mx1* and *Ifnb1* mRNA levels in SCR control and hnRNP M KD cells at 4 h following ISD transfection. (N) qRT-PCR of ISGs (*Ifit1* and *Irf7*) in SCR control and hnRNP M KD cells at 4 h following ISD transfection (O) qRT-PCR of *Mx1* transcript in SCR control and hnRNP M KD cells treated with recombinant IFN- β for 4 h. All experiments represent 3 biological replicates where values are means \pm SEM, n = 3.

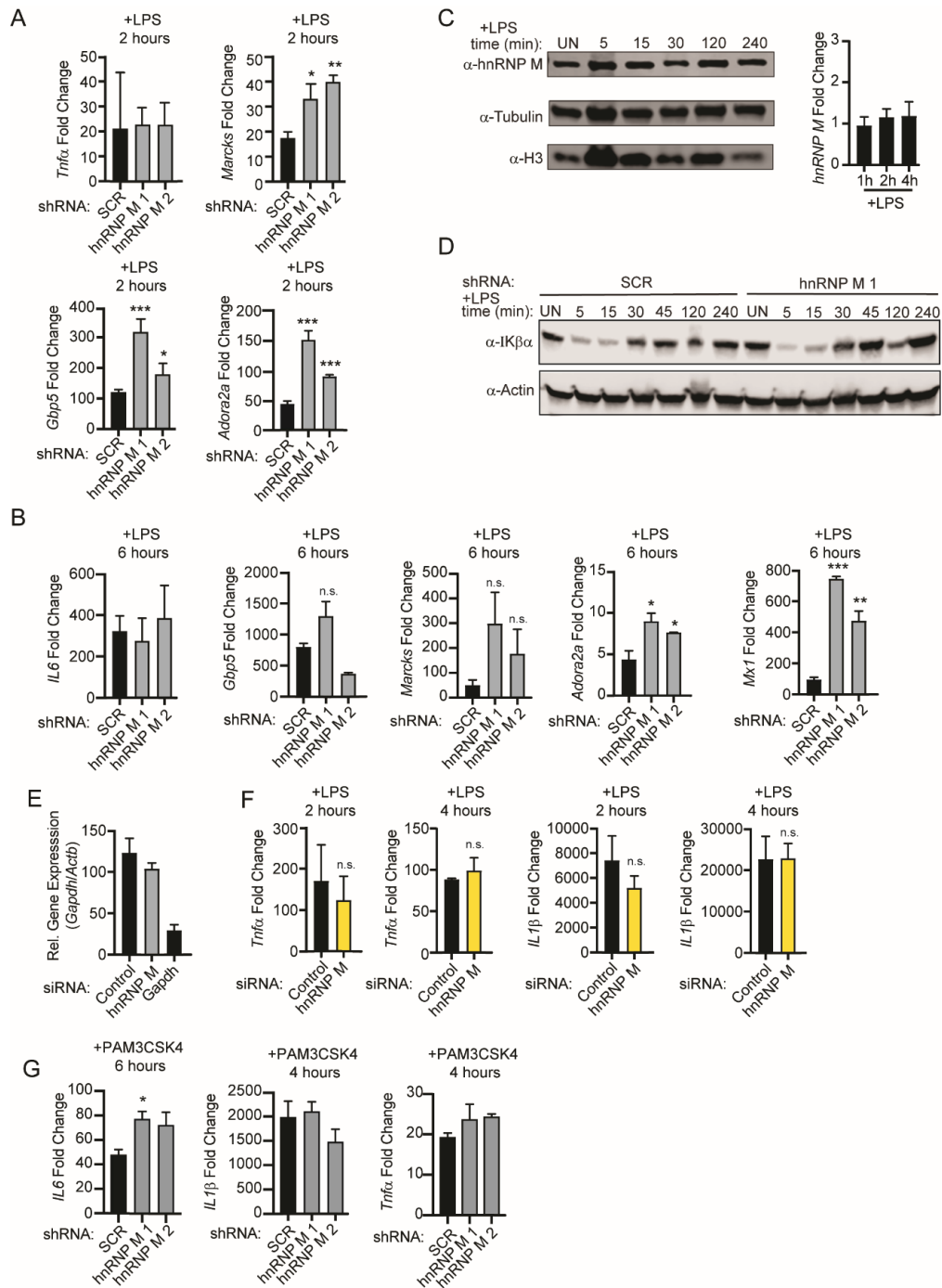


Figure 17 (Figure S2). hnRNP M-dependent gene expression profiles are similar among diverse immune stimuli.

(a) *Tnfa*, *Marcks*, *Gbp5*, and *Adora2a* expression by RT-qPCR in LPS-treated cells of SCR, hnRNP M KD 1, and hnRNP M KD 2 2hr post-treatment. (b) *IL6*, *Gbp5*, *Marcks*, *Adora2a*, and *Mx1* expression by RT-qPCR in SCR, hnRNP M KD1, and hnRNP M KD 2 6hr post-LPS treatment. (c) Western blot analysis of endogenous hnRNP M in RAW 264.7 macrophages treated with LPS for 5, 15, 30, 120, and 240 mins. RT-qPCR of *hnRNP M* expression in RAW 264.7 cells treated with LPS for 1hr, 2hr, and 4hr. (d) Western blot analysis of α IK β in SCR control and hnRNP M KD 1 macrophages treated with LPS for 5, 15, 30, 45, 120, and 240 mins. (e) RT-qPCR demonstrating effective depletion of GAPDH in siRNA transfected BMDMs. (f) RT-qPCR of *Tnfa* and *IL1 β* in negative control and hnRNP M siRNA BMDMs treated with 10 ng/ml of LPS for 2hrs and 4hrs. (g) RT-qPCR of *IL6*, *Tnfa*, and *IL1 β* in SCR control and hnRNP M KD macrophages treated with PAM3CSK4 for 6hrs and 4hrs.

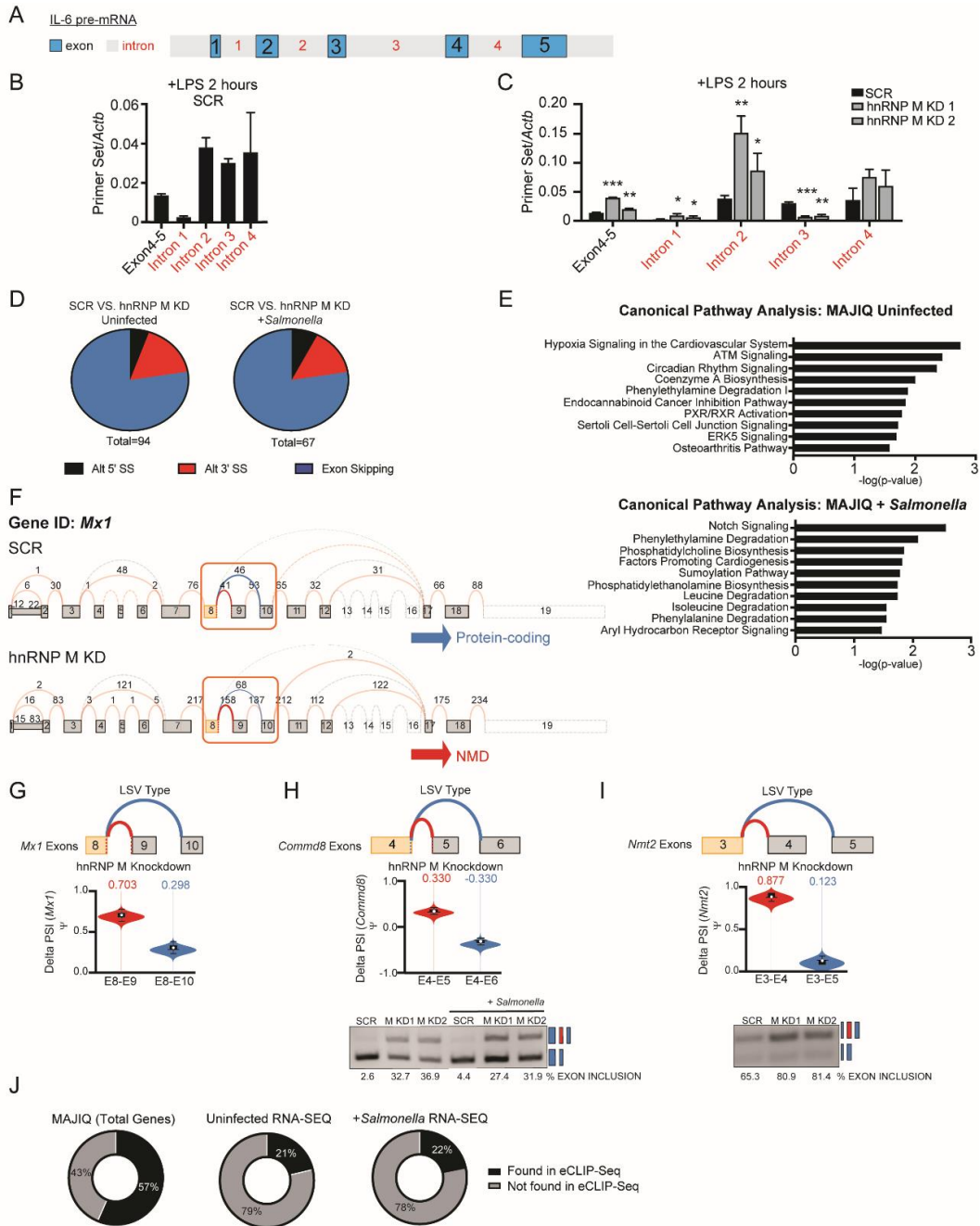


Figure 18 (Figure 3). hnRNP M Influences Gene Expression Outcomes at the Level of Pre-mRNA Splicing

(A) Diagram of *IL6* pre-mRNA with introns (gray) and exons (blue). (B) qRT-PCR of *IL6* exon-exon and intron-exon junctions in SCR control macrophages at 2 h post-LPS treatment. (C) qRT-PCR of *IL6* exon-exon and intron-exon junctions in SCR versus hnRNP M KD1 and KD2 at 2 h post-LPS treatment. (D) Categorization of alternative splicing events identified via MAJIQ in uninfected SCR versus hnRNP M KD1 samples and in *Salmonella*-infected SCR versus hnRNP M KD1 samples. (E) Ingenuity Pathway Analysis of hnRNP M-dependent genes from MAJIQ analysis in uninfected and *Salmonella*-infected cells. (F) VOILA output of *Mx1* transcript model in SCR and hnRNP M KD1 cells infected with *Salmonella*. (G) Violin plots depicting the delta PSI of hnRNP M-dependent local splicing variations in *Mx1*. (H) As in (G) but for *Commd8*, alongside semiquantitative RT-PCR validation. (I) As in (H) but for *Nmt2*. (B) and (C) are representative of two independent experiments that showed the same result with values representing means (SD), n = 3.

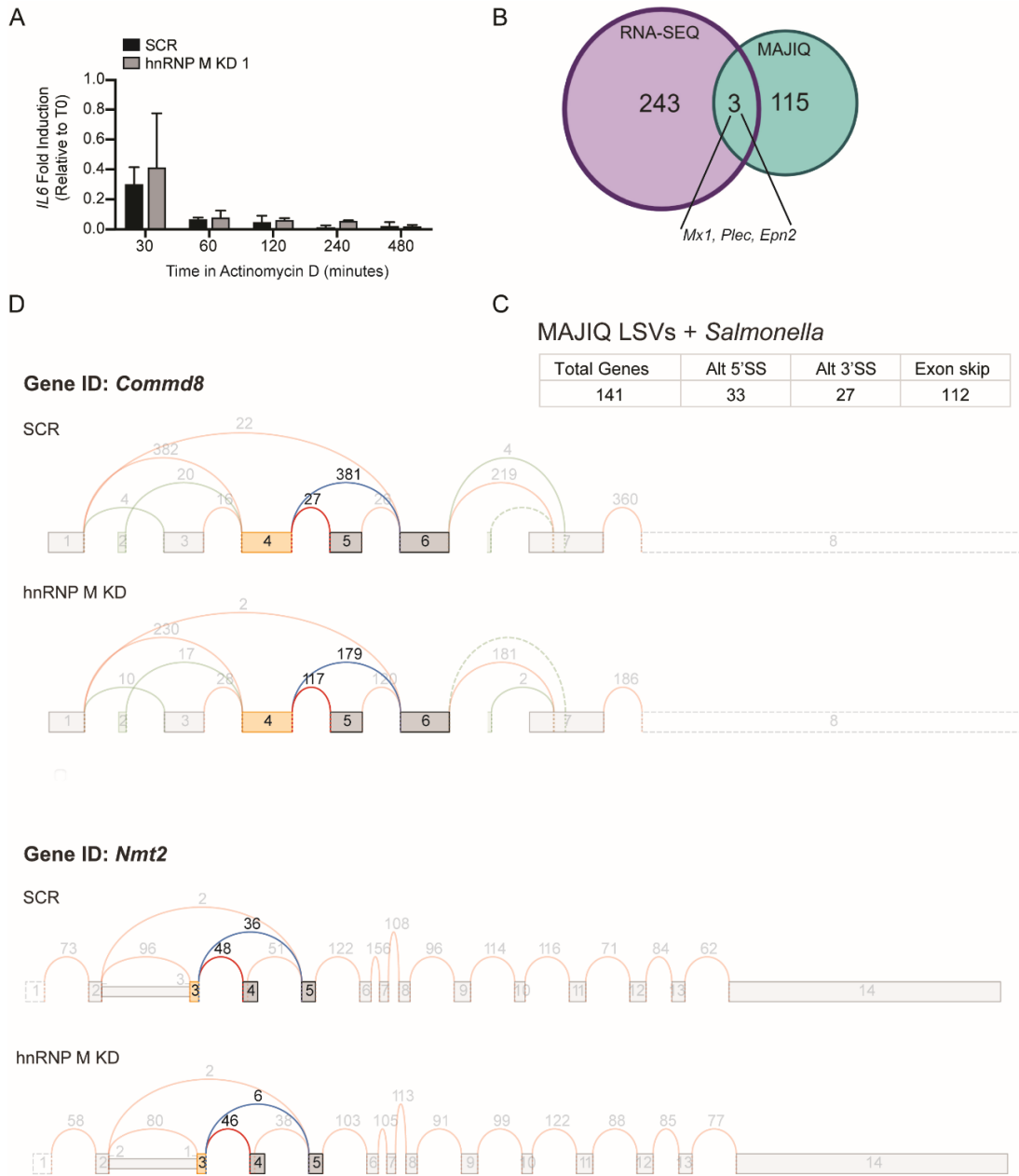


Figure 19 (Figure S3). hnRNP M Influences Gene Expression Outcomes at the Level of Pre-mRNA Splicing

(a) *IL6* expression by RT-qPCR in SCR, hnRNP M KD1 cells treated with LPS for 1hr then treated with Actinomycin D for 0, 30, 60, 120, 240, and 480 mins. (b) Venn diagram to represent overlap between hnRNP M-regulated transcripts identified via RNA-Seq analysis (unique genes identified in Salmonella and uninfected analyses) and hnRNP M-dependent LSVs identified via MAJIQ analysis (total number of unique LSV events from both Salmonella and uninfected conditions). (c) Categorization of alternative splicing events identified via MAJIQ in uninfected vs. Salmonella-infected samples. (d) Full VOILA-generated tracks for *CommD8* and *Nmt2*. Significant LSVs are shown in color.

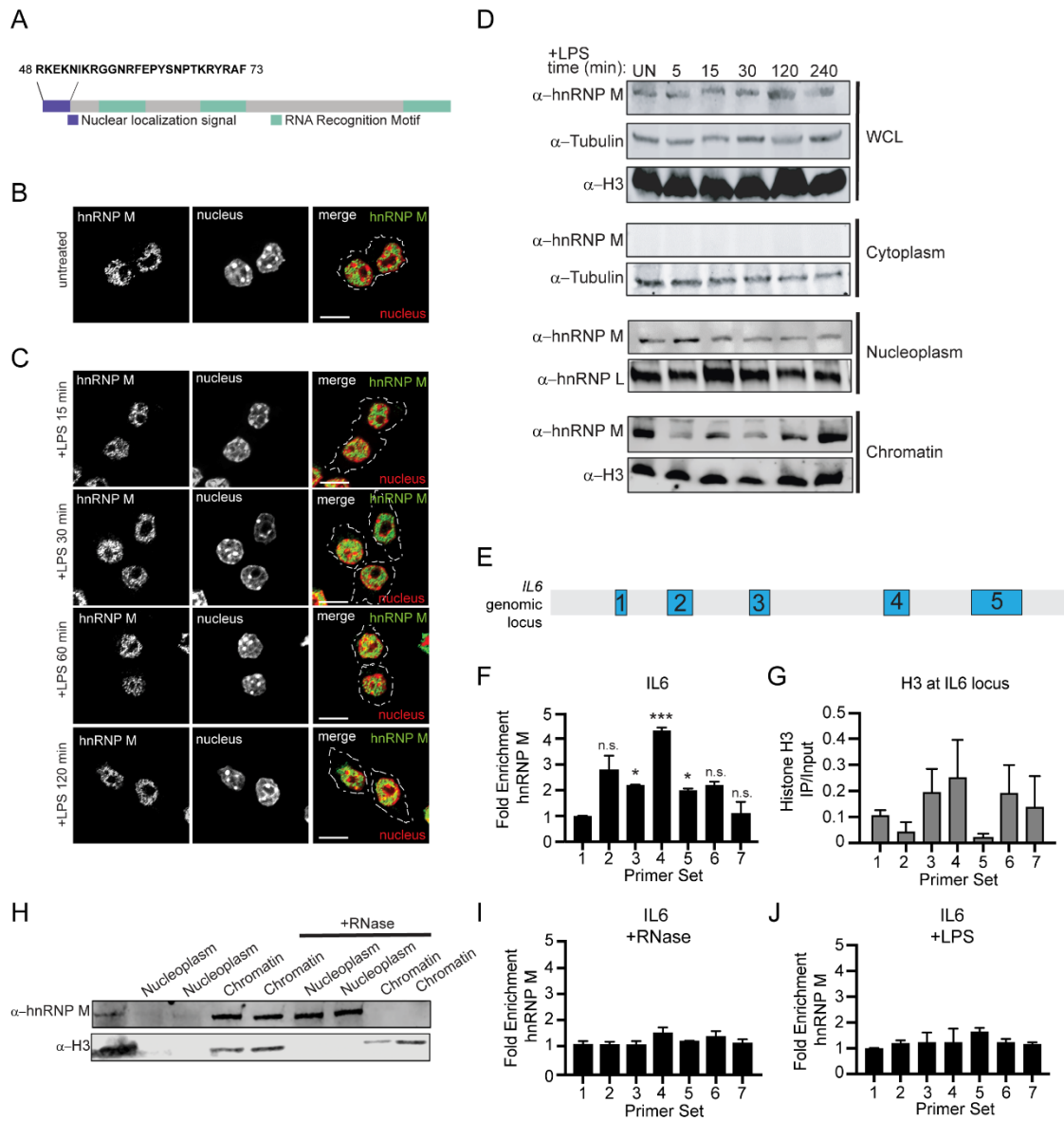


Figure 20 (Figure 4) hnRNP M Is a Nuclear Protein that Associates with the *IL6* Genomic Locus in an RNA-Dependent Fashion

(A) Schematic diagram of hnRNP M, highlighting the nuclear localization signal (purple) and three RNA Recognition Motifs (green). (B) Immunofluorescence images of uninfected RAW 264.7 macrophages immunostained with anti-hnRNP M (green). (C) Immunofluorescence images of RAW 264.7 macrophages stimulated with LPS for the respective time points and immunostained with anti-hnRNP M (green). Scale bar, 10 μ m. (D) Western blot analysis of cellular fractions with anti-hnRNP M and loading controls of cytoplasm (tubulin), nucleoplasm (hnRNP L) and chromatin (H3) fractions of uninfected and LPS stimulated RAW 264.7 macrophages. (E) ChIP-qPCR primers designed to tile the *IL6* locus. (F) qPCR of ChIP at the *IL6* genomic locus with anti-hnRNP M in resting RAW 264.7 macrophages. (G) As in (F) but using an anti-histone H3 antibody. (H) Western blot analysis of nuclear and chromatin fractions with anti-hnRNP M and Histone H3 (control) with untreated and RNase-treated nuclear fractions. (I) As in (F) but with 30 min incubation at 37 with RNase A. (J) As in (F) but with macrophages treated with 100 ng/mL LPS for 1 h. (K) Venn diagrams representing hnRNP M eCLIP (ENCODE) gene overlap with our MAJIQ, uninfected RNA-seq, and Salmonella-infected RNA-seq results. (F) and (G) values are means \pm SEM representative of 2 biological replicates, n = 2. (I) and (J) values are means \pm SEM representative of 3 biological replicates, n = 3.

(a) Immunofluorescence microscopy of 3xFLAG-hnRNP M in untreated and LPS-treated macrophages (1hr and 2hr post-treatment). (b) Immunofluorescence microscopy of hnRNP U in untreated and LPS-treated macrophages (2hr post-treatment). (c) Western blot of whole cell lysate, cytoplasm, nucleoplasm, and chromatin of fractionated stable 3xFL-hnRNP M-expressing macrophages over a time-course of LPS treatment. (d) Western blot analysis of cellular fractions with anti-hnRNP M and loading controls of cytoplasm (tubulin), nucleoplasm (Snrp70) and chromatin (H3) fractions of uninfected and LPS stimulated hnRNP M KD 1 macrophages. (e) RNA sequence of IL6 introns 2 and 3. Consensus or near-consensus hnRNP M binding sites are highlighted in yellow.

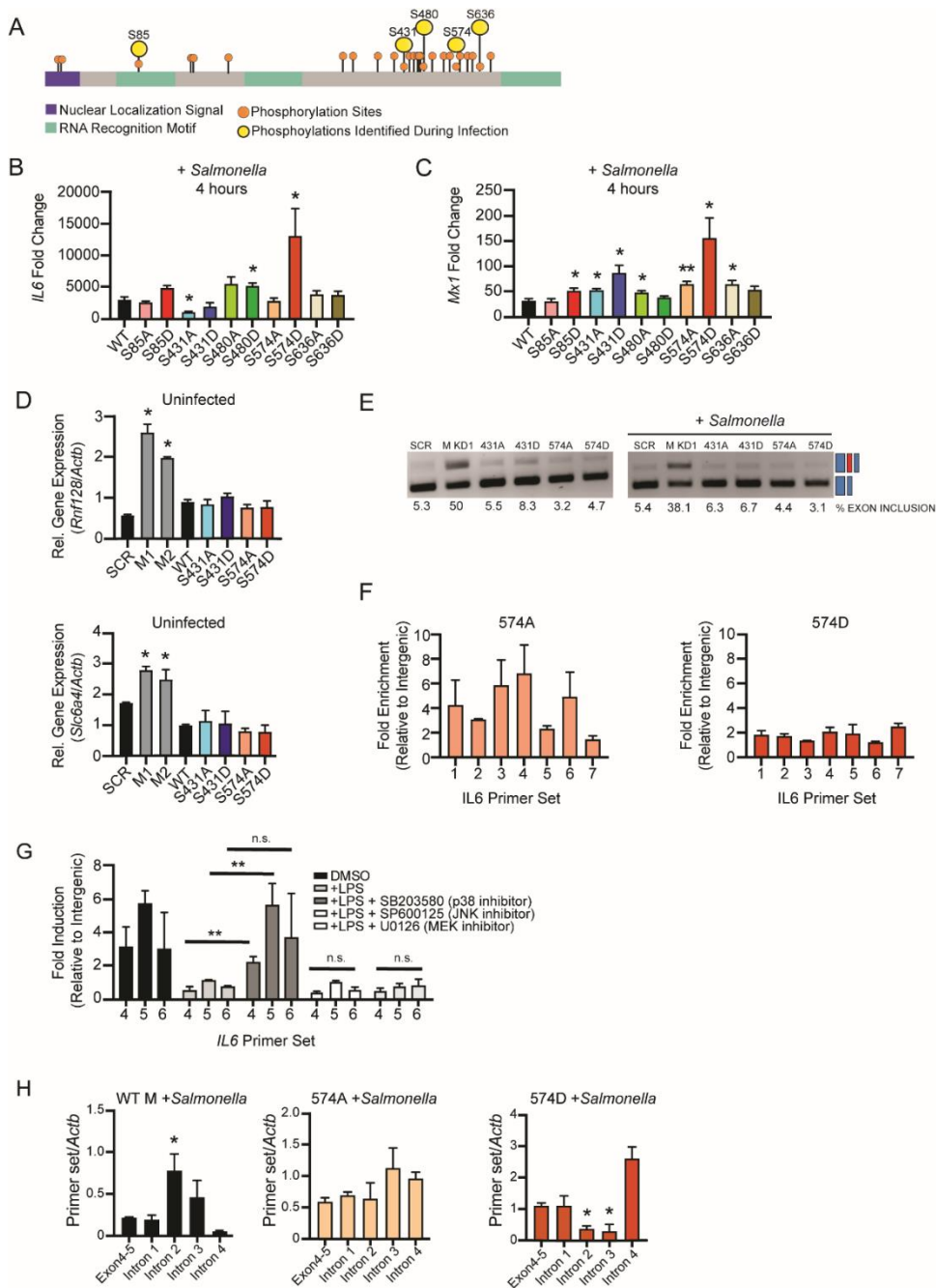


Figure 22 (Figure 5) Phosphorylation of hnRNP M at S574 Downstream of TLR4 Activation Controls Its Ability to Repress Expression of Innate Immune Transcripts

(A) Protein diagram of hnRNP M indicating location of phosphorylation sites identified by SILAC/mass spectrometry (Penn et al., 2018) with nuclear localization signal shown in purple and RNA-recognition motifs (RRM) shown in green. (B) qRT-PCR of mature *IL6* in wild-type (WT) hnRNP M-FLAG and phosphomutants in macrophages infected with *Salmonella* for 4 h. (C) As in (B) but for *Mx1*. (D) qRT-PCR of *Rnf128* and *Slc6a4* in uninfected, WT 3xFL-hnRNP M, and phosphomutants. (E) Semiquantitative PCR of *Commd8* alternative splicing in cells expressing SCR or hnRNP M KD constructs alongside phosphomutant-expressing alleles. (F) ChIP-qPCR of hnRNP M-S574A/D alleles at the *IL6* genomic locus. (G) ChIP-qPCR of wild-type 3xFL-hnRNP M in the presence of 100 ng/mL LPS and various MAPK inhibitors (SB203580, SP600125, and U0126). (H) RT-qPCR of *IL6* intron-exon junctions and the exon 4–5 mature junction in 3xFL-hnRNP M and 3xFL-hnRNP M 574A and 574D phosphomutants, in macrophages infected with *Salmonella* for 4 h. (B)–(D) are representative of 3 biological replicates with values indicating means \pm SEM, n = 3. (F)–(H) are representative of 2 biological replicates values indicating means \pm SEM, n = 2. (I) is representative of 2 independent experiments that showed the same result with values representing means (SD), n = 3.

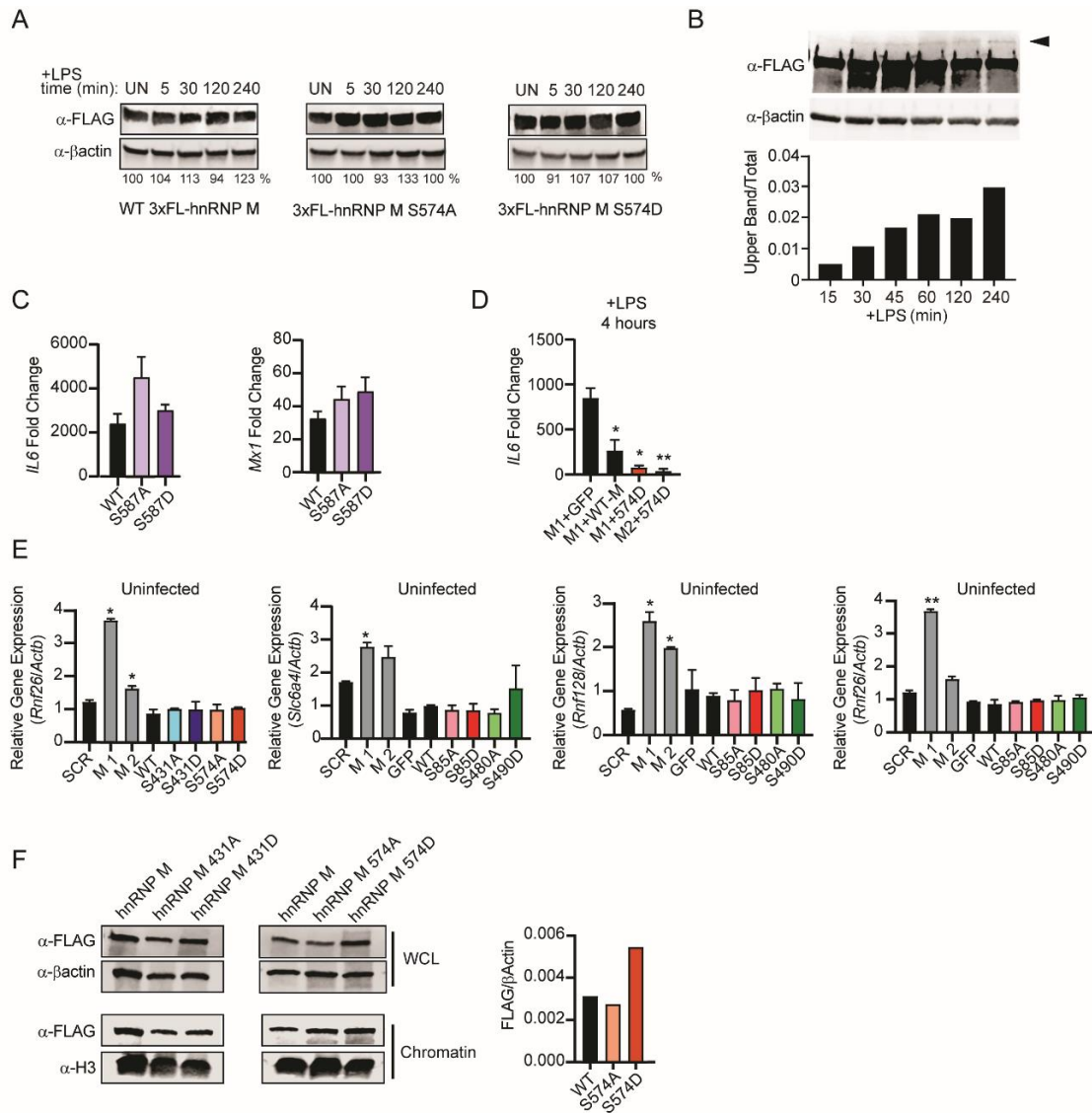


Figure 23 (Figure S5) Phosphorylation of hnRNP M at S574 Downstream of TLR4 Activation Controls Its Ability to Repress Expression of Innate Immune Transcripts

(a) Western blot analysis of 3xFL-hnRNP M WT, S574A, S574D phosphomutants stably expressed in RAW 264.7 macrophages treated with LPS for 5, 30, 120, and 240 mins. (b) Western blot analysis of phosphorylation events of 3xFL-hnRNP M WT stably expressed in RAW 264.7 macrophages treated with LPS for 15, 30, 45, 60, 120, and 240 mins. (c) *IL6* and *Mx1* expression by RT-qPCR, 2hr post-LPS treatment in 3xFL-hnRNP M WT and 3xFLhnRNP M S587A/D-expressing macrophages. (d) IL6 expression by RT-qPCR, 4hr post-LPS treatment in hnRNP M KD 1 macrophages complemented with 3xFL-GFP, 3xFL-hnRNP M WT, or S574D and hnRNP M KD 2 macrophages complemented with S574D. (e) Expression by RT-qPCR of *Rnf26*, *Slc6a4*, and *Rnf128* for 3xFL-hnRNP M WT, hnRNP M KD 1 and hnRNP M KD 2, and 3xFL-S431A/D, S574A/D, S85A/D, S480A/D-expressing macrophages. (f) Western blot of whole cell lysate and chromatin of fractionated stable 3xFL-hnRNP M WT, 3xFL-hnRNP M 431A/D and 3xFL-hnRNP M 574A/D-expressing macrophages. FLAG expression was quantified over β actin.

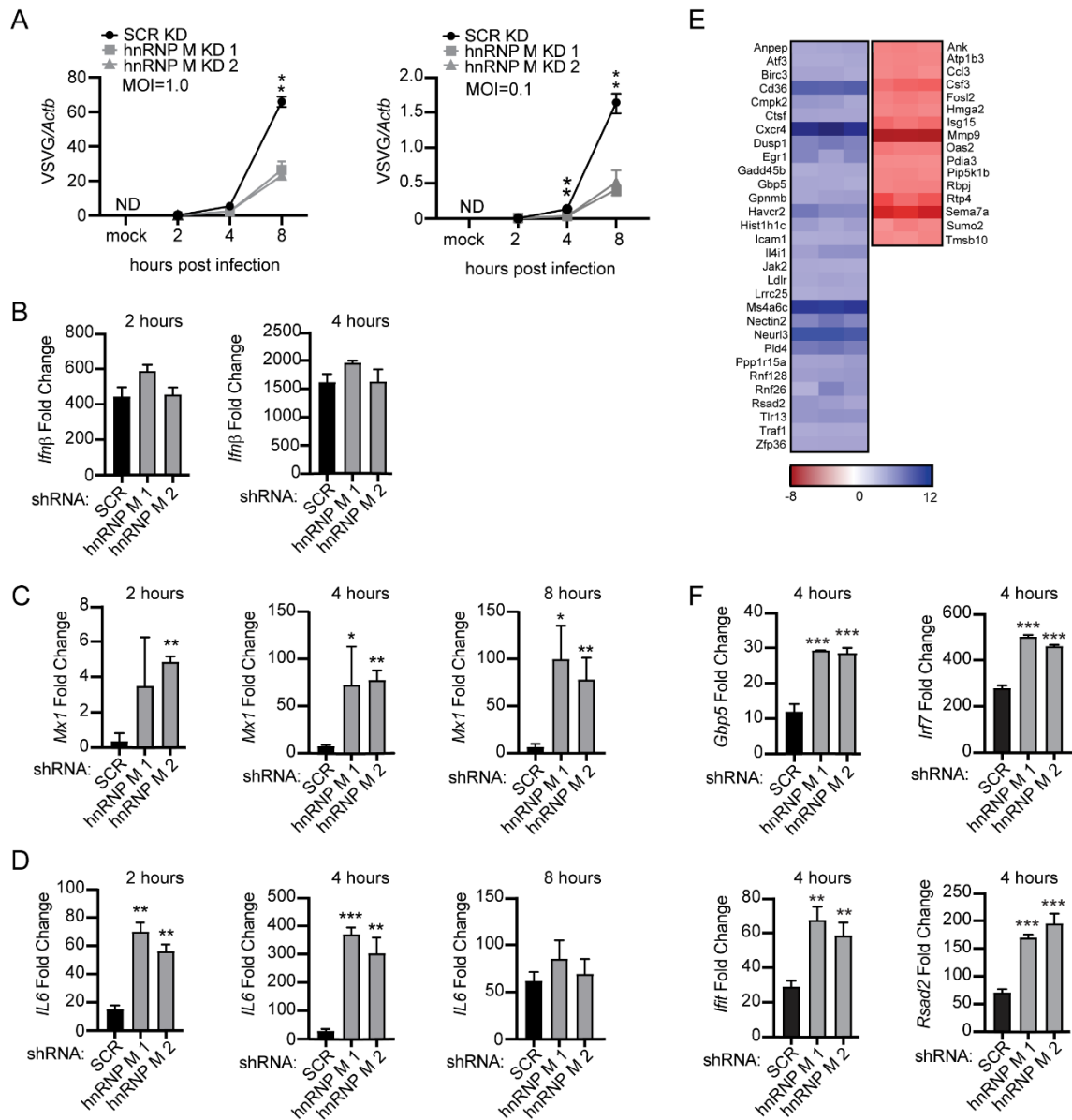


Figure 24 (Figure 6) Knockdown of hnRNP M Enhances a Macrophage's Ability to Control Viral Infection

(A) Viral replication in hnRNP M KD and SCR control RAW 264.7 macrophages infected with VSV (MOI = 1.0, MOI = 0.1, or Mock) at 2, 4, and 8 h post-infection. (B) qRT-PCR of *Ifnb1* mRNA levels in SCR control and hnRNP M KD cells at 2 and 4 h post-infection, MOI = 1. (C) qRT-PCR of *Mx1* transcript in VSV-infected SCR control and hnRNP M KD cells at 2, 4, and 8 h post-infection, MOI = 1. (D) qRT-PCR of *IL6* transcript in SCR control and hnRNP M KD cells at 2, 4, and 8 h post-infection MOI = 1. (E) Differential gene expression in hnRNP M KD cells compared to SCR control macrophages from earlier RNA-seq analysis (Figure 1) highlighting known viral response genes. (F) qRT-PCR of *Ifit*, *Irf7*, *Rsad2*, and *Gbp5* mRNA levels in SCR control and hnRNP M KD cells at 4 h post-infection, MOI = 1. (A)–(E) are representative of 2 biological replicates with values indicating means \pm SEM, n = 2. (F) is representative of 2 independent experiments that showed the same result with values representing means (SD), n = 3.

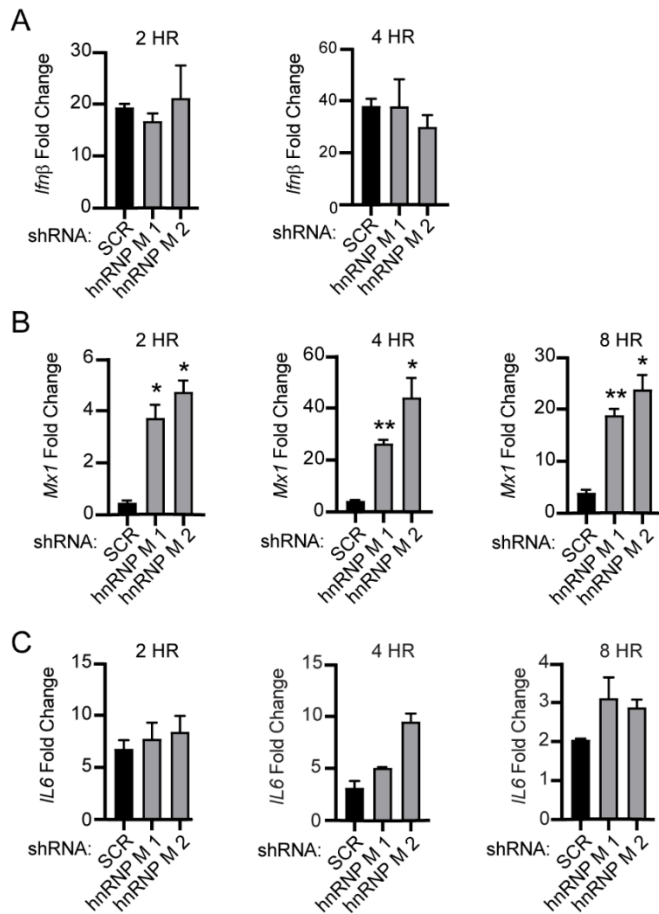


Figure 25 (Figure S6) Knockdown of hnRNP M Enhances a Macrophage’s Ability to Control Viral Infection

(a) RT-qPCR of *Ifnb1* mRNA levels in SCR control and hnRNP M KD cells at 2hr and 4hr post-infection, MOI=0.1. (b) RT-qPCR of *Mx1* transcript in VSV infected SCR control and hnRNP M KD cells at 2hr, 4hr, and 8hr post-infection, MOI=0.1. (c) RT-qPCR of *IL6* transcript in SCR control and hnRNP M KD cells at 2hr, 4hr, and 8hr post-infection, MOI=0.1. All figures are representative of 2 biological replicates.

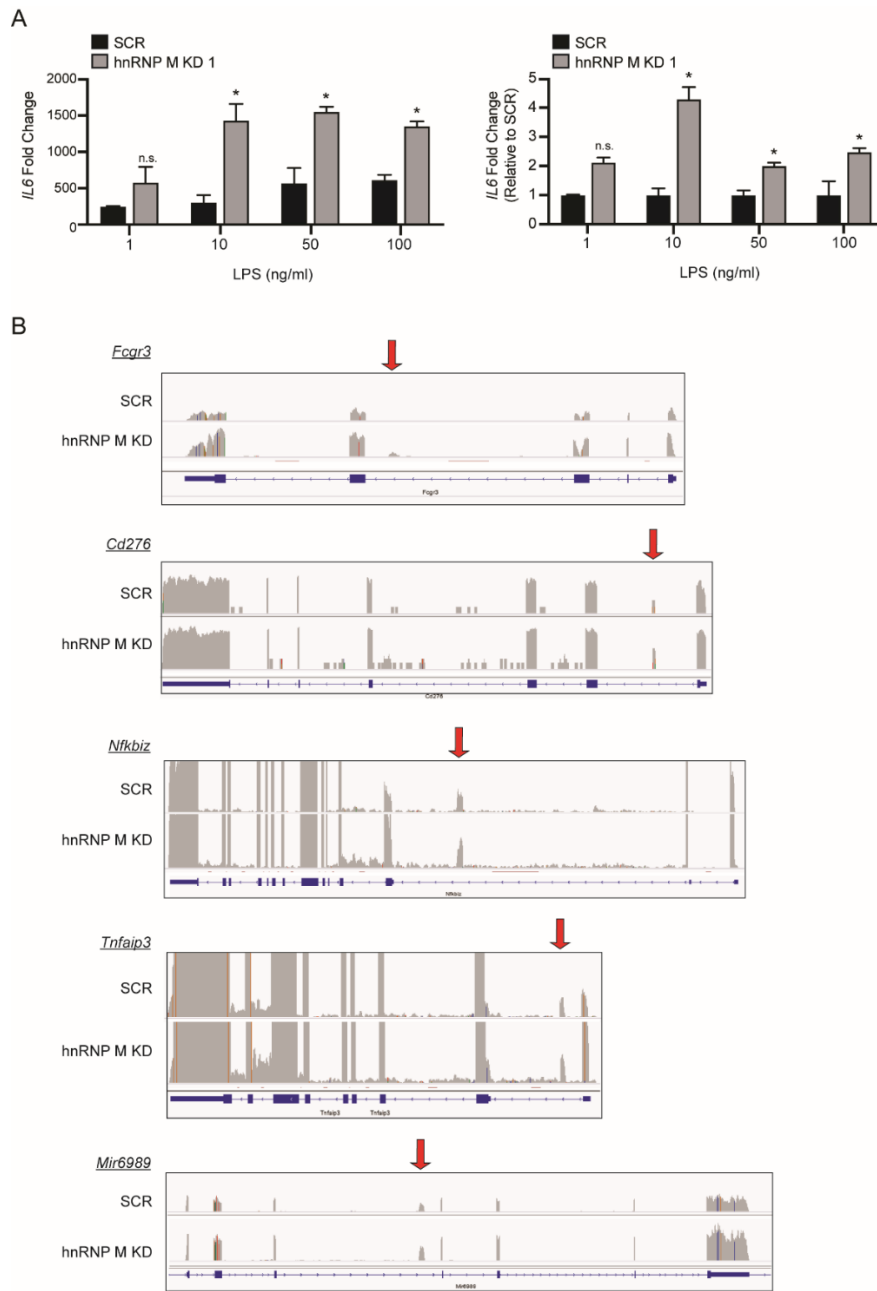


Figure 26 (Figure S7). hnRNP M can respond to low levels of innate immune stimuli and may influence differential inclusion of cryptic exons.

(a) RT-qPCR of IL6 mRNA levels in SCR control and hnRNP M KD cells at 2h treated with 100ng/ml, 50ng/ml, 10ng/ml and 1ng/ml. Data is expressed as fold-change over time = 0 as well as fold-change relative to SCR. (a) is representative of 2 biological replicates with values indicating means \pm SD, n=2. Statistical significance was determined using two-tailed students' t-test. *P < 0.05, **P < 0.01, n.s.= not significant.

(b) Screenshots of IGV viewer of Salmonella-infected SCR and hnRNP M KD RNA-Seq reads at Fcgr3, Cd276, Nfkbiz, Tnfaip3, and Mir6989. Red arrows indicate potential cryptic exons.

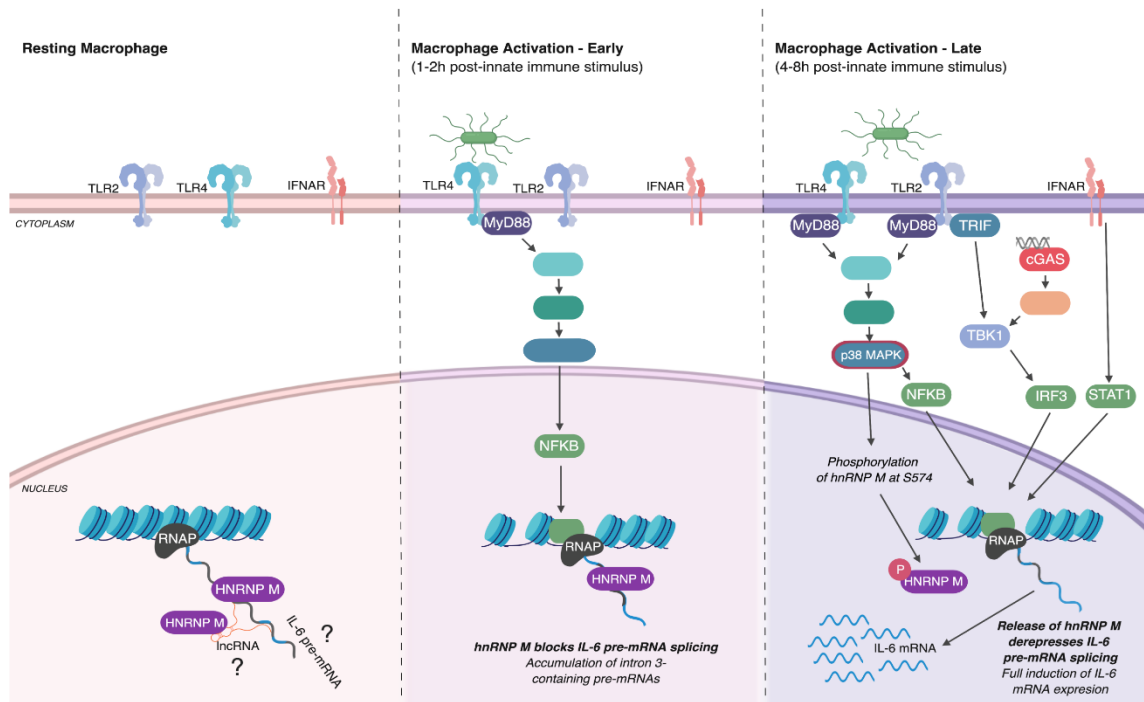


Figure 27 (Figure 7) Proposed Model for hnRNP M-Dependent Repression for IL6 Expression in Resting, Early-, and Late-Activated Macrophages

(Left) In resting macrophages, hnRNP M associates with chromatin, at the *IL6* genomic locus, through interactions with RNA. These interactions may be direct with target transcripts expressed at low levels or spuriously or indirect via protein interactions with other RNA binding proteins or through interactions with other chromatin-associated RNAs, e.g., lincRNAs. (Middle panel) When macrophages receive an innate immune stimulus, they transcriptionally activate genes like *IL6*. A population of “poised” hnRNP M can associate with chromatin-bound premRNAs in these cells, slowing *IL6* intron removal and preventing full maturation of *IL6* nascent transcripts. (Right) As

early macrophage activation proceeds, hnRNP M is phosphorylated at S574 in a p38-MAPK-dependent fashion. Phosphorylation of hnRNP M releases it from the *IL6* genomic locus, relieves inhibition of *IL6* splicing, and allows for full induction of *IL6* gene expression. Figure generated using BioRender software.

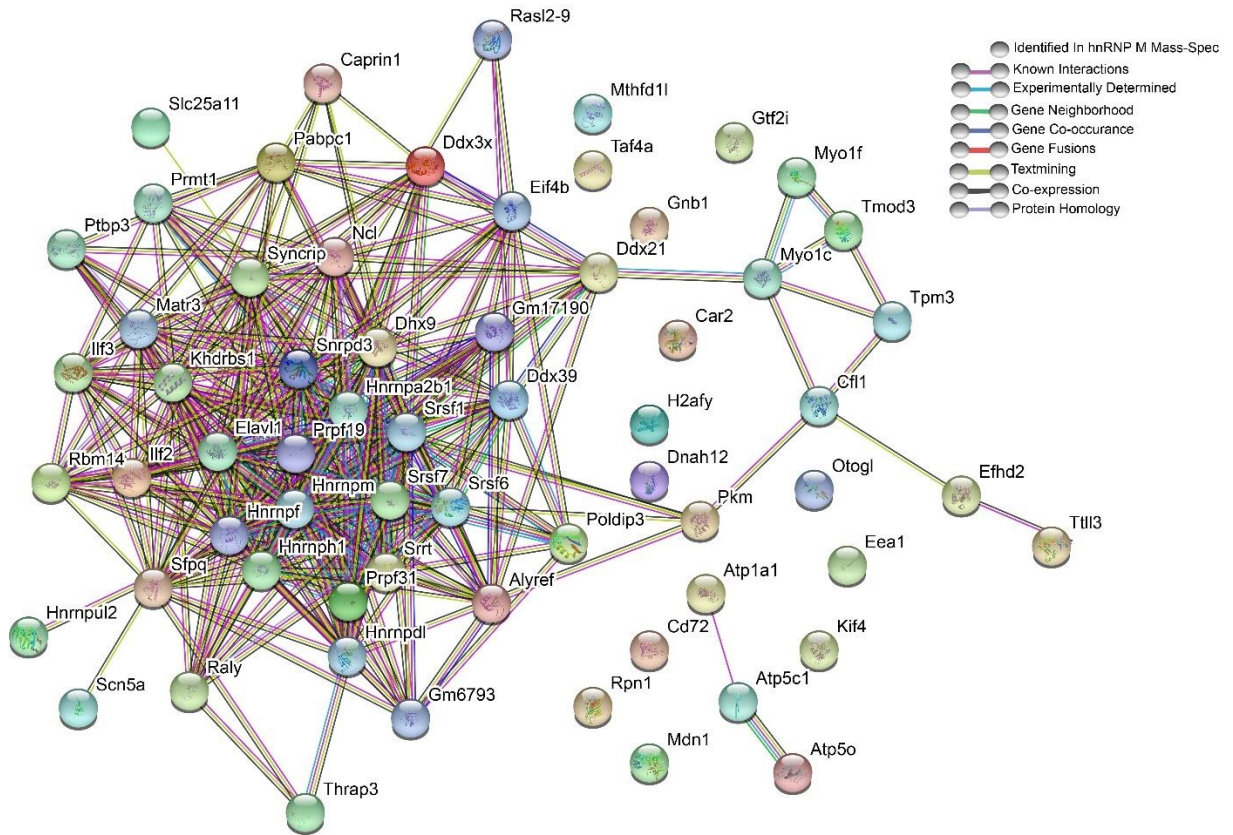


Figure 28 hnRNP M Interacts with Paraspeckle-Associated Proteins, SFPQ, ILF3, and MATR3 in Resting Macrophages

Proteins identified by Nuclear IP-LC/MS with hnRNP M are represented by circles. Data was overlapped with STRING Databases.

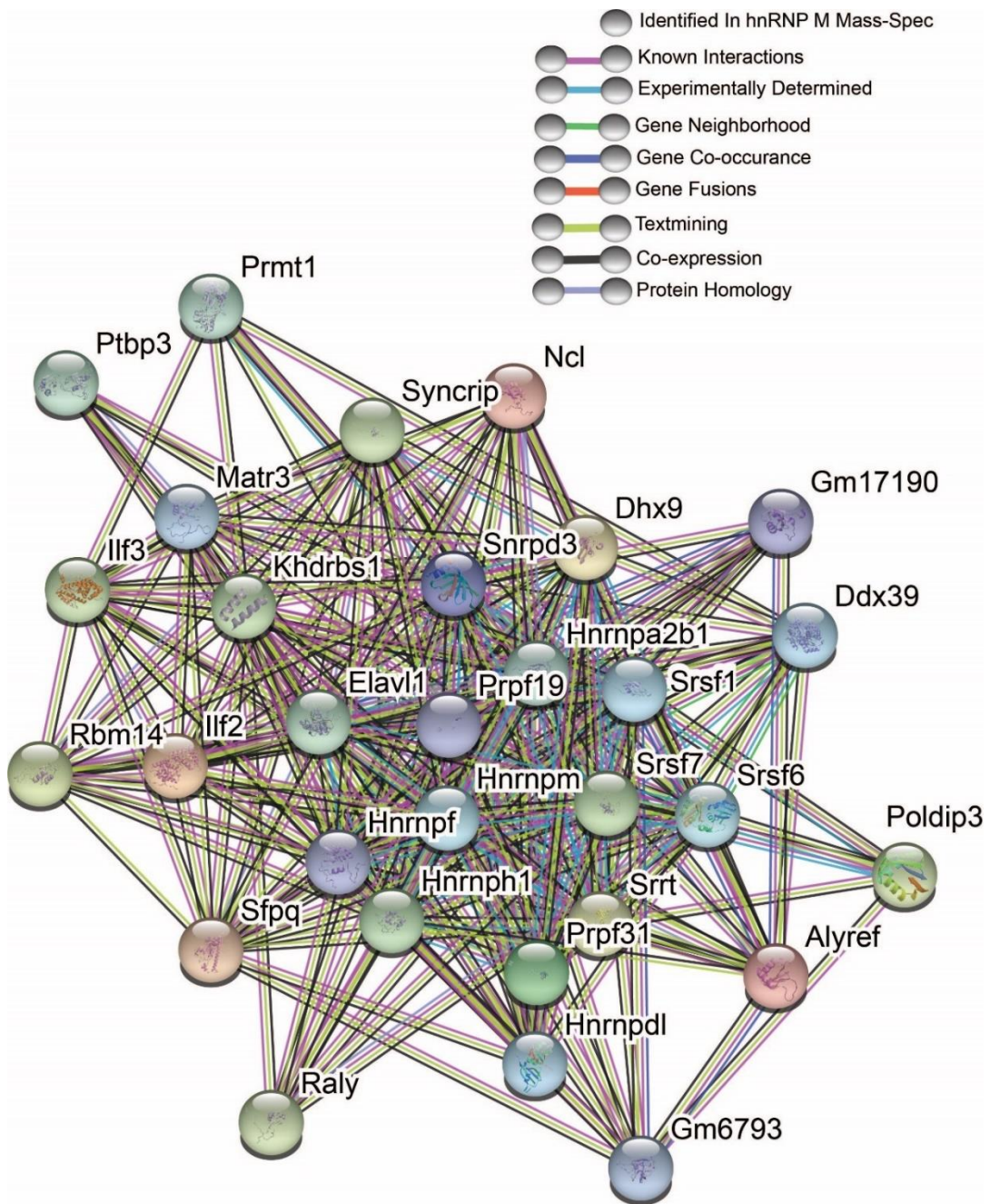


Figure 29 Zoom-In of hnRNP M Interactions with Paraspeckle-Associated Proteins, SFPQ, ILF3, and MATR3 in Resting Macrophages

Proteins identified by Nuclear IP-LC/MS with hnRNP M are represented by circles. Data was overlapped with STRING Databases.

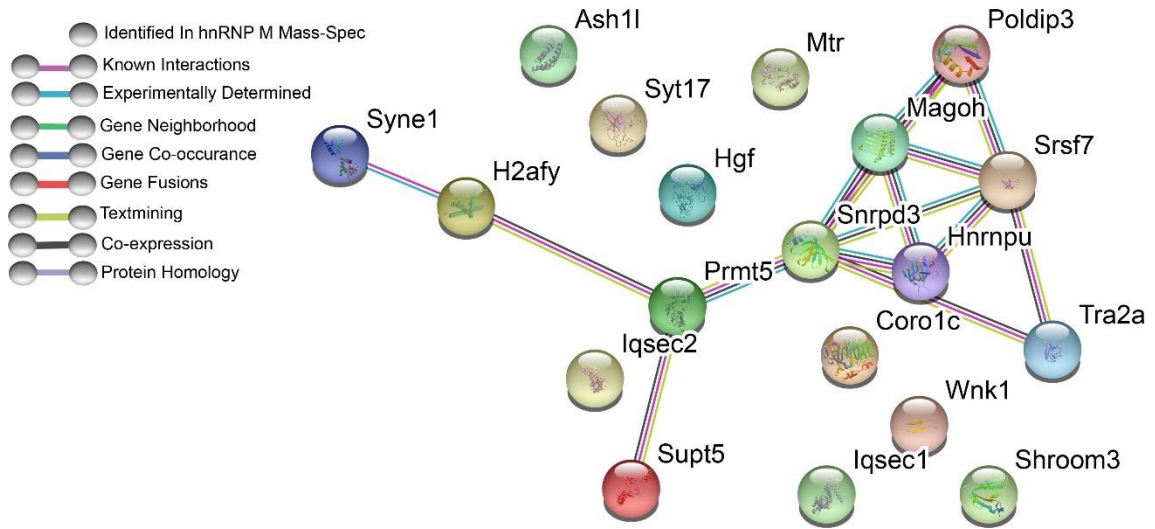


Figure 30 hnRNP M Dissolves Interactions with Majority of Protein Partners Upon Innate Immune Sensing in Macrophages

Macrophages were treated for 2h with LPS. Proteins identified by Nuclear IP-LC/MS with hnRNP M are represented by circles. Data was overlapped with STRING Databases.

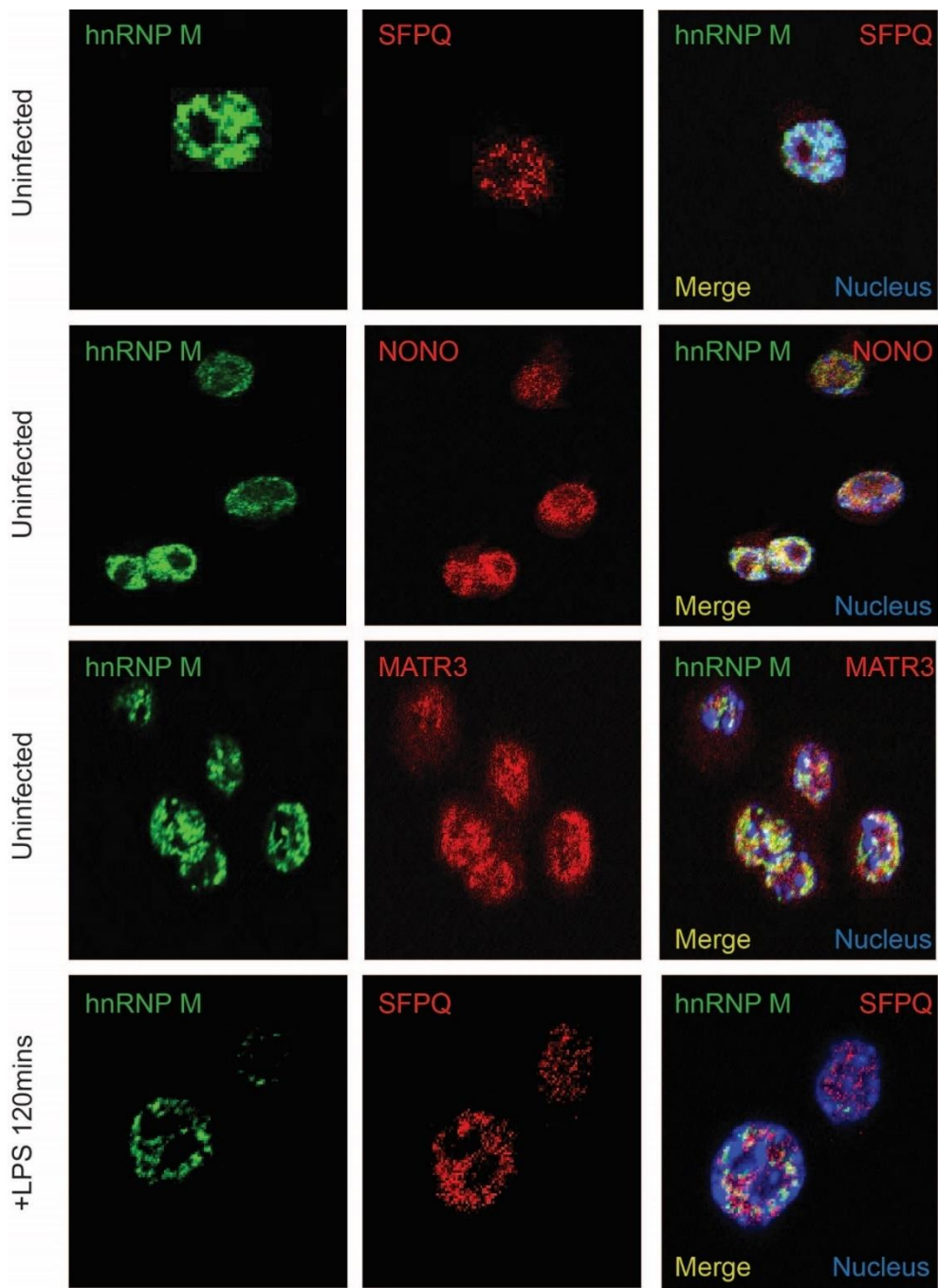


Figure 31 hnRNP M Colocalizes with Paraspeckle-Associated Proteins, SFPQ, NONO and MATR3

Immunofluorescence of RAW 264.7 cells and co-stained for endogenous hnRNP M, SFPQ, MATR3, or NONO treated with LPS for the respective time point. Green, endogenous hnRNP M; red, SFPQ, NONO, or MATR3; blue, DAPI.

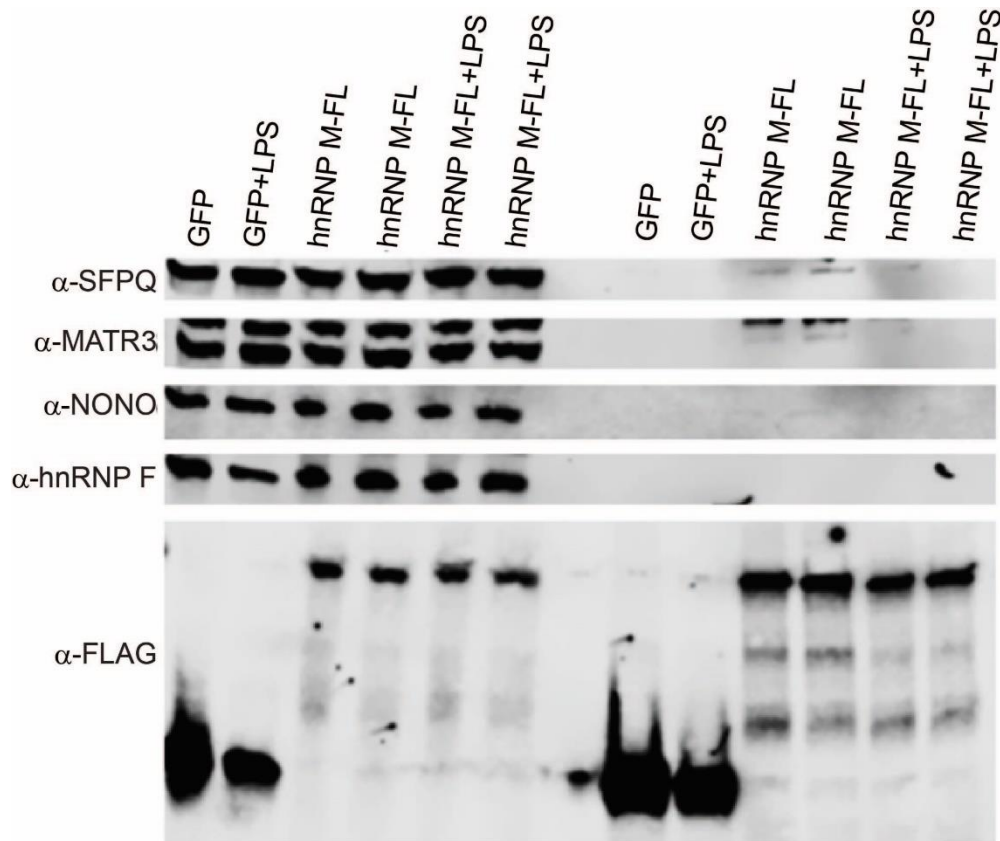


Figure 32 hnRNP M Coimmunoprecipitates with NONO, SFPQ, and MATR3

Co-immunoprecipitation (IP) of 3xFLAG (FL)-hnRNP M stable expressing RAW 264.7 cells. Whole cell lysates (WCL) and co-IPs probed for endogenous SFPQ, NONO, MATR3, and hnRNP F.

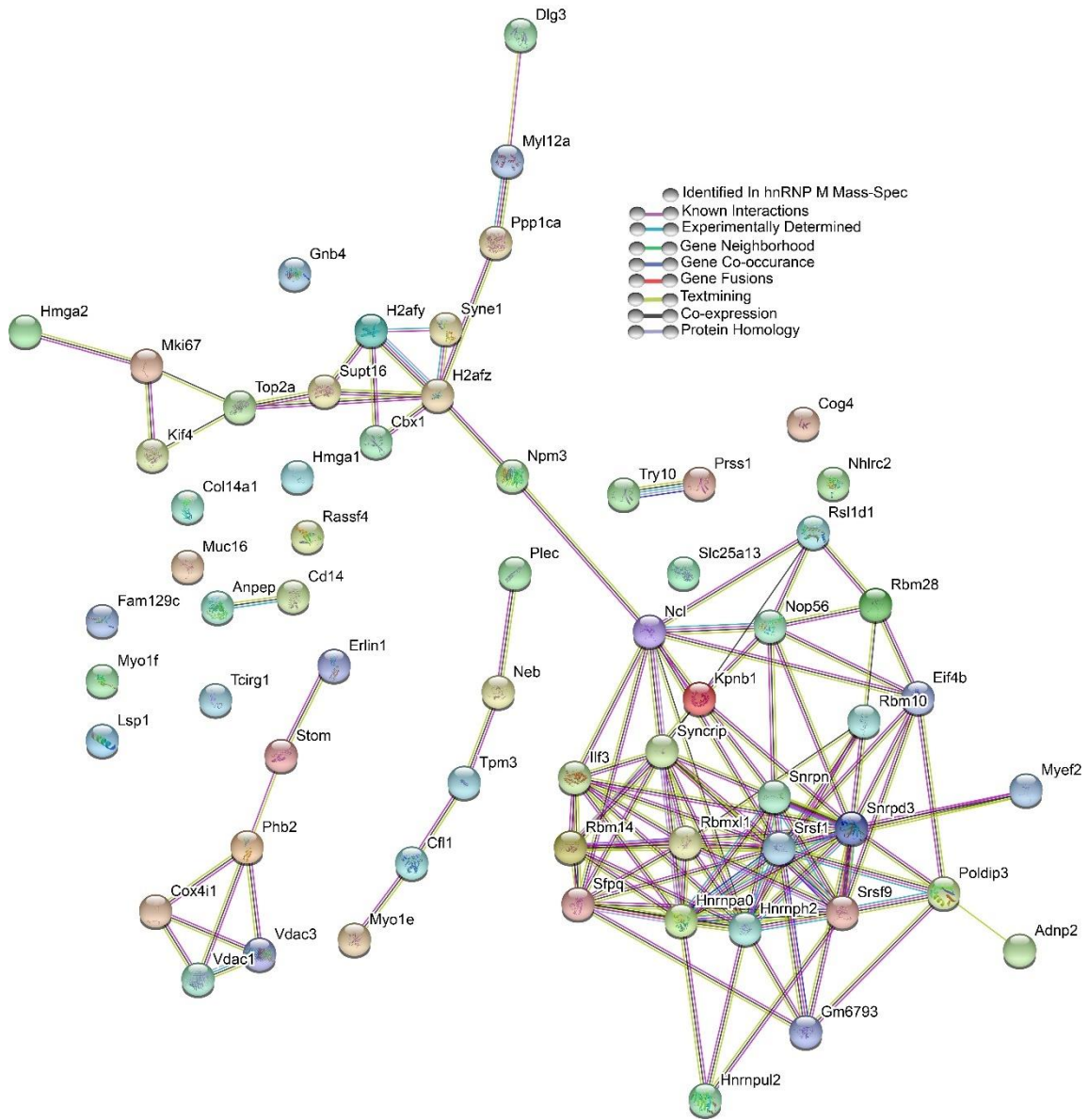


Figure 33 hnRNP M S574A Interacts with Similar Protein Partners as WT hnRNP

M

Proteins identified by Nuclear IP-LC/MS with 3xFL-hnRNP M S574A are represented by circles. Data was overlapped with STRING Databases.

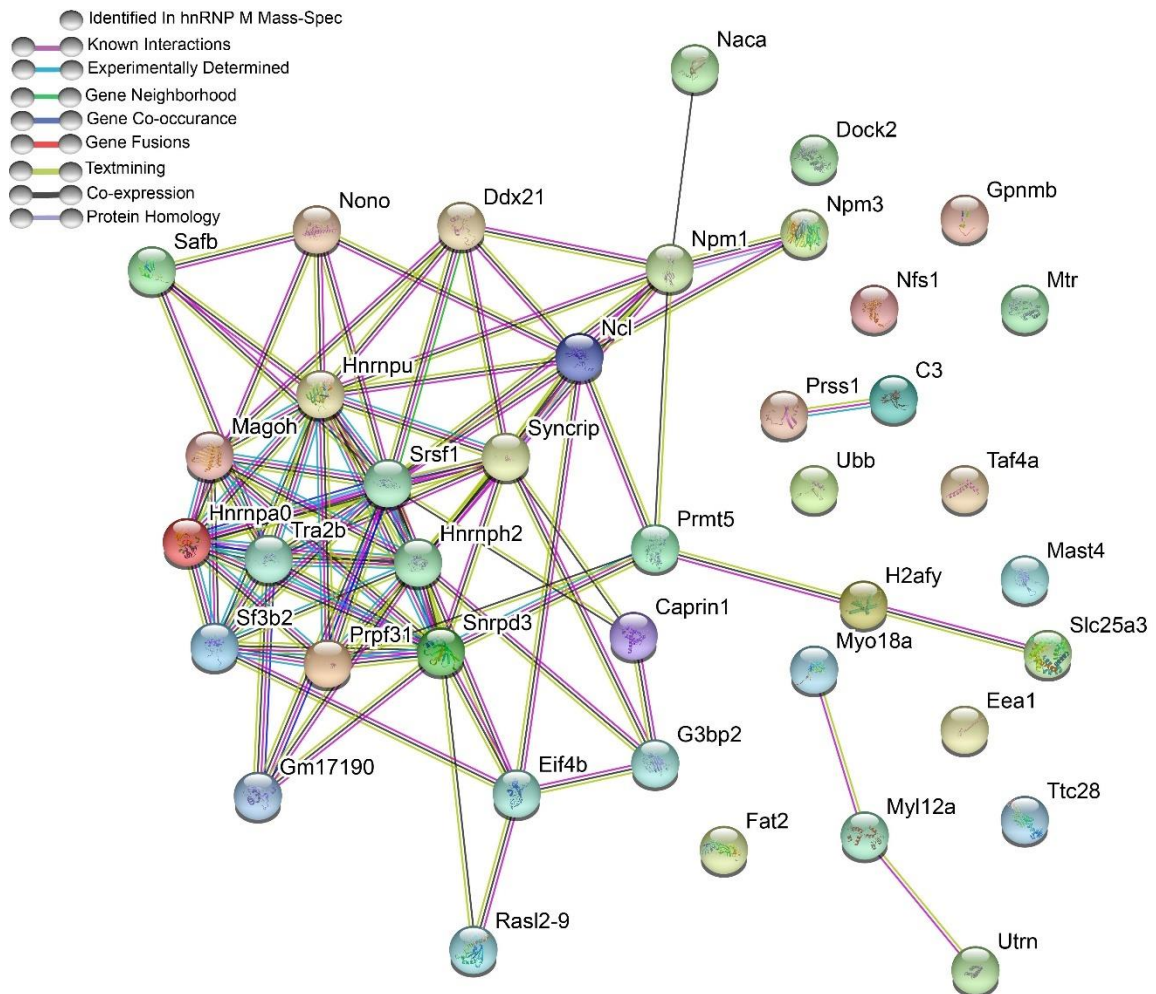


Figure 34 hnRNP M S574A Gains NONO Interaction Following Innate Immune Sensing in Macrophages

Macrophages were treated for 2h with LPS. Proteins identified by Nuclear IP-LC/MS with hnRNP M are represented by circles. Data was overlapped with STRING Databases.

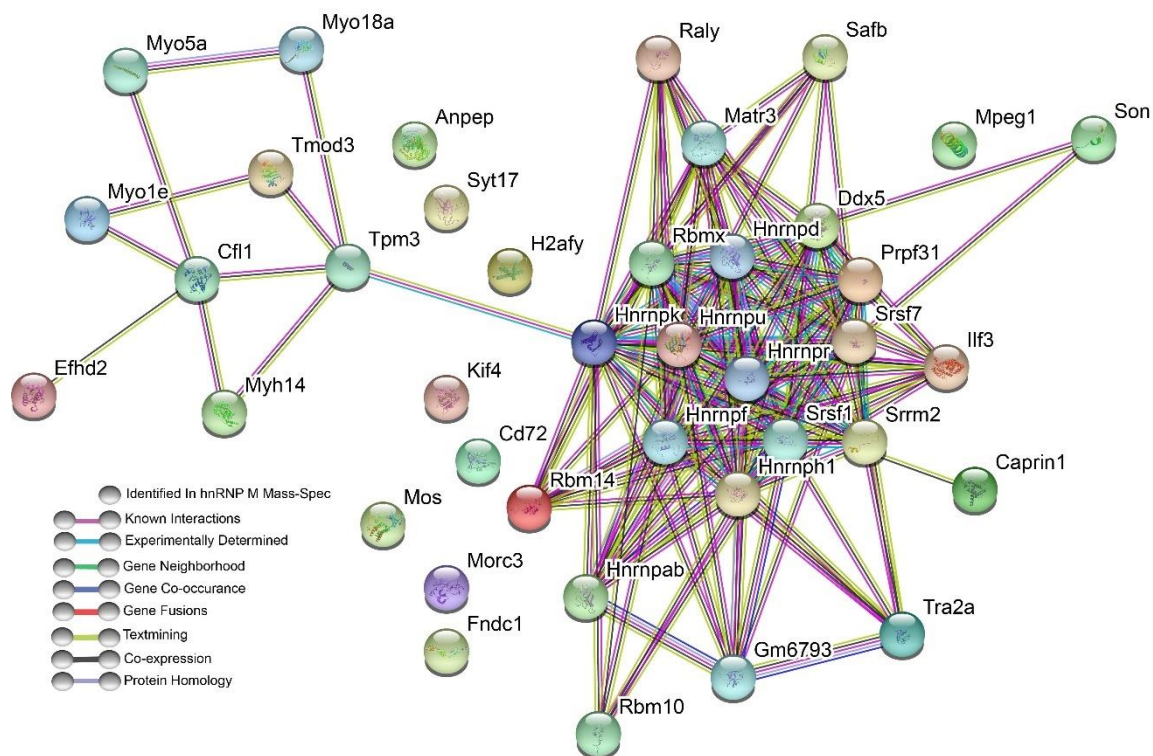


Figure 35 hnRNP M S574D Displays Interactions with MATR3 and ILF3, but not SFPQ or NONO

Proteins identified by Nuclear IP-LC/MS with hnRNP M are represented by circles. Data was overlapped with STRING Databases.

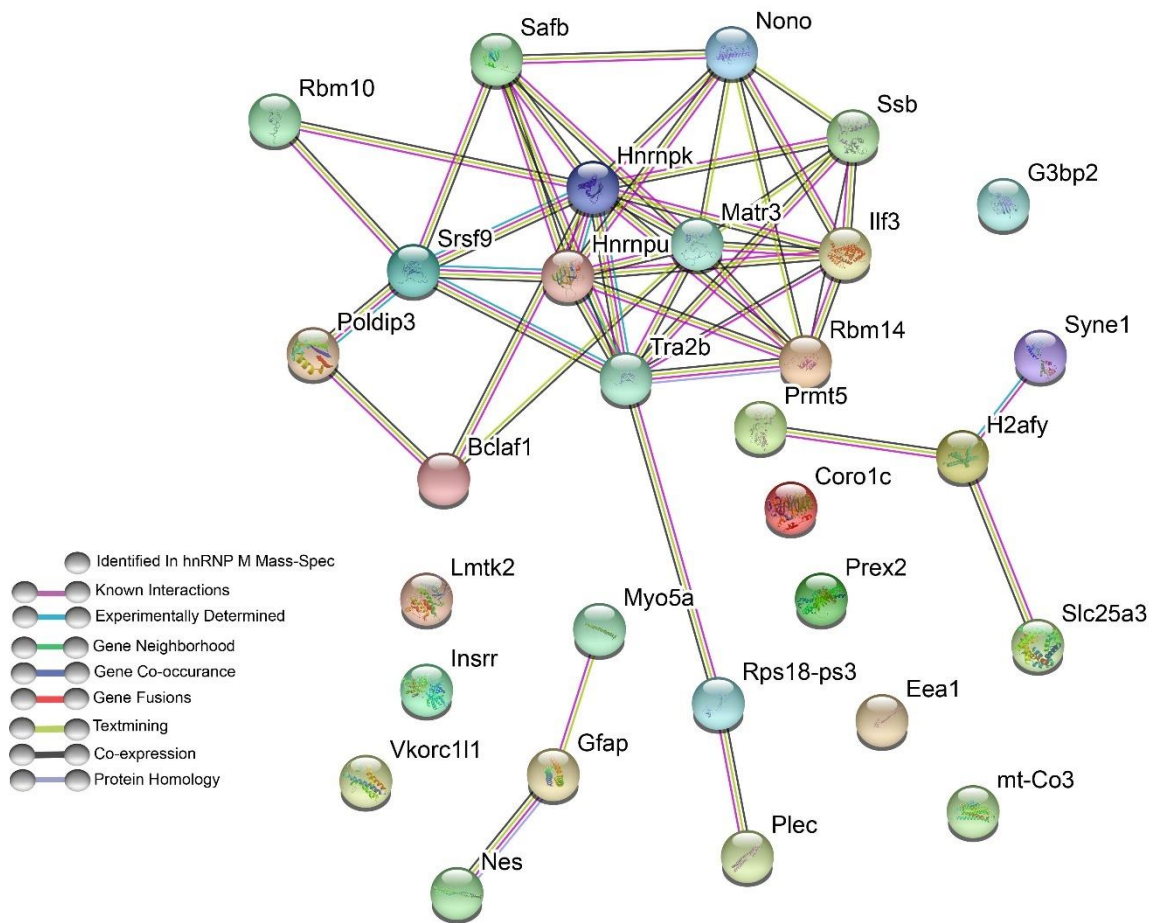


Figure 36 hnRNP M S574D Dissolves Interactions with Majority of Protein Partners Upon Innate Immune Sensing in Macrophages Similar to WT hnRNP M

Macrophages were treated for 2h with LPS. Proteins identified by Nuclear IP-LC/MS with hnRNP M are represented by circles. Data was overlapped with STRING Databases.

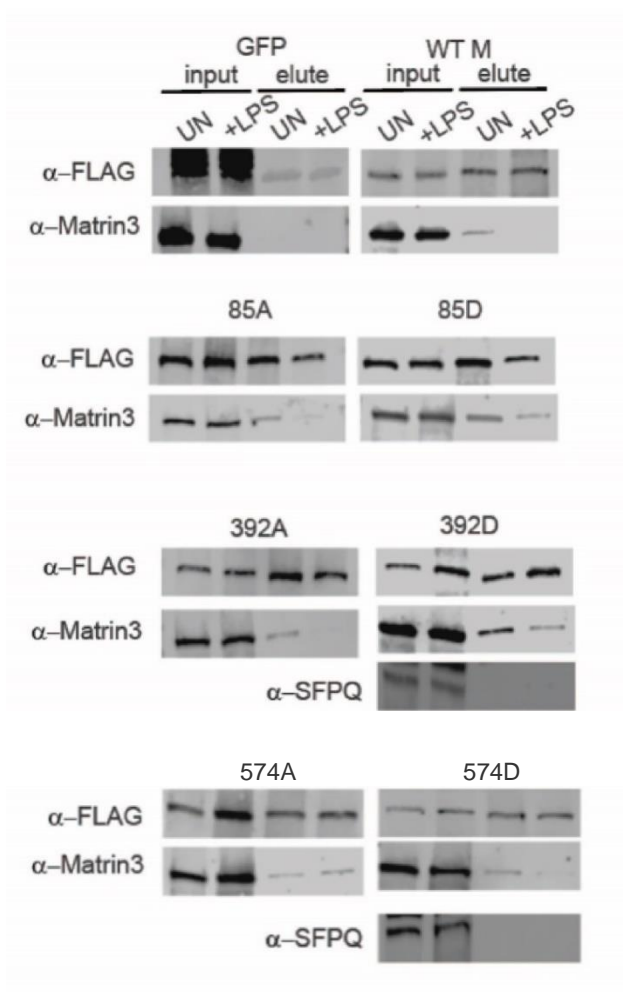


Figure 37 hnRNP M S574D and S574A Show Differentially Interactions with MATR3 In Resting and Upon Innate Immune Sensing in Macrophages

Co-immunoprecipitation (IP) of 3xFLAG (FL)-tagged hnRNP M or 3xFLAG (FL)-tagged GFP stably expressing RAW 264.7 cells. Whole cell lysates (WCL) and co-IPs probed for endogenous MATR3 and SFPQ. Macrophages were treated for 2h with LPS.

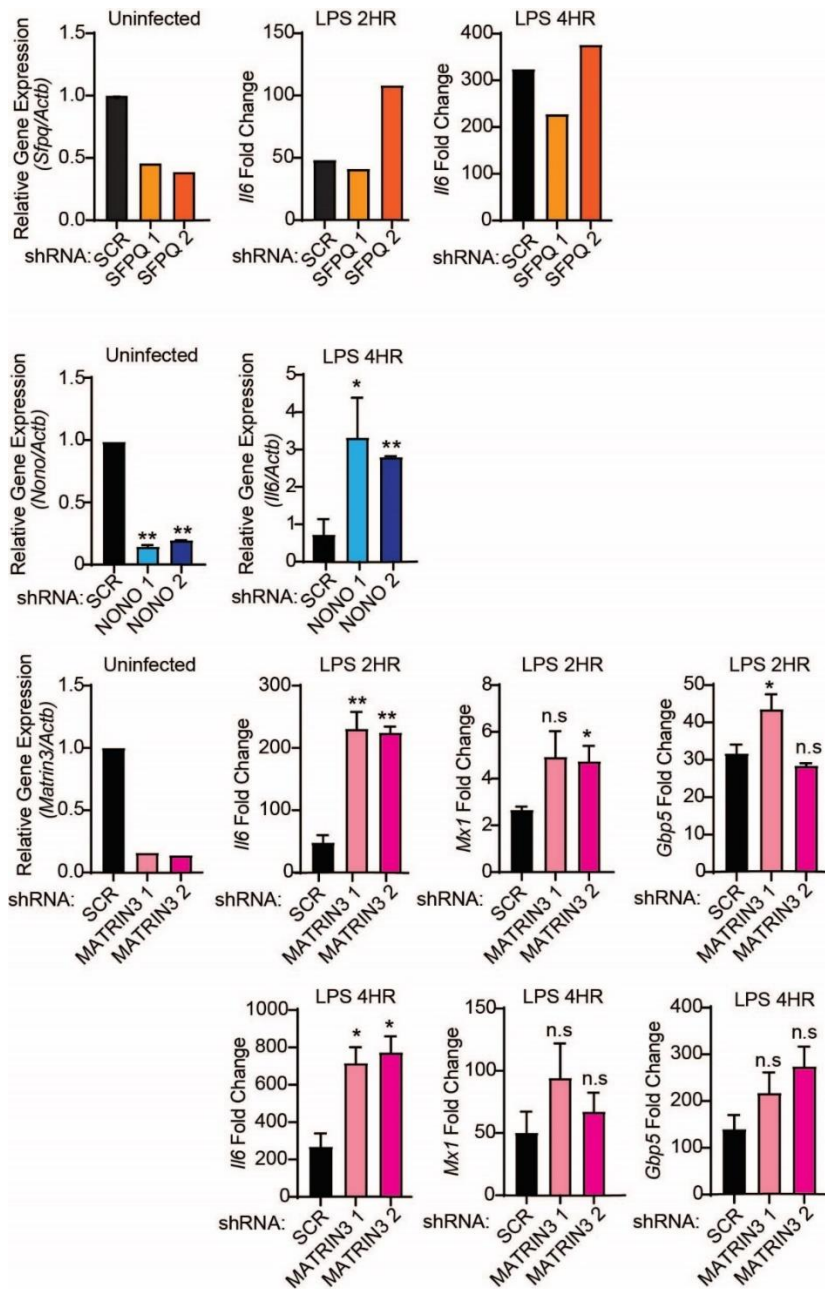


Figure 38. NONO and MATRIN3 Knockdown Stimulates Innate Immune Gene Expression

qRT-PCR of *Sfpq* and *Il6* in LPS-treated hnRNP F KD cells at 2 h and 4h. Values are mean (SD) representative of 2 biological replicates. qRT-PCR of *Nono* and *Il6* in LPS-treated hnRNP F KD cells at 4h. qRT-PCR of *Matr3*, *Il6*, *Mx1*, and *Gbp5* in LPS-treated hnRNP F KD cells at 2h and 4h. Values are mean (SD) representative of 2 biological replicates.

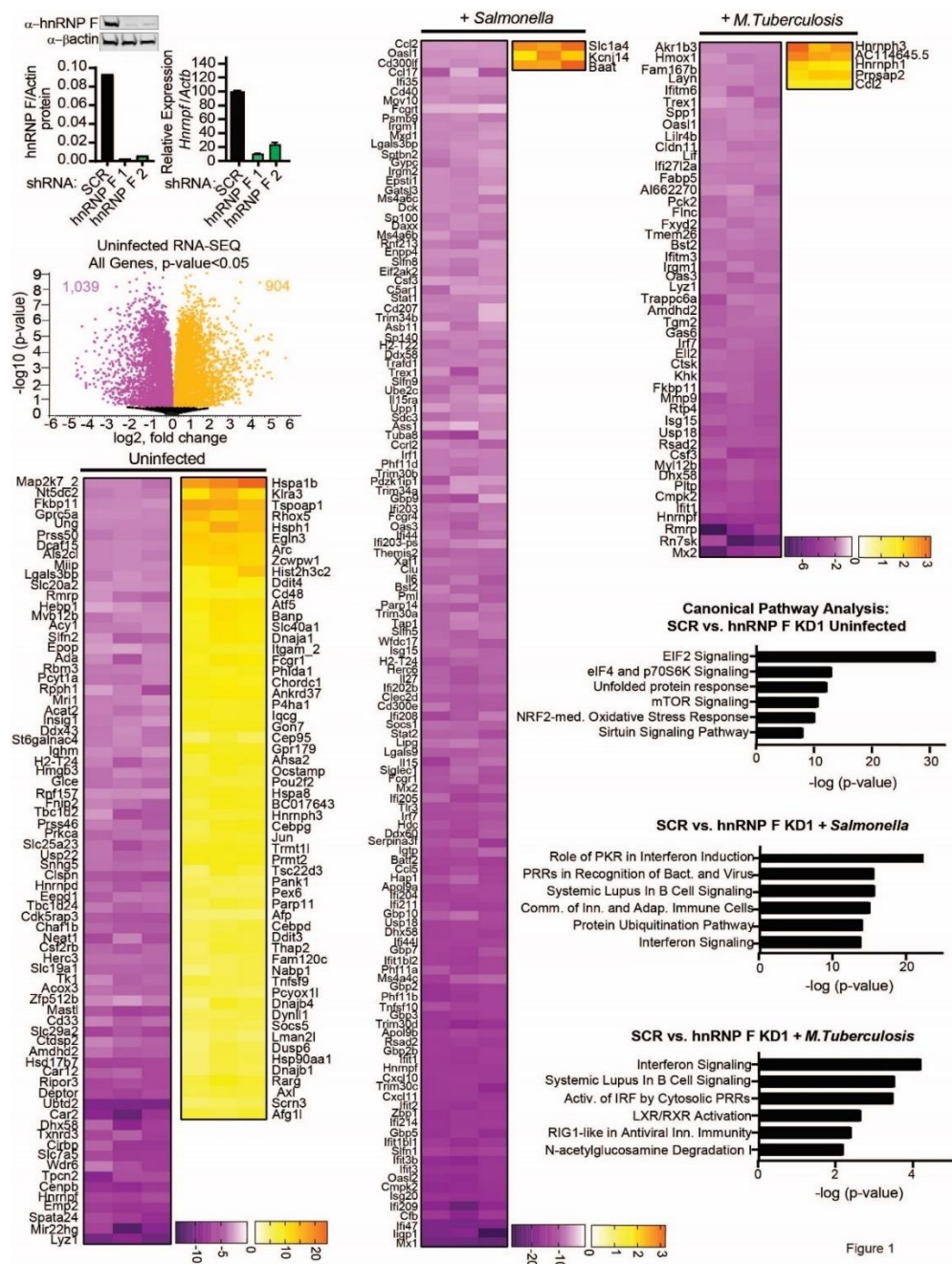


Figure 39. hnRNP F Regulates Expression of Interferon-Stimulatory Genes During *Salmonella* Typhimurium and *Mycobacterium Tuberculosis* Infection

(A) Western blot analysis and qRT-PCR of hnRNP F in RAW 264.7 macrophages. Values are mean (SD) representative of 3 biological replicates. (B) Volcano plot (t test) showing gene expression analysis of hnRNP F KD RNA-seq data from uninfected cells. Downregulated genes are in purple, and upregulated genes are in orange. (C) Gene expression analysis of hnRNP F KD cells compared to SCR control for uninfected cells. Each column represents a biological replicate. (D) Gene expression analysis of hnRNP F KD cells compared to SCR control for *Salmonella*-infected cells. (E) Gene expression analysis of hnRNP F KD cells compared to SCR control for *Tuberculosis*-infected cells. (F) Ingenuity pathway analysis of gene expression changes in uninfected, *Salmonella*-infected, and *Tuberculosis*-infected cells.

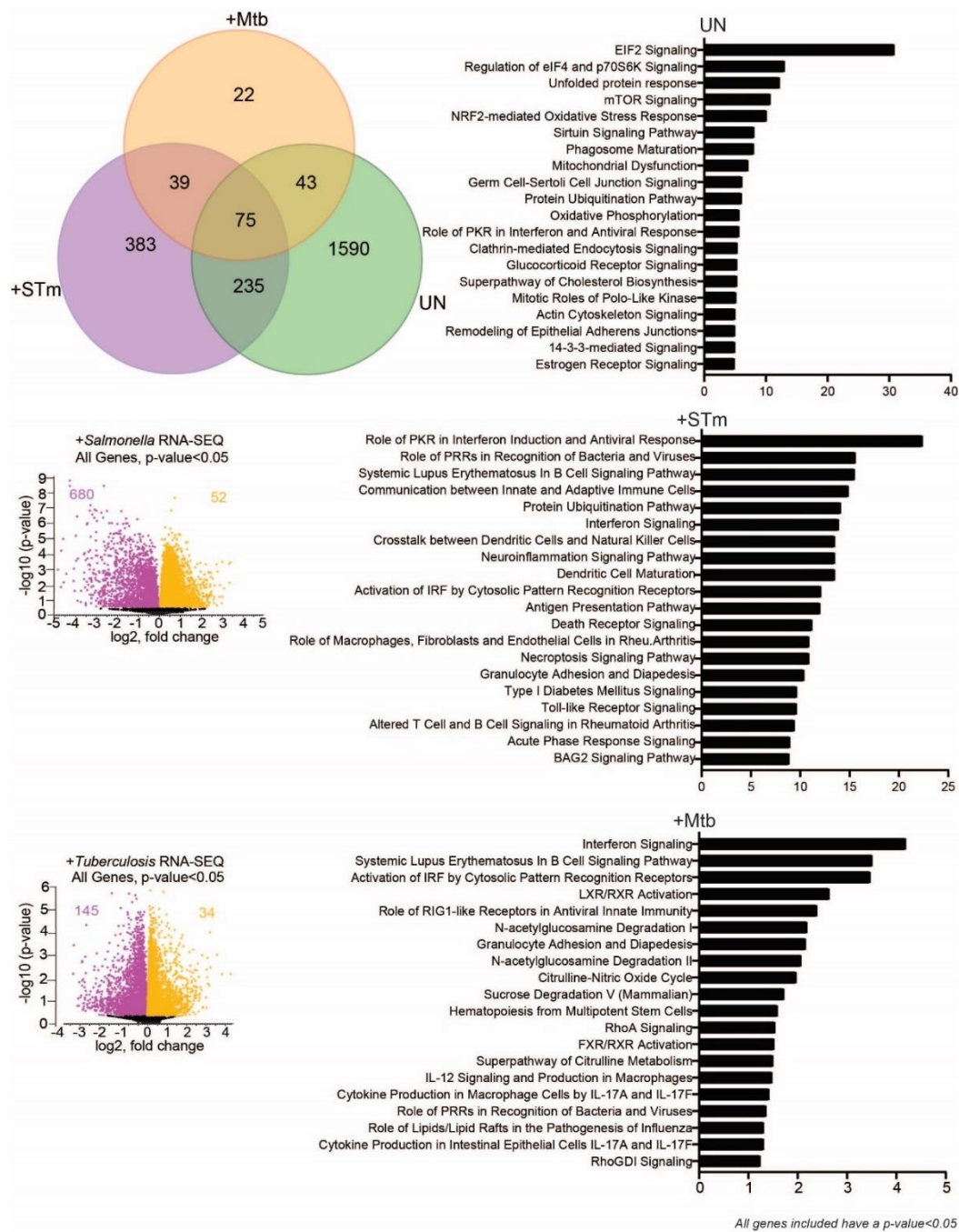


Figure 40. hnRNP F Regulates Expression of Interferon-Stimulatory Genes During *Salmonella* Typhimurium and *Mycobacterium Tuberculosis* Infection

Venn diagram displaying overlap of genes found in RNA-Seq analysis of uninfected, *Salmonella*-infected, and *Tuberculosis*-infected hnRNP F KD1 samples. Genes utilized in diagram were from heat maps displayed previously. (B) Volcano plot (t test) showing gene expression analysis of hnRNP F KD RNA-seq data from *Salmonella*-infected and *Tuberculosis*-infected samples. X axis shows \log^2 fold change of gene expression, and y axis shows statistical significance. Downregulated genes are plotted on the left in purple, and upregulated genes are on the right in orange. Gene counts are all genes with $p\text{-value} < 0.05$. (C) All hits from Ingenuity pathway analysis of RNA-Seq differential expression in uninfected, *Salmonella*-infected, and *Tuberculosis*-infected hnRNP F KD1 cells.

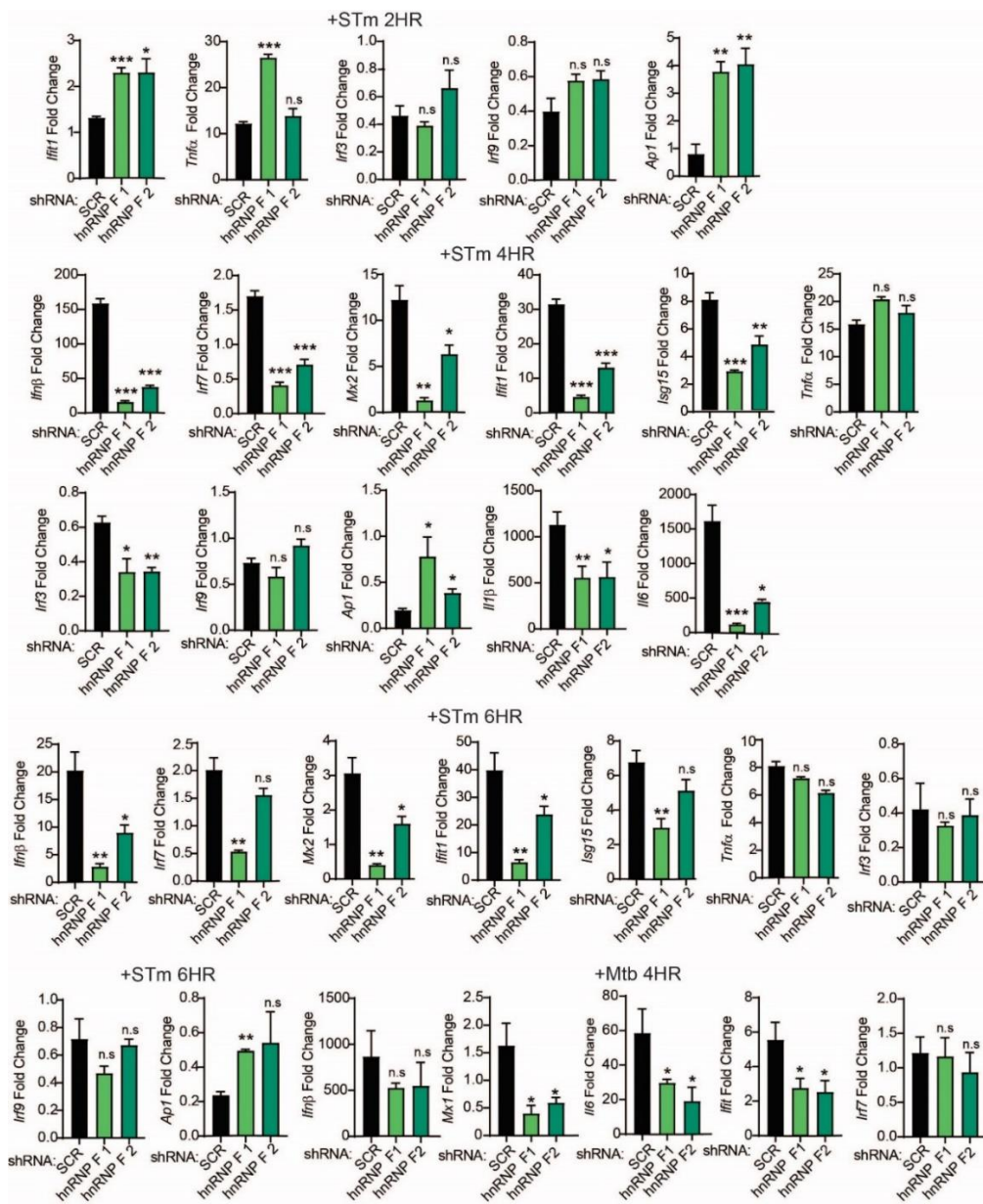


Figure 41. hnRNP F Regulates Expression of Interferon-Stimulatory Genes During *Salmonella* Typhimurium and *Mycobacterium Tuberculosis* Infection

(A) qRT-PCR of *Infβ*, *Ifit1*, *Tnfx*, *Irf3*, *Irf9*, and *Ap1* in *Salmonella*-infected hnRNP F KD cells at 2 h post-infection. (B) qRT-PCR of *Infβ*, *Irf7*, *Mx2*, *Ifit1*, *Isg15*,

Tnfa, *Irf3*, *Irf9*, *Ap1*, *IL1 β* , and *IL6* in *Salmonella*-infected hnRNP F KD cells at 4 h post-infection. (C) qRT-PCR of *Inf β* , *Irf7*, *Mx2*, *Ifit1*, *Isg15*, *Tnfa*, *Irf3*, *Irf9*, and *Ap1* in *Salmonella*-infected hnRNP F KD cells at 6 h post-infection. (D) qRT-PCR of *Inf β* , *Mx1*, *Ifit1*, and *IL6* in *Tuberculosis*-infected hnRNP F KD cells at 6 h post-infection (A)–(D) represent 4 biological replicates \pm SEM, n = 4. For all experiments in this study, statistical significance was determined using two-tailed Students' t test. *p < 0.05, **p < 0.01, ***p < 0.001, n.s., not significant.

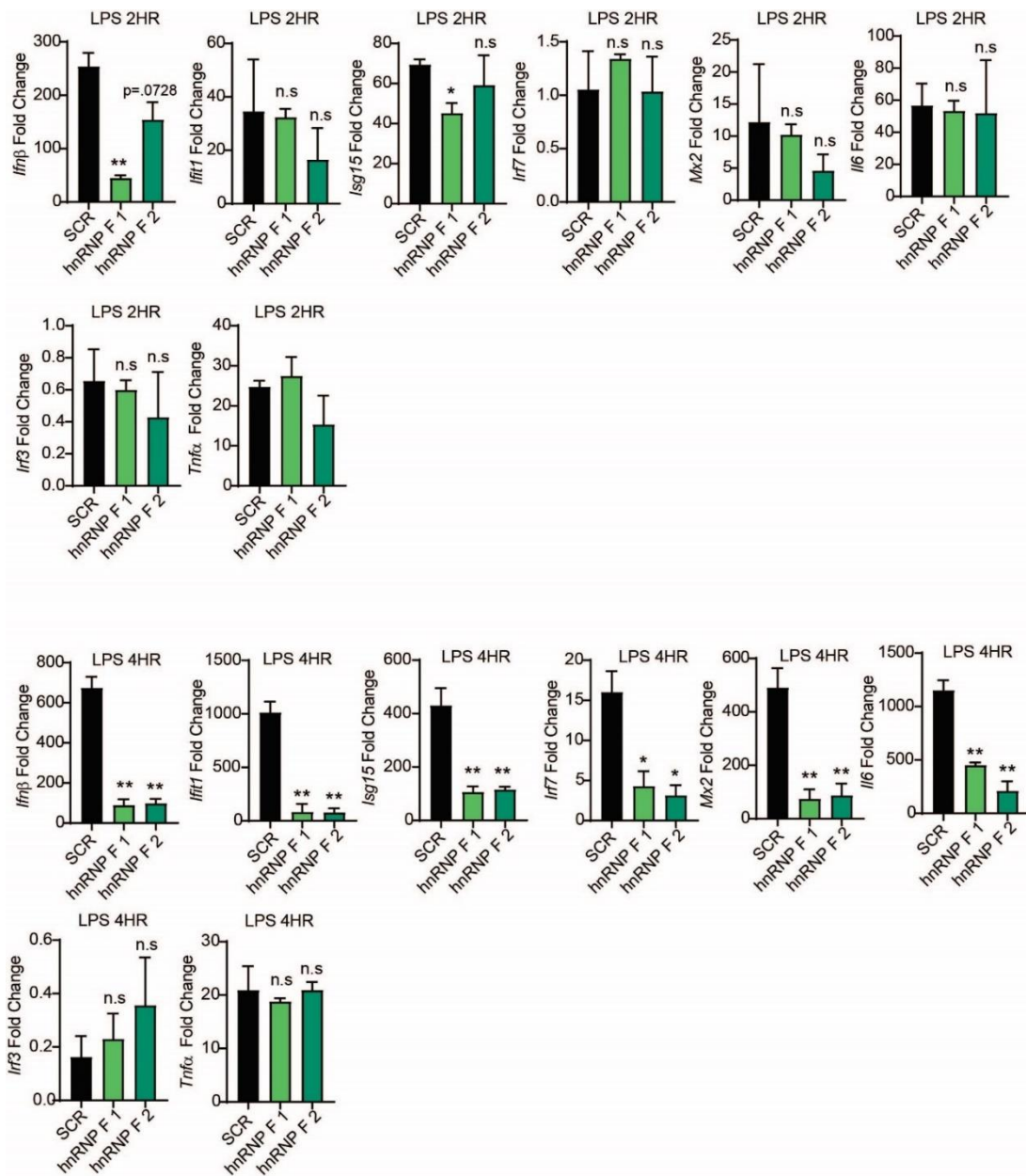


Figure 42. hnRNP F-dependent Regulation of Innate Immune Gene Expression

Occurs Downstream of TLR4

(A) qRT-PCR of *Infβ*, *Ifit1*, *Isg15*, *Irf7*, *Mx2*, *Il6*, *Irf3*, and *Tnfa* in hnRNP F KD cells treated with LPS for 2h and 4h. All experiments represent 4 biological replicates where values are means \pm SEM, n = 4. For all experiments in this study, statistical significance was determined using two-tailed Students' t test. *p < 0.05, **p < 0.01, ***p < 0.001, n.s., not significant.

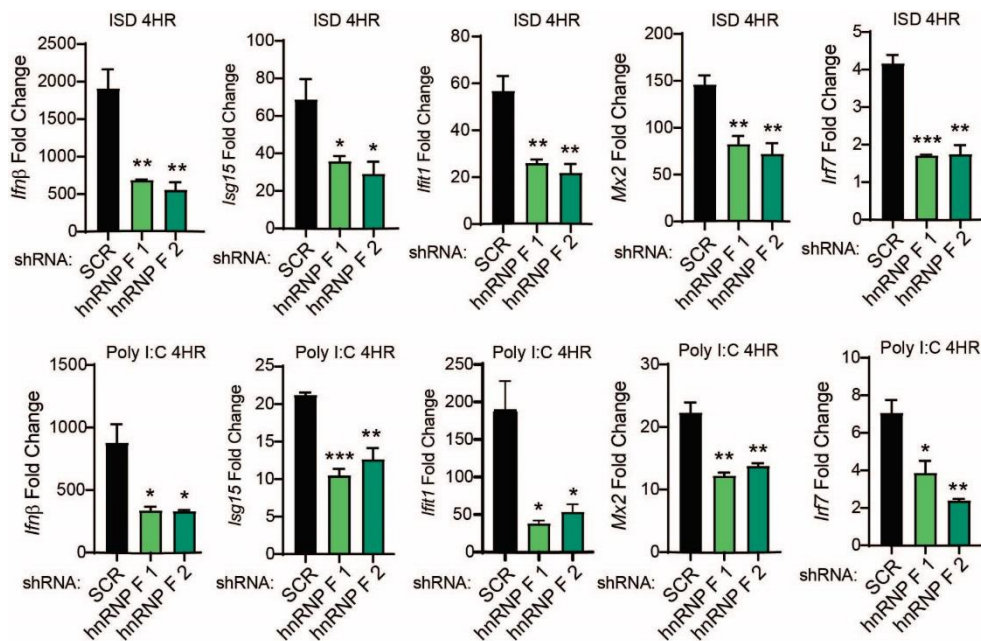


Figure 43. hnRNP F-dependant Regulation of Innate Immune Gene Expression

Occurs Downstream of DNA-Sensing and RNA-Sensing

qRT-PCR of *Ifnb1*, *Isg15*, *Ifit1*, *Mx2*, and *Irf7* mRNA levels in SCR control and hnRNP F KD cells at 4 h following ISD transfection. qRT-PCR of *Ifnb*, *Isg15*, *Ifit1*, *Mx2*, and *Irf7* in SCR control and hnRNP F KD cells at 4 h following polyI:C transfection. All experiments represent 3 biological replicates where values are means \pm SEM, n = 3.

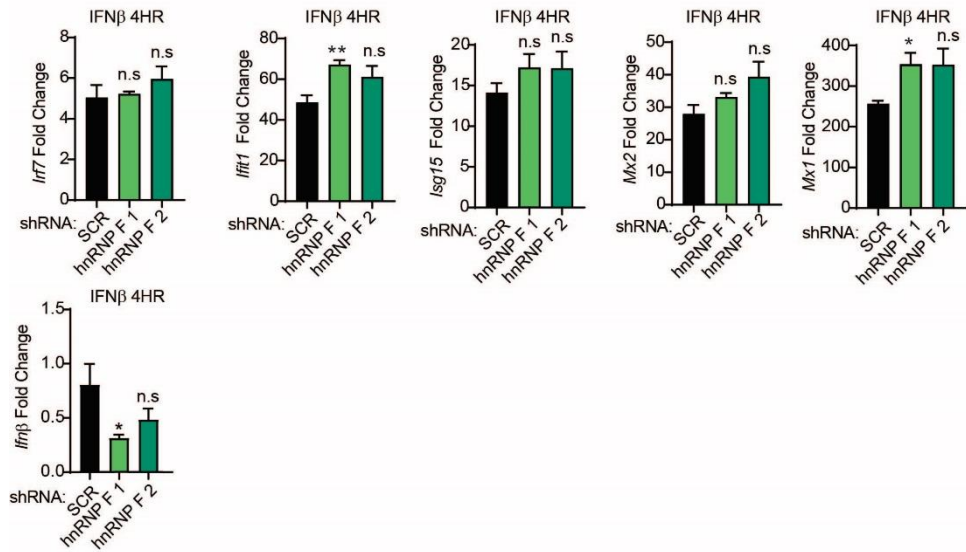


Figure 44. hnRNP F-Dependent Regulation is Independent of IFNAR Signaling

qRT-PCR of *Irf7*, *Ifit1*, *Isg15*, *Mx2*, *Mx1*, and *Irfb1* in SCR control and hnRNP F KD cells at 4h following treatment of recombinant IFN-β for 4h. All experiments represent 3 biological replicates where values are means ± SEM, n = 3.

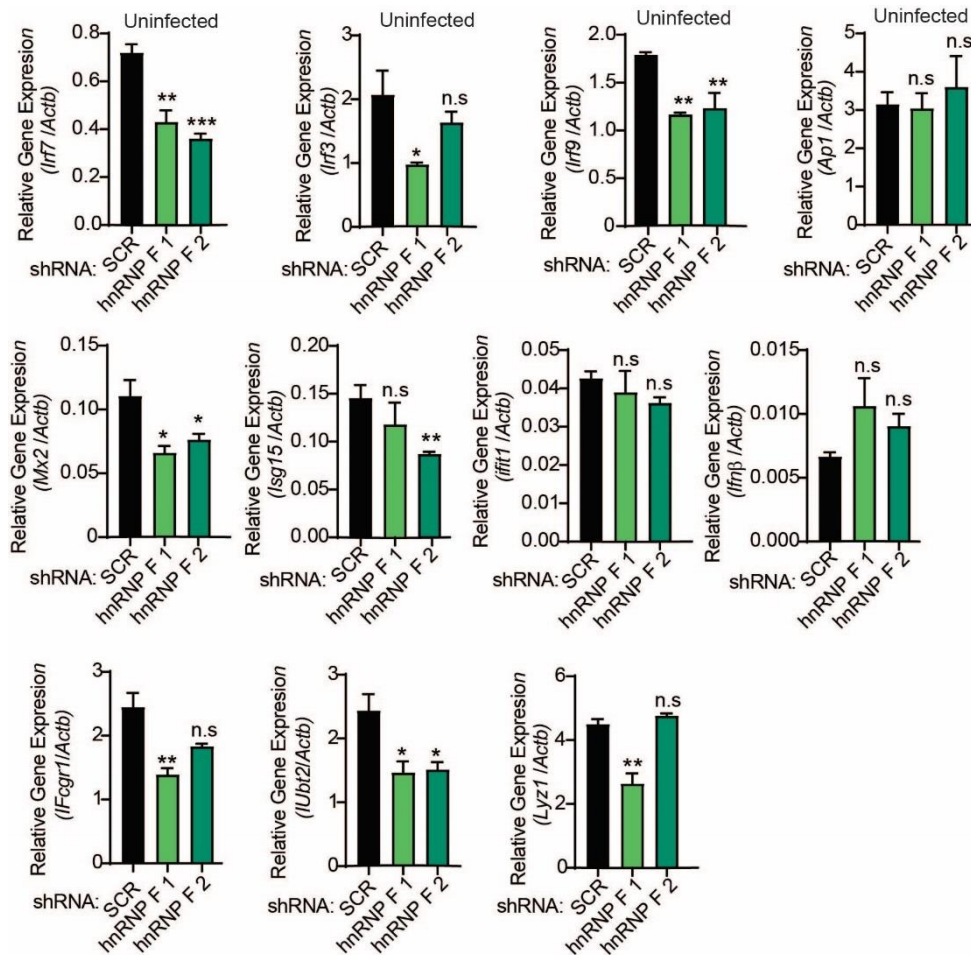


Figure 45. hnRNP F Knockdown Macrophages Show Differences in *Irf3* and *Irf7*

Expression at Baseline

qRT-PCR of *Irf7*, *Irf3*, *Irf9*, *Ap1*, *Mx2*, *Isg15*, *Ifit1*, and *Ifnb* in uninfected hnRNP

F KD cells. qRT-PCR of *Fcgr1*, *Ubt2*, and *Lyz1* in uninfected hnRNP F KD cells. All

experiments represent 3 biological replicates where values are means \pm SEM, n = 3.

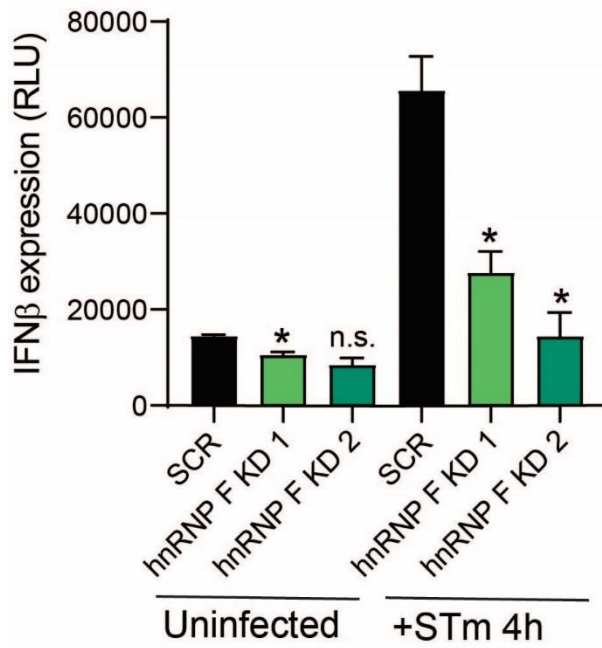


Figure 46. hnRNP F Depletion Leads to Loss of IFN β Protein During *Salmonella* Infection

IFN stimulated response element reporter cells expressing luciferase with relative light units measured as a readout for IFN- β protein in hnRNP F Knockdown and SCR control cells infected with *Salmonella* for 4h.

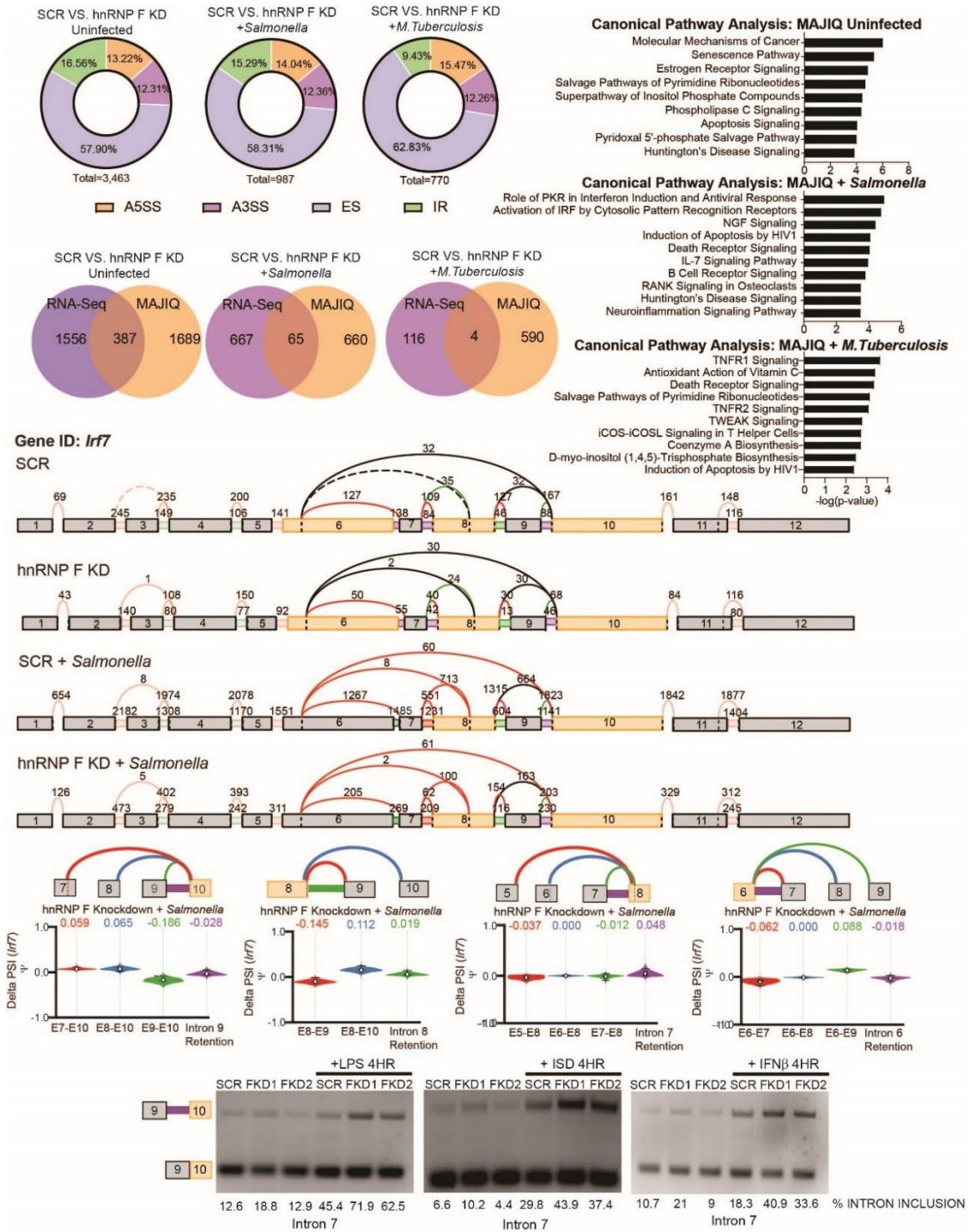


Figure 47. MAJIQ Analysis of hnRNP F Reveals *Irf7* Alternative Splicing

Categorization of alternative splicing events identified via MAJIQ in uninfected SCR versus hnRNP F KD1 samples, in *Salmonella*-infected SCR versus hnRNP F KD1 samples, and in *Tuberculosis*-infected SCR versus hnRNP F KD1 samples. MAJIQ genes used had a deltaPSI of 0.2 or greater. (B) Ingenuity Pathway Analysis of hnRNP F-dependent genes from MAJIQ analysis in uninfected, *Salmonella*-infected, and *Tuberculosis*-infected cells. The top nine hits are displayed. (C) Venn diagrams displaying overlap of genes identified through differential expression analysis and genes identified in MAJIQ analysis in uninfected, *Salmonella*-infected, and *Tuberculosis* infected hnRNP F KD samples. Genes included in differential expression analysis were the same used in the heat map diagrams. MAJIQ genes used had a deltaPSI of 0.2 or greater. (D) VOILA output of *Irf7* transcript model in uninfected SCR and hnRNP F KD1 cells and cell infected with *Salmonella*. (E) Violin plots depicting the delta PSI of hnRNP F-dependent local splicing variations in *Irf7* in *Salmonella*-infected samples. (F) Semiquantitative RT-PCR validation of hnRNP F-dependent intron inclusion of *Irf7* in hnRNP F KD cells treated with LPS, ISD, or IFNB for 4 h. (F) is representative of two independent experiments that showed the same result with values representing means (SD), n = 2. (F) and (G) values are means \pm SEM representative of 2 biological replicates, n = 2.

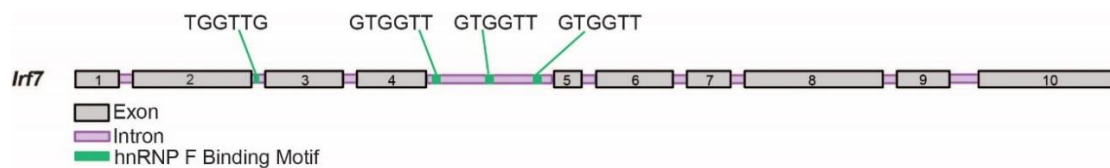


Figure 48. Canonical *Irf7* Transcript Reveals hnRNP F Binding Sites Aligning With MAJIQ Identified Splice Sites

Diagram of *Irf7* pre-mRNA with introns in purple and exons in gray. Green represents identified sites with similarity to hnRNP F consensus motifs.

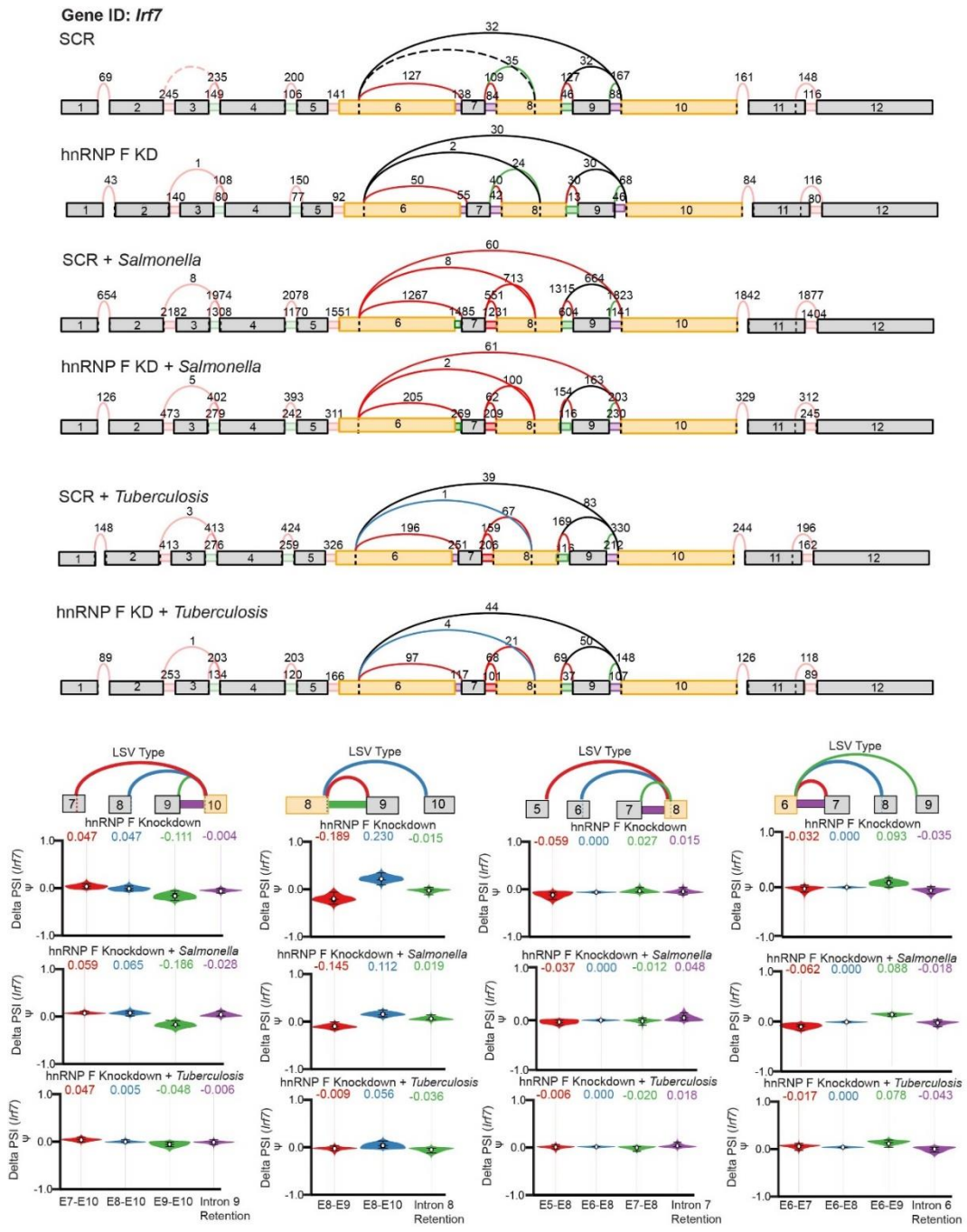


Figure 49. MAJIQ Analysis of hnRNP F Reveals *Irf7* Alternative Splicing

VOILA output of *Irf7* transcript model in uninfected SCR and hnRNP F KD1 cells, cells infected with *Salmonella*, cells infected with *Tuberculosis*. Violin plots depicting the delta PSI of hnRNP F-dependent local splicing variations in *Irf7* in uninfected SCR and hnRNP F KD1 cells, cells infected with *Salmonella*, cells infected with *Tuberculosis*.

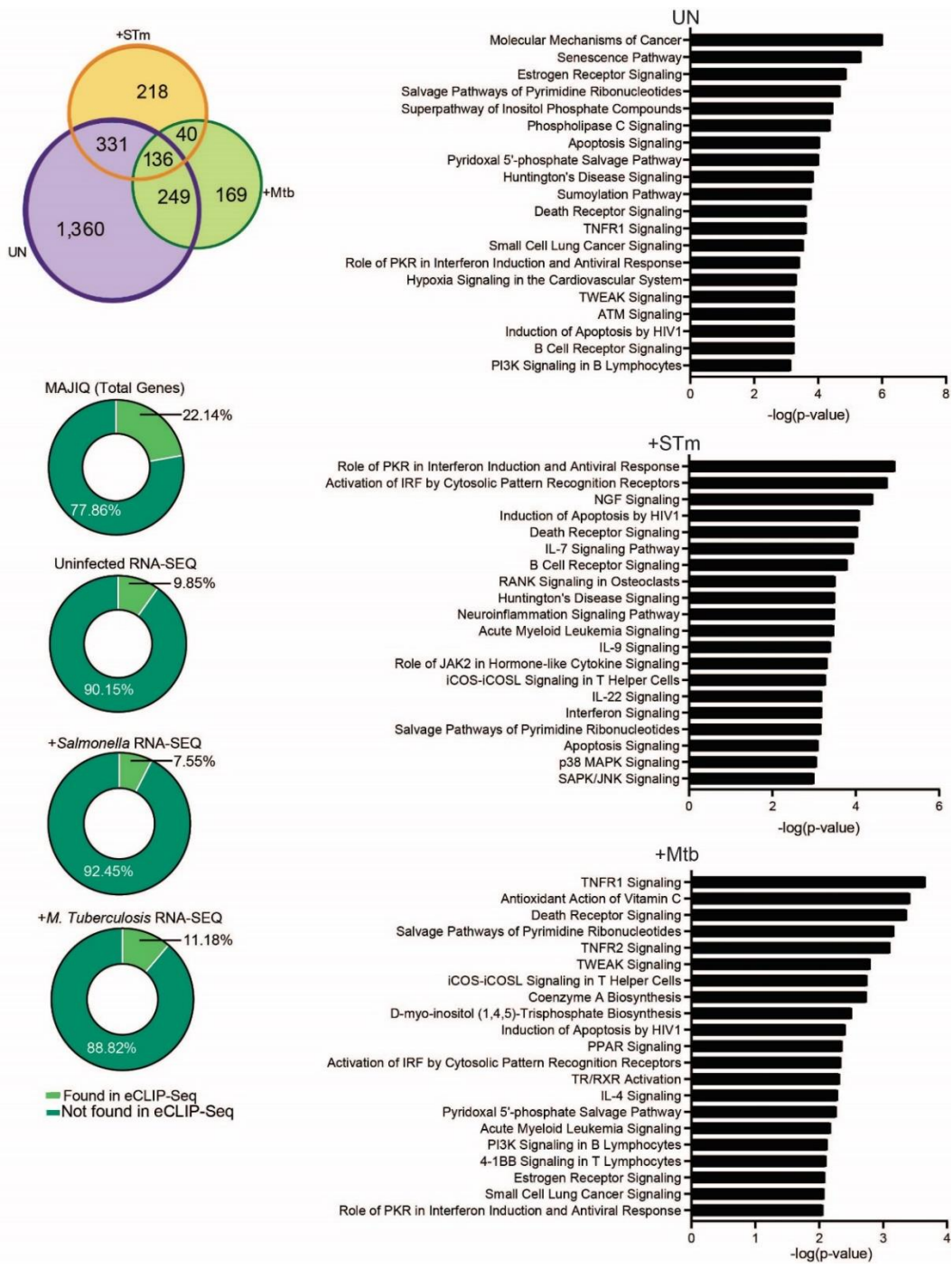


Figure 50. Supplemental MAJIQ Analysis of hnRNP F

Venn diagram displaying overlap of genes found in MAJIQ analysis of uninfected, *Salmonella*-infected, and *Tuberculosis*-infected hnRNP F KD1 samples. MAJIQ genes used had a deltaPSI of 0.2 or greater. (B) All hits from Ingenuity pathway analysis of MAJIQ changes in uninfected, *Salmonella*-infected, and *Tuberculosis*-infected cells. (C) Venn diagrams representing hnRNP M eCLIP (ENCODE) gene overlap with our MAJIQ, uninfected RNA-seq, *Salmonella*-infected RNA-seq, and *Tuberculosis*-infected RNA-seq results.

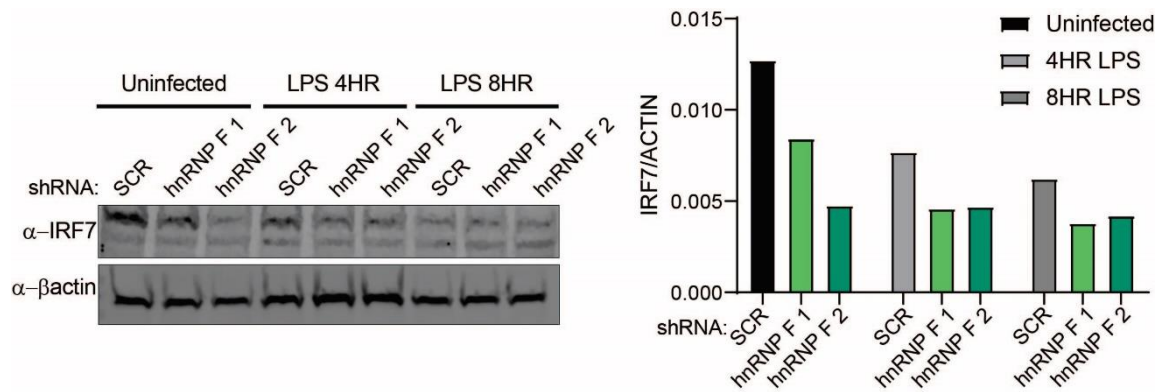


Figure 51. Expression and Splicing Changes of *Irf7* in hnRNP F Knockdown Cells Leads to Decrease Protein Levels

Immunoblot analysis of IRF7 in SCR control cells vs. hnRNP F KD cells treated with LPS for 4h and 8h using endogenous IRF7 antibody. Protein expression was quantified using Odyssey Fc by LI-COR.

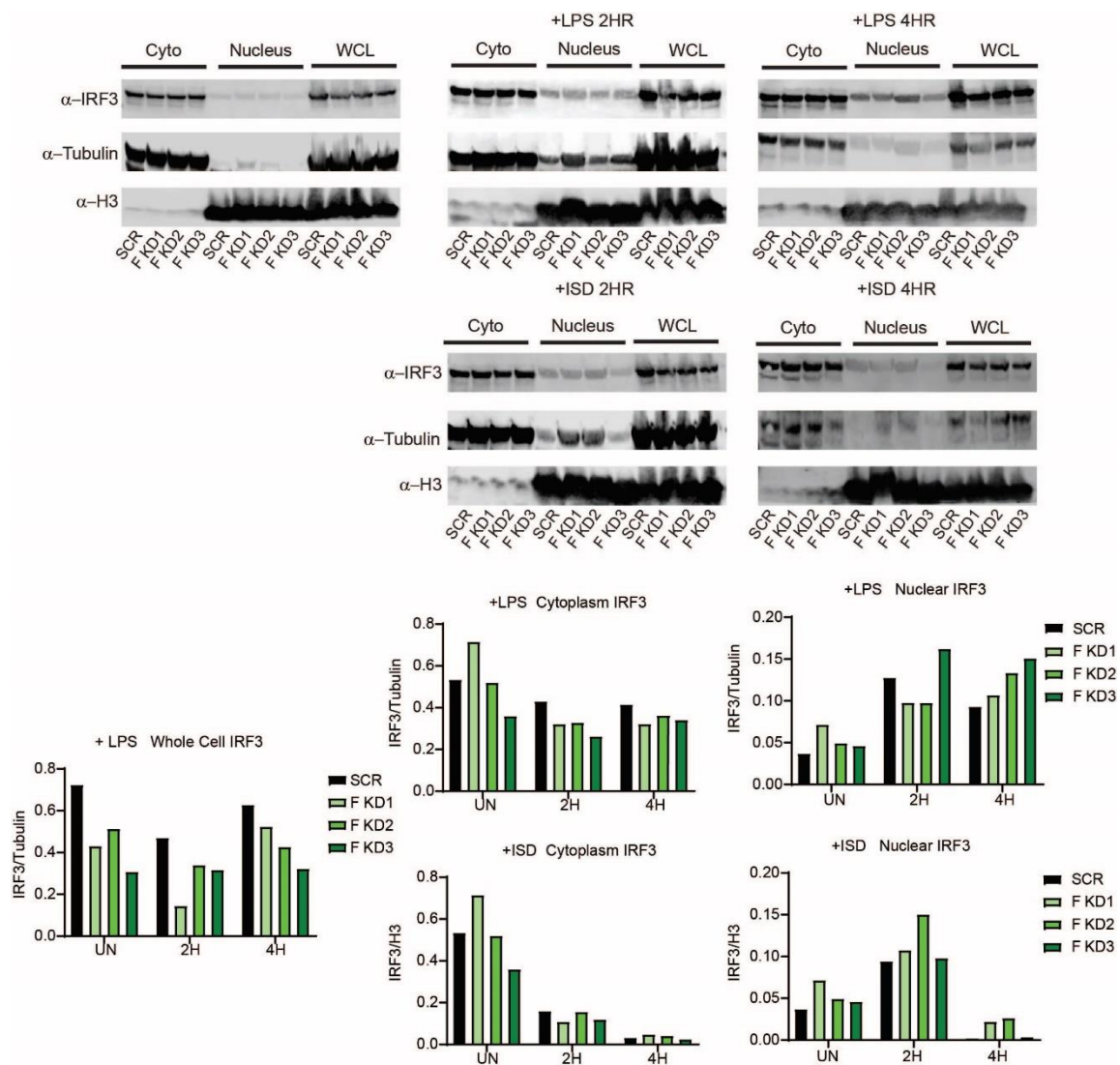


Figure 52. Nuclear Fractionation in hnRNP F Knockdown Cells Shows No Difference in IRF3 Localization Upon Innate Immune Agonists

Nuclear Fraction of SCR control cells and hnRNP F KD cells was performed with cells treated with LPS for 2h and 4h or ISD for 2h or 4h. Immunoblot analysis of IRF3 in SCR control cells vs. hnRNP F KD cells using endogenous IRF3 antibody.

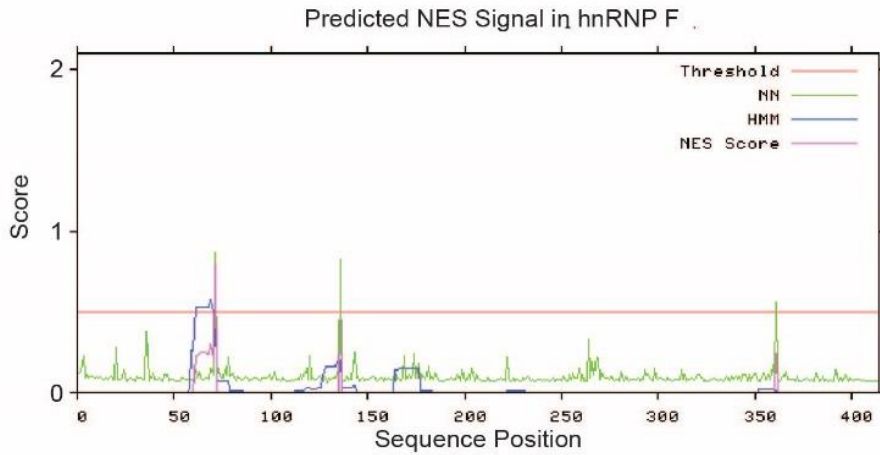
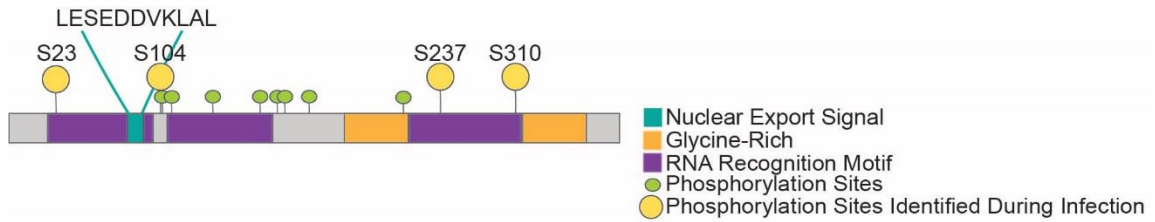


Figure 53. hnRNP F Protein Diagram

Schematic diagram of hnRNP F, highlighting the nuclear export signal (blue), three RNA Recognition Motifs (purple), and Glycine-Rich regions shown in orange. Protein diagram of hnRNP F indicating location of phosphorylation sites identified by SILAC/mass spectrometry (Penn et al., 2018) with nuclear localization signal shown in blue, RNA-recognition motifs (RRM) shown in purple, and Glycine-Rich regions shown in orange. Nuclear Export Signal identified using NetNES 1.1.

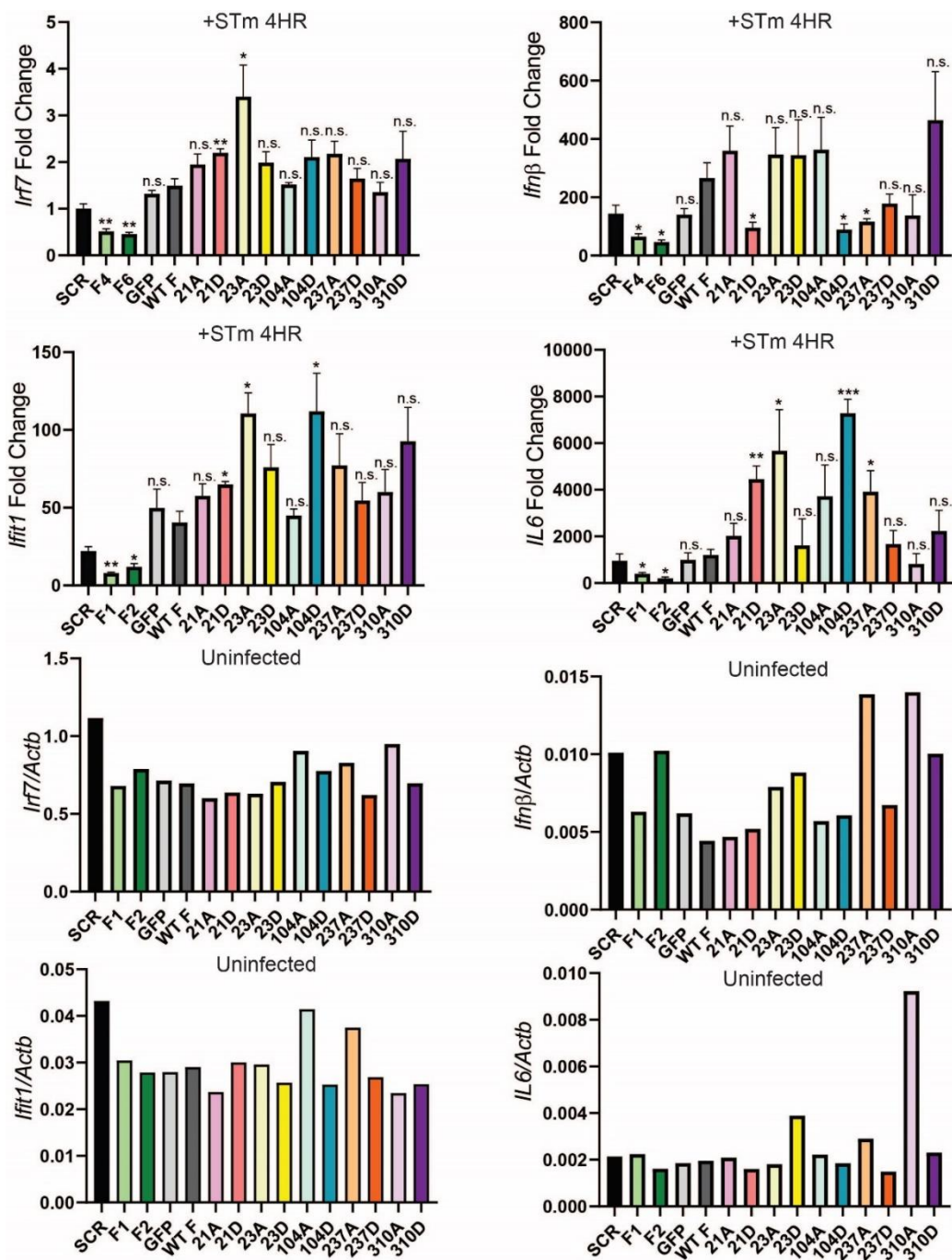


Figure 54. Phosphorylation of hnRNP F at Several Serines Controls Its Ability to Regulate Expression of *Ifnb1* and ISGs

qRT-PCR of Fold Induction Relative to FL-GFP of *Irf7*, *Ifnb1*, *Ifit1*, and *IL6* in WT FL-hnRNP F and phoshomutants in macrophages infected with *Salmonella* for 4h.

qRT-PCR of relative gene expression of *Irf7*, *Ifnb1*, *Ifit1*, and *IL6* in WT FL-hnRNP F and phoshomutants in resting macrophages.

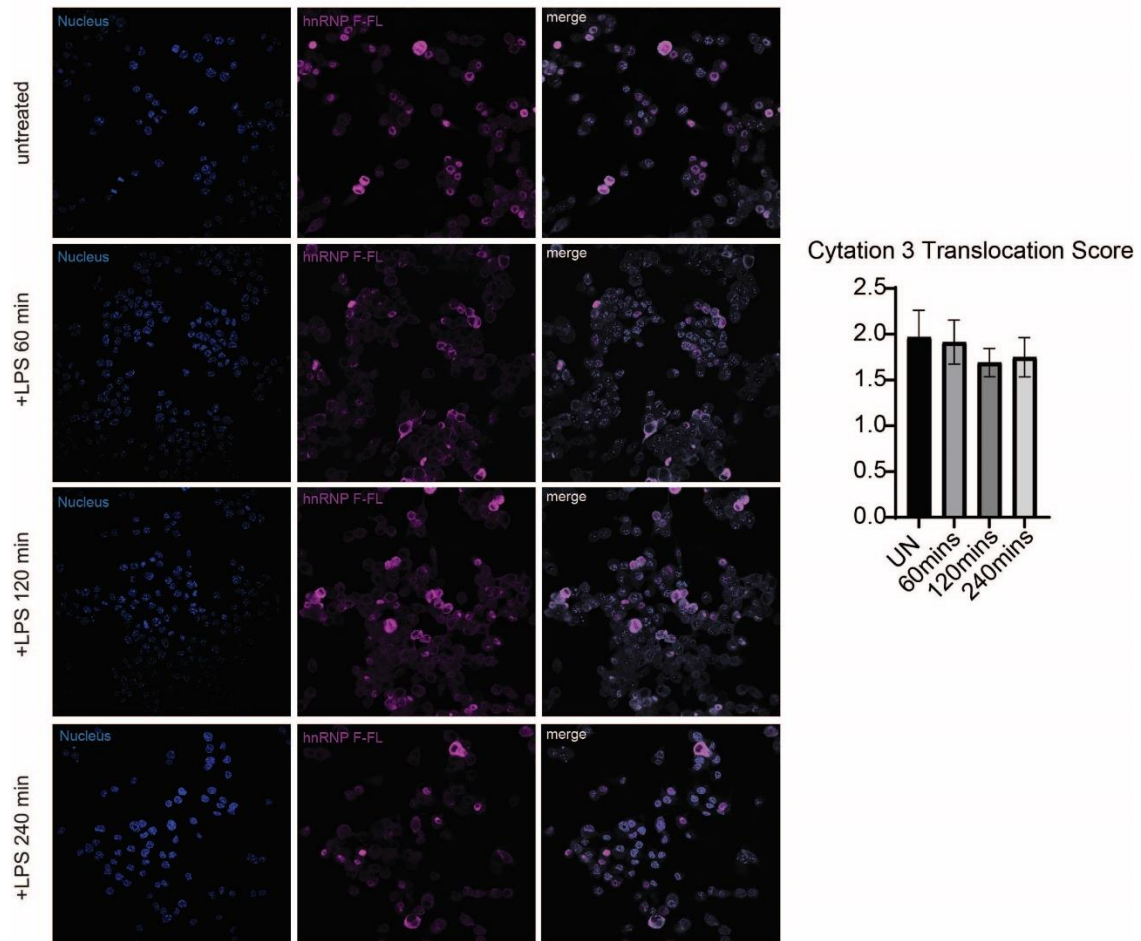


Figure 55. hnRNP F is Found in Nuclear and Cytoplasmic Compartments Upon LPS Treatment

Immunofluorescence of RAW 264.7 cells stably expressing FL-hnRNP F treated with LPS for the respective time points. Purple, FL-hnRNP F; blue, DAPI. Using Cytation 3 Software, cellular compartments of the cytoplasm and nucleus were quantified for translocation of hnRNP F.

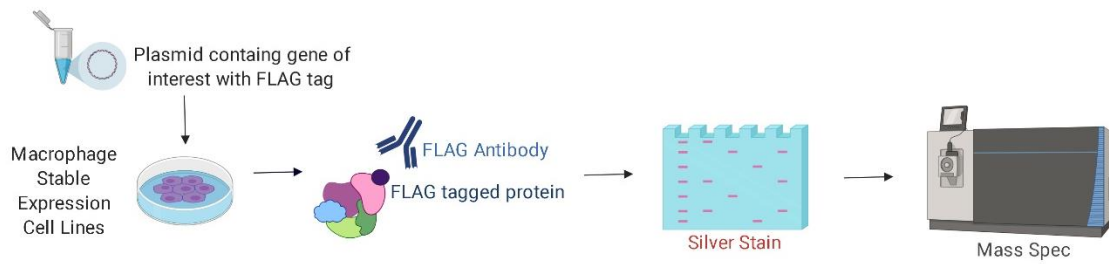


Figure 56. Immunoprecipitation with Mass Spectrometry Experimental Design

Schematic of approach for immunoprecipitation and mass spectrometry (IP-MS)

identification of hnRNP F binding partners in macrophages.

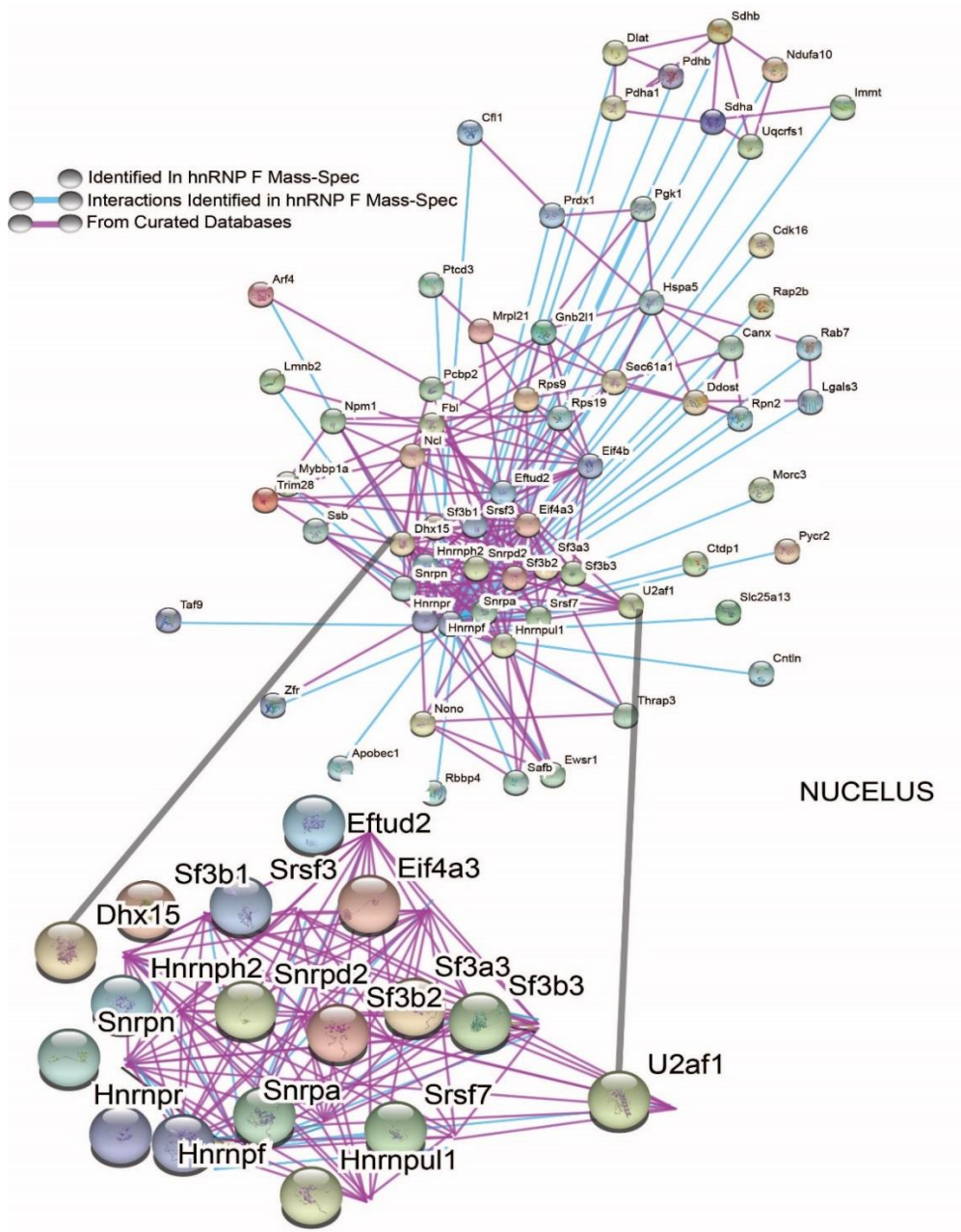


Figure 57. hnRNP F Interacts with Many Nuclear Splicing Proteins

Proteins identified by Nuclear IP-LC/MS with hnRNP F are represented by circles. Data was overlapped with STRING Databases for known interactions.

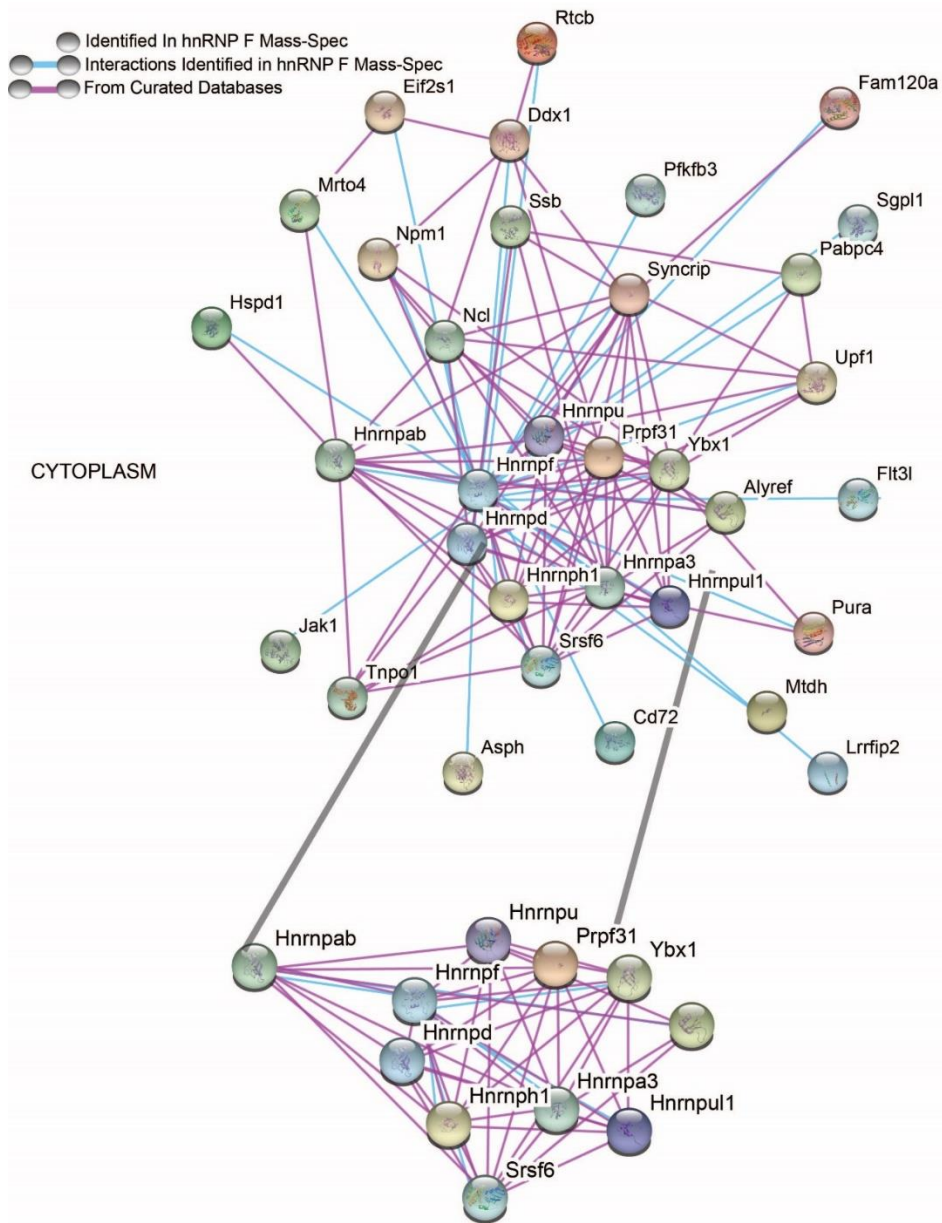


Figure 58. hnRNP F Interacts with Other hnRNPs in Cytoplasm Fractions

Proteins identified by Nuclear IP-LC/MS with hnRNP F are represented by circles. Data was overlapped with STRING Databases for known interactions.

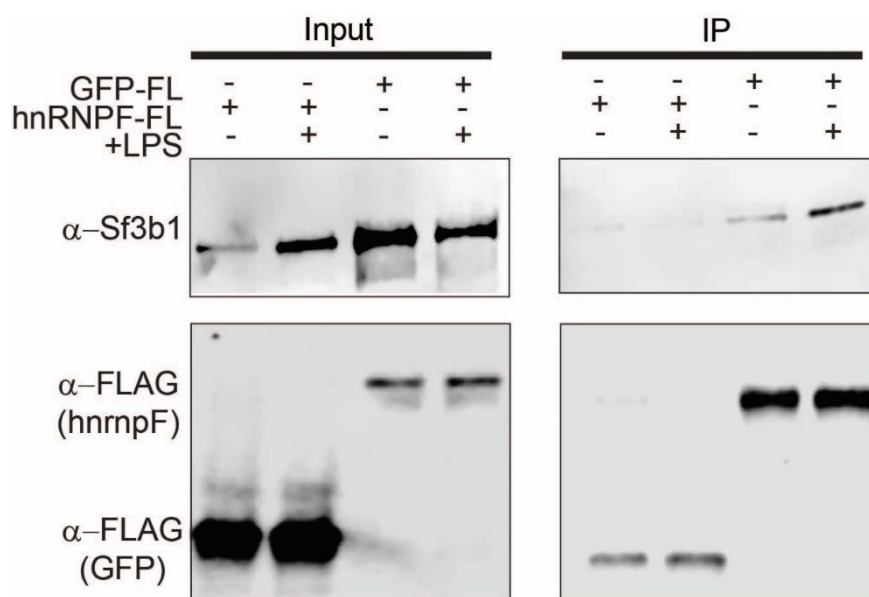


Figure 59. hnRNP F Interacts with SF3B1 In Resting and LPS-treated Cells

Nuclear immunoprecipitation of 3xFLAG-hnRNP F stably expression RAW 264.7 cells. Nuclear lysates were probed for endogenous SF3B1.

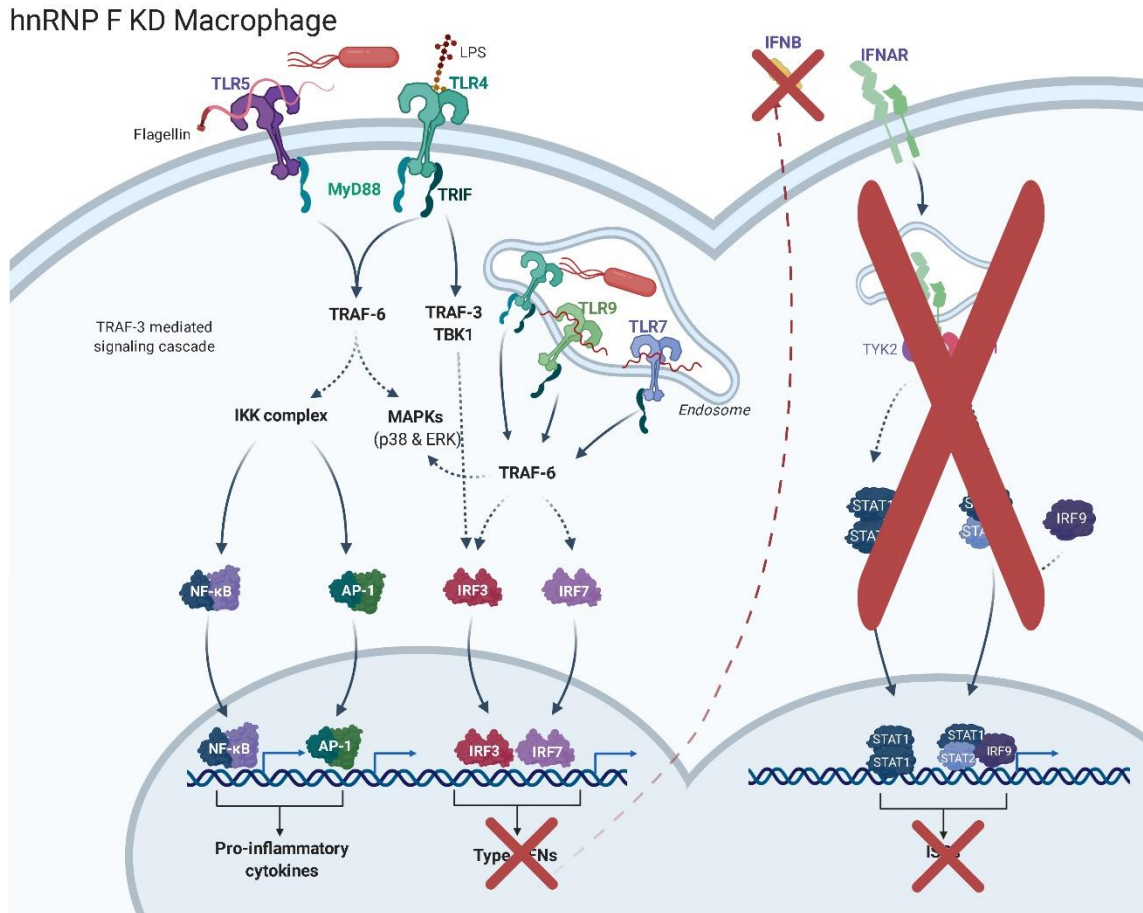


Figure 60. Proposed model of hnRNP F Regulating Type I Interferon Production Leading to Decreased ISG Expression

hnRNP F regulates several factors required to activate IFNβ expression. This decrease in IFNβ leads to an overall decrease in IFNAR signaling and STAT activation. This overall leads to a decrease in ISG expression. Model created using BioRender software.

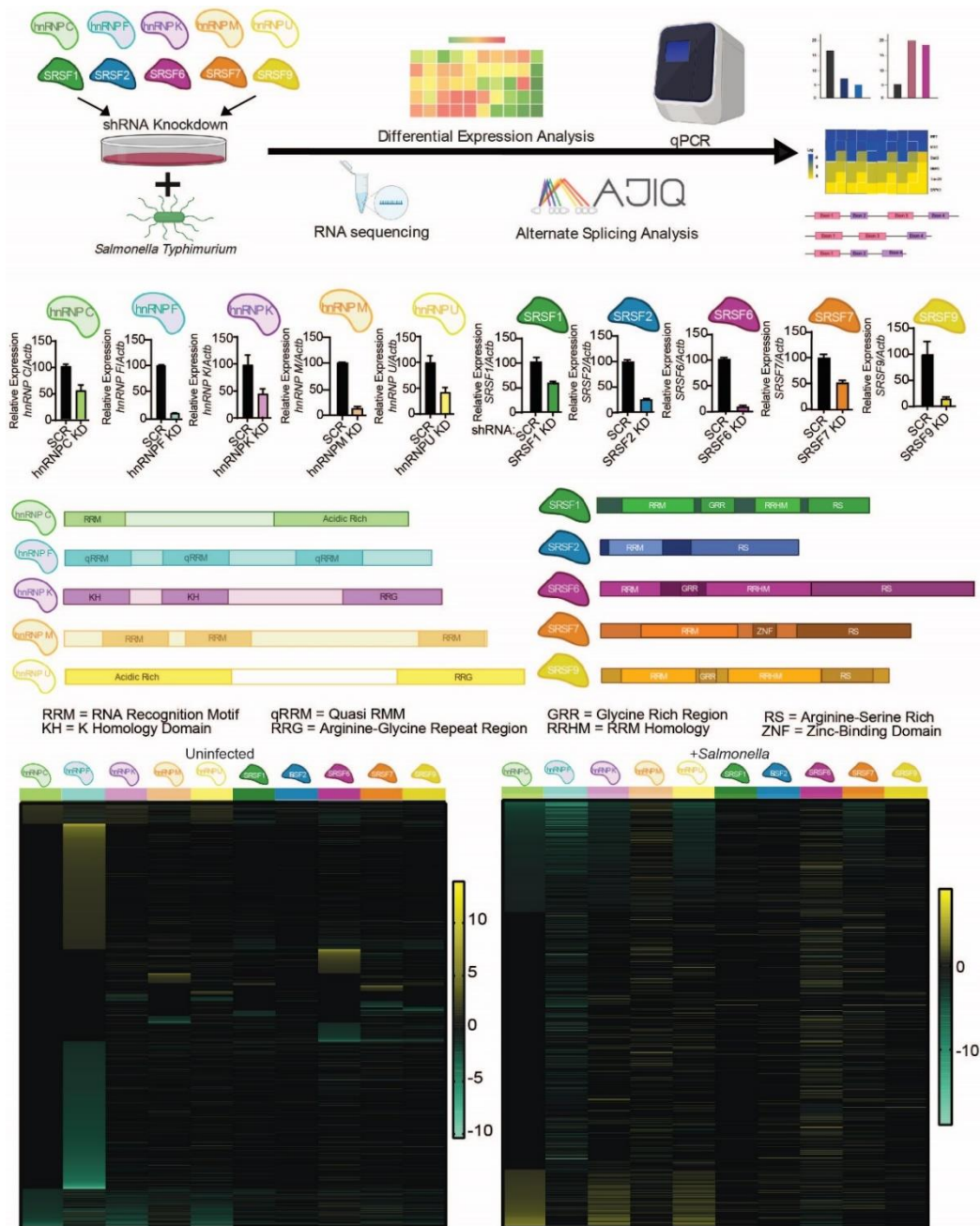


Figure 61. RNA-Seq Reveals Hundreds of hnRNP and SRSF-dependent Gene Expression In Resting and *Salmonella*-Infected Macrophages

qRT-PCR of repective hnRNP and SRSF knockdowns in RAW 264.7 macrophages. Values are mean (SD) representative of 3 biological replicates. Protein diagrams of hnRNP and SRSF RBPS. Genes represented in Heatmaps were significantly differentially expressed ($p < 0.05$) in at least one knockdown cell line.

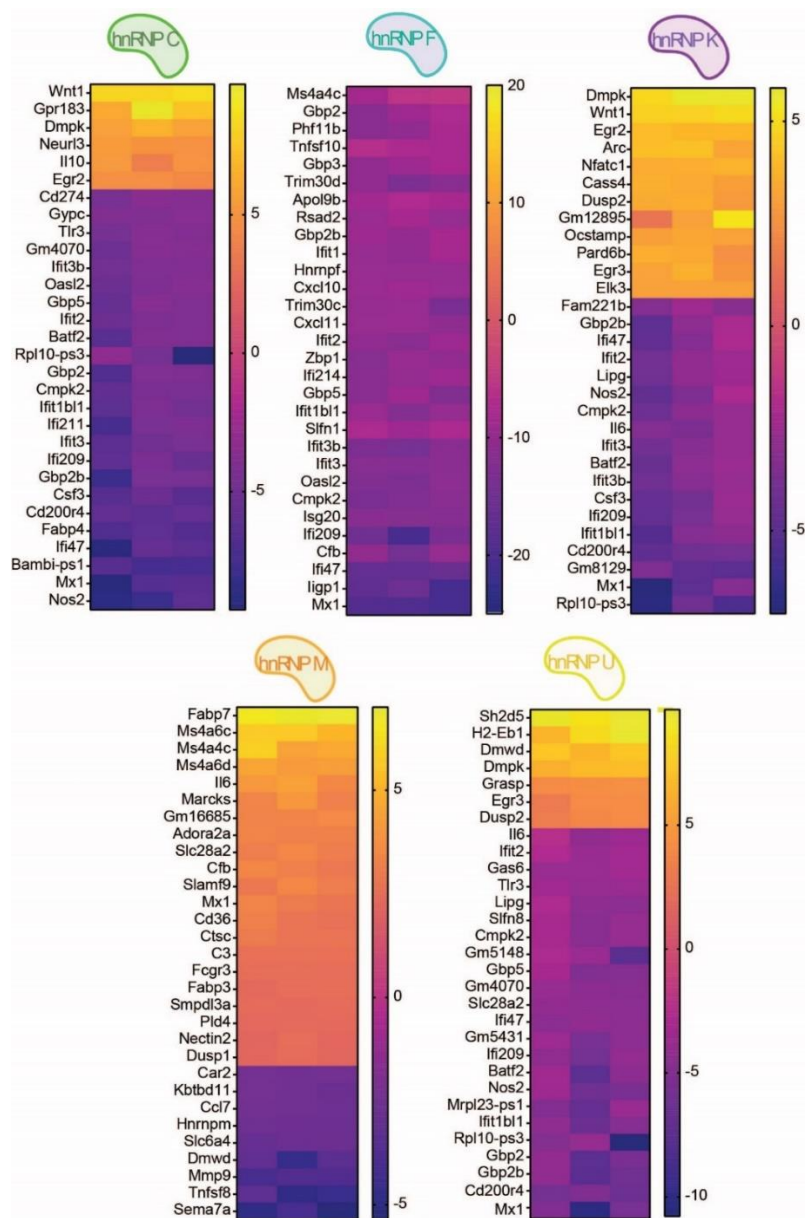


Figure 62. RNA-Seq Reveals hnRNP-dependent Gene Expression In *Salmonella*-Infected Macrophages

Genes represented in Heatmaps were the top 30 significantly differentially expressed ($p < 0.05$) in at least one knockdown cell line.

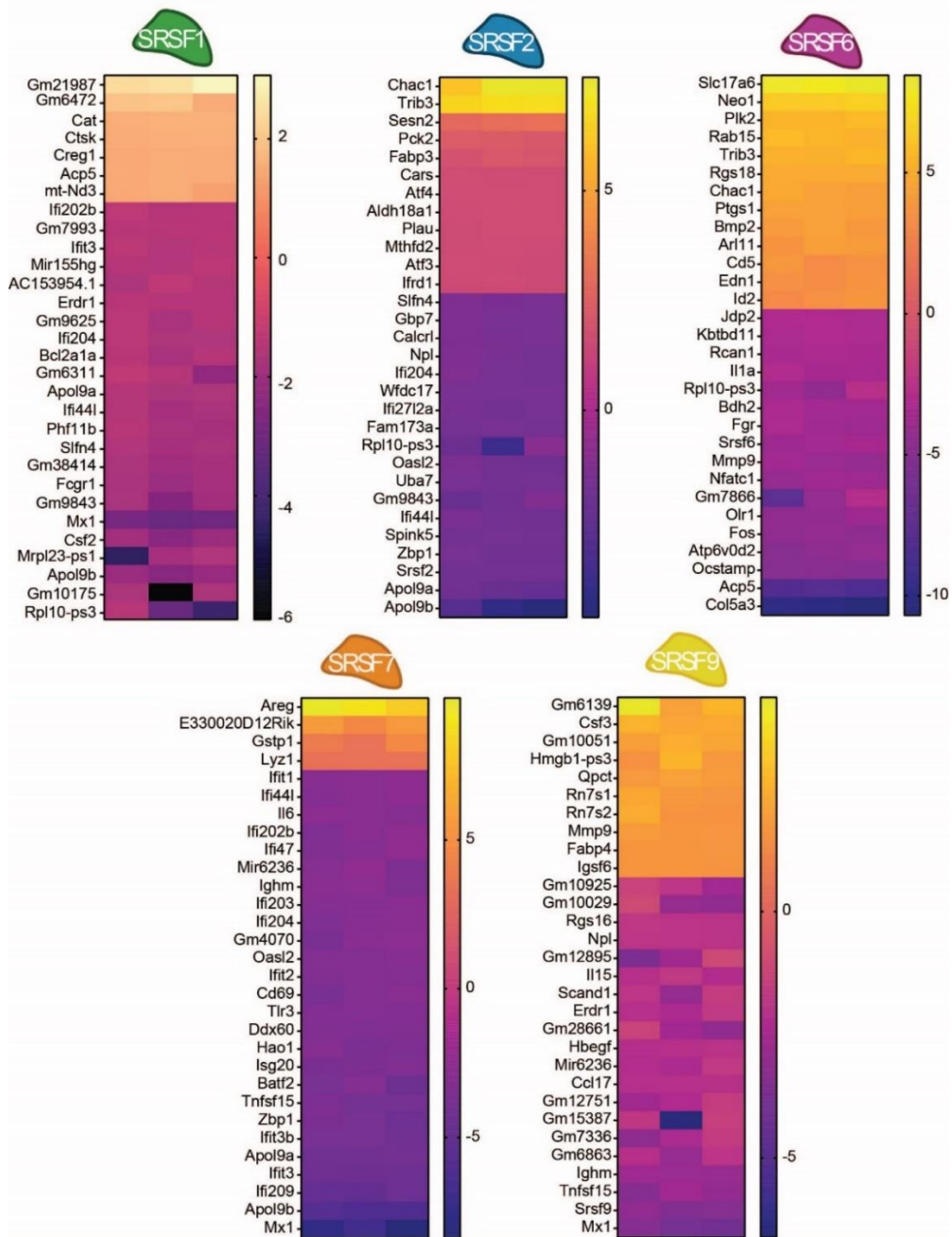


Figure 63. RNA-Seq Reveals SRSF-dependent Gene Expression In *Salmonella*-Infected Macrophages

Genes represented in Heatmaps were the top 30 significantly differentially expressed ($p < 0.05$) in at least one knockdown cell line.

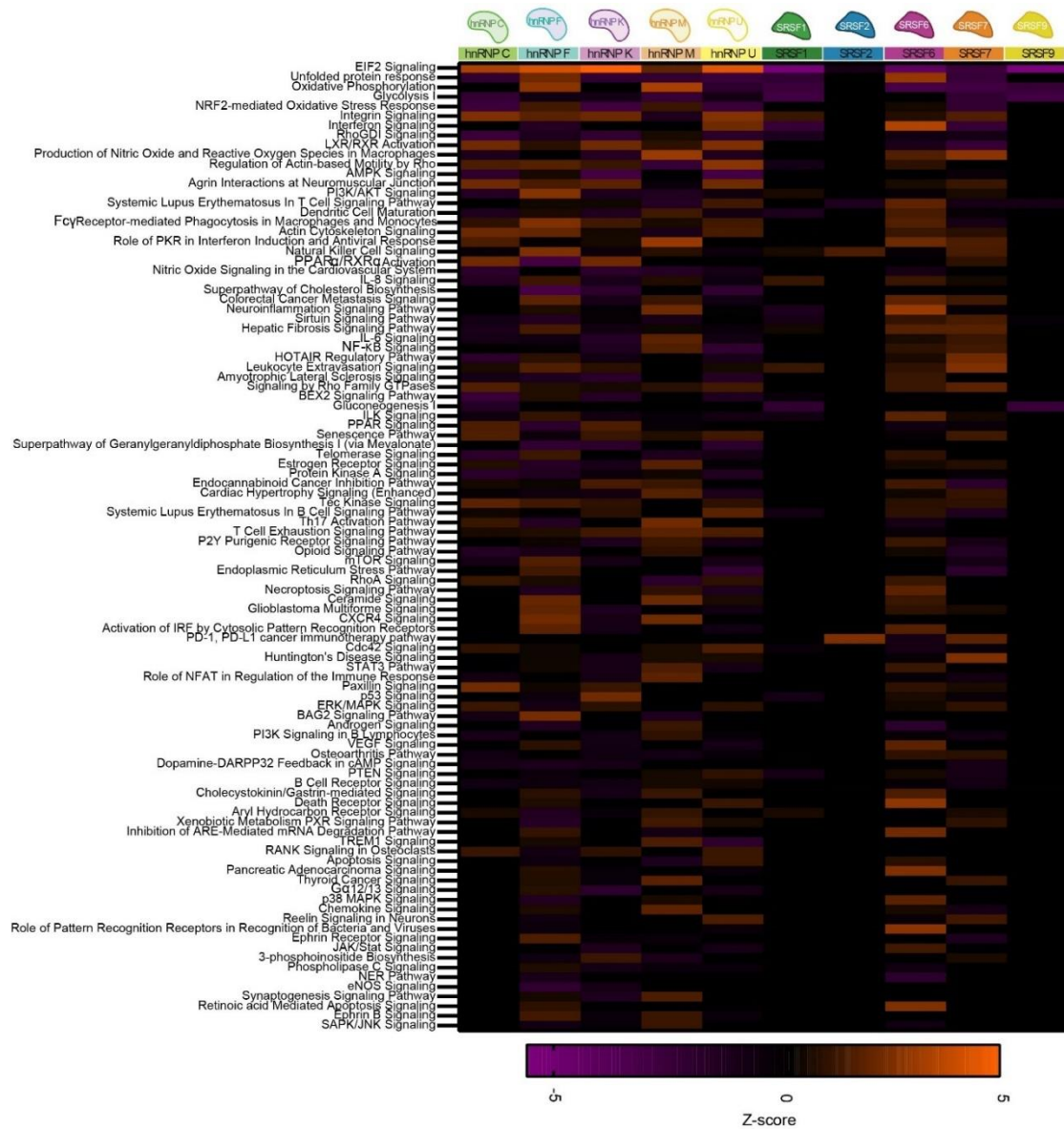


Figure 64. IPA Analysis of hnRNP and SRSF-dependent Gene Expression Shows Regulation of mRNA Translational in Resting Macrophages

Comparison Ingenuity Pathway Analysis of gene expression changes in uninfected hnRNP and SRSF knockdowns. Genes utilized in IPA were significantly differentially expressed ($p < 0.05$).

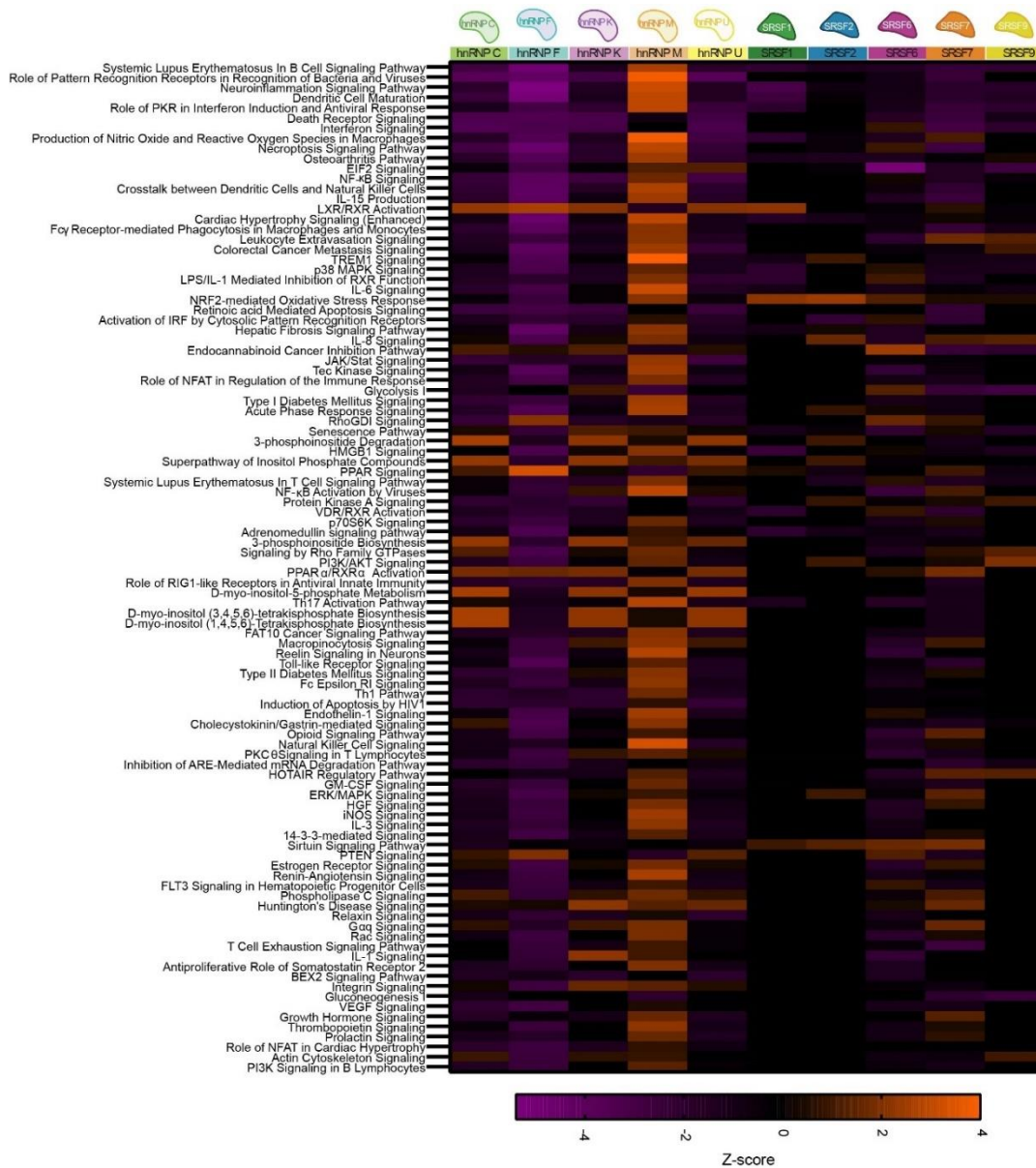


Figure 65. IPA Analysis of hnRNP and SRSF-dependent Gene Expression Shows Similar Regulation between hnRNP C, U, and K in *Salmonella*-Infected Macrophages

Comparison Ingenuity Pathway Analysis of gene expression changes in *Salmonella*-infected hnRNP and SRSF knockdowns. Genes utilized in IPA were significantly differentially expressed ($p < 0.05$).

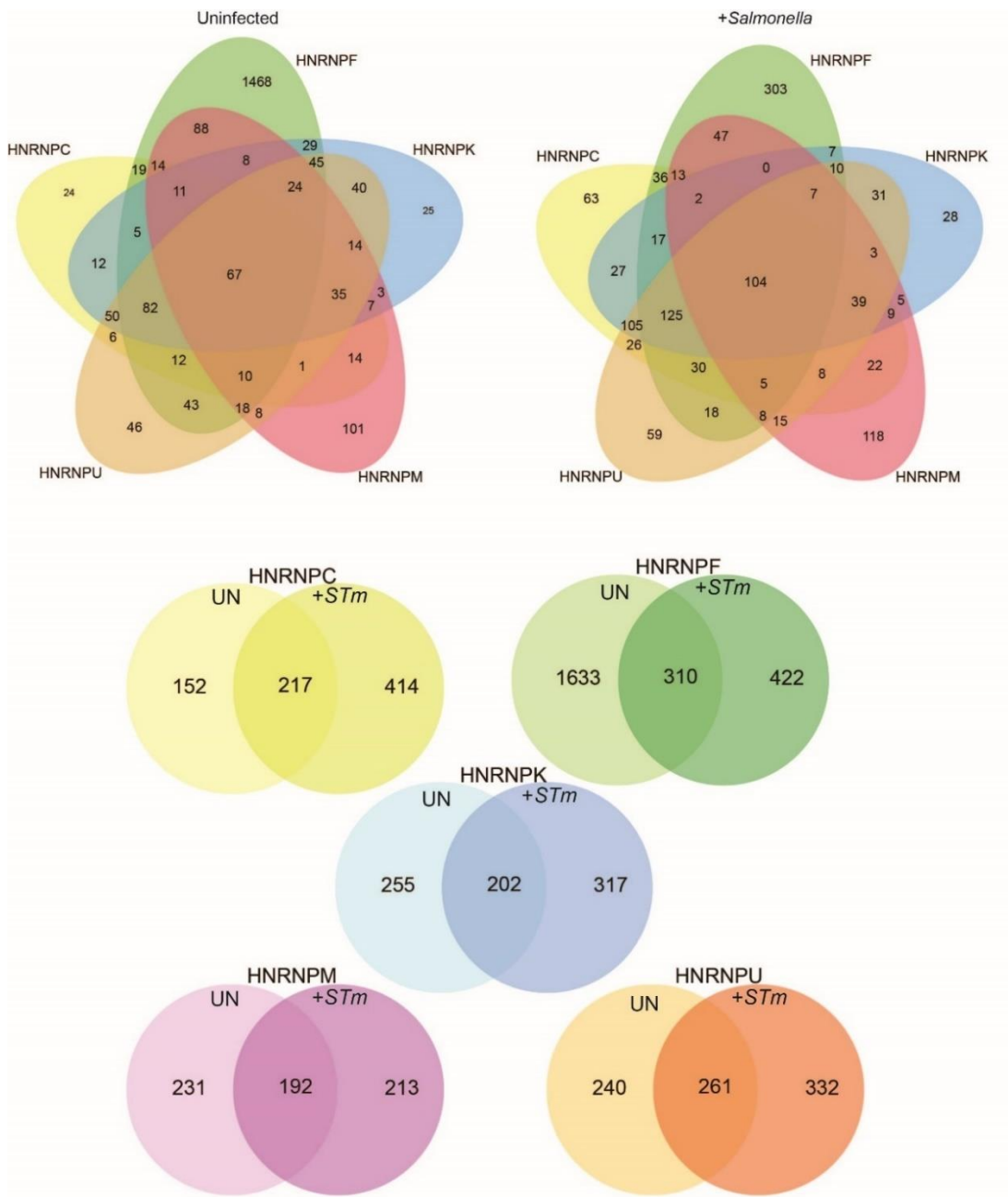


Figure 66. hnRNPs Co-regulate Gene Expression and Show Distinct Regulation

Occuring During Innate Immune Sensing

Venn diagrams illustrate diversification of hnRNP protein function in macrophages following *Salmonella* infection. Number in circles indicate differentially expressed genes ($p < 0.05$).

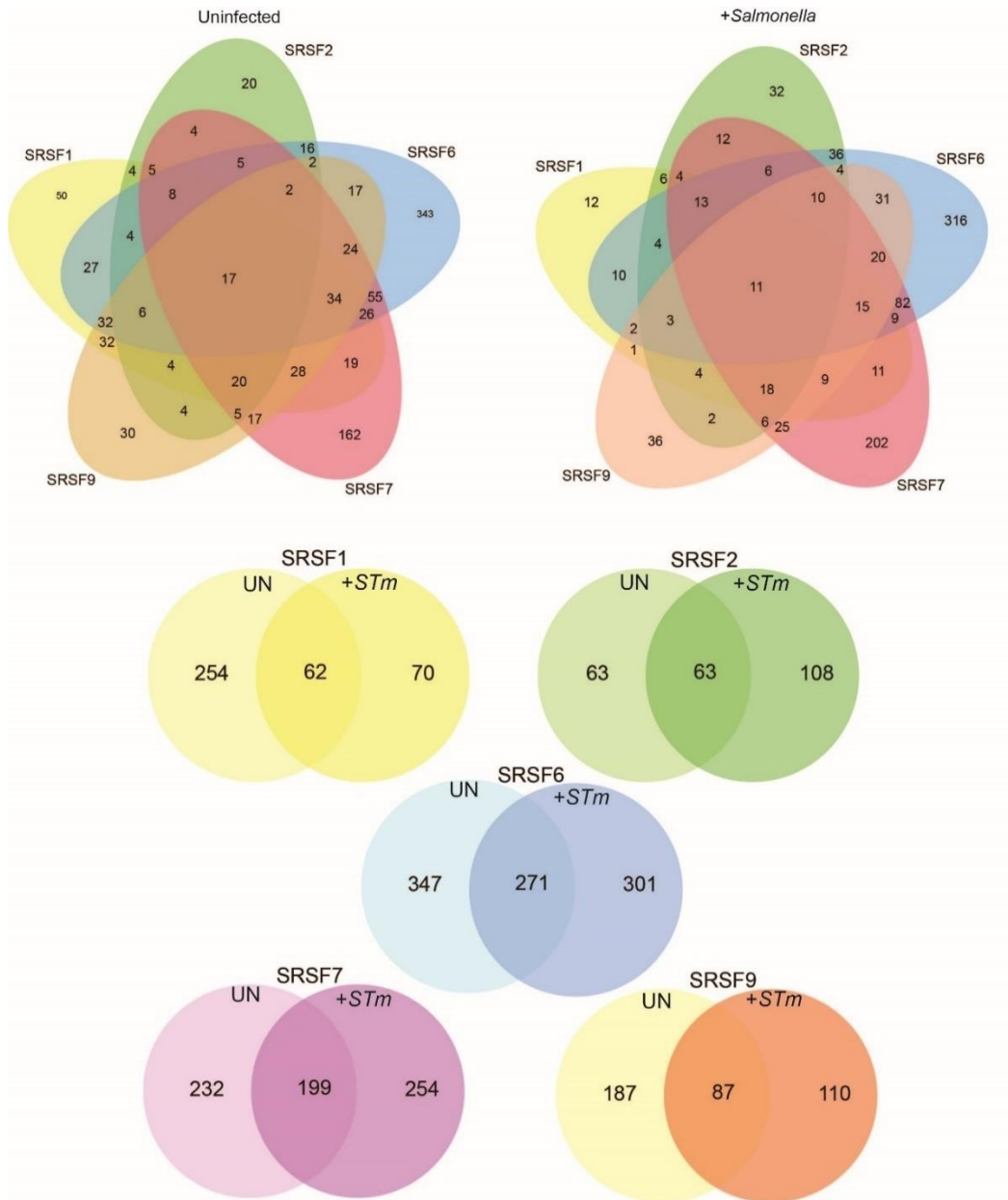


Figure 67. SRSFs Show Distinct Regulation Occuring During Innate Immune Sensing, But Not Co-Regulation of Gene Expression

Venn diagrams illustrate diversification of SRSF protein function in macrophages following *Salmonella* infection. Number in circles indicate differentially expressed genes ($p < 0.05$).

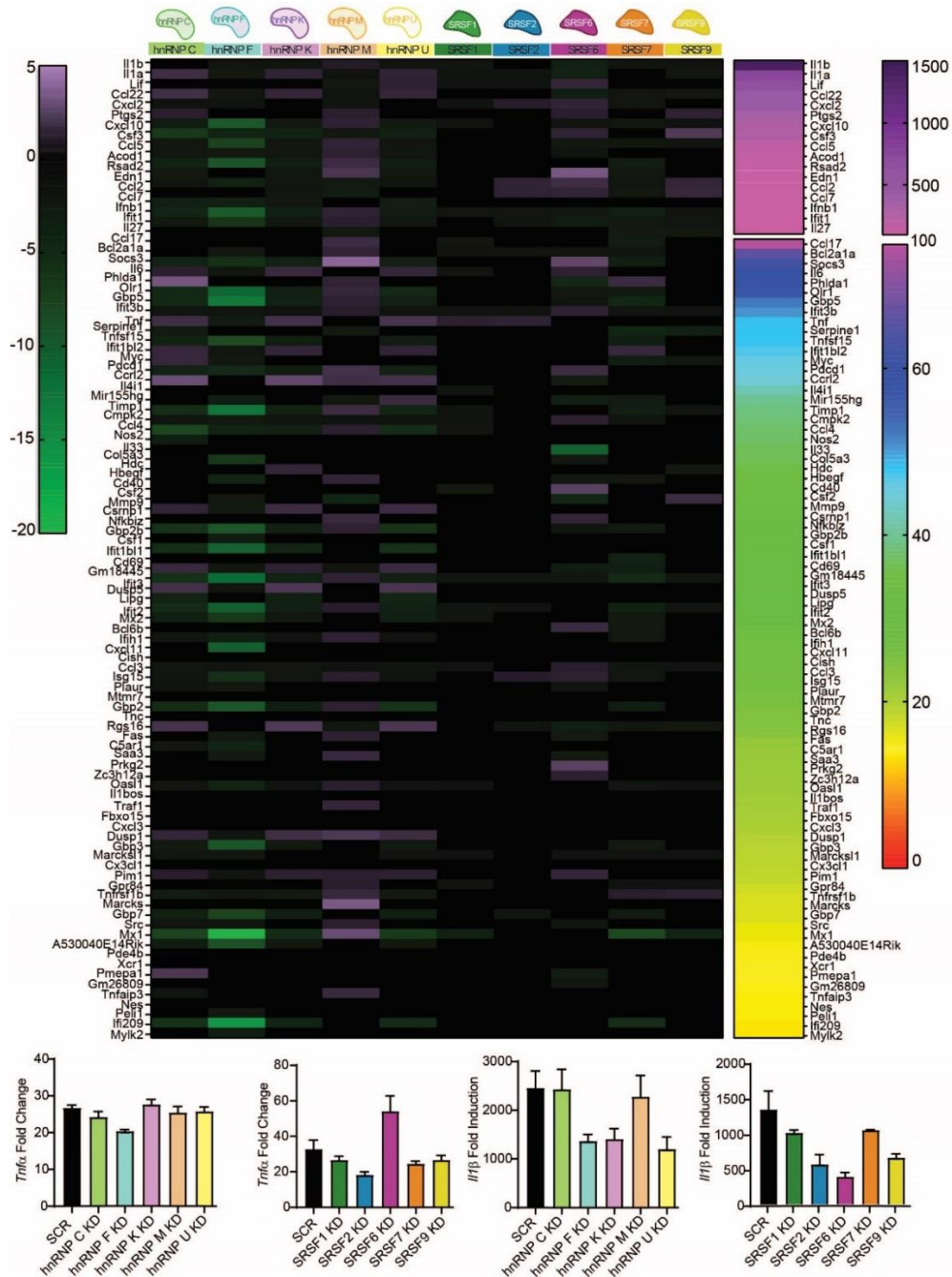


Figure 68. hnRNPs and SRSFs Regulate Specific Innate Immune Genes Upon *Salmonella*-Infection

Top 100 upregulated genes upon Salmonella infection are displayed. Genes represented in Heatmaps were significantly differentially expressed ($p < 0.05$) in at least one knockdown cell line.

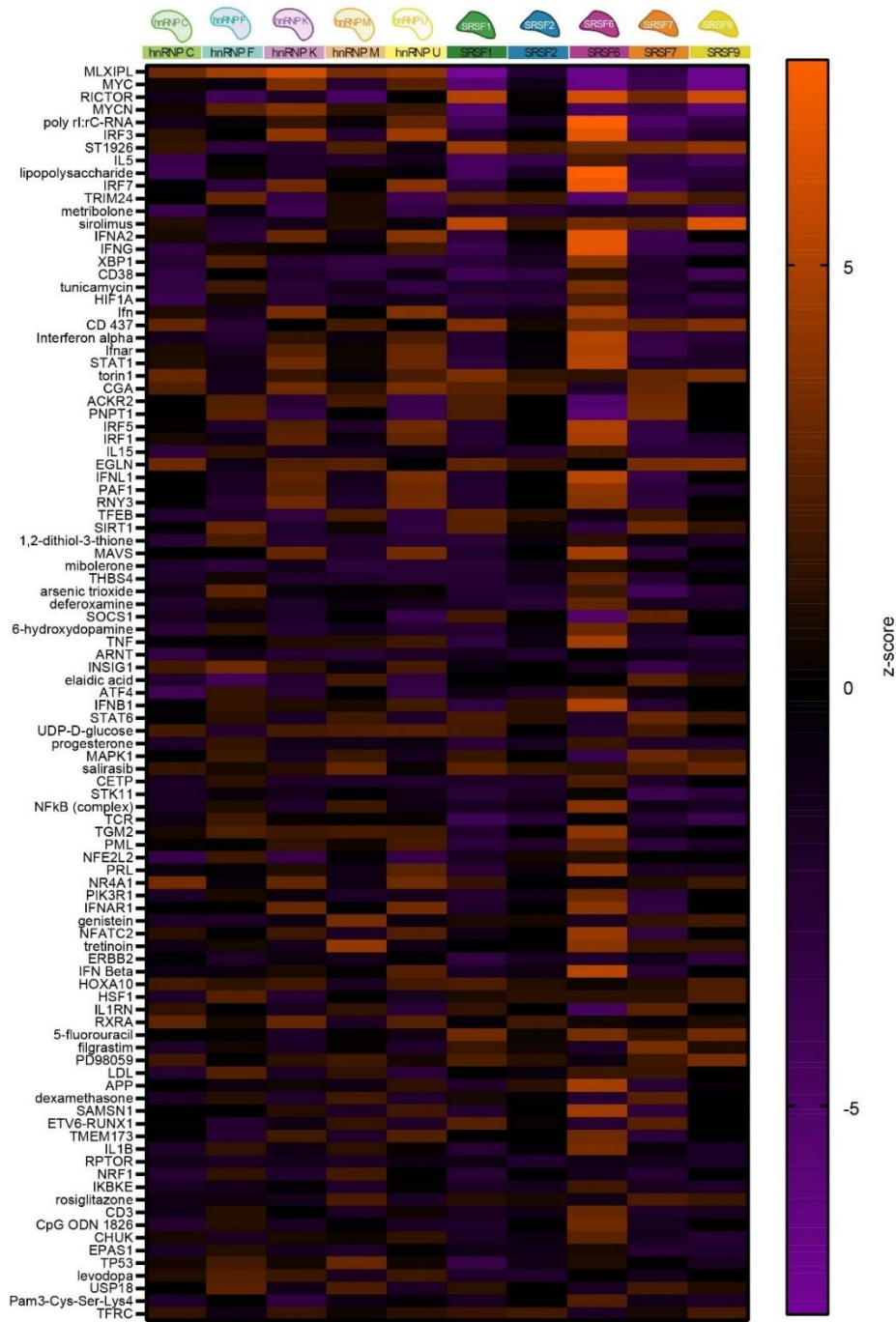


Figure 69. IPA Analysis of hnRNP and SRSF-dependent Gene Expression Shows Regulation of mRNA Translational in Resting Macrophages

Upstream Regulator Ingenuity Pathway Analysis of gene expression changes in uninfected hnRNP and SRSF knockdowns. Genes utilized in IPA were significantly differentially expressed ($p < 0.05$).

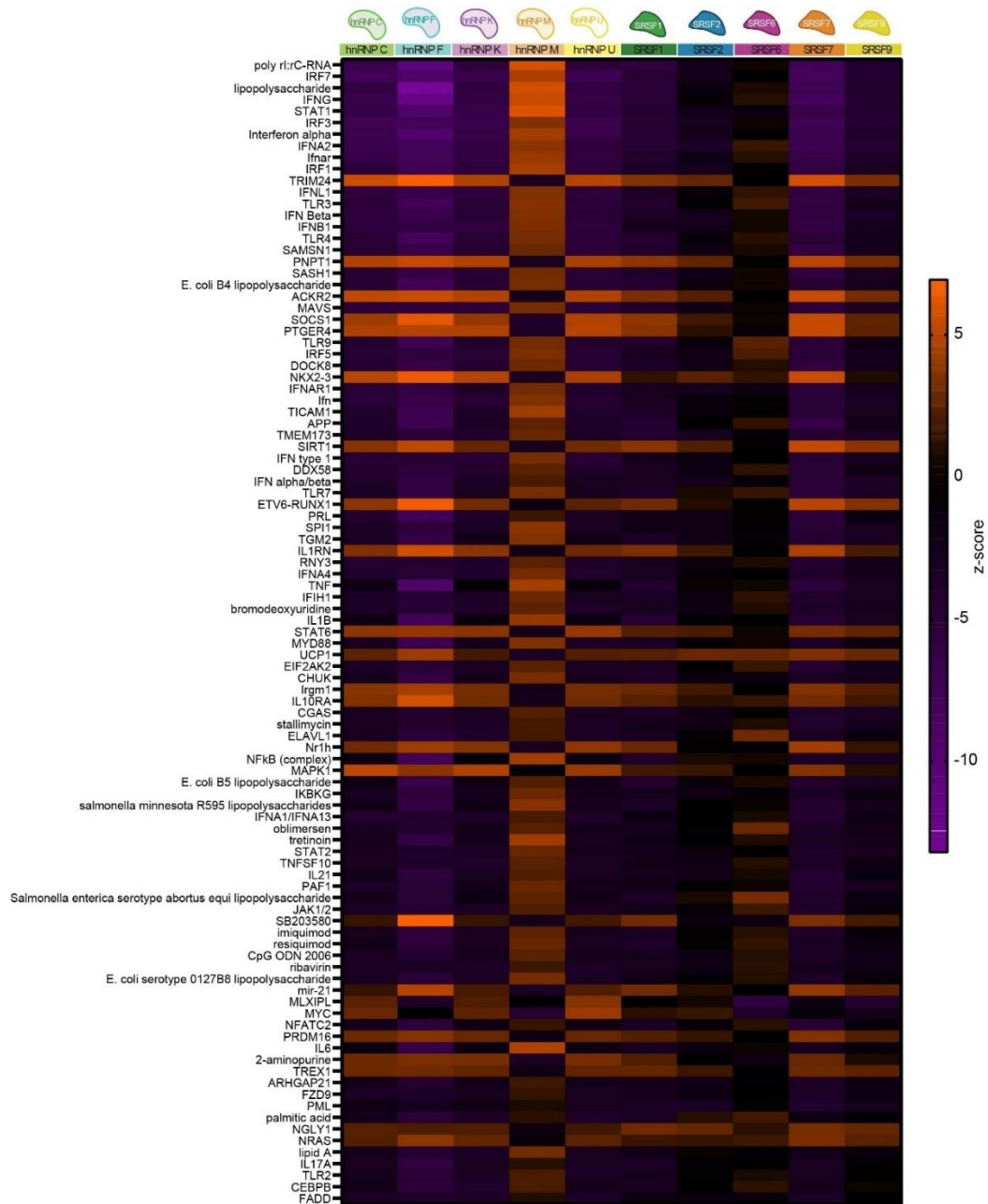


Figure 70. IPA Analysis of hnRNP and SRSF-dependent Gene Expression Shows Similar Regulation between hnRNP C, U, and K in *Salmonella*-Infected Macrophages

Upstream Regulator Ingenuity Pathway Analysis of gene expression changes in *Salmonella*-infected hnRNP and SRSF knockdowns. Genes utilized in IPA were significantly differentially expressed ($p < 0.05$).

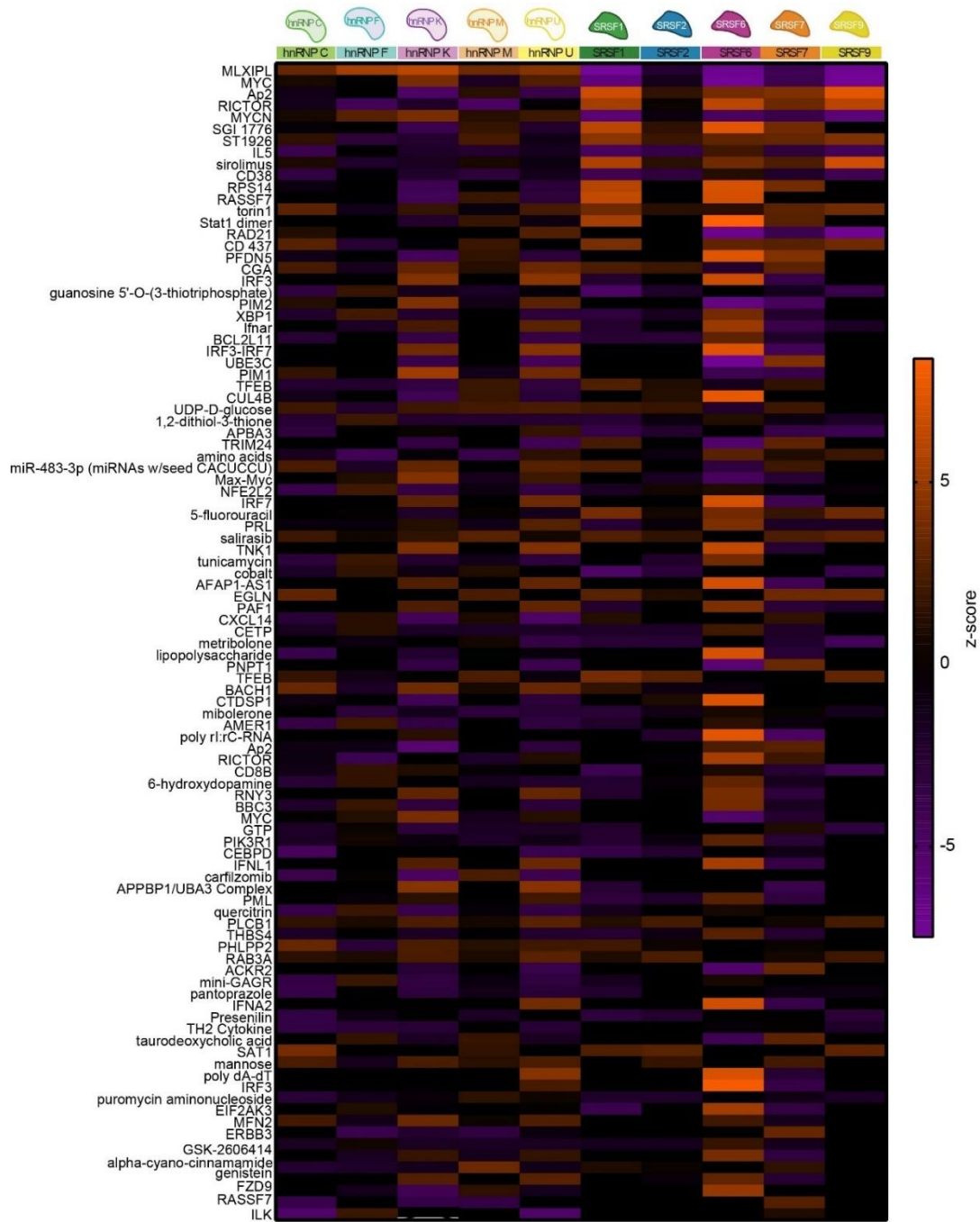


Figure 71. IPA Analysis of hnRNP and SRSF-dependent Gene Expression Shows Regulation of mRNA Translational in Resting Macrophages

Causal Ingenuity Pathway Analysis of gene expression changes in uninfected hnRNP and SRSF knockdowns. Genes utilized in IPA were significantly differentially expressed ($p < 0.05$).

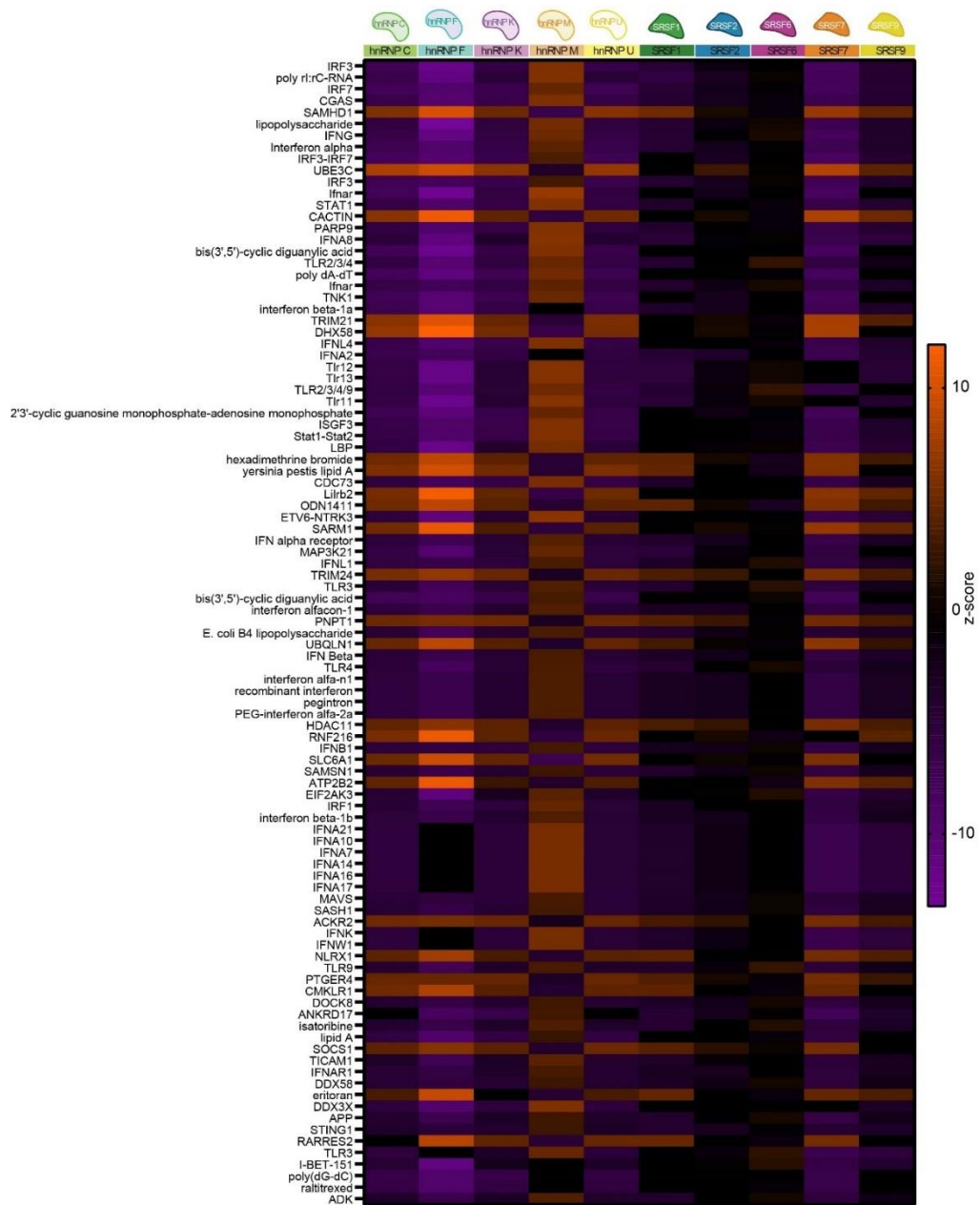


Figure 72. IPA Analysis of hnRNP and SRSF-dependent Gene Expression Shows Similar Regulation between hnRNP C, U, and K in *Salmonella*-Infected Macrophages

Causal Ingenuity Pathway Analysis of gene expression changes in *Salmonella*-infected hnRNP and SRSF knockdowns. Genes utilized in IPA were significantly differentially expressed ($p < 0.05$).

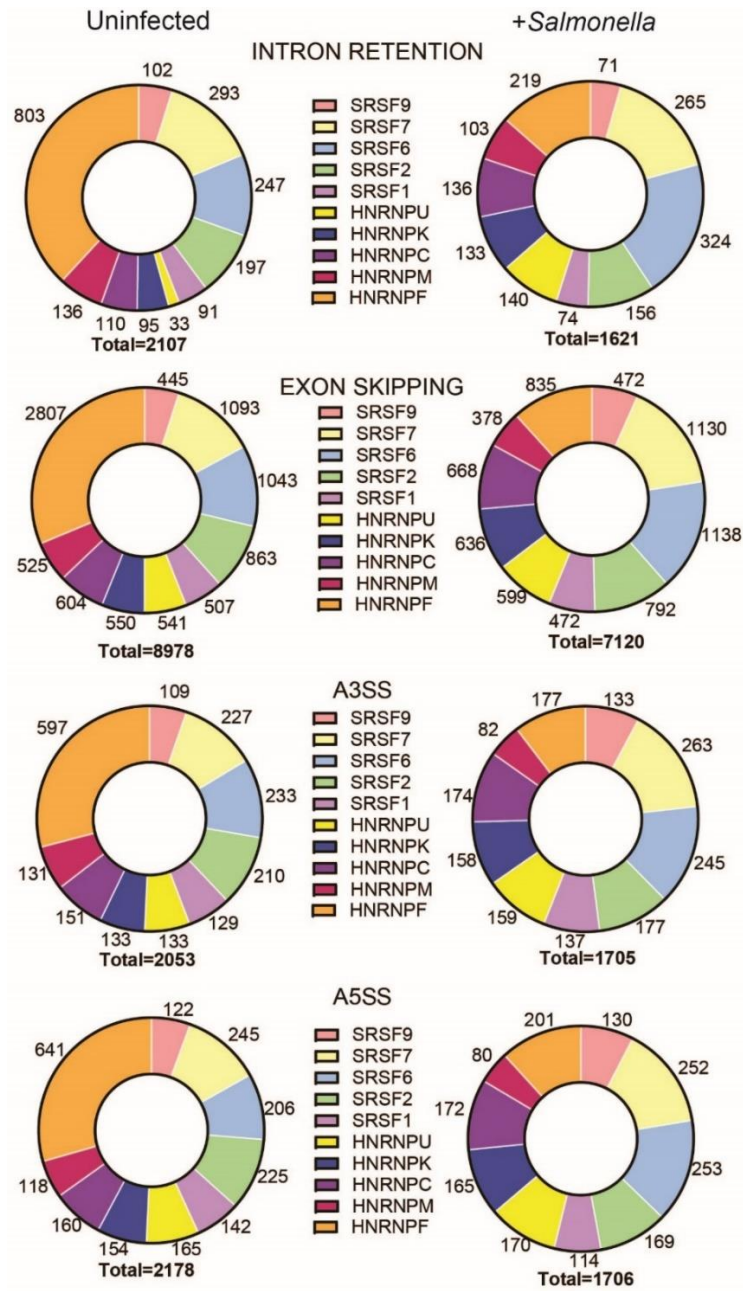


Figure 73. Thousands of Alternative Splicing Events are Regulated by hnRNPs and SRSFs in Macrophages

Categorization of alternative splicing events identified via MAJIQ in uninfected SCR vs. respective hnRNP and SRSF knockdown samples and in *Salmonella*-infected SCR vs. respective hnRNP and SRSF knockdown samples.

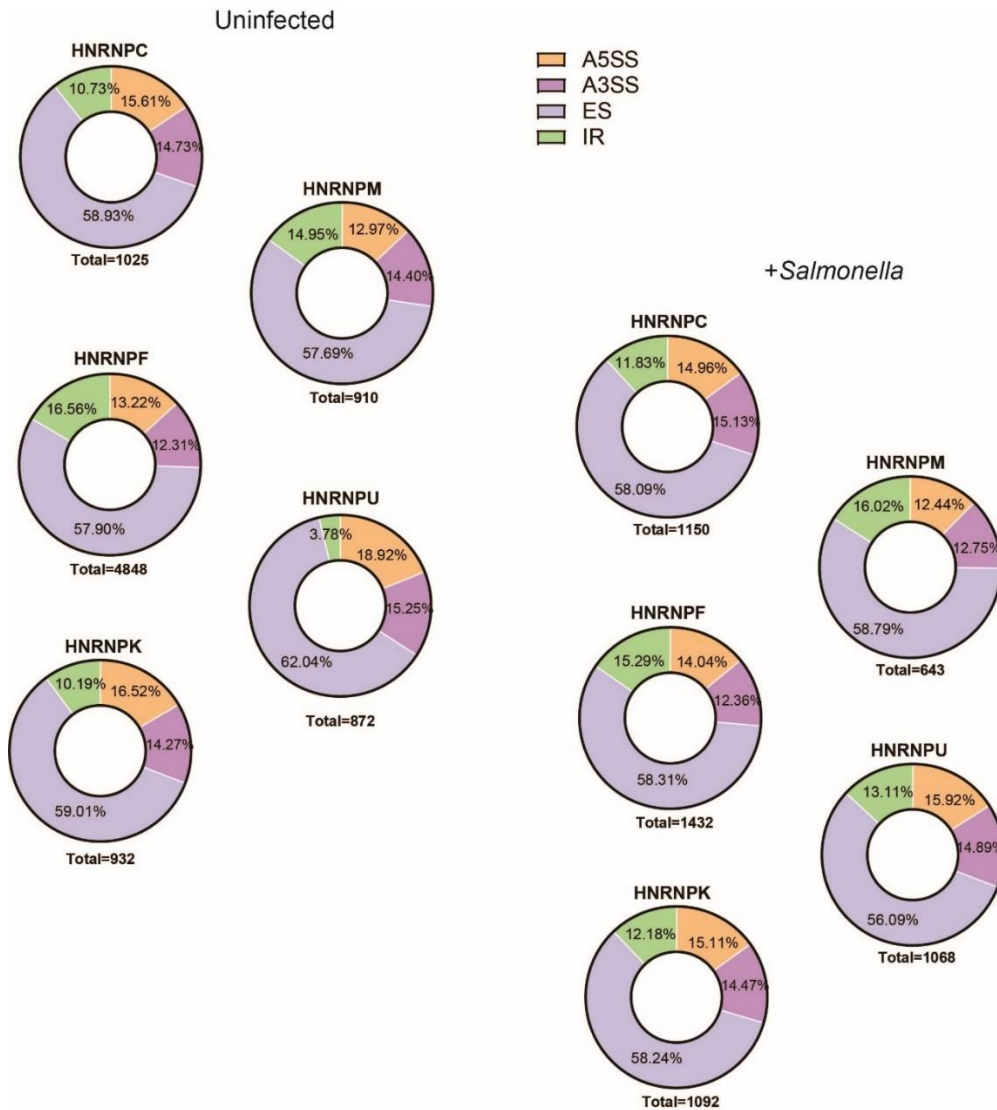


Figure 74. Thousands of hnRNP-dependent Alternative Splicing Events Identified in Macrophages

Categorization of alternative splicing events identified via MAJIQ in uninfected SCR vs. respective hnRNP knockdown samples and in *Salmonella*-infected SCR vs. respective hnRNP knockdown samples.

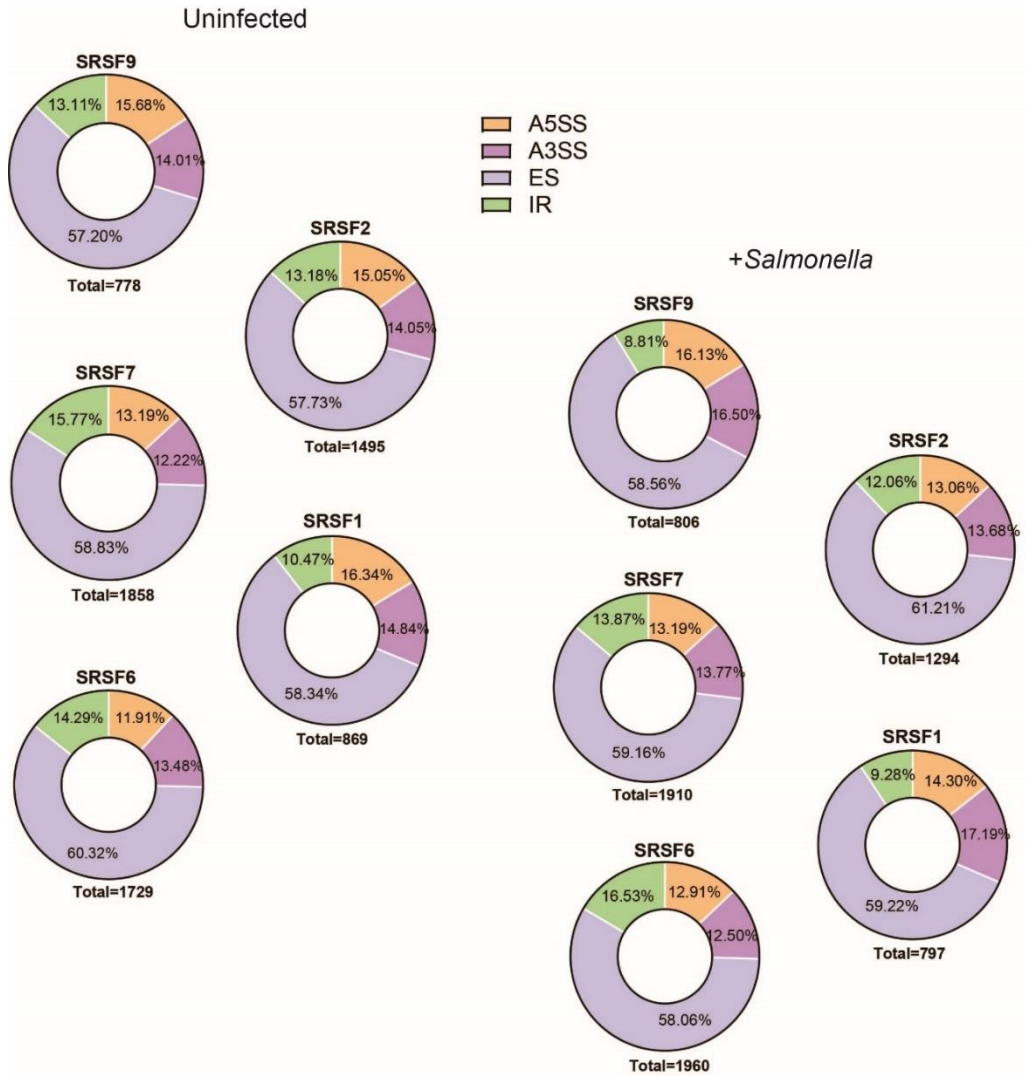


Figure 75. Thousands of SRSF-dependent Alternative Splicing Events Identified in Macrophages

Categorization of alternative splicing events identified via MAJIQ in uninfected SCR vs. respective SRSF knockdown samples and in *Salmonella*-infected SCR vs. respective SRSF knockdown samples.

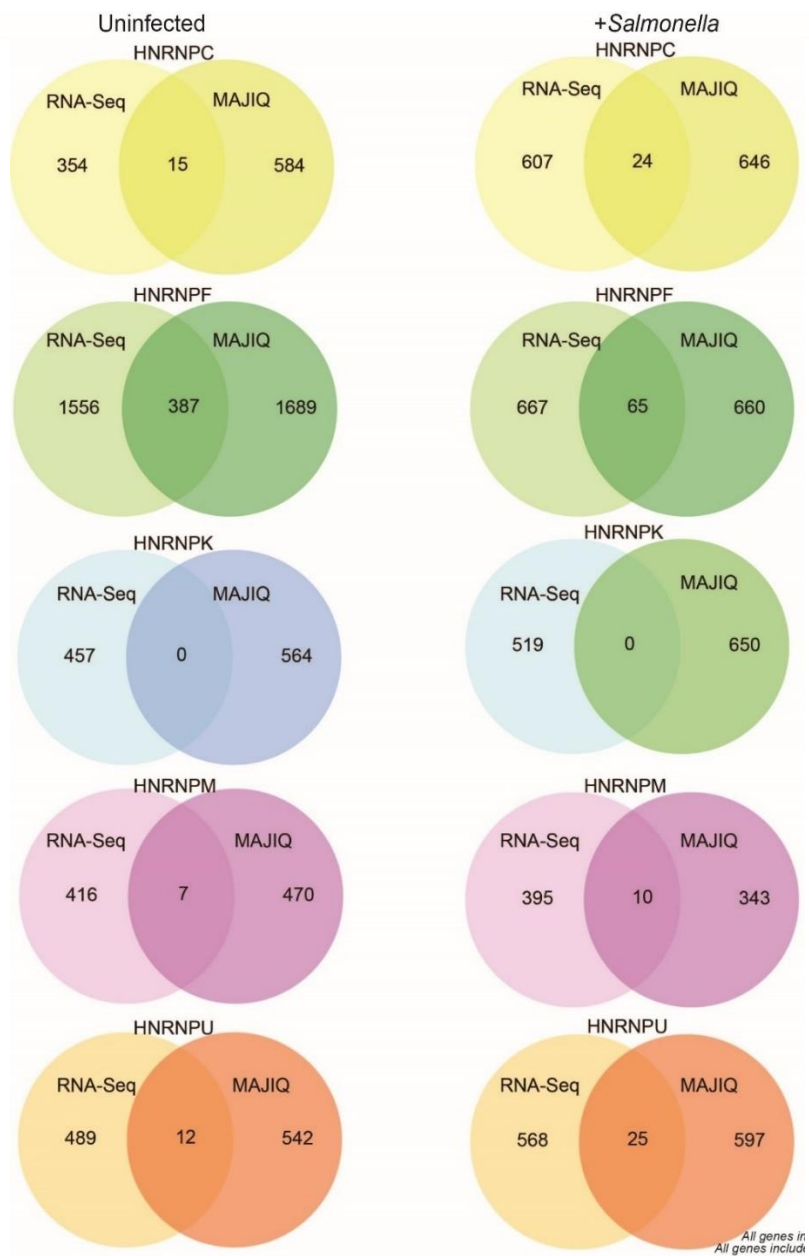


Figure 76. Gene Expression Changes Do Not Correlate To Splicing Regulation

Genes whose splicing and expression are regulated by loss of individual hnRNPs.

UN = uninfected macrophages; +STm = 4h *Salmonella*-infection.

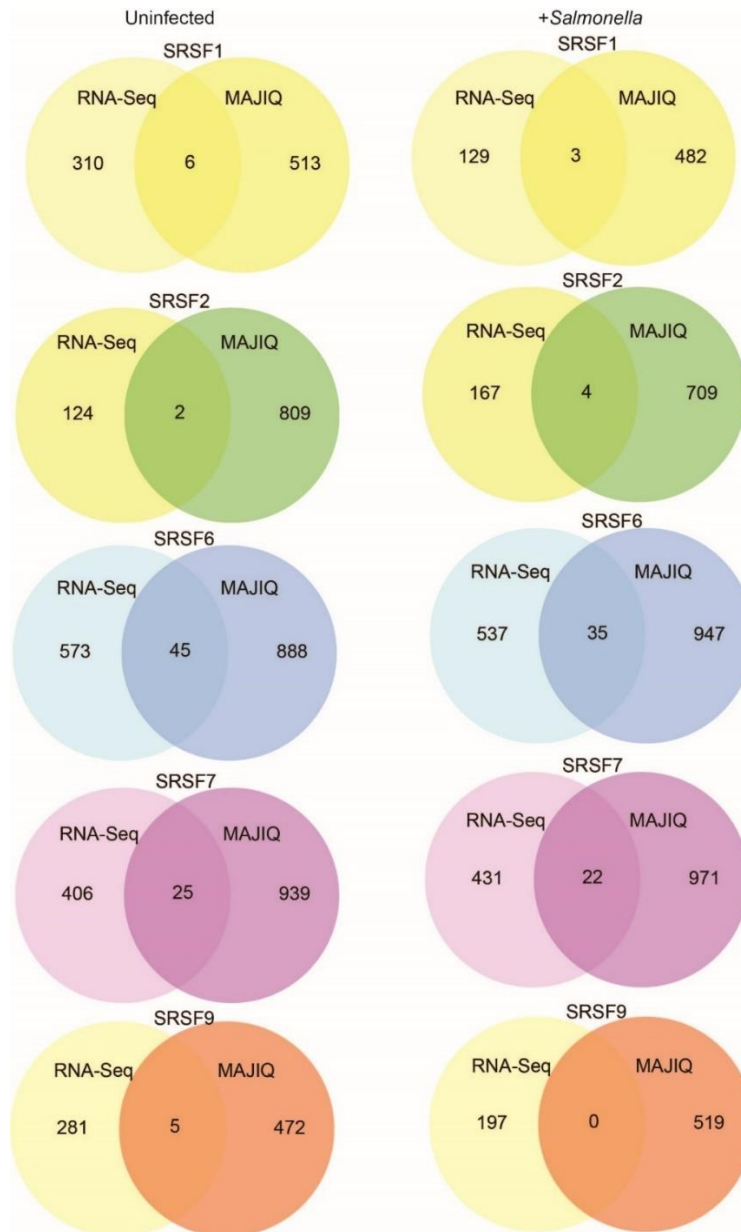


Figure 77. Gene Expression Changes Do Not Correlate To Splicing Regulation

Genes whose splicing and expression are impacted by loss of individual SRSFs.

UN = uninfected macrophages; +STm = 4h *Salmonella*-infection.

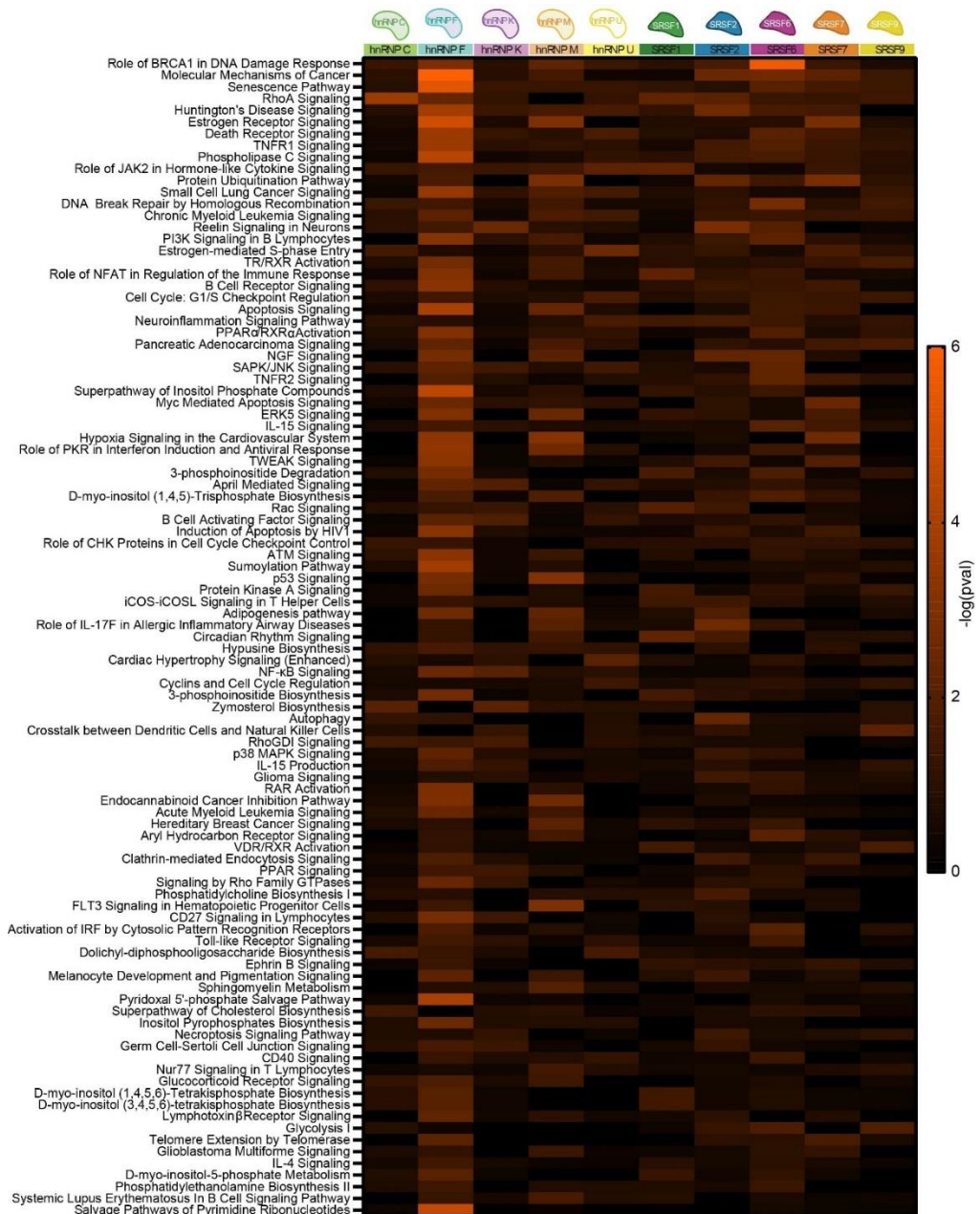


Figure 78. IPA Analysis of hnRNP and SRSF-dependent Splicing Shows

Regulation of Cancer in Resting Macrophages

Upstream Regulator Ingenuity Pathway Analysis of MAJIQ splicing changes in uninfected hnRNP and SRSF knockdowns. Genes utilized in IPA were significantly differentially expressed ($p < 0.05$).

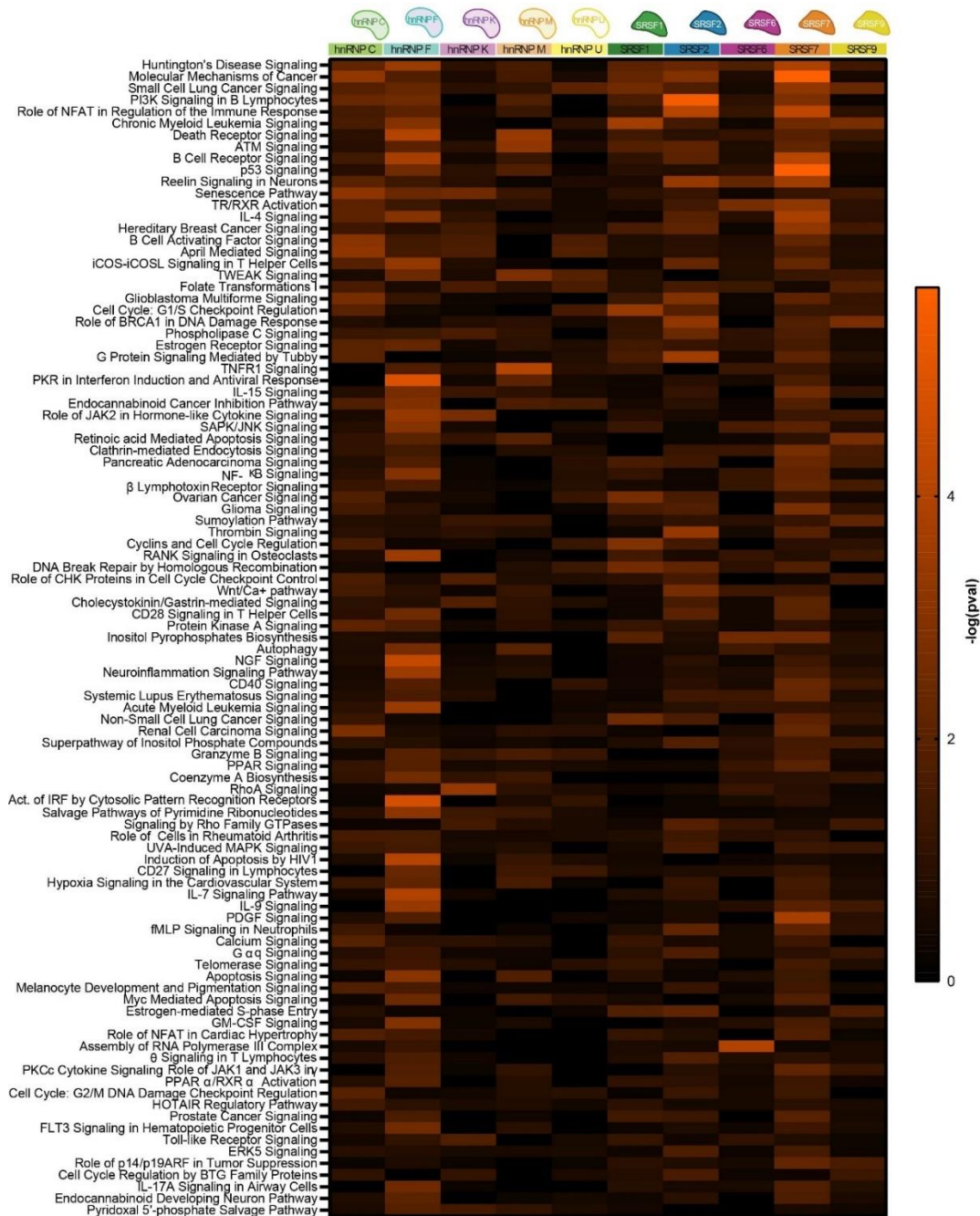


Figure 79. IPA Analysis of hnRNP and SRSF-dependent Splicing Shows in *Salmonella*-Infected Macrophages

Upstream Regulator Ingenuity Pathway Analysis of MAJIQ splicing changes in *Salmonella*-infected hnRNP and SRSF knockdowns. Genes utilized in IPA were significantly differentially expressed ($p < 0.05$).

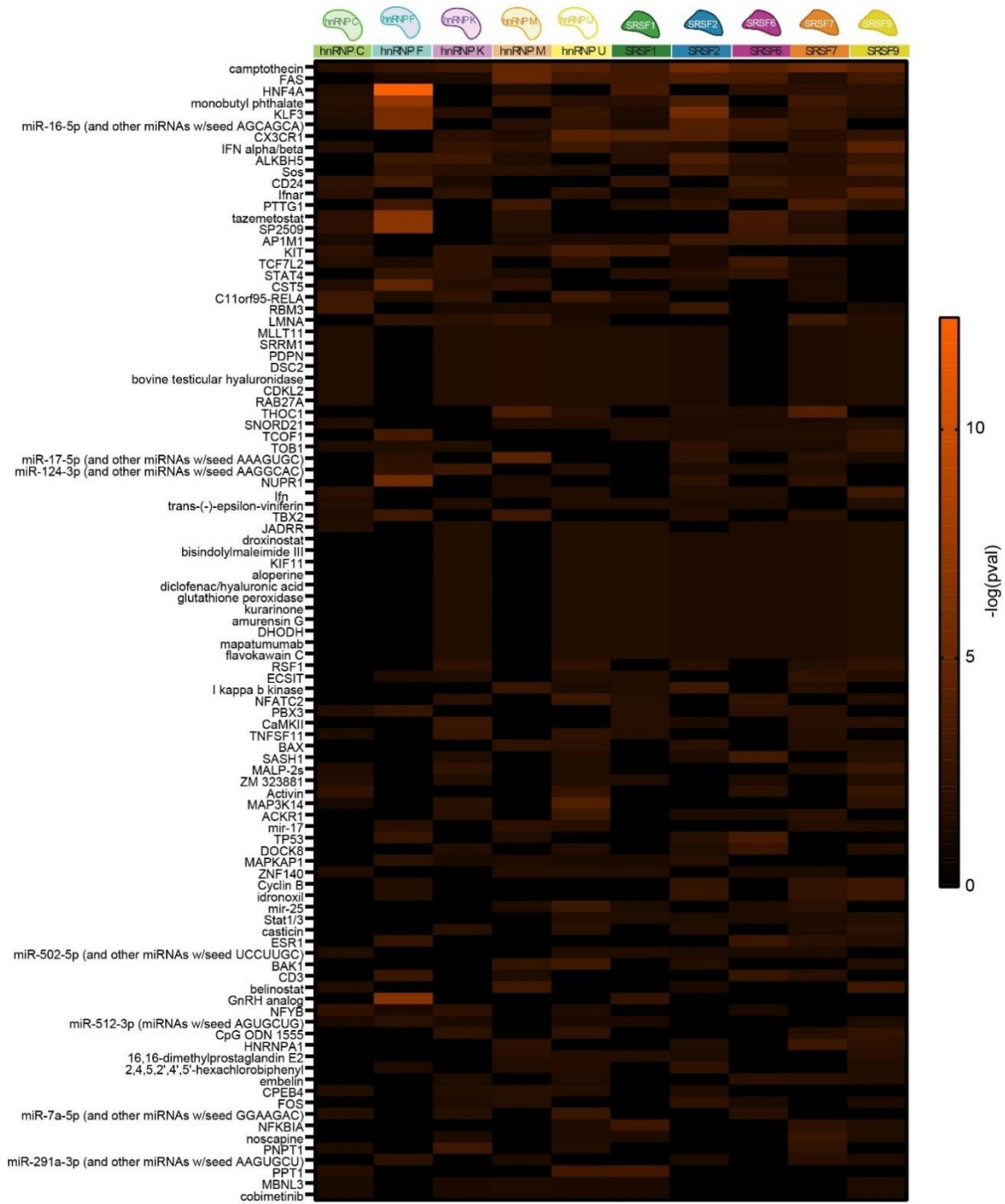


Figure 80. IPA Analysis of hnRNP and SRSF-dependent Splicing Shows Regulation of Cancer in Resting Macrophages

Causal Ingenuity Pathway Analysis of gene expression changes in uninfected hnRNP and SRSF knockdowns. Genes utilized in IPA were significantly differentially expressed ($p < 0.05$).

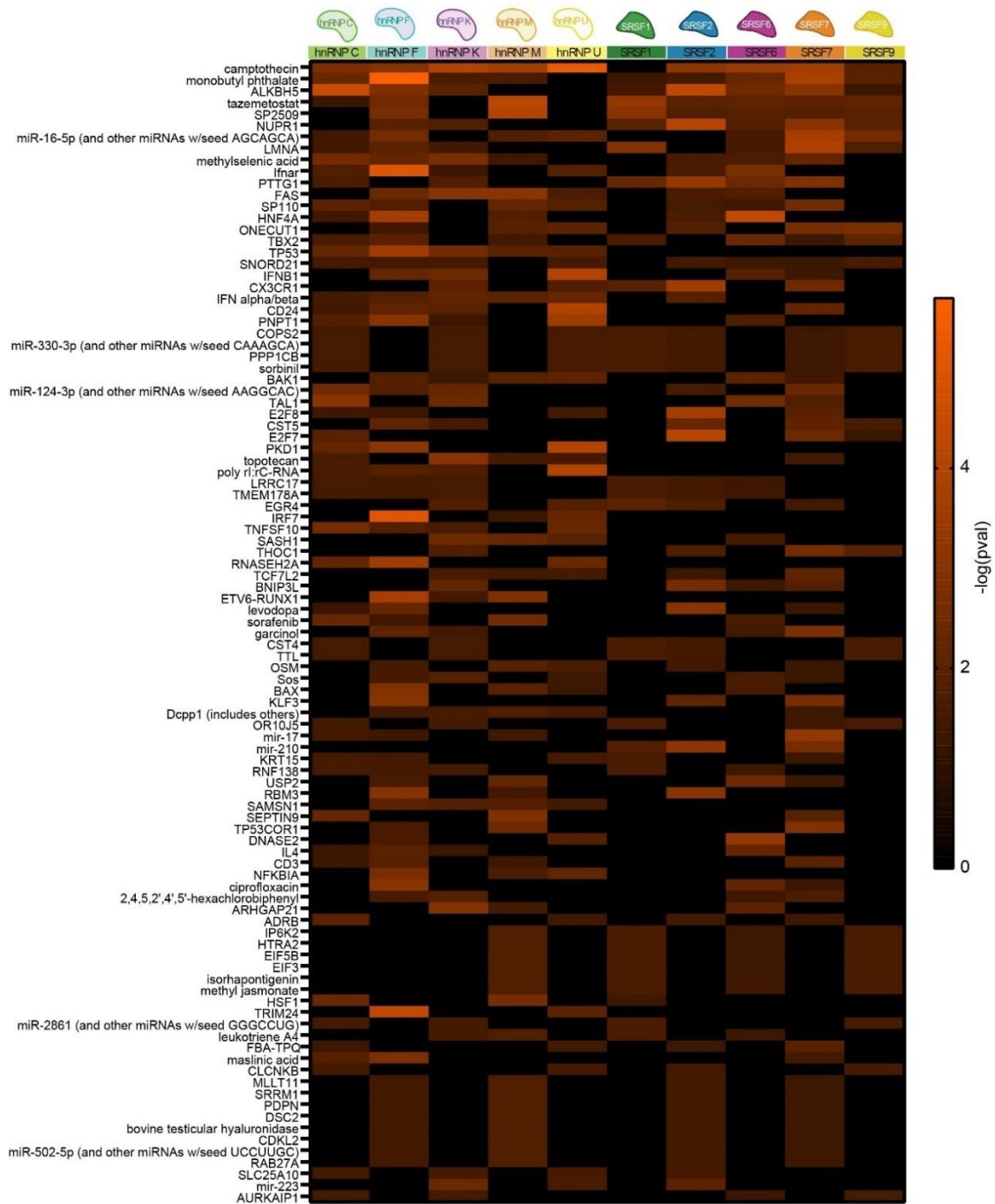


Figure 81. IPA Analysis of hnRNP and SRSF-dependent Splicing Shows in *Salmonella*-Infected Macrophages

Causal Ingenuity Pathway Analysis of gene expression changes in *Salmonella*-infected hnRNP and SRSF knockdowns. Genes utilized in IPA were significantly differentially expressed ($p < 0.05$).

APPENDIX B

TABLES

Table 1. hnRNP M RNA-Seq Gene Expression Changes

RNA-Seq Uninfected		RNA-Seq + <i>Salmonella</i>	
GENE NAME	FOLD INDUCTION	GENE NAME	FOLD INDUCTION
Hpgd	13.90711	Fabp7	6.765286
Cxcr4	9.354822	Ms4a6c	5.454133
Ms4a6c	7.745006	Ms4a4c	4.956656
Csf3r	7.714053	Ms4a6d	4.288573
Fabp7	5.976491	Il6	3.957798
S1pr1	5.387236	Marcks	3.499546
Cd33	4.585221	Gm16685	3.373171
Ms4a6d	4.420621	Adora2a	3.23969
Neur13	3.949566	Ighm	3.19321
Pros1	3.932567	Slc28a2	3.177709
Prss46	3.472838	Cfb	3.166876
Prss50	3.46898	Slamf9	3.116945
St6gal1	3.419711	Rpl27-ps3	3.017322
Ighm	3.19321	Mx1	3.008578
Cd36	3.104169	Cd36	2.828894
Il10ra	3.085386	Ctsc	2.787805
Gm12166	2.956821	C3	2.569081
Fabp4	2.923715	Fcgr3	2.480588
Aph1c	2.916988	Fabp3	2.4082
Fosb	2.85088	Smpdl3a	2.352208
Atf3	2.832853	Pld4	2.271779
Tnfrsf1b	2.814419	Nectin2	2.247367
Tgfbr1	2.740644	Dusp1	2.241607
Fcgr3	2.73009	Cd300e	2.21221
Clec4a3	2.694922	Gm5431	2.182886
Il7r	2.691738	Havcr2	2.170636
Tmem86a	2.672264	Fcgr2b	2.150546
Cav2	2.651061	Spen	2.146736
Gm6377	2.615475	C3ar1	2.115022
Cd300c2	2.58364	Cd300c2	2.104473
Fabp3	2.555074	Siglece	2.089605
Smpdl3a	2.51753	Edn1	2.089051
Ptafr	2.485913	Cd276	2.056106
Pld4	2.390038	Tgm2	2.027966
Plk2	2.379248	Fcgr4	1.997097
Btg2	2.363222	Gm10260	1.99323
C3ar1	2.210747	Il10ra	1.978782
Wfdc17	2.139324	Sema4a	1.955406
Cd276	2.135795	Ccl2	1.938053
Itgam_1	2.060784	Ass1	1.925226
Ctsc	2.051702	Adgre1	1.866584
Egr2	2.046845	Il4i1	1.857245
Tgm2	2.039586	Pik3r6	1.817064

Table 2. hnRNP M RNA-Seq Gene Expression Changes Cont.

RNA-Seq Uninfected		RNA-Seq + <i>Salmonella</i>	
GENE NAME	FOLD INDUCTION	GENE NAME	FOLD INDUCTION
Egr1	1.995767	Bcl3	1.802364
Dusp1	1.995471	Tnfsf9	1.799192
Mpeg1	1.96516	Fcgr1	1.797059
Bhlhe41	1.959191	Igsf6	1.796179
Xdh	1.939404	Lacc1	1.793885
Lst1	1.919394	Zc3h12c	1.793278
Lsp1	1.897235	Gngt2	1.786466
Gnpda1	1.891593	Gm4070	1.762879
Tlr13	1.876798	Plk2	1.735775
Myo1f	1.868713	Bcl2a1a	1.731698
Rap2b	1.824333	Rsad2	1.728779
Jun	1.818452	Lsp1	1.728275
Arl11	1.803489	Cmpk2	1.716878
Rnf26_1	1.800696	Fabp4	1.709066
Havcr2	1.800502	Stat5a	1.705524
Fblim1	1.779344	Napsa	1.704077
Mcoln2	1.774978	Ppp1r15a	1.686405
Rnf128	1.761964	Gk	1.68233
Rab32	1.75113	Myo1f	1.677152
Tnfaip2	1.726583	GpnmB	1.675334
Dhrs3	1.725571	Arhgef3	1.672991
Litaf	1.714146	Tnfaip3	1.661885
Ctsf	1.705514	Nfkbiz	1.658248
Cxcl16	1.703797	Syk	1.651344
Gstm1	1.702554	Tagap	1.645342
Gngt2	1.701373	Iltgal	1.638434
Zfp385a	1.688385	Tmem51	1.636726
Pbxip1	1.687734	Mpeg1	1.635068
Hist1h1c	1.68698	Cebpb	1.63348
GpnmB	1.672091	Dusp2	1.627537
Napsa	1.658448	Ctsf	1.621343
Fos	1.652633	Fam129a	1.620868
Cotl1	1.646704	Zfp36	1.62075
Slc15a4	1.638645	Saa3	1.617704
Tmem51	1.636726	Slc44a1	1.610821
Id3	1.631679	Ldlr	1.600648
Slc44a1	1.628823	Ptafr	1.600574
Ier2	1.613946	Fam177a	1.598248
MsrB1	1.611736	Birc3	1.591189
Il10rb	1.603	Anpep	1.587615
Bcl2a1d	1.597259	Myo1g	1.58755
Ctnnb1	1.585479	Tnfrsf1b	1.587515
Slc6a8	1.582178	Il18	1.582494
Nceh1	1.57352	Tnfaip2	1.546983
Sptssa	1.571322	Cxcl16	1.538268
Gyg	1.565705	Traf1	1.533961
Rgs2	1.565309	Gbp5	1.531947
Plin2	1.563214	Blnk	1.531359

Table 3. hnRNP M RNA-Seq Gene Expression Changes Cont.

RNA-Seq Uninfected		RNA-Seq + <i>Salmonella</i>	
GENE NAME	FOLD INDUCTION	GENE NAME	FOLD INDUCTION
B4galt1	1.550249	Atf3	1.530953
Rnh1	1.536697	Gadd45	1.526009
Tbc1d16	1.521571	Lrrc25	1.515623
Zfp36	1.515133	Jak2	1.509944
Fabp5	1.507761	Icam1	1.501014
Cybb	1.506247	Capg	-1.43733
Anpep	1.50344	Ubald2	-1.50115
Alox5ap	1.500911	Rab31	-1.50144
Pdia3	-1.50295	Pdia3	-1.51841
Tubb6	-1.50417	Atp1b3	-1.5477
Tmsb10	-1.50845	Snx9	-1.56831
Sumo2	-1.53189	Ets2	-1.60419
Ccl3	-1.54719	Plau	-1.60747
Pip5k1b	-1.56974	Naa25	-1.60934
Hmga2	-1.58317	Gm26619	-1.6641
Atp1b3	-1.58414	Mrps6	-1.67118
Ank	-1.5913	Spp1	-1.67374
Cpne8	-1.59717	Tfdp1	-1.67919
Fcrl1	-1.61248	Serinc2	-1.69061
Rbpj	-1.61302	Tmem98	-1.70829
Tfdp1	-1.61335	Dhrs9	-1.71239
Slc6a12	-1.61529	Rpl10-ps3	-1.73337
Snx9	-1.62045	Spink5	-1.77682
Preld2	-1.64498	Epn2	-1.79498
Slc16a3	-1.65921	Ccz1	-1.81366
Fosl2	-1.65925	Ier3	-1.86244
Mrps6	-1.68031	Acy1	-1.8627
Acot7	-1.71671	Ccl17	-1.86471
Oas2	-1.71742	Ccnd1	-1.87697
Ehd1	-1.75186	Lif	-1.88307
Ccnd1	-1.78697	Rgs16	-1.91798
Marcks1	-1.81918	Csf3	-1.99019
Bnip3	-1.84262	Npl	-2.01377
Ak4	-1.84773	Timp1	-2.02017
Ets2	-1.85673	Hmga2	-2.04688
Acy1	-1.86399	Ccl2	-2.14895
Isg15	-1.88973	Dmpk	-2.16457
Odc1	-1.95677	Tnfsf15	-2.17432
Gm28037	-1.96705	Odc1	-2.24711
Layn	-1.96945	Pdia3	-2.34015
Naa25	-2.00186	Scin	-2.42501
Plekha3	-2.06644	Car2	-2.49682
Ccz1	-2.12175	Kbtbd11	-2.58657
Gm9803	-2.13322	Ccl7	-2.59416
Rtp4	-2.18593	Hnrpm	-2.72047
Npl	-2.19264	Gm18445	-2.80579
Spp1	-2.25665	Slc6a4	-2.88423

Table 4. hnRNP M RNA-Seq Gene Expression Changes Cont.			
RNA-Seq Uninfected		RNA-Seq + <i>Salmonella</i>	
GENE NAME	FOLD INDUCTION	GENE NAME	FOLD INDUCTION
Dmpk	-2.4654	Dmwd	-3.67138
Emp2	-2.65804	Mmp9	-3.86347
Hnrpm	-2.69036	Tnfsf8	-4.12014
Fosl1	-2.78138	Sema7a	-4.72083
Spink5	-2.80455		
Gm18445	-2.80579		
Tmem26	-3.02585		
Flt1	-3.09266		
Serinc2	-3.27645		
Rgs16	-3.53479		
Car2	-3.73217		
Gm21987	-4.1013		
Dmwd	-4.16092		
Slc6a4	-4.72442		
Mmp9	-6.9746		
1810011H11Rik	2.333564		
AB124611	1.783388		

Table 5. hnRNP M Regulated Genes with hnRNP M Consensus Motif Binding Sites + *Salmonella*

	Upregulated genes		Downregulated genes		
	GUGGUGG	GGUUGGUU		GUGGUGG	GGUUGGUU
Fabp7			Uald2	+	
Ms4a6c	+		Rab31	+	+
Ms4a4c	+	+	Pdia3	+	+
Ms4a6d	+		Atp1b3	+	+
Il6	+		Snx9	+	+
Marcks	+		Ets2	+	
Gm16685	+		Plau	+	
Adora2a	+		Naa25	+	+
Slc28a2	+		Gm26619	+	
Cfb			Mrps6	+	
Slamf9			Spp1	+	
Mx1	+		Tfdp1	+	+
Cd36	+	+	Serinc2	+	
Ctsc	+		Tmem98	+	
C3	+	+	Dhrs9		
Fcgr3	+	+	Rpl10-ps3		
Fabp3			Spink5	+	
Smpd13a	+		Epn2	+	+
Pld4	+		Ccz1	+	
Nectin2	+	+	Ier3		
Dusp1			Acy1	+	
Cd300e	+		Ccl17		
Gm5431	+	+	Ccnd1	+	
Siglece	+		Lif	+	
Havcr2	+	+	Rgs16	+	
Fcgr2	+		Csf3		
Spen	+	+	Npl	+	+
C3ar1	+		Timp1	+	
Cd300c2	+		Hmga2	+	+
Edn1			Ccl2		
Cd276			Dmpk	+	
Tgm2	+	+	Tnfsf15	+	
Fcgr4	+	+	Odc1	+	
Gm10260			Gm9260		
IL10ra	+		Scin	+	+
Sema4a	+		Car2		
Ccr12			Kbtbd11	+	
Ass1	+		Ccl7		
Adgre	+	+	Hnrnpm	+	
Pik3r6	+		Slc6a4	+	+
Il4i1	+		Dmwd		
Bcl3	+		Mmp9	+	
Tnfsf9			Tnfsf8	+	
Fcgr1	+		Sema7a	+	
Igsf6	+	+			
Lacc1	+	+			
Zc3h12c	+				
Gngt2					
Plk2					
Gm4070	+				
Bcl2a1a					
Rsad2	+				
Lsp1	+	+			
Cmpk2	+				
Fabp4	+				
Stat5a	+	+			
Napsa	+				

**Table 6. hnRNP M Regulated Genes with hnRNP M Consensus Motif Binding Sites
Cont.**

+ *Salmonella*

Upregulated genes

Downregulated genes

	GUGGUGG	GGUUGGUU		GUGGUGG	GGUUGGUU
Napsa	+				
Ppr1r15a					
Gk	+	+			
Myo1f	+				
Gpnmb	+	+			
Arhgef3	+	+			
Tnfaip3	+				
Nfkbiz	+	+			
Syk	+	+			
Tagap		+			
Itgal	+	+			
Mpeg1					
Cebpb					
Dusp2					
Ctsf					
Fam129a	+				
Zfp36					
Saa3	+				
Slc44a1	+	+			
Ldlr	+				
Ptafr	+	+			
Acp2	+				
Fam177a	+				
Birc3	+				
Anpep	+				
Myo1g	+				
Tnfrsf1b	+	+			
Il18	+				
Tnfaip2					
Cxcl16					
Traf1	+	+			
Gbp5	+				
Blnk	+				
Atf3					
Lrrc25	+				
Jak2	+	+			
Gadd45b					
Icam1	+	+			

Table 7. hnRNP M RNA-Seq and MAJIQ Hits Overlap with ENCODE Data

MAJIQ GENES (UN+SAL)	Found in eCLIP (ENCODE)	RNA-Seq Uninfected	Found in eCLIP (ENCODE)	RNA-Seq + <i>Salmonella</i>	Found in eCLIP (ENCODE)
1190007I07Rik				Fabp7	
Acvr1	*	Hpgd		Ms4a6	
Aldh3a2		Cxcr4		Ms4a4c	
Amotl1	*	Ms4a6c		Ms4a6d	
Asxl1	*	Csf3r		Il6	
Atxn2	*	Fabp7		Marcks	*
Auh	*	S1pr1		Gm16685	
Ccne2		Cd33		Adora2a	*
Chka	*	Ms4a6d		Ighm	*
Cnot4	*	Neurl3		Slc28a2	
Commd8		Pros1	*	Cfb	
Dcaf8	*	Prss46		Slamf9	
Desi2	*	Prss50		Rpl27-ps3	
Dock10		St6gal1	*	Mx1	
Dtx2	*	Ighm		Cd36	
Ercc8		Cd36		Ctsc	*
Frm4a	*	Il10ra		C3	
Gfod1	*	Gm12166		Fcgr3	
Gm29247		Fabp4		Fabp3	
Hps5		Aph1c		Smpdl3a	
Ist1	*	Fosb		Pld4	
Kat6a	*	Atf3		Nectin2	
Kat6a		Tnfrsf1b		Dusp1	
Klf7	*	Tgfr1	*	Cd300e	
Ktn1	*	Fcgr3		Gm5431	
Lrmp		Clec4a3		Havcr2	
Mdm4	*	Il7r		Fcgr2b	
Mx1		Tmem86a		Spen	*
Nmt2	*	Cav2		C3ar1	
Numb		Gm6377		Cd300c2	
Pak1	*	Cd300c2		Siglece	
Pds5b	*	Fabp3		Edn1	
Phactr4	*	Smpdl3a	*	Cd276	*
Plec	*	Ptafr		Tgm2	
Plxnc1		Pld4		Fcgr4	
Rpl22	*	Plk2		Gm10260	
Sec14l1	*	Btg2		Il10ra	
Senp1		C3ar1		Sema4a	
Senp6	*	Wfdc17		Ccr12	
Smc6		Cd276	*	Ass1	*
Tbc1d7		Itgam_1		Adgre1	
Tex30		Ctsc	*	Il4i1	*
Tmem87a	*	Egr2		Pik3r6	
Trmu	*	Tgm2		Bcl3	
Ubqln1	*	Egr1	*	Tnfrsf9	
Xpo6		Dusp1		Fcgr1	
Zfyve27	*	Mpeg1		Igsf6	
Zmynd8	*	Bhlhe41		Lacc1	
1110051M20Rik		Xdh		Zc3h12c	
4833420G17Rik		Lst1		Gngt2	

Table 8. hnRNP M RNA-Seq and MAJIQ Hits Overlap with ENCODE Data Cont.

MAJIQ GENES (UN+SAL)	Found in eCLIP (ENCODE)	RNA-Seq Uninfected	Found in eCLIP (ENCODE)	RNA-Seq + <i>Salmonella</i>	Found in eCLIP (ENCODE)
Ankra2		Lsp1		Gm4070	
Aplp2	*	Gnpda1		Plk2	
Atf2	*	Tlr13		Bcl2a1a	
Ccdc77		Myo1f		Rsad2	
Ccdc82	*	Rap2b		Lsp1	
Clk4	*	Jun		Cmpk2	
Csnk1d	*	Arl11		Fabp4	
Def8	*	Rnf26_1		Stat5a	*
Dmac2		Havcr2		Napsa	
Ehmt1	*	Fblim1		Ppp1r15a	
Emsy	*	Mcoln2	*	Gk	
Epn2	*	Rnf128		Myo1f	
Fbxo34	*	Rab32		Gpnmb	
Foxd2os		Tnfaip2	*	Arhgef3	*
Foxo3	*	Dhrs3	*	Tnfaip3	*
Gabpb2		Litaf	*	Nfkbiz	*
Ggta1		Ctsf		Syk	
Gm46430		Cxcl16		Tagap	
Golgb1	*	Gstm1		Itgal	
Herc2	*	Gngt2		Tmem51	*
Lair1		Zfp385a		Mpeg1	
Luzp1	*	Pbxip1		Cebpb	
Lyar		Hist1h1c		Dusp2	
Mettl2		Gpnmb		Ctsf	
Mycbp2	*	Napsa		Fam129a	
Myo18a	*	Fos		Zfp36	
Ncapg2	*	Cotl1		Saa3	
Nsmaf	*	Slc15a4	*	Slc44a1	*
Panx1		Tmem51		Ldlr	
Patz1	*	Id3		Ptafr	
Ppcdc		Slc44a1	*	Fam177a	
Ppp2r5c	*	Ier2	*	Birc3	
Pradc1		Msrb1		Anpep	
Prepl		Il10rb		Myo1g	
Prr14	*	Bcl2a1d		Tnfrsf1b	
Ptger4		Ctnnb1	*	Il18	
Ptpn4	*	Slc6a8		Tnfaip2	*
Rnf20		Nceh1		Cxcl16	
Snx12		Sptssa	*	Traf1	
Sptan1		Gyg		Gbp5	
Srrm2	*	Rgs2		Blnk	
St7	*	Plin2		Atf3	
Tmem161b	*	B4galt1	*	Gadd45b	
Tmem229b		Rnh1		Lrrc25	
Tmem80		Tbc1d16		Jak2	*
Ttc13	*	Zfp36		Icam1	
Vegfa		Fabp5		Capg	*
Zmym3		Cybb		Ubal2	
		Anpep		Rab31	*

Table 9. hnRNP M RNA-Seq and MAJIQ Hits Overlap with ENCODE Data Cont.

MAJIQ GENES (UN+SAL)	Found in eCLIP (ENCODE)	RNA-Seq Uninfected	Found in eCLIP (ENCODE)	RNA-Seq + <i>Salmonella</i>	Found in eCLIP (ENCODE)
		Alox5ap		Pdia3	
		Pdia3		Atp1b3	*
		Tubb6		Snx9	*
		Tmsb10		Ets2	*
		Sumo2		Plau	*
		Ccl3		Naa25	
		Pip5k1b	*	Gm26619	
		Hmga2	*	Mrps6	*
		Atp1b3	*	Spp1	
		Ank	*	Tfdp1	*
		Cpne8	*	Serinc2	
		Fcrl1		Tmem98	
		Rbpj	*	Dhrs9	
		Tfdp1	*	Rpl10-ps3	*
		Slc6a12		Spink5	
		Snx9	*	Epn2	*
		Preli2	*	Ccz1	
		Slc16a3		Ier3	
		Fosl2		Acy1	
		Mrps6	*	Ccl17	
		Acot7		Ccnd1	
		Oas2		Lif	
		Ehd1		Rgs16	
		Ccnd1		Csf3	
		Marcksl1	*	Npl	
		Bnip3	*	Timp1	
		Ak4	*	Hmga2	*
		Ets2	*	Ccl2	
		Acy1		Dmpk	
		Isg15		Tnfsf15	
		Odc1	*	Odc1	*
		Gm28037		Pdia3	
		Layn		Scin	
		Naa25	*	Car2	
		Plekha3		Kbtbd11	*
		Ccz1		Ccl7	
		Gm9803		Hnrnp	*
		Rtp4		Gm18445	
		Npl		Slc6a4	
		Spp1		Dmwd	
		Dmpk		Mmp9	
		Emp2		Tnfsf8	
		Hnrnp		Sema7a	*
		Fosl1			
		Spink5			
		Gm18445			
		Tmem26			
		Flt1			
		Serinc2			

Table 10. hnRNP M RNA-Seq and MAJIQ Hits Overlap with ENCODE Data Cont.

MAJIQ GENES (UN+SAL)	Found in eCLIP (ENCODE)	RNA-Seq Uninfected	Found in eCLIP (ENCODE)	RNA-Seq + <i>Salmonella</i>	Found in eCLIP (ENCODE)
		Car2			
		Gm21987			
		Dmwd			
		Slc6a4			
		Mmp9			

Table 11 hnRNP M Mass Spec Overlap with Serine Mutants In Uninfected and LPS treated Macrophages

UNINFECTED				+LPS						
574A + 574D	WT+ 574D	WT +574A	WT, 574A, + 574D	574D + 574A	WT + 574A	WT + 574D	WT, 574A, + 574D			
AMPN	CD72	EIF4B	CAPR1	CO3	METH	CORO1C	HNRPU			
F8WGL3	EFHD2	IF4B	KIF4	EEA1	SMD3	SYNE1	HNRPU			
ILF3	HNRPF	POLDIP3	B2RXM2	ROA0	MGN	POLDIP3	ANM5			
RBM10	RALY	PDIP3	ANXA2P2	ATPA			TRA2			
RBM14	ROAA	SFPQ	AXA2L	MPCP						
SRSF1	SRSF7	CAPRIN1		NONO						
CAPR1	MATR3	KIF4		SAFB1						
KIF4	CAPR1	B2RXM2		G3BP2						
B2RXM2	KIF4	ANXA2P2		SRSF1						
ANXA2P2	B2RXM2									
	ANXA2P2									